National Technical University of Athens

School of Naval Architecture and Marine Engineering
Division of Ship and Marine Hydrodynamics

Nonlinear water waves over varying bathymetry: Theoretical and numerical study using variational methods

BY

Christos E. Papoutsellis

A thesis submitted for the degree of
Doctor of Philosophy

Supervisor: G. A. Athanassoulis, Professor (NTUA)

2016

Advisory Committee

G. A. Athanassoulis	Professor, National Technical University of Athens, **Supervisor**
K. A. Belibassakis	Associate Professor, National Technical University of Athens
G. K. Politis	Professor, National Technical University of Athens

Examination Committee

G. A. Athanassoulis	Professor, National Technical University of Athens
K. A. Belibassakis	Associate Professor, National Technical University of Athens
G. K. Politis	Professor, National Technical University of Athens
K. I. Spyrou	Professor, National Technical University of Athens
I. G. Stratis	Professor, University of Athens
D. J. Frantzeskakis	Professor, University of Athens
V. Ch. Katsardi	Lecturer, University of Thessaly

Acknowledgements

Apart from my personal endeavour, the completion of the challenging quest for a doctoral degree would not be possible without the continuous encouragement and support from other people. The least I can do is devote this section to them.

Firstly, I owe my deepest gratitude to my Master and PhD supervisor Gerassimos Athanassoulis for being the first person that introduced me to the field of water waves and gave me the opportunity to work in National Technical University of Athens. I am indebted for his guidance, the time he devoted and the things that he taught me throughout these years. I am grateful for believing in me, for motivating me to be a better scientist and for inducing me to conduct original research defying the temptation to follow beaten tracks. I consider myself very fortunate that I had the opportunity to collaborate with him in this beautiful subject.

My sincere gratitude extends to Kostas Belibassakis for his help and advice. His willingness to provide codes, data and expertise significantly accelerated the passage from theory to numerical computation which is invaluable for the understanding of water waves. This thesis would not have been possible had it not been for the original contributions of both the aforementioned professors.

I would also like to express my gratitude to professors Gerassimos Politis and Kostas Spyrou for discussions during the finalisation of this manuscript.

My thanks also goes to my officemates. First, to Ivi Tsantili for helpful and interesting discussions during my first years. To Aris Kapelonis, for his important help during the whole process of the PhD. The stimulating discussions with him played an important role in my preoccupation with water waves and my overall scientific development. Many thanks to Alkis Milidis for sharing of thoughts and ideas during his stay in our office, and to Kostas Mamis, Angeliki Karperaki and Nikos Vasilikis for interesting discussions. I am also grateful to Alexis Charalampopoulos. I had the opportunity to closely collaborate with Alexis in the context of his diploma thesis, during which, he significantly advanced the efficiency of the proposed numerical method and contributed to the study of solitary waves.

I would also like to thank my "neighbours" Dimitris Manolas and Georgios Papadakis for their support and encouragement. Special thanks to Dimitris for sharing his expertise on the problem of water waves and its numerical solution.

Many thanks to Marinos Manolesos and professor Spyros Voutsinas for fruitful discussions and their encouragement. I would also like to thank my colleagues Ioannis Georgiou, Theodoros Gerostathis, Evangelos Filippas, Theodosios Papathanassiou, Vasileios Tsarsitalidis, Panagiotis Schoinas, Kostas Diakakis and many others in the Laboratory of Naval and Marine Hydrodynamics for interesting discussions in several scientific subjects. I would also like to thank professor Maria Perel for her hospitality during my stay in Saint Petersburg in the context of the conference Days on Diffraction 2015.

I also acknowledge the financial support provided from National Technical University of Athens, School of Naval and Marine Engineering, Section of Naval and Marine Hydrodynamics and the administrative support of Anastasia Tsoni, Mika Stylianou and Marillia Kassapi.

Many thanks and greetings to my friends, inside and outside the institution, for their support and encouragement from my first years in the School of Applied Mathematics and Physical Sciences till now.

This thesis would not be possible without the unconditional support of my parents Efstratios and Mirsini. Thank you for making it possible to follow my dream. Many thanks to my brothers Stavros and Vaggelis for believing in me and understanding my will to pursue my studies.

Above all, I thank my partner Ioanna Kocheila-Noulelli for her unconditional love and patience and for being by my side all these years. I could not have accomplished my goal without your presence.

Abstract

The understanding of the motion of water waves is of fundamental importance for many applications related to disciplines such Naval and Marine Hydrodynamics, Coastal and Environmental Engineering, and Oceanography. Even under the simplifying assumptions that fluid is ideal and the flow irrotational, the complete mathematical formulation of the free-boundary problem of water waves is very complicated and its theoretical and numerical study comprises a contemporary direction of research.

In the first part of this thesis, a new system of two *Hamiltonian* equations is derived, governing the evolution of free-surface waves. This system is coupled with a time-independent Coupled Mode System (CMS), called the *substrate* problem, that accounts for the internal fluid kinematics. The derivation is based on the use of Luke's variational principle in conjunction with an appropriate series representation of the velocity potential. The critical feature of this approach, initiated in (Athanassoulis & Belibassakis 1999, 2000), is the use of an enhanced vertical modal expansion that serves as an exact representation of the velocity potential in terms of horizontal modal amplitudes. Herein, we study further and justify this expansion. In particular, it is proved that under appropriate smoothness assumptions, the modal amplitudes exhibit rapid decay, ensuring that the infinite series can be termwise differentiated in the non-uniform fluid domain, including its physical boundaries. This justifies the variational procedure and proves that the resulting system, called Hamiltonian/Coupled-Mode System (HCMS), is an exact reformulation of the complete hydrodynamic problem, and therefore it is valid for fully nonlinear waves and significantly varying seabeds. In fact, it is a modal version of Zakharov/Craig-Sulem Hamiltonian formulation (Zakharov 1968, Craig & Sulem 1993) with a new, versatile and efficient representation of the Dirichlet to Neumann operator (DtN) operator, needed for the closure of the non-local evolution equations. No smallness assumptions are made, that is, the present approach is a *non-pertubative* one. In HCMS, the DtN operator is defined in terms of one of the unknown modal amplitudes, namely, the free-surface modal amplitude. Its computation avoids the numerical solution of the Laplace equation in the whole fluid domain, required in direct numerical methods, and the evaluation of higher-order horizontal derivatives, required in Boussinesq or other higher-order pertubative methods. Instead, a system of horizontal second order partial differential equations needs to be solved.

In the second part of the thesis, our theoretical results are exploited for the numerical solution of various nonlinear water wave problems. The backbone of our numerical

method is the computation of the DtN operator through its modal characterization which is achieved by a fourth-order finite-difference method. The accuracy and convergence of the new characterization of the DtN operator is assessed in test cases of highly non-uniform domains and our theoretical findings concerning the rate of decay of the modal amplitudes are numerically verified. This preparatory investigation demonstrates that a small number of modes suffices for the accurate computation of the DtN operator even in extremely deformed domains. Subsequently, a number of physically interesting water-wave problems, over flat as well as varying bathymetry, are considered. The first application concerns the computation of steady travelling periodic waves above a flat bottom for a wide range of nonlinearity and shallowness conditions up to the breaking limit. Next, we turn to the time integration of the new evolution equations by employing a fourth-order Runge-Kutta for the simulation of wave interactions with variable bathymetry and vertical walls. Computations are validated against predictions from laboratory experiments and other numerical methods in connection with several nonlinear phenomena. In particular we study the interaction of solitary waves with a vertical wall (reflection) and a plane beach (shoaling) and the transformation of regular incident waves past submerged obstacles (harmonic generation) or undulating bathymetry (Bragg scattering). Numerical results on the interaction of a solitary wave with an undulating bottom patch are also provided. The present method provides stable and accurate long time simulations of nonlinear waves in various depths, from deep to shallow waters, avoiding the computational burden of direct numerical methods as well as the use of filtering techniques, frequently required in pertubative approaches.

Περίληψη

Η κατανόηση της κίνησης των υδάτινων κυμάτων είναι ουσιαστικής σημασίας για πολλές εφαρμογές που σχετίζονται με τομείς όπως η Ναυτική και Θαλάσσια Υδροδυναμική, η Παράκτια και Περιβαλλοντική Μηχανική, και η Ωκεανογραφία. Ακόμη και υπό τις απλοποιητικές υποθέσεις του ιδανικού ρευστού και της αστρόβιλης ροής, η πλήρης μαθηματική διατύπωση του κυματικού προβλήματος με την ελεύθερη επιφάνεια είναι ιδιαίτερα πολύπλοκη και η θεωρητική και αριθμητική της μελέτη αποτελεί μία σύγχρονη κατεύθυνση έρευνας.

Στο πρώτο μέρος της παρούσας διατριβής, εξάγεται ένα νέο σύστημα δύο μη-τοπικών εξελικτικών εξισώσεων *Hamilton*, οι οποίες περιγράφουν την δυναμική των μη-γραμμικών κυμάτων ελεύθερης επιφάνειας. Αυτό το σύστημα είναι συζευγμένο με ένα χρονοανεξάρτητο κινηματικό υποπρόβλημα που αναπαριστά την κινηματική του υποκείμενου ρευστού. Η διαδικασία βασίζεται στη χρήση της μεταβολικής αρχής του (Luke 1967) σε συνδυασμό με μία κατάλληλη αναπαράσταση του δυναμικού της ταχύτητας σε μορφή συγκλίνουσας σειράς. Το βασικό χαρακτηριστικό αυτής της μεθοδολογίας, η οποία εισήχθη με τις εργασίες (Athanassoulis & Belibassakis 1999, 2000) είναι η χρήση ενός βελτιωμένου αναπτύγματος κατακόρυφων ιδιοσυναρτήσεων, το οποίο οδηγεί σε μια ακριβή αναπαράσταση του δυναμικού της ταχύτητας συναρτήσει των συντελεστών (πλατών) των ιδιομορφών που συνθέτουν το ανάπτυγμα. Σε αυτή την εργασία, το ανωτέρω ανάπτυγμα μελετάται λεπτομερώς για την περίπτωση των πλήρως μη-γραμμικών υδατίνων κυμάτων. Συγκεκριμένα, αποδεικνύεται ότι, υπό κατάλληλες υποθέσεις λειότητας, τα πλάτη των ιδιομορφών μειώνονται ταχέως, εξασφαλίζοντας έτσι ότι το ανάπτυγμά μπορεί να παραγωγίζεται κατά όρους στο χωρίο του ρευστού, μέχρι και τα ανομοιόμορφα φυσικά του σύνορα (ελεύθερη επιφάνεια και πυθμένας). Το γεγονός αυτό, νομιμοποιεί τους χειρισμούς στην μεταβολική διαδικασία που ακολουθείται, και αποδεικνύει ότι το προκύπτον σύστημα (Hamiltonian/Coupled-Mode System (HCMS)), είναι μία ακριβής αναδιατύπωση του πλήρους υδροδυναμικού προβλήματος. Στην ουσία είναι μία εναλλακτική εκδοχή της Zakharov/Craig-Sulemδιατύπωσης κατα Hamilton (Zakharov 1968, Craig & Sulem 1993) με μία νέα, ευέλικτη και αποδοτική αναπαράσταση του τελεστή Dirichlet to Neumann (DtN), ο οποίος υπεισέρχεται στην διατύπωση των μη-τοπικών εξελικτικών εξισώσεων. Εν προκειμένω, ο τελεστής DtNεκφράζεται μέσω του πρώτου όρου του αναπτύγματος του δυναμικού ταχύτητας. Δεν γίνεται χρήση καμίας ασυμπτωτικής υπόθεσης, δηλαδή, η παρούσα μέθοδος είναι *μη-διαταρακτική*. Ο υπολογισμός του τελεστή DtNπαρακάμπτει την αριθμητική επίλυση της εξίσωσης Laplacεσε όλο το υγρό χωρίο, όπως απαιτείται στις ευθείες αριθμητικές μεθόδους, καθώς και την υ-

λοποίηση υψηλής τάξεως οριζοντίων παραγώγων, όπως απαιτείται σε μεθόδους τύπου Boussinesq ή σε υψηλοτάξιες διαταρακτικές μεθόδους.

Στο δεύτερο μέρος της διατριβής, τα θεωρητικά μας αποτελέσματα εφαρμόζονται για την αριθμητική επίλυση μη-γραμμικών προβλημάτων υδάτινων κυμάτων. Το θεμελιώδες στοιχείο της αριθμητικής μεθόδου είναι ο υπολογισμός του τελεστή DtN, μέσω της επίλυσης του υποκειμένου κινηματικού προβλήματος στην μορφή οριζόντιων διαφορικών εξισώσεων. Η ακρίβεια και σύγκλιση αυτού του υπολογισμού αξιολογείται σε δοκιμαστικές περιπτώσεις έντονα ανομοιόμορφων χωρίων και τα θεωρητικά ευρήματα, σχετικά με το ρυθμό μείωσης των πλατών του αναπτύγματος, επιβεβαιώνονται αριθμητικά. Αυτή η προκαταρκτική διερεύνηση καταδεικνύει ότι ένας μικρός αριθμός όρων του αναπτύγματος αρκεί για τον ακριβή υπολογισμό του τελεστή DtN, ακόμη και σε περιπτώσεις έντονα παραμορφωμένων χωρίων. Στην συνέχεια, θεωρούμε διάφορα προβλήματα μη-γραμμικών υδάτινων κυμάτων, πάνω από σταθερή ή μεταβαλλόμενη βαθυμετρία. Η πρώτη εφαρμογή αφορά τον υπολογισμό οδευόντων περιοδικών κυμάτων σε σταθερό βάθος, για ένα ευρύ φάσμα συνθηκών μη-γραμμικότητας και ρηχότητας, έως το όριο θραύσεως. Στη συνέχεια, θεωρούμε την αριθμητική ολοκλήρωση των εξελικτικών εξισώσεων, η οποία επιτυγχάνεται με την μέθοδο Runge-Kutta τετάρτης τάξεως, και υλοποιείται για την προσομοίωση των αλληλεπιδράσεων υδάτινων κυμάτων με μεταβαλλόμενο πυθμένα ή με κατακόρυφα σύνορα. Οι υπολογισμοί επαληθεύονται με την χρήση διαθέσιμων αποτελεσμάτων από εργαστηριακά πειράματα ή/και άλλες αριθμητικές μεθόδους. Συγκεκριμένα, μελετάται η αλληλεπίδραση μοναχικών (solitary) κυμάτων με κατακόρυφο τοίχο (ανάκλαση) και με κεκλιμένο επίπεδο (ρήχωση). Επίσης, μελετάται ο μετασχηματισμός μονοχρωματικών κυματισμών που κινούνται πάνω από βυθισμένα εμπόδια (γένεση αρμονικών) ή κυματοειδή βαθυμετρία (ανάκλαση Bragg). Επιπλέον, δίνονται αποτελέσματα για την περίπτωση μοναχικού κύματος σε βαθυμετρία που αποτελείται από ένα κυματοειδές τμήμα σε έναν κατά τα άλλα σταθερό πυθμένα. Η παρούσα μέθοδος επιτυγχάνει ευσταθείς και ακριβείς προσομοιώσεις ισχυρά μη-γραμμικών κυμάτων σε ύδατα ενδιαμέσου και μικρού βάθους, αποφεύγοντας το υπολογιστικό κόστος των ευθέων αριθμητικών μεθόδων καθώς και τη χρήση τεχνικών φιλτραρίσματος, που συχνά απαιτούνται σε διαταρακτικές μεθόδους.

Contents

List of Notation

Against each entry is the page at which the notation is introduced.

General:

d	11	Horizontal dimension, $d = 1$ or 2.
D_h^η	11	Fluid domain vertically confined by the free and bottom surface parametrised by η and h respectively.
$\Gamma^\eta,\ \Gamma_h$	11	Vertical boundaries of D_h^η: Free and bottom surface.
X	11	The common projection of Γ^η and Γ_h on the horizontal plane $\{z = 0\}$.

Space-time variables and differential operators:

$\boldsymbol{x}$	11	Horizontal variables $\boldsymbol{x} = (x_1, x_2)$. If $d = 1$ we write $\boldsymbol{x} = x$.
z	11	Vertical variable.
t	11	Time variable.
$\nabla_{\boldsymbol{x}}$	12	Gradient operator in $\mathbb{R}^d$. $\nabla_{\boldsymbol{x}} = (\partial_{x_1}, \partial_{x_2})$
∇	12	Gradient operator in $\mathbb{R}^d \times \mathbb{R}^d$. $\nabla = (\nabla_{\mathbf{x}}, z) = (\partial_{x_1}, \partial_{x_2}, \partial_z)$
∂_t	12	Time derivative, $\partial_t = \frac{\partial}{\partial t}$.
Δ	12	Laplace operator on $\mathbb{R}^d \times \mathbb{R}^d$, $\Delta = \partial_{x_1}^2 + \partial_{x_2}^2 + \partial_z^2$.
∂_a	30	Denotes collectively the derivative with respect to $a = x_1, x_2$ or t.

Functional spaces:

$C^k([a, b])$	23	Space of k-times continuously differentiable functions in the interval $[a, b]$.
$L^2(a, b)$	23	Space of square integrable functions on the interval (a, b), with associated norm $\|F\|_{L^2(a,b)} = \left(\int_a^b F^2 dz\right)^{1/2}$.
$H^k(a, b)$	24	Sobolev spaces of functions defined on the interval (a, b).
$C^k(X)$	24	Space of k-times continuously differentiable functions on $X \subset \mathbb{R}^d$.

List of Figures

Introduction

Background literature

Gravity driven waves, propagating on the surface of water, are inextricably linked with phenomena that take place in the marine environment. The understanding of the motion of *water waves*, also called *gravity waves* or *free surface waves*, is of fundamental importance for the understanding of the interactions that take place among the sea, the seabed and the atmosphere. Due to their connection with a broad range of applications, the study of water waves has been a longstanding preoccupation of scholars from various disciplines, such as naval, coastal, civil engineering, oceanography and mathematics. Numerous developments have been documented up to now in the existing vast literature which is constantly enriched by contributions, involving rigorous mathematical analysis, numerical computations and experiments. Closely related topics that motivate a constantly growing interest on water waves, include the design of coastal structures, offshore platforms for oil extraction, offshore wind energy turbines or wave energy converters, ships etc.

Water waves abound in the natural environment where they develop a quite diverse and complex behaviour. They can, for example, diffract in the presence of obstacles, form coherent structures that travel along large distances or even break when approaching the shore. Feynman, initiating his short exposition on surface waves, in Volume I of (Feynman et al. 1964), aptly described their distinct character by using the following phrase

"*Now, the next waves of interest, that are easily seen by everyone and which are usually used as an example of waves in elementary courses, are water waves. As we shall soon see, they are the worst possible example, because they are in no respects like sound and light; they have all the complications that waves can have.*"

The mathematical formulation that describes water waves is very hard to deal with, since, it involves the already complicated equations of hydrodynamics in conjunction with the presence of a fluid domain with an unknown boundary, called *free surface*. Even under the suitably simplifying physical assumptions of an ideal fluid, irrotational flow and non-breaking waves, the governing equations comprise a set of partial differential equations, for the velocity potential of the fluid and the *free surface elevation*, which is tough to perceive mathematically. Early attempts for the study of this problem mainly concerned the treatment of the linearised formulation (Craik

2004). Historically, the first attempts to study nonlinear wave motion were made around the 19^{th} century, the most notable of which is that of (Stokes 1847) which dealt with waves of permanent form, observed earlier by Russel. Stoke's original approach was to recast the hydrodynamic problem in a frame of reference travelling with constant speed and then expand the periodic free surface elevation and potential in Fourier series along the direction of propagation. Using perturbation expansions for the Fourier coefficients he obtained meaningful solutions, valid for waves of relatively small amplitude in deep water, and provided insight into nonlinear wave motion which was not understood at that time. Another observation of Russell mentioned the existence of a "wave of translation", which was described as a "*...large solitary elevation, a rounded, smooth and well-defined heap of water, which continues its course along the channel apparently without change of form or diminution of speed*". This observation drew the attention of (Boussinesq 1872) who realised that the persistence and longevity of Russel's solitary wave, implied that the fluid motion over flat bottom evolves in such a way that the horizontal fluid velocity does not significantly depends on the depth. In this framework, Boussinesq expressed the velocity potential as a Taylor series, an even order polynomial in the vertical variable with space-time dependent coefficients given in terms of the unknown potential on the flat bottom. In this way, he derived a reduced two component evolutionary system, now called *Boussineq* equations, that govern small amplitude long waves, and admit of a closed form solitary wave solution. Equally important reduced equations with similar properties were derived by (Saint-Venant 1871) and (Korteweg & de Vries 1895) and took the names of the respective authors. Although the above model equations improved the understanding on nonlinear water waves, they are not themselves very useful in modern applications involving large waves and significantly varying seabeds that substantially affect the wave motion. In this cases, fluid motion becomes more complicated and its analytical treatment is a very difficult task.

In the 60s, the classical formulation of irrotational water waves, was revisited from the perspective of first principles of mechanics. The first contribution on that matter is due to Petrov (Petrov 1964) who provided a Lagrangian reformulation in which the dynamic free surface condition is derived from the stationarity of the Lagrangian action functional, constrained by the kinematical equations of potential flow and free surface impermeability. Luke, on the other hand, proposed an unconstrained variational formulation for irrotational free surface flow (Luke 1967). In *Luke's variational principle* the action functional is the space-time integral of the pressure field in the fluid domain and its Euler-Lagrange equations are equivalent to the complete hydrodynamical problem. Not much later, Zakharov derived the Hamiltonian reformulation of the problem (Zakharov 1968). Zakharov's Hamiltonian is the total energy of the fluid, under the constraint of potential flow, considered as a functional on the free surface elevation and the trace of the velocity potential on the free surface, the *free surface potential*. The corresponding Hamilton's equations are equivalent to the two nonlinear free surface conditions (kinematic and dynamic), coupled with the kinematical subproblem of the interior potential flow.

Petrov's formulation did not find application and is in general overlooked. On the other hand,

Witham immediately recognized that Luke's action functional, being free of kinematic constraints, can be simplified by using asymptotic expansions on the unknown potential (Whitham 1967). In this way, he rederived the Boussinesq equations and put forth a variational study of slowly varying wavetrains. Concerning the Hamiltonian formulation, Zakharov himself, introduced a second order expansion of the velocity potential in powers of the free surface elevation and, after some simplifications, derived a single evolution equation that describes weakly nonlinear waves in deep water, known as the *nonlinear Schrödinger equation*. The Hamiltonian structure of water waves was later rediscovered (Broer 1974, Miles 1977) and further studied in (Benjamin & Olver 1982). Craig and Sulem presented Zakharov's formulation in a more elegant form, by introducing an appropriate *Dirichlet to Neumann* operator (DtN), which represents the required normal fluid velocity on the free surface corresponding to potential flow (Craig & Sulem 1993). In this latter form, the Hamiltonian system for water waves is usually called the *Zakharov/Craig-Sulem formulation* (ZCS). The distinctive feature of the ZCS formulation, which separates it from other nonlinear evolution equations, is that the presence of DtN, being determined from the solution of a boundary value problem on the fluid domain, makes ZCS a nonlocal formulation which needs special treatment from both a theoretical and a numerical point of view.

For implementing numerical solution schemes for the complete ZCS formulation, an accurate and efficient evaluation of the DtN operator is of fundamental importance. First numerical methods were presented in (West et al. 1987) and (Dommermuth & Yue 1987), where spectral representations in the direction of propagation where employed. This approach, called *Higher Order Spectral* method (HOS), was extended in the variable bottom case in (Liu & Yue 1998) and further elaborated in (Gouin et al. 2016). In a similar line of work, Craig and Sulem, based on the analytic dependence of the DtN operator on the free-surface elevation, proposed its expansion in the form of a functional Taylor (Volterra-Taylor) series, implemented recursively in the Fourier space (Craig & Sulem 1993). As pointed out in (Schaffer 2008), the HOS and DtN expansions are equivalent. Further developments and applications of these methods in the flat bottom case can be found for instance in (Milder 1990, Nicholls 1998, Bateman et al. 2001, Craig & Nicholls 2002, Craig et al. 2006, Xu & Guyenne 2009). DtN expansions have been also generalized to the case of variable bathymetry, assuming that the seabed surface is a small perturbation of the horizontal plane (Smith 1998, Guyenne & Nicholls 2005, Craig et al. 2005). Another possibility, proposed in (Nicholls & Reitich 2001*a*), (Nicholls & Reitich 2001*b*), (Nicholls & Reitich 2006), (Nicholls 2007) is the transformed field expansion method, which implements an improved expansion for the velocity potential, having superior numerical characteristics both in accuracy and stability of the computation of DtN. Extension of this approach to the variable bathymetry case has been presented in (Guyenne & Nicholls 2007). It should be emphasized that the implementation of the aforementioned series expansions is based on spatial periodicity in conjunction with the assumption that the irregular geometry is a small perturbation of a canonical domain (an horizontal uniform strip), which permits the velocity potential or the DtN to be perturbed. These facts introduce some limitations, especially for non-periodic problems and

general domains, e.g. domains with essentially different depths in various subregions. In addition, there is evidence that the truncation of the DtN in the Hamiltonian of the ZCS formulation leads to problems that are generally ill-posed, especially when high-order wave numbers enter the computations (Milder 1990, Ambrose et al. 2014). A comparison of some of the above mentioned methods of computation of the DtN operator can be found in (Nicholls 2007) and (Wilkening & Vasan 2015).

Throughout the last decades, many scientists turned to the direct solution of the complete formulation of water waves, providing meaningful computations of nonlinear waves which are not restricted by smallness assumptions. Various *direct numerical methods* have been developed in this context, solving the boundary value problem (Laplace equation) for the substrate kinematics either by the finite element method (Cai et al. 1998, Rycroft & Wilkening 2013, Gagarina et al. 2014) or by the finite difference method (Bingham & Zhang 2007, Engsig-Karup et al. 2009). Such methods provide high-quality numerical results, but computations may become slow or inefficient in large domains, since they require the discretization of the free surface and the vertical coordinate. Another class of numerical methods involves boundary integral equations (Longuet-Higgins et al. 1976, Grilli et al. 1994, Clamond & Grue 2001, Grilli et al. 2001). These methods attain dimensional reduction (elimination of the vertical coordinate) at the expense of the evaluation of integrals along the surfaces that enclose the fluid domain. Although this approach is flexible enough to deal with complex geometries, floating or submerged structures, its implementation requires the inversion of full matrices and becomes inefficient in large domains. Interesting surveys of various numerical methods applied for the solution of the water waves problem can be found in (Dias & Bridges 2006) and in the chapters of the collective volume (Ma 2010).

As already mentioned, nonlinear wave propagation in the presence of variable bathymetry plays a central role in most branches of coastal oceanography. Traditionally in these fields, the most popular line of work is the derivation of model equations derived by simplifying the complete formulation of the problem on the basis of asymptotic expansions and smallness assumptions on the shallowness, nonlinearity or bottom variation. Important developments in this line of work include the equations derived in (Serre 1953, Peregrine 1967, Green & Naghdi 1976, Miles & Salmon 1985). After the introduction of the ZCS formulation, the derivation of asymptotic models was revisited in several works. See for instance (Craig & Groves 1994, Craig et al. 1997, Lannes & Bonneton 2009, Matsuno 2016) and the monograph (Lannes 2013) for more details and references. It is well known that asymptotic models are valid for wave propagation over weakly varying seabeds governed by weak dispersion or nonlinearity (Dingemans 1997, Barthelemy 2004). The extension of the range of validity of these models is the purpose of a great deal of effort that led to the development of various improvement techniques and more sophisticated models, usually called Boussinesq Type Models (BTMs), see e.g. (Nwogu 1993, Madsen et al. 2002, Zou & Fang 2008, Bingham et al. 2009, Bonneton et al. 2011, Memos et al. 2015) and the review (Brocchini 2013). These models have become very popular because they are characterised

by adequate physical accuracy and their numerical solution requires reasonable computational resources. Nevertheless, BTMs derived through a perturbation procedure, inherit the presence of higher-order (horizontal) space and space-time derivatives and high polynomial nonlinearities which make the implementation of numerical schemes quite involved. Other authors preferred to avoid the use asymptotic expansions in small parameters, and proposed the derivation of model equations, on the basis of well chosen simplified representations of fluid quantities in conjunction with variational principles or depth integration, see for instance (Isobe & Abohadima 1998, Kakinuma 2001, Kim et al. 2001, Klopman et al. 2010, Clamond & Dutykh 2012, Zhao et al. 2014). Notwithstanding the attractive structure of simple model equations (a few horizontal evolution equations).

In another axis of research, several authors proposed equations that govern linear waves over varying bathymetry. Berkhoff introduced a mild bottom slope approximation and derived a single linear equation modelling waves in slowly varying depth (Berkhoff 1972). Berkoff's *mild-slope* equation was extended by the introduction of vertical eigenfunction expansions for the unknown velocity potential (Massel 1993, Porter & Staziker 1995). This approach, called *coupled mode method* in the relevant literature, aims at a dimensional reduction of the wave propagation problem through its reformulation in terms of an unknown sequence of horizontal modal amplitudes that are introduced through the eigenfunction expansion. Athanassoulis and Belibassakis pointed out the deficiency of these eigenfunction expansions, in accurately satisfying the boundary condition on the uneven seabed, and proposed a remedy by appropriately introducing an additional term in the expansion. Using this enhanced expansion, in conjunction with the variational formulation of linear waves, they derived a *consistent coupled mode system*, valid for waves over uneven seabed (Athanassoulis & Belibassakis 1999). This enhancement technique led subsequently to the computation of scattered linear waves due to steep bathymetry (Belibassakis et al. 2001, 2011), and the extension of Stoke's second order theory in the variable bottom case (Belibassakis & Athanassoulis 2002). An interesting discussion on the properties of multi-modal linear models can be found in (Chamberlain & Porter 2006). The application of the coupled mode method in the context of the fully nonlinear problem was initiated in (Athanassoulis & Belibassakis 2000) where equations on the free surface elevation and the modal amplitudes are presented for the first time. These equations were further developed and led to the computation of nonlinear waves over flat and variable bottom (Athanassoulis & Belibassakis 2007, Belibassakis & Athanassoulis 2011). As pointed out in the latter works, the essential advantage of working with such enhanced expansions is their ability to converge rapidly on the whole non-uniform fluid domain and up to the boundaries, leading essentially to an exact reformulation of the problem rather than a simplified one. Thus, in principle, the number of terms required in the truncated enhanced series for an accurate representation of the velocity potential is expected to be small. This feature was demonstrated numerically in (Athanassoulis & Belibassakis 1999) and (Belibassakis & Athanassoulis 2011), while a proof was announced in (Athanassoulis & Belibassakis 2003). Other representation of the velocity potential are of course

possible leading to reformulations of similar mathematical structure. We mention, for instance, the approach followed in (Tian & Sato 2008, Yates & Benoit 2015, Rault et al. 2016) where the fluid domain is transformed to a uniform strip and the corresponding velocity potential is represented using Chebyshev vertical functions.

The above literature review is by no means complete. It gives, however, a flavour of the diversity of the methods employed for the study of water waves.

Overview of the Thesis

The main purpose of this thesis is to further study the idea of Athanassoulis and Belibassakis (Athanassoulis & Belibassakis 1999, Belibassakis & Athanassoulis 2011) in the context of fully nonlinear water waves and to delve deeper into its connection with the Hamiltonian ZCS formulation (Zakharov 1968, Craig & Sulem 1993) . The first step is to provide an extension and justification of enhanced modal expansions of smooth fields defined on non-uniform domains with smooth boundaries. We show that the infinite modal series can be differentiated term by term everywhere in the domain, including the boundaries, permitting us to develop exact coupled mode theories for general domains. This justifies the subsequent variational treatment of the hydrodynamic problem that eventually leads to the main result of this thesis; namely, the exact modal reformulation of ZCS formulation. The new Hamiltonian equations are coupled with a system of time independent partial differential equations on the sequence of horizontal modal amplitudes that is introduced through the modal expansion. The solution of the latter system, called *substrate* system, determines the DtN operator required for the time evolution and moreover can be used for the computation of the velocity potential or velocity field in the entire fluid domain. For the computation of water waves governed by the new formulation, called *Hamiltonian Coupled Mode System* (HCMS), we propose a fourth-order finite-difference approach. The convergence and accuracy of the new modal characterisation of the DtN operator are examined in several test cases of highly deformed domains where our theoretical findings are also verified. Computations of nonlinear water waves governed by HCMS are compared with theoretical, experimental and numerical predictions.

The manuscript is divided into three parts. The first two parts, each divided into four chapters, contain the main material. The theoretical framework and the methodology is developed in the first part. Numerical schemes and results are presented in the second part. The third part contains appendices related to the theoretical developments of this work.

In Chapter 1, the physical assumptions and the classical differential formulation of the problem is introduced. The associated mathematical reformulations are also presented.

In Chapter 2, we focus on a technique that aims at the enhancement of conventional eigenfunction expansions of the velocity potential in water wave problems. This technique, initiated in (Athanassoulis & Belibassakis 1999) for linear water waves over varying bathymetry, is generalized and justified. In particular, by estimating the rate of decay of the terms in the

modal series, it is shown that termwise space and time differentiation is permitted, provided sufficient smoothness conditions are satisfied by the velocity potential and the fluid domain.

In Chapter 3, the variational reformulation of the hydrodynamic problem using Luke's variational principle is undertaken. The first step is taken by the derivation of Euler-Lagrange (EL) equations on the basis of a generic series representation in terms of prescribed vertical functions and unknown horizontal functions. The EL equations corresponding to the exact modal series expansion, established in the previous chapter, are further elaborated leading eventually to the derivation of an evolutionary two component system, essentially equivalent with the ZCS formulation. In this context, the DtN operator is determined by the solution of a boundary value problem (BVP) for a system of partial differential equations (PDEs) on the horizontal modal amplitudes, instead of a BVP for the velocity potential in the whole fluid domain.

In Chapter 4, the generic EL equations are applied to the derivation of simplified models. Some existing models are derived by performing appropriate simplifications to our new EL equations. A new nonlocal model is also derived and its linear dispersive properties are examined.

In Chapter 5, a fourth-order finite-difference method is outlined for the solution of the substrate modal system in one horizontal dimension and several types of lateral boundary conditions (periodic, vertical impermeable walls, matching or excitation boundary condition). Our first numerical results concern the computation of the DtN operator in periodic test cases over flat bottom, for which close form solutions are available. In particular, we focus on the assessment of the convergence and accuracy of the new modal representation of the DtN operator in terms of the number of modes used in the truncated series expansion.

In Chapter 6, steady periodic waves travelling above a flat bottom are considered. After applying the travelling wave assumption on the HCMS we propose a numerical scheme for the approximate solution of the resulting, time independent, nonlinear system. The proposed algorithm computes steady waves for a broad range of shallowness conditions and wave heights up to their maximal values.

In Chapter 7, numerical schemes applicable to HCMS are developed for two different configurations. The first one corresponds to a wave tank laterally confined by vertical impermeable walls and is suitable for the investigation of the initial-boundary value problem. In the second configuration, HCMS is appropriately modified, via a sponge layer technique, so that it can simulate wave generation and absorption in a numerical wave tank.

In Chapter 8, the numerical schemes are implemented for simulations of water waves. After the preliminary assessment of the convergence, the accuracy, and the conservation properties of our scheme, we pursue with simulations of several interesting phenomena. In particular, we consider the interaction of solitary waves with varying bathymetry (shoaling) and walls (reflection) and the interaction of regular waves with submerged obstacles (harmonic generation) and sinusoidal bottoms (Bragg reflection). The validity of our computations is demonstrated by comparisons with experimental measurements and direct numerical methods. The interaction of a solitary wave with a sinusoidal bottom patch is also considered.

All algorithms were implemented in MATLAB with an Intel Core i7-2600, 3.40 GHz. The manuscript was prepared in LaTeX.

Main original contributions

- The analysis deployed in Chapter 2 establishes that appropriately enhanced eigenfunction expansions of wave fields defined on nonuniform strip-like domains are termwise differentiable, provided that the field in the vertical (transverse) direction and the domain are sufficiently smooth.

- The HCMS, derived in Chapter 3, comprises a new set of evolution equations for nonlinear water wave propagation in the presence of varying bathymetry, free of any smallness assumption concerning the deformation of the boundaries of the fluid domain or horizontal spatial periodicity. That is, HCMS is an exact (non-pertubative) reformulation of the fully nonlinear water problem, in the form of two evolution equations, coupled with a time-independent kinematical substrate problem.

- Fourth-order finite-difference schemes, applicable to HCMS, are developed. The solution of the truncated substrate problem is validated against analytical solutions and its convergence is systematically investigated with respect to the number of terms kept in the series expansion as well as the spatial discretization. Steady travelling periodic waves above a flat seabed (Chapter 6) and unsteady water waves over varying bathymetry (Chapter 7) are considered.

- The developed schemes are validated against highly accurate computations of fully nonlinear steady water waves and experimental measurements concerning the transformation of regular waves due to varying bathymetry.

- Simulations involving the interaction of solitary waves with vertical walls or varying bathymetry are also performed and validated against experimental predictions and other numerical methods. The case of a solitary wave interacting with a sinusoidal bottom patch is also considered.

The HCMS formulation was first announced in (Athanassoulis, Papoutsellis & Belibassakis 2013). Some details on the derivation of HCMS were given in (Athanassoulis & Papoutsellis 2015*a*), together with first simulations of the transformation of incident regular water waves over submerged obstacles. In (Athanassoulis & Papoutsellis 2015*b*), the convergence and accuracy of the coupled mode method for the computation of the DtN operator was demonstrated in some test cases. In (Papoutsellis 2015), some details of the numerical scheme were given together with applications on the propagation of water waves over undulating bathymetry. Further numerical results are presented in (Papoutsellis, Athanassoulis & Charalampopoulos 2016) where the propagation of solitary waves is considered, over flat or varying bathymetry.

Part I

The physical problem and its mathematical modelling

Chapter 1

Formulations of the water waves problem

In this preliminary chapter, we present three mathematical formulations of the *water waves problem* that constitute the basic framework of this thesis.

1.1 Physical assumptions and classical formulation

A Cartesian coordinate system $O\mathbf{x}z$ is adopted, where $\mathbf{x} \in \mathbb{R}^d$, $d = 1, 2$, denotes the horizontal variable(s) and z denotes the upward pointing vertical variable. The problem of water waves arises when one considers the motion of a fluid with an unknown or *free surface*, under the influence of gravity. Our starting point, in formulating this classical hydrodynamical problem, is the long-standing physical model of oceanography, according to which, the fluid is vertically bounded by the *free surface* and a fixed impermeable *bottom surface*, and is assumed to be homogeneous, inviscid and incompressible. Assuming that the free and bottom surfaces are parametrized by smooth functions $\eta(\mathbf{x}, t)$ and $h(\mathbf{x})$, the unknown fluid domain at time t is defined by

$$D_h^\eta(X; t) = \{(\mathbf{x}, z) \in \mathbb{R}^{d+1} : \ \mathbf{x} \in X \subset \mathbb{R}^d, \quad -h(\mathbf{x}) < z < \eta(\mathbf{x}, t)\}, \tag{1.1}$$

so that the free and bottom surface are given respectively by

$$\Gamma^\eta(X; t) = \{(\mathbf{x}, z) \in \mathbb{R}^{d+1} : \ \mathbf{x} \in X \subset \mathbb{R}^d, \quad z = \eta(\mathbf{x}, t)\}, \tag{1.2}$$

$$\Gamma_h(X) = \{(\mathbf{x}, z) \in \mathbb{R}^{d+1} : \ \mathbf{x} \in X \subset \mathbb{R}^d, \quad z = -h(\mathbf{x})\}. \tag{1.3}$$

The *free surface elevation* η represents the spatiotemporal deviation of Γ^η from the plane of quiescence $\{z = 0\}$, while the *bathymetry* h fixes the shape of the bottom in time. In the above definitions X denotes the common projection of Γ^η and Γ_h on the horizontal plane $\{z = 0\}$. In order to assure that the surfaces Γ_h and Γ^η do not intersect, we assume that the total depth of

the fluid $H(\mathbf{x},t)=\eta(\mathbf{x},t)+h(\mathbf{x})>0$ for any $(\mathbf{x},t)$. The outward normal vectors on Γ^η and Γ_h are written as

$$N_\eta=(-\nabla_{\mathbf{x}}\eta,1),\qquad N_h=(-\nabla_{\mathbf{x}}h,-1),\tag{1.4a,b}$$

respectively, where $\nabla_{\mathbf{x}}=(\partial_{x_1},\partial_{x_2})$ denotes the horizontal gradient (see Figure 1.1). On the time dependent domain $D_h^\eta(X;t)$, an unknown vector function $\vec{V}(\mathbf{x},z,t)$ is ascribed, called velocity field, which determines at time t the fluid particle velocity at $(\mathbf{x},z)$. This vector field, in the absence of rotational effects ($\operatorname{curl}\vec{V}=0$), is represented in terms of the so called *velocity potential* $\Phi(\mathbf{x},z,t)$ through the relation $V(\mathbf{x},z,t)=\nabla\Phi(\mathbf{x},z,t)$, where ∇ denotes the gradient with respect to $\mathbf{x}=(x_1,x_2)$ and z. Under these assumptions and notations, the fluid motion is described in terms of the velocity potential $\Phi(\mathbf{x},z,t)$ and the free surface elevation $\eta(\mathbf{x},t)$, by the following set of equations

$$\Delta\Phi=0,\quad \text{in } D_h^\eta,\tag{1.5}$$

$$N_h\cdot\nabla\Phi=0,\quad \text{on } z=-h,\tag{1.6}$$

$$\partial_t\eta=N_\eta\cdot\nabla\Phi,\quad \text{on } z=\eta,\tag{1.7}$$

$$\partial_t\Phi+\frac{1}{2}(\nabla\Phi)^2+g\eta=-\frac{P_{\text{surf}}}{\rho},\quad \text{on } z=\eta,\tag{1.8}$$

where g is the acceleration of gravity, ρ is the constant density of the fluid and P_{surf} is the known external surface pressure applied to a finite portion of the free surface Γ^η. Eq. (1.5) expresses the *incompressibility* of the homogeneous fluid, $\operatorname{div}\vec{V}=0$, and the *irrotationality* of the flow. Eqs. (1.6) and (1.7) state that no fluid particles cross the upper and bottom surface and are called the *bottom impermeability condition* and the *free surface kinematic condition*, respectively. Eq. (1.8) is the Bernoulli equation evaluated on the free surface Γ^η. It is derived by spatial integration of the Euler equation and evaluation on $z=\eta$, and is usually called *dynamic free surface condition*. More details on the derivation of Eqs. (1.5)-(1.8) can be found in several books, e.g. (Stoker 1957, Witham 1974, Debnath 1994, Lannes 2013).

Notation 1.1. In order to abbreviate notation, the boundary values (traces) of the various fields will be denoted by using brackets with a subscript defining the boundary. For example, Eq. (1.6) will be written as $N_h\cdot[\nabla\Phi]_{z=-h}=0$.

Eq. (1.6) is a boundary condition for Φ on the bottom surface Γ_h while Eqs. (1.7), (1.8) are two boundary conditions on the upper, free surface Γ^η. In order for the formulation to be complete, the set of equations (1.5)-(1.8) must be closed by appropriate conditions on the remaining boundaries of $D_h^\eta(X;t)$. In the case of a horizontally unbounded fluid one assumes that for any time t

$$\eta(\mathbf{x},t)\to 0\ \text{ as }\ |\mathbf{x}|\to\infty\quad\text{and}\quad |V(\mathbf{x},z,t)|\to 0\ \text{ as }\ |(\mathbf{x},z)|\to\infty.\tag{1.9}$$

In the case where the fluid domain is enclosed by a vertical impermeable surface denoted by S,

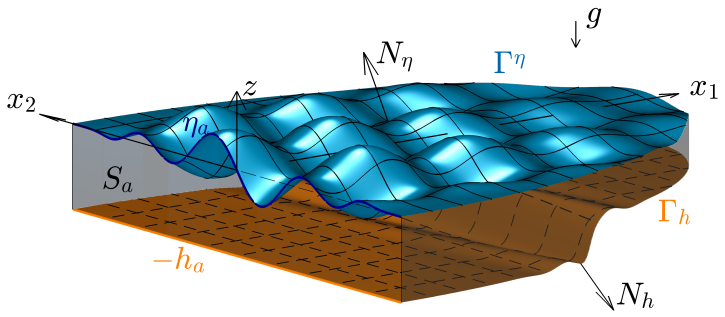

Figure 1.1: Geometric configuration of the fluid domain D_h^η.

then the normal velocity on S must vanish:

$$n_S \cdot [\nabla\Phi]_S = 0, \tag{1.10}$$

where n_S is the unit normal vector on S. Another possibility, suitable for the study of propagation and transformation of incident waves, is to introduce a plane vertical surface

$$S_a = \{(x_1, x_2, z) : x_1 = a,\ -h_a \le z \le \eta_a\}, \tag{1.11}$$

where η_a and h_a denote the prescribed surface elevation and depth at $x_1 = a$, on which the velocity field or the velocity potential are known. Then, the unilaterally bounded horizontal extent of the fluid domain is $X = \{(x_1, x_2) : x_1 \ge a, x_2 \in \mathbb{R}\}$ and the lateral boundary conditions on η and Φ are written respectively as $[\eta]_{x_1=a} = \eta_a$ and

$$[\partial_{x_1}\Phi]_{x_1=a} = V_a, \tag{1.12}$$

where, V_a denotes the known fluid velocity on the matching surface S_a. Alternatively, one could use

$$[\Phi]_{x_1=a} = \Phi_a, \tag{1.13}$$

instead, where Φ_a denotes the known velocity potential on the matching surface S_a. We further assume that η_a and V_a vanish and h_a tends to a positive constant as $|x_2| \to \infty$. The fluid far from the excitation boundary S_a is assumed to be at rest, i.e., $|\nabla\Phi| + |\eta| \to 0$ as $|\mathbf{x}| \to \infty$.

1.2 Luke's Lagrangian formulation

Luke provided a variational principle for irrotational water waves, governed by Eqs. (1.5)-(1.8), in the case of a horizontally unbounded fluid of finite depth with zero external surface pressure (Luke 1967). More precisely, he delivered a functional $\mathcal{S}$, defined on the fields (η, Φ), and showed that the *Euler-Lagrange* (EL) equations of $\mathcal{S}$ are given by Eqs. (1.5)-(1.8) with $P_{\text{surf}} = 0$. This functional reads

$$\mathcal{S}[\eta, \Phi] = \int \int_X \int_{-h}^{\eta} \left[\partial_t \Phi + \frac{1}{2} (\nabla \Phi)^2 + gz \right] dz d\mathbf{x} dt, \tag{1.14}$$

and the corresponding EL equations are derived, in the usual way, by requiring the first variation of $\mathcal{S}$ to vanish. This is expressed by the following variational equation

$$\delta \mathcal{S}[\eta, \Phi; \delta\eta, \delta\Phi] = \delta_\Phi \mathcal{S}[\eta, \Phi; \delta\Phi] + \delta_\eta \mathcal{S}[\eta, \Phi; \delta\eta] = 0, \tag{1.15}$$

where $\delta_\Phi \mathcal{S}[\eta, \Phi; \delta\Phi]$ and $\delta_\eta \mathcal{S}[\eta, \Phi; \delta\eta]$ denote the partial Gâteaux derivatives of the functional $\mathcal{S}[\eta, \Phi]$ with respect to Φ and η in the directions $\delta\Phi$ and $\delta\eta$, respectively. In the case of an horizontally unbounded fluid, the so called admissible variations $\delta\Phi$ and $\delta\eta$ are arbitrary functions that satisfy $\delta\Phi(\mathbf{x}, z, t_1) = \delta\Phi(\mathbf{x}, z, t_2) = \delta\eta(\mathbf{x}, t_1) = \delta\eta(\mathbf{x}, t_2) = 0$ and $\delta\Phi \to 0$ and $\delta\eta \to 0$ as $|\mathbf{x}| \to \infty$. Luke's variational principle is verified by calculating $\delta_\Phi \mathcal{S}[\eta, \Phi; \delta\Phi]$ and $\delta_\eta \mathcal{S}[\eta, \Phi; \delta\eta]$,

$$\delta_\Phi \mathcal{S}[\eta, \Phi; \delta\Phi] = \int \int_X \int_{-h}^{\eta} \left[\partial_t \delta\Phi + (\nabla\Phi) \cdot (\nabla\delta\Phi) \right] dz d\mathbf{x} dt, \tag{1.16}$$

$$\delta_\eta \mathcal{S}[\eta, \Phi; \delta\eta] = \int \int_X \left[\partial_t \Phi + \frac{1}{2} (\nabla\Phi)^2 + gz \right]_{z=\eta} d\mathbf{x} dt, \tag{1.17}$$

integrating by parts in space and time in Eq. (1.15), and applying the usual arguments of the calculus of variations. We refer to (Luke 1967, Miles 1977) and the books (Witham 1974, Section 13.2), (Debnath 1994, Chapter 1), (van Groesen & Molenaar 2007, Chapter 6.3) for more details. The functional (1.14) can be easily modified to incorporate the presence of external surface pressure and the velocity matching condition (1.12) by adding to it the appropriate boundary terms. The extended functional, still denoted by $\mathcal{S}$, reads

$$\mathcal{S}[\eta, \Phi] = \int \int_X \left\{ \int_{-h}^{\eta} \left[\partial_t \Phi + \frac{1}{2} (\nabla\Phi)^2 + gz \right] dz + \int_X \frac{P_{\text{surf}}}{\rho} \eta \right\} d\mathbf{x} dt + \int \int_{\mathbb{R}} \int_{-h_a}^{\eta_a} V_a [\Phi]_{x_1 = a} \, dz dx_2 dt, \tag{1.18}$$

and its stationarity is equivalent with equations (1.5)-(1.8) and (1.12). Indeed, repeating the previous derivation, one easily finds that

$$\begin{aligned}\delta_\Phi \mathcal{S}[\eta,\Phi;\delta\Phi] = \int_{t_0}^{t_1}\int_X \Big\{ \Big(-\partial_t\eta + N_\eta \cdot [\nabla\Phi]_{z=\eta}\Big)\,[\delta\Phi]_{z=\eta} \\ - \int_{-h}^{\eta} \Delta\Phi\delta\Phi dz + N_h\cdot[\nabla\Phi]_{z=-h}\,[\delta\Phi]_{z=-h}\Big\} d\mathbf{x}dt \\ + \int_{t_0}^{t_1}\int_{\mathbb{R}}\int_{-h}^{\eta}\Big(-[\partial_{x_1}\Phi]_{x_1=a} + V_a\Big)\,[\delta\Phi]_{x_1=a}\,dzdx_2dt,\end{aligned} \tag{1.19}$$

and

$$\delta_\eta \mathcal{S}[\eta,\Phi;\delta\eta] = \int_{t_0}^{t_1}\int_X \left\{ [\partial_t\Phi]_{z=\eta} + \frac{1}{2}(\nabla\Phi)^2_{z=\eta} + g\eta + \frac{P_{\text{surf}}}{\rho}\right\}\delta\eta d\mathbf{x}dt, \tag{1.20}$$

where integration by parts (in space ant time) has been performed for the derivation of Eq. (1.19). The result follows after invoking the variational equation (1.15) in conjunction with the arbitrariness of $\delta\eta$ and $\delta\Phi$.

1.3 Zakharov/Craig-Sulem formulation and the Dirichlet to Neumann Operator

Zakharov pointed out that the knowledge of the free surface elevation $\eta(\mathbf{x},t)$ and the trace of the potential on the free surface,

$$\psi(\mathbf{x},t) = \Phi(\mathbf{x},\eta(\mathbf{x},t),t) = [\Phi]_{z=\eta}\,, \tag{1.21}$$

suffices for the determination of the flow in the fluid domain $D_h^\eta(X;t)$ (Zakharov 1968). This happens because the linear boundary value problem for Φ, consisting of the Laplace equation (1.5), the bottom impermeability (Neumann) condition (1.6), the non-homogeneous Dirichlet condition (1.21) and appropriate lateral boundary conditions, is in general solvable.[1]. Craig and Sulem introduced the Dirichlet to Neumann Operator (DtN) and extended Zakharov's formulation in the finite depth case (Craig & Sulem 1993). It is possible to extend further this approach in order to include the matching condition Eq. (1.12) at $x_1 = a$. In this case, the DtN operator[2], $\psi \to G[\eta,h]\psi$, is defined by

$$G[\eta,h]\psi = N_\eta\cdot[\nabla\Phi]_{z=\eta}\,, \tag{1.22}$$

[1] A rigorous proof of this statement in the case of a laterally unbounded fluid can be found in (Lannes 2005).

[2] Strictly speaking, this operator is the rescaled DtN operator; $G[\eta,h]$ maps the Dirichlet data ψ to the Neumann data, $\partial_n\Phi \equiv (|\nabla_{\mathbf{x}}\eta|^2+1)^{-\frac{1}{2}} N_\eta\cdot[\nabla\Phi]_{z=\eta}$, multiplied by the scalar function $(|\nabla_{\mathbf{x}}\eta|^2+1)^{\frac{1}{2}}$.

where Φ solves the boundary value problem

$$\Delta\Phi = 0, \quad \text{in} \quad D_h^\eta, \tag{1.23a}$$

$$N_h \cdot [\nabla\Phi]_{z=-h} = 0, \tag{1.23b}$$

$$[\Phi]_{z=\eta} = \psi, \tag{1.23c}$$

$$[\partial_{x_1}\Phi]_{x_1=a} = V_a, \tag{1.23d}$$

together with vanishing at infinity conditions. Applying the chain rule for the $(t, \mathbf{x})$- differentiation of Eq. (1.21) we obtain

$$[\partial_t\Phi]_{z=\eta} = \partial_t\psi - [\partial_z\Phi]_{z=\eta}\,\partial_t\eta, \tag{1.24a}$$

$$[\nabla_{\mathbf{x}}\Phi]_{z=\eta} = \nabla_{\mathbf{x}}\psi - [\partial_z\Phi]_{z=\eta}\,\nabla_{\mathbf{x}}\eta. \tag{1.24b}$$

Combining Eq. (1.24b) with Eq. (1.22) and solving for $[\partial_z\Phi]_{z=\eta}$ yields

$$[\partial_z\Phi]_{z=\eta} = \frac{G[\eta,h]\psi + \nabla_{\mathbf{x}}\eta\cdot\nabla_{\mathbf{x}}\psi}{1+|\nabla_{\mathbf{x}}\eta|^2}. \tag{1.25}$$

Taking into account Eqs. (1.24) and Eq. (1.25), the kinematic and dynamic free surface conditions, (1.7), (1.8), are written, after straightforward manipulations, as an evolutionary system on the free surface elevation η and free surface potential ψ:

$$\partial_t\eta = G[\eta,h]\psi, \tag{1.26}$$

$$\partial_t\psi = -g\eta - \frac{1}{2}|\nabla_{\mathbf{x}}\psi|^2 + \frac{\left(G[\eta,h]\psi + \nabla_{\mathbf{x}}\psi\cdot\nabla_{\mathbf{x}}\eta\right)^2}{2\left(1+|\nabla_{\mathbf{x}}\eta|^2\right)}. \tag{1.27}$$

The above equations were also derived by Watson and West in a slightly different form, see Eqs. (A4a,b) of (Watson & B.West 1975). The latter equations are obtained from Eqs. (1.26), (1.27) by noting that $G[\eta,h]\psi$, in view of Eqs. (1.24b), (1.22), is rewritten as

$$G\left[\eta,h\right]\psi = -\nabla_{\mathbf{x}}\eta\cdot\nabla_{\mathbf{x}}\psi + \left((\nabla_{\mathbf{x}}\eta)^2+1\right)W[\eta,h]\psi, \tag{1.28}$$

where $W\left[\eta,h\right]\psi = [\partial_z\Phi]_{z=\eta}$ is the free surface vertical velocity corresponding to the velocity potential satisfying (1.23). Evidently, $G[\eta,h]$ is a linear operator on ψ (and V_a). On the other hand, $G[\cdot,\cdot]$ is a nonlinear operator on (η,h) and this is suitably emphasised by the present notation, which is due to (Craig & Sulem 1993). Another, well-known property is that $G[\eta,h]$ is self-adjoint.

1.4 On the Hamiltonian structure of irrotational water waves

Zakharov also showed that Eqs. (1.26), (1.27), in the case of an infinite depth fluid in the absence of external surface pressure, comprise a Hamiltonian system (Zakharov 1968)

$$\partial_t \eta = \delta_\psi \mathscr{H}, \tag{1.29a}$$
$$\partial_t \psi = -\delta_\eta \mathscr{H}, \tag{1.29b}$$

where $\mathscr{H}$ is the Hamiltonian, that equals to the total energy of the fluid, and $\delta_\eta = \delta/\delta\eta$ and $\delta_\psi = \delta/\delta\psi$ denote variational derivatives with respect to η and ψ respectively, see also (Broer 1974, Miles 1977). The Hamiltonian, given by the sum of the kinetic energy K and potential energy V, is written

$$\mathscr{H} = K + V, \tag{1.30a}$$
$$K = \frac{1}{2}\int_X \int_{-h(\mathbf{x})}^{\eta(\mathbf{x},t)} \left(\nabla\Phi(\mathbf{x},z,t)\right)^2 dz d\mathbf{x}, \tag{1.30b}$$
$$V = \frac{1}{2} g \int_X \eta(\mathbf{x},t)^2 d\mathbf{x}. \tag{1.30c}$$

In order to verify the Hamiltonian structure of Eqs. (1.26), (1.27), via the DtN formalism, we shall start by expressing the kinetic energy functional K in terms of η and ψ. We assume for simplicity an horizontally unbounded fluid, $X = \mathbb{R}^2$. Using Green's identity in conjunction with the definition of DtN operator, Eqs. (1.22), (1.23), we have

$$K[\eta,\psi] = \frac{1}{2}\int_X \psi\, G[\eta,h]\psi \, d\mathbf{x}. \tag{1.31}$$

It turns out that the computation of the variation of $K[\eta,\psi]$ requires the derivative of the DtN operator $G[\eta,h]\psi$ with respect to the free surface elevation η. This derivative, also called *shape derivative*, was calculated in (Lannes 2005, Th. 3.20):

Theorem 1.1. *The mapping $\eta \mapsto G[\eta,h]\psi$ is well defined, differentiable and for all $\delta\eta$ one has*

$$\delta_\eta G[\eta,h]\psi\cdot\delta\eta = -G[\eta,h]\left(\frac{G[\eta,h]\psi + \nabla_{\mathbf{x}}\eta\cdot\nabla_{\mathbf{x}}\psi}{|\nabla_{\mathbf{x}}\eta|^2+1}\delta\eta\right) - \nabla_{\mathbf{x}}\cdot\left[\left(\nabla_{\mathbf{x}}\psi - \frac{G[\eta,h]\psi + \nabla_{\mathbf{x}}\eta\cdot\nabla_{\mathbf{x}}\psi}{|\nabla_{\mathbf{x}}\eta|^2+1}\nabla_{\mathbf{x}}\eta\right)\delta\eta\right]. \tag{1.32}$$

Applying Theorem 1.1, it was shown in the master thesis (Papoutsellis 2012) that

Lemma 1.1. *The first variation of the kinetic energy functional $K[\eta,\psi]$ in the direction $\delta\eta$ reads*

$$\delta_\eta K[\psi,\eta;\delta\eta] = \int_X \left\{ \frac{1}{2}|\nabla_{\mathbf{x}}\psi|^2 - \frac{\left(G[\eta,h]\psi + \nabla_{\mathbf{x}}\psi\cdot\nabla_{\mathbf{x}}\eta\right)^2}{2\left(|\nabla_{\mathbf{x}}\eta|^2+1\right)} \right\} \delta\eta \, d\mathbf{x}.$$

Proof. A straightforward calculation and application of Theorem 1.1 yields

$$\begin{aligned}
\delta_\eta K[\psi,\eta;\delta\eta] =& \frac{1}{2}\int_X \psi \, \left(\delta_\eta G[\eta,h]\psi\cdot\delta\eta\right) d\mathbf{x} \\
=& \frac{1}{2}\int_X \Bigg\{ -\psi\, G[\eta,h]\left(\frac{G[\eta,h]\psi + \nabla_{\mathbf{x}}\eta\cdot\nabla_{\mathbf{x}}\psi}{|\nabla_{\mathbf{x}}\eta|^2+1}\delta\eta\right) \\
& - \psi\,\nabla_{\mathbf{x}}\cdot\left[\left(\nabla_{\mathbf{x}}\psi - \frac{G[\eta,h]\psi + \nabla_{\mathbf{x}}\eta\cdot\nabla_{\mathbf{x}}\psi}{|\nabla_{\mathbf{x}}\eta|^2+1}\nabla_{\mathbf{x}}\eta\right)\delta\eta\right] \Bigg\} d\mathbf{x}.
\end{aligned}$$

Using the self-adjointness of $G\,[\eta,h]$ for the first term and integration by parts for the second we obtain

$$\begin{aligned}
\delta_\eta K[\psi,\eta;\delta\eta] =& \frac{1}{2}\int_X \Bigg\{ -G[\eta,h]\psi\frac{G[\eta,h]\psi + \nabla_{\mathbf{x}}\eta\cdot\nabla_{\mathbf{x}}\psi}{|\nabla_{\mathbf{x}}\eta|^2+1} \\
& + \nabla_{\mathbf{x}}\psi\cdot\left[\nabla_{\mathbf{x}}\psi - \frac{G[\eta,h]\psi + \nabla_{\mathbf{x}}\eta\cdot\nabla_{\mathbf{x}}\psi}{|\nabla_{\mathbf{x}}\eta|^2+1}\nabla_{\mathbf{x}}\eta\right] \Bigg\}\delta\eta d\mathbf{x},
\end{aligned}$$

and after some algebra we obtain the result. □

Taking the variational derivatives of the Hamiltonian $\mathscr{H}[\eta,\psi]$ and using the above lemma one easily verifies that the Hamiltonian equations (1.29) are identical to Eqs. (1.26) and (1.27). This derivation has been recently extended in the moving bottom case in (Mélinand 2015).

The above Hamiltonian structure brings out the fact that free surface waves are essentially fields on the dimensionally reduced $(\mathbf{x},t)$ space. The evolution of the canonical functional variables (η,ψ) is naturally constrained by the kinematics of the interior flow, encoded in the definition of the DtN operator $G[\eta,h]\psi$. During the evolution, the only information required from the solution of the full boundary value problem (1.23) is the action of $G[\eta,h]$ on ψ. Thus, the water waves system (1.26), (1.27) evolves in time, given a procedure that determines $G[\eta,h]\psi$ at any t.

Chapter 2

Rapidly convergent series expansion of smooth functions defined on a non-planar strip

Strip-like domains, i.e., domains delimited in one direction by a pair of surfaces, are encountered in many physical and engineering applications. Apart from free surface waves in water of finite depth, which is the subject of this thesis, prominent examples are sound waves in nearshore sea environments, acoustic waves in non-uniform ducts, electromagnetic waves in curved or varying cross-section, etc. Very often, the mathematical formulation of these problems, involves a boundary value problem on a highly non-uniform strip-like domain whose horizontal extent is much larger than the vertical one, and in general contains a large number of wavelengths of the underlying wave-field. Apparently, this makes the implementation of direct numerical methods (e.g., boundary-element method) very demanding. On the other hand, if the domain is (or can be simplified to) a uniform strip, then usually the method of separation of variables provides us with an analytical or semi-analytical solution in the form of eigenfunctions expansions. Motivated by this fact, various authors introduced solution techniques, based on the approximation of the unknown field, say $\Phi(\mathbf{x}, z, t)$ defined on the domain $D_h^\eta(X)$, by a series representation (or a finite-series ansatz) of the form

$$\Phi(\mathbf{x}, z, t) = \sum_n \varphi_n(\mathbf{x}, t) Z_n(z; \mathbf{x}, t). \tag{2.1}$$

In (2.1), the functions $\{Z_n\}_n$ are prescribed functions of the transverse direction which can possibly depend on $(\mathbf{x}, t)$ while $\{\varphi_n\}_n$ are unknown functions that must be determined. As a rule, $\{Z_n\}_n$ are defined by means of a vertical (transverse) Sturm-Liouville problem, obtained by separation of variables in a uniform strip $\{-h_0 < z < 0\}$, adapted to the interval $-h(\mathbf{x}) \le z \le \eta(\mathbf{x}, t)$ (the so called *reference waveguide* at $(\mathbf{x}, t)$, (Brekhovskikh & Godin 1992, Sec. 7.1)). In this connection, the functions Z_n are also called *local modes*, and the series (2.1) is referred to as the *local-mode*

series expansion. Elaborating this series representation in conjunction with the mathematical formulation of the wave propagation problem under study, one can derive horizontal differential equations that determine the modal amplitudes $\varphi_n = \varphi_n(\mathbf{x}, t)$. This technique, usually called *coupled-mode theory* (CMT) or *coupled-mode method* (CMM) in the relevant literature, aims at a dimensional reduction of the original wave propagation problem and, provided that the required number of modes for a satisfactory solution is small, it offers a promising solution method. The origin of CMT goes back to early 50s, first appearing in the context of electromagnetic (Stevenson 1951*a*), and acoustic (Stevenson 1951*b*) waveguides of varying cross sections (horns). Since then, CMT has been applied to the study of various types of waveguides : microwave and optical waveguides (sometimes under the name generalized telegraphist's equations) (Huang 1994, Barybin & Dimitriev 2002, Dusseaux & Faure 2008); duct acoustics (horns) (Bi et al. 2007, Mercier & Maurel 2013, Maurel et al. 2014); duct acoustics with mean flow (Mercier & Maurel 2015); hydroacoustics (Brekhovskikh & Godin 1992, Sec. 7.1), (Mcdonald 1996, Belibassakis et al. 2014, Stotts & Koch 2015, Pannatoni 2016); seismology and geophysics (Maupin 1988, Harris & Block 2005); water waves (Massel 1993, Porter & Staziker 1995, Chamberlain & Porter 1995, Athanassoulis & Belibassakis 1999, 2000, Belibassakis et al. 2001, Athanassoulis & Belibassakis 2007, Belibassakis et al. 2011, Belibassakis & Athanassoulis 2011); hydroelasticity (Belibassakis & Athanassoulis 2006).

Expansion (2.1) can be viewed in two different perspectives: either as a convenient ansatz, used to obtain an approximate reformulation of the full problem, or as an exact, convergent series expansion of the looked-for field Φ, enabling an exact reformulation of the full problem in terms of the local amplitudes $\{\varphi_n\}_n$. In this thesis we focus on the second approach, which was initiated heuristically by Athanassoulis and Belibassakis in late 90's, in the context of water waves (Athanassoulis & Belibassakis 1998, 1999, 2000). The medium can be nonhomogeneous, and the wave equation can be quite general, covering all cases mentioned above. To avoid technical difficulties, we assume that the medium parameters do not exhibit discontinuities, that is, no interfaces with matching conditions are present. Nevertheless, the approach presented herein seems also to be applicable to problems with interfaces, which are common in geophysical applications; see e.g. (Belibassakis & Athanassoulis 2006, Belibassakis et al. 2014), where promising first results have been obtained for such problems, even without rigorous proofs concerning convergence.

A known deficiency in the application of the conventional CMT in non-uniform waveguides is that the vertical functions $Z_n = Z_n(\mathbf{x}, z, t)$ inherit the boundary conditions of the reference waveguide problem, which, in general, are inconsistent with the physical boundary conditions on the wavefield Φ. The simplest inconsistent case is a Neumann condition on the surface Γ_h:

$$\partial_n \Phi \equiv |N_h|^{-1} \left(-\nabla_{\mathbf{x}} h \cdot [\nabla_{\mathbf{x}} \Phi]_{z=-h} - [\partial_z \Phi]_{z=-h} \right) = 0. \tag{2.2}$$

When $\nabla_{\mathbf{x}} h \neq 0$, Eq. (2.2) implies that $[\partial_z \Phi]_{z=-h}$ is not identically zero. However, the boundary

condition satisfied by the eigenfunctions Z_n at $z = -h$ is, most of the times, homogeneous. Many authors, in an attempt to avoid this problem, replaced the smoothly varying, nonplanar boundary by a piecewise planar (staircase) boundary; see e.g. (Smith 1983, Luo et al. 2011) for applications to acoustic problems and (Devillard et al. 1988, Seo 2014) for water-wave problems. This method may provide satisfactory solutions, at points far from the staircase boundary, for 2D and axisymmetric geometries, but becomes inappropriate for fully 3D environments and for complicated boundary conditions. (Rutherford & Hawker 1981) used perturbation theory to construct a first-order (with respect to the slop) correction to each vertical function, in the context of hydroacoustics. (Godin 1997) questioned the approach of Rutherford and Hawker, arguing that they erroneously considered a termwise differentiation of the local-mode series expansion. Although this (correct) observation is practically useless, since the termwise differentiation is inevitable in formulating any CMT, it points out the main prerequisite for developing an exact CMT: the series expansion (2.1) should be term-by-term differentiable (two times, for second-order differential operators) in order that the steps leading to a coupled-mode reformulation to be justifiable (exact).

A sufficient condition in order that the series expansion (2.1) is two times termwise differentiable is

$$\|\partial_\alpha^s (\varphi_n Z_n)\|_\infty = \max \{|\partial_\alpha^s(\varphi_n(\mathbf{x},t)Z_n(z;\mathbf{x},t))|, \quad (\mathbf{x},t) \in X \times I\} = O(n^{-2}) \tag{2.3}$$

where $\alpha \in \{t, x_1, x_2, z\}$, $s = 1, 2$, and X, I are the ranges of the parametric variables $\mathbf{x}$, t (see Section 2.1). In this work we rigorously establish a method permitting to construct a vertical basis system $\{Z_n\}_n$ such that the above criterion is satisfied for any smooth enough boundaries Γ^η, Γ_h and field Φ. The construction is based on the enhancement of the basis $\{Z_n\}_{n\in\mathbb{N}}$, provided by the reference waveguide (Sturm-Liouville) problem, by two *additional* or *boundary modes*, Z_{-2} and Z_{-1}, taking care of the boundary behavior of the field Φ on the boundaries Γ^η and Γ_h. Under these circumstances, the expansion (2.1) becomes rapidly convergent, and enables an exact semi-separation of variables for the non-separable geometries of strip-like domains with nonplanar boundaries. The CMT arising by using the enhanced coupled-mode series will be called *consistent coupled-mode theory* (CCMT) or *consistent coupled-mode method* (CCMM).

2.1 Enhanced eigenfunction expansion of smooth functions defined on a strip-like domain

In this section, we prove that a function Φ, defined on the non-uniform strip-like domain $D_h^\eta(X;t)$,

$$D_h^\eta(X) = \{(\mathbf{x}, z) \in X \times \mathbb{R} : \mathbf{x} \in X, -h(\mathbf{x}) < z < \eta(\mathbf{x}, t)\},$$

can be expanded in a rapidly convergent series of the form

$$\Phi(\mathbf{x}, z, t) = \varphi_{-2}(\mathbf{x}, t)\, Z_{-2}\left(z; \eta(\mathbf{x}, t), h(\mathbf{x})\right) + \varphi_{-1}(\mathbf{x}, t)\, Z_{-1}\left(z; \eta(\mathbf{x}, t), h(\mathbf{x})\right) + \sum_{n=0}^{\infty} \varphi_n(\mathbf{x}, t) Z_n\left(z; \eta(\mathbf{x}, t)\,, h(\mathbf{x})\right), \quad (2.4)$$

where $\{Z_n\}_{n\geq 0}$ are the eigenfunctions of a reference waveguide, and Z_{-2} , Z_{-1} are appropriately selected *boundary modes* corresponding to the two transverse non-uniform boundaries of D_h^η, Γ^η and Γ_h (see Eqs. (1.2), (1.3)). The local depth of the strip-like domain $D_h^\eta(X;t)$ is denoted by $H(\mathbf{x}, t)$, and we assume that for any $(\mathbf{x}, t) \in X \times I$,

$$H(\mathbf{x}, t) = \eta(\mathbf{x}, t) + h(\mathbf{x}) > 0.$$

For later use we also introduce the subdomains $D_h^\eta(\tilde{X}_{\text{part}})$ consisting of all points of $D_h^\eta(X)$ with $\mathbf{x} \in \tilde{X}_{\text{part}}$, $\tilde{X}_{\text{part}}$ being an open subregion, finite or infinite, of X. A scalar field $\Phi = \Phi(\mathbf{x}, z, t)$ is defined on the closed domain $\overline{D_h^\eta}(\tilde{X}_{\text{part}}) \times I$, where and $I = [t_0, t_1]$. Smoothness conditions on the field Φ and the boundaries Γ^η, Γ^h will be introduced subsequently.

The reference waveguide and the boundary modes

The reference waveguide or local vertical Sturm-Liouville problem, is chosen as follows

$$\partial_z^2 Z_n + \left(k_n^2 - Q(\mathbf{x}, z)\right) Z_n = 0, \quad z \in (-h(\mathbf{x}), \eta(\mathbf{x}, t)), \quad (2.5a)$$

$$\mathscr{B}_\eta Z_n \equiv \left[\partial_z Z_n - \mu_0 Z_n\right]_{z=\eta} = 0, \quad (2.5b)$$

$$\mathscr{B}_h Z_n \equiv \left[\partial_z Z_n\right]_{z=-h} = 0. \quad (2.5c)$$

where $Q(\mathbf{x}, z)$ is a bounded, smooth function[1], and μ_0 is a real constant. The eigensystem $\{k_n, Z_n,\ n \geq 0\}$ of the reference waveguide (2.5) is dependent on μ_0, $Q(\mathbf{x}, z)$ and the ends of the vertical interval $\eta = \eta(\mathbf{x}, t)$, $h = h(\mathbf{x}, t)$ for any $(\mathbf{x}, t) \in X \times \mathbb{R}$. This implies that $\{k_n, Z_n(z),\ n \geq 0\}$ are functions of $(\mathbf{x}, t)$: $k_n = k_n(\mathbf{x}, t)$ and $Z_n(z) = Z_n(z; \mathbf{x}, t)$. In the present

[1]The case where the function $Q(\mathbf{x}, z)$ exhibits discontinuities along a number of surfaces, corresponding to stratified media, is excluded from our analysis herein. The asymptotics of eigenvalues and eigenfunctions is different and more complicated in this case; see e.g., (Athanassoulis & Papanicolaou 1997).

work the eigenfunction $Z_n(z)$ are normalised so that

$$[Z_n]_{z=\eta} = 1. \tag{2.6}$$

From the general theory of Sturm-Liouville problems we recall the following well-known results, which will be used in the sequel:

(i) If the function $Q(\mathbf{x}, \cdot)$ belongs to $C^k([-h, \eta])$, then $Z_n \in C^{k+2}([-h, \eta])$.

(ii) the system of functions $\{Z_n\}_{n\in\mathbf{N}}$ forms an orthogonal basis of the space of square integrable functions, $L^2(-h, \eta)$.

(iii) For large values of n, the functions k_n, Z_n and the L^2- norm

$$\|Z_n(\mathbf{x}, \cdot, t)\|_{L^2(-h(\mathbf{x}),\eta(\mathbf{x}))} \equiv \left(\int_{-h(\mathbf{x})}^{\eta(\mathbf{x},t)} Z_n^2(\mathbf{x}, z, t)dz\right)^{1/2},$$

exhibit the following asymptotic behavior:

$$k_n(\mathbf{x}, t) = \frac{n\pi}{H(\mathbf{x}, t)} + \frac{O(1)}{n} = O(n), \tag{2.7a}$$

$$Z_n(\mathbf{x}, z, t) = \frac{\cos(k_n(z + h))}{\cos(k_n H(\mathbf{x}, t))} + \frac{O(1)}{n} = O(1), \tag{2.7b}$$

$$||Z_n||^2_{L^2(-h,\eta)} = \frac{H(\mathbf{x}, t)}{2} + \frac{O(1)}{n} = O(1), \tag{2.7c}$$

Asymptotic results (2.7) are classical and can be found in various books; see, e.g., (Birkhoff & Rota 1989, Chapter 10). It is worth noting that the leading-order asymptotic terms, shown in Eqs. (2.7), are not dependent on the coefficient function $Q(\mathbf{x}, z)$; they are only dependent on the boundary points η and h, revealing the critical role played by the latter on the asymptotics and, through them, on the rate of convergence of the expansion (2.4), as we shall see in the sequel.

The additional vertical functions, or boundary modes, Z_{-2} and Z_{-1}, are associated with the free surface Γ_η and bottom Γ_h respectively and are defined so that the enhanced representation (2.4) to be able to recover the non-identically vanishing values $\mathscr{B}_\eta\Phi$ and $\mathscr{B}_h\Phi$ (compare with Eqs. (2.5b) and (2.5c)). In this connection, Z_{-2} and Z_{-1}, are selected to be smooth functions satisfying the following boundary conditions

$$[Z_{-2}]_{z=\eta} = 1, \qquad [Z_{-1}]_{z=\eta} = 1, \tag{2.8a}$$

$$\mathscr{B}_\eta Z_{-2} = 1/h_0, \quad \mathscr{B}_h Z_{-1} = 0, \tag{2.8b}$$

$$\mathscr{B}_h Z_{-2} = 0, \qquad \mathscr{B}_h Z_{-1} = 1/h_0, \tag{2.8c}$$

where the constant h_0 (reference depth) is introduced for dimensional consistency. Conditions (2.8a) serve for normalization (compare with Eq. (2.6)), while conditions (2.8b) and (2.8c) are

imposed in order to separate the influence of the two boundary modes Z_{-2}, Z_{-1}; the former will act on the free surface but not on the bottom, and the latter inversely. Among the infinite possible choices, we pick out the one corresponding to the least degree polynomials in the vertical variable z [2]. Then, we easily find

$$Z_{-2} = \frac{\mu_0 h_0 + 1}{2h_0}\frac{(z+h)^2}{\eta+h} - \frac{\mu_0 h_0 + 1}{2h_0}(\eta + h) + 1, \tag{2.9a}$$

$$Z_{-1} = \frac{\mu_0 h_0 - 1}{2h_0}\frac{(z+h)^2}{\eta+h} + \frac{1}{h_0}(z+h) - \frac{\mu_0 h_0 + 1}{2h_0}(\eta + h) + 1. \tag{2.9b}$$

Smoothness conditions on the field to be expanded and the boundaries

Definition 2.1 (Vertical Smoothness Condition)**.** *A function $F(\mathbf{x}, z, t)$, defined on $\bar{D}_h^\eta \times I$, considered as a function of z at a specific point $(\mathbf{x}, t) \in X \times I$, will be denoted as $F(\mathbf{x}, \cdot, t)$. We shall say that $F(\mathbf{x}, \cdot, t)$ satisfies a local vertical smoothness condition* VSC$(k; \mathbf{x}, t)$ *if $F(\mathbf{x}, \cdot, t) \in H^k(-h(\mathbf{x}), \eta(\mathbf{x}, t))$ where $H^k(-h(\mathbf{x}), \eta(\mathbf{x}, t))$ is the standard Sobolev space of functions defined on the interval; see* (Brezis 2011, Chapter 8). $\tilde{X}_{\text{part}}$ may be replaced by X if the uniform boundedness of the Sobolev norm holds true in X.

It is recalled that $H^k(-h, \eta)$ is continuously embedded in $C^{k-1}([-h, \eta])$ ((Brezis 2011, p. 217)), which ensures that the boundary values of the vertical derivatives $\partial_z^m F(\mathbf{x}, z, t)$, at $z = \eta$ and $z = -h$ are well-defined and bounded for $0 \le m \le k-1$.

In studying the $(\mathbf{x}, t)$ differentiability of the enhanced series expansion (2.4) (in Section 2.3), smoothness conditions will also be required for the functions $\eta(\mathbf{x}, t)$ and $h(\mathbf{x})$, that parametrize the vertical boundary surfaces Γ^η and Γ_h. As in the case of field functions, we distinguish between local and uniform boundary smoothness conditions.

Definition 2.2 (Boundary Smoothness Condition)**.** *We shall say that the functions $\eta(\mathbf{x}, t)$ and $h(\mathbf{x})$ (or the boundaries Γ^η, Γ_h) satisfy a local boundary smoothness condition* BSC$(\mathbf{x}, t)$ *if $\partial_t \eta$, $\partial_{x_i}\eta$, $\partial_{x_i}^2\eta$ and $\partial_{x_i}h$, $\partial_{x_i}^2 h$ exist at $(\mathbf{x}, t) \in X \times I$. Further, we shall say that $h(\mathbf{x})$, $\eta(\mathbf{x}, t)$ satisfy a uniform boundary smoothness condition* BSC$(\tilde{X}_{part} \times I)$ *if the local* BSC$(\mathbf{x}, t)$ *holds true for all $(\mathbf{x}, t) \in \tilde{X}_{part} \times I$, and the norms $\|\eta\|_{C^1(X_{part} \times I)}$, $\|\eta(\cdot, t)\|_{C^2(X_{\text{part}})}$, $\|h\|_{C^2(X_{part})}$ are uniformly bounded in I. ($\tilde{X}_{part}$ may be replaced by X if the stated conditions hold true on X).*

The fundamental expansion theorem

Theorem 2.1. *Assume that $\Phi(\mathbf{x}, \cdot, t)$ satisfy the* VSC$(k = 2; \mathbf{x}, t)$*. Then, the quantities*

$$\varphi_{-2}(\mathbf{x}, t) = h_0 \mathscr{B}^\eta \Phi, \qquad \varphi_{-1}(\mathbf{x}, t) = h_0 \mathscr{B}_h \Phi \tag{2.10a, b).}$$

[2] Other choices are also possible without affecting the validity of our results.

and

$$\Phi^*(\mathbf{x}, z, t) = \Phi(\mathbf{x}, z, t) - \varphi_{-2}(\mathbf{x}, t)Z_{-2} - \varphi_{-1}(\mathbf{x}, t)Z_{-1} \tag{2.11}$$

are well-defined, and

(i) *The series expansion* (2.4) *converges uniformly on* $[-h(\mathbf{x}), \eta(\mathbf{x}, t)]$*, and the modal amplitudes* $\varphi_n = \varphi_n(\mathbf{x}, t)$*,* $n \geq 0$ *are given by*

$$\varphi_n = \|Z_n\|_{L^2}^{-2} \int_{-h}^{\eta} \Phi^* Z_n dz, \quad n \geq 0. \tag{2.12}$$

(ii) *If* $Q(\mathbf{x}, \cdot) \in C^2([-h, \eta])$*, the modal amplitudes* φ_n *satisfy the following local asymptotic estimate (with respect ot* n*)*

$$|\varphi_n| \leq A(\mathbf{x}, t)\, n^{-2}. \tag{2.13}$$

(iii) *If* $Q(\mathbf{x}, \cdot) \in C^4([-h, \eta])$ *and* Φ *satisfies the* VSC$(k = 4; \mathbf{x}, t)$*, then the asymptotic estimate* (2.13) *is improved to*

$$|\varphi_n| \leq A_2(\mathbf{x}, t)\, n^{-4}. \tag{2.14}$$

The latter estimate cannot be improved further under the present choice of the boundary modes.

Proof. The modal amplitudes φ_{-2} and φ_{-1} are well-defined since from our smoothness assumptions $\Phi(\mathbf{x}, \cdot, t) \in H^2(-h(\mathbf{x}, t), \eta(\mathbf{x}, t))$. It follows directly that $\Phi^*(\mathbf{x}, \cdot, t)$ is also well-defined.

(i) Applying the boundary operators $\mathscr{B}^\eta$ and $\mathscr{B}_h$ to both members of Eq. (2.11) and taking into account the boundary conditions of Z_{-2} and Z_{-1}, (2.8b) and (2.8c), we readily find that $\mathscr{B}^\eta \Phi^* = \mathscr{B}_h \Phi^* = 0$. Thus, $\Phi^*(\mathbf{x}, \cdot, t)$ satisfies the same vertical boundary conditions as the eigenfunctions $\{Z_n\}_{n \geq 0}$, of the regular Sturm-Liouville problem (2.5). Consequently, by standard Sturm-Liouville theory (see e.g. (Coddington & Levinson 1955, Theorem 4.1)), the function Φ^* admits of a uniformly convergent series expansion

$$\Phi^*(\mathbf{x}, z, t) = \sum_{n=0}^{\infty} \varphi_n(\mathbf{x}, t) Z_n\left(z; \eta(\mathbf{x}, t), h(\mathbf{x})\right), \tag{2.15}$$

where φ_n are given by Eqs. (2.12). Substituting the above series expansion of Φ^* in Eq. (2.11), and solving for Φ, we obtain the series expansion (2.4), having already established its uniform convergence.

(ii) Using the Sturm-Liouville differential equation (2.5a), the modal amplitudes φ_n (defined

by Eqs. (2.12)), are equivalently written as

$$\varphi_n = \|Z_n\|_{L^2}^{-2} k_n^{-2} \int_{-h}^{\eta} Q_n^* \Phi^* \partial_z^2 Z_n dz, \quad n \geq 0, \tag{2.16}$$

with

$$Q_n^* = \left(1 - \frac{Q(\mathbf{x}, z)}{k_n^2}\right)^{-1}. \tag{2.17}$$

The assumption $Q(\mathbf{x}, \cdot) \in C_b(D_h^\eta)$, implies that the sequence $\{Q_n^*\}_{n\geq 0}$, is well defined, continuous and bounded for large values of n and satisfies the estimates

$$|Q_n^*(\mathbf{x}, z)| \leq A_0 = O(1), \quad \text{for all} \quad z \in [-h, \eta], \tag{2.18a}$$

$$|\partial_z^m Q_n^*(\mathbf{x}, z)| \leq A_m \frac{\|Q(\mathbf{x}, \cdot)\|_{C^m}}{k_n^2} = O(n^{-2}), \quad \text{for all} \quad z \in [-h, \eta], \tag{2.18b}$$

which are proved in Appendix A (see Proposition A.1). Under the present assumptions, $\Phi^* \in H^2(-h(\mathbf{x}), \eta(\mathbf{x}, t))$, thus, after performing two integration by parts, Eq. (2.16) takes the form

$$\varphi_n = k_n^{-2} \|Z_n\|_{L^2}^{-2} \left([Q_n^* \Phi^* \partial_z Z_n]_{-h}^{\eta} - [\partial_z (Q_n^* \Phi^*) Z_n]_{-h}^{\eta} + \int_{-h}^{\eta} \partial_z^2 (Q_n^* \Phi^*) Z_n dz \right). \tag{2.19}$$

The boundary terms in the parenthesis, in the right-hand side of Eq. (2.19), can be written as

$$[Q_n^* \Phi^* \partial_z Z_n]_{-h}^{\eta} - [Q_n^* \partial_z \Phi^* Z_n]_{-h}^{\eta} - [\partial_z Q_n^* \Phi^* Z_n]_{-h}^{\eta} = - [\partial_z Q_n^* \Phi^* Z_n]_{-h}^{\eta}, \tag{2.20}$$

since the first two of them cancel out because of the boundary conditions $\mathscr{B}^\eta \Phi^* = \mathscr{B}_h \Phi^* = 0$. The right-hand side of the above equation has the following asymptotic behaviour, obtained by using Eqs. (2.6), (2.7b) and (2.18b) (for $m = 1$), applied for $z = \eta$ and $z = -h$:

$$[\partial_z Q_n^* \Phi^* Z_n]_{-h}^{\eta} = [\partial_z Q_n^* \Phi^* Z_n]_{z=\eta} - [\partial_z Q_n^* \Phi^* Z_n]_{z=-h} = O(k_n^2). \tag{2.21}$$

Using Eqs. (2.20) and (2.21), we write Eq. (2.19) in the form

$$\varphi_n = k_n^{-2} \|Z_n\|_{L^2}^{-2} \left(O(k_n^{-2}) + \int_{-h}^{\eta} \partial_z^2 (Q_n^* \Phi^*) Z_n dz \right), \tag{2.22}$$

thus, it remains to estimate the integral appearing in the above right hand side. This is easily done by means of the inequality

$$\int_{-h}^{\eta} \partial_z^2 (Q_n^* \Phi^*) Z_n dz \leq 2 \|Q_n^*\|_{C^2} \|\Phi_n^*\|_{H^2} \|Z_n\|_{L^2}, \tag{2.23}$$

which is proved in Appendix A; see Proposition A.2 for details. Now, using the estimates

$\|Q_n^*\|_{C^2} = 1 + O(n^{-2})$, $\|Z_n\|_{L^2} = O(1)$ and $\|\Phi^*\|_{H^2} = O(1)$, we conclude that the above integral is bounded, hence, Eq. (2.22), in conjunction with (2.7a), yields (2.13).

(iii) Substituting Z_n in Eq. (2.19), by $k_n^{-2} Q_n^* \partial_z^2 Z_n$ (see Eq. (2.5a)), we obtain

$$\varphi_n = k_n^{-4} \|Z_n\|_{L^2}^{-2} \left(O(1) + \int_{-h}^{\eta} \partial_z^2 (Q_n^* \Phi^*) \partial_z^2 Z_n dz \right). \tag{2.24}$$

Thus, in order to prove estimate (2.14), we need to prove that the integral appearing in the parenthesis of the above equation is $O(1)$. Under the assumptions $Q(\mathbf{x}, \cdot) \in C^4([-h, \eta])$ and $\Phi^*(\mathbf{x}, \cdot, t) \in H^4(-h, \eta)$, it is legitimate to perform two integrations by parts, obtaining

$$\begin{aligned} &\int_{-h}^{\eta} \partial_z^2 (Q_n^* \Phi^*) \partial_z^2 Z_n dz = \\ &= \left[Q_n^* \partial_z^2 (Q_n^* \Phi^*) \partial_z Z_n \right]_{-h}^{\eta} - \left[\partial_z \left(Q_n^* \partial_z^2 (Q_n^* \Phi^*) \right) Z_n \right]_{-h}^{\eta} + \int_{-h}^{\eta} \partial_z^2 \left(Q_n^* \partial_z^2 (Q_n^* \partial_z^2 \Phi^*) \right) Z_n dz. \end{aligned} \tag{2.25}$$

Expanding the derivatives appearing above, and using the estimates (2.7b) and (2.18), we find that the boundary terms in the right hand side of Eq. (2.25) are of order $O(1)$. Further, the last integral term of Eq. (2.25) satisfies the inequality

$$\int_{-h}^{\eta} \partial_z^2 \left(Q_n^* \partial_z^2 (Q_n^* \Phi^*) \right) Z_n dz \leq 13 \|Q_n^*\|_{C^4} \|\Phi^*\|_{H^4} \|Z_n\|_{L^2}, \tag{2.26}$$

which is proved in Appendix A; see Proposition A.3. Since $\|Q_n^*\|_{C^2} = 1 + O(n^{-2})$, $\|Z_n\|_{L^2} = O(1)$ and $\|\Phi^*\|_{H^2} = O(1)$, the right hand side of the above inequality is bounded, and the estimate (2.14) is readily obtained from Eq. (2.24).

The estimate (2.14), asserted in (iii), cannot be improved further because of the presence of the boundary terms in the right-hand side of Eq. (2.24). These terms are non-zero even for the simplest reference waveguide, with $Q(\mathbf{x}, z) = 0$ in Eq. (2.5a), which results in $Q_n^*(\mathbf{x}, z) = 1$. Indeed, in this simplest case, Eq. (2.24) simplifies to

$$\varphi_n = -k_n^{-4} \|Z_n\|_{L^2}^{-2} \left(\int_{-h}^{\eta} \partial_z^2 \Phi^* \partial_z^2 Z_n dz \right), \tag{2.27}$$

which, after the substitution $Z_n = -k_n^2 \partial_z^2 Z_n$ and two integration by parts, takes the form

$$\varphi_n = -k_n^{-4} \|Z_n\|_{L^2}^{-2} \left(\left[\partial_z^2 \Phi^* \partial_z Z_n \right]_{-h}^{\eta} - \left[\partial_z^3 \Phi^* Z_n \right]_{-h}^{\eta} + \int_{-h}^{\eta} \partial_z^4 \Phi^* Z_n dz \right). \tag{2.28}$$

It is now clear that the boundary terms in the right hand side of Eq. (2.28) cannot be zero, as far as $\partial_z^2 \Phi^*$, $\partial_z^3 \Phi^*$ are free of any restrictions concerning their boundary values. Thus, even if Φ is smoother, e.g. $\Phi(\mathbf{x}, \cdot, t) \in H^6([-h, \eta])$, in which case the last (integral) term in the right-hand side of Eq. (2.28) can be reformulated, by using once again the relation $Z_n = -k_n^2 \partial_z^2 Z_n$, and

becomes $O(n^{-2})$, the presence of the boundary values of $\partial_z^2\Phi^*$, $\partial_z^3\Phi^*$, blocks the order of $\varphi_n(\mathbf{x},t)$ to $O(n^{-4})$. □

Corollary 2.1. *If $\Phi(\mathbf{x},\cdot,t)$ satisfies the uniform* VSC$(k=2;\tilde{X}_{\text{part}})$*, then the series expansion (2.4) is uniformly convergent in the subdomain $\overline{D_h^\eta}(\tilde{X}_{\text{part}})$, and the estimate (2.13) is uniform in $\tilde{X}_{\text{part}}\times I$, that is $\|\varphi_n\|_{\infty,\,\tilde{X}_{\text{part}}\times I}=O(n^{-2})$. Further, if $\Phi(\mathbf{x},\cdot,t)$ satisfies the stronger uniform* VSC$(k=4;\tilde{X}_{\text{part}})$*, then the estimate (2.14) becomes uniform in $\tilde{X}_{\text{part}}\times I$, which implies that $\|\varphi_n\|_{\infty,\,\tilde{X}_{\text{part}}\times I}=O(n^{-4})$.*

Remark 2.1. Theorem 2.1 was first announced in (Athanassoulis & Belibassakis 2003) for a flat upper boundary, and a proof of assertion (i) for the case $Q(\mathbf{x},z)=0$, and under more restrictive assumptions for the field Φ and the boundaries η and h, was presented in (Belibassakis & Athanassoulis 2006).

Remark 2.2. The validity of Theorem 2.1 is not affected by the values of the parameters μ_0 and h_0, or by the choice of the additional functions Z_{-2} and Z_{-1} as far as the conditions (2.8b) and (2.8c) hold true.

Remark 2.3. According to assertions (i) and (ii) of Theorem 2.1, a function $\Phi(\mathbf{x},\cdot,t)\in H^2(-h(\mathbf{x}),\eta(\mathbf{x},t))$ is expanded as a uniformly convergent series

$$\Phi=\mathscr{B}^\eta\Phi Z_{-2}+\mathscr{B}_h\Phi Z_{-1}+\sum_{n=0}^{\infty}\frac{k_n^2}{\|Z_n\|_{L^2}^2}\int_{-h}^{\eta}\left(\Phi-\mathscr{B}^\eta\Phi Z_{-2}-\mathscr{B}_h\Phi Z_{-1}\right)Z_n dz\frac{Z_n}{k_n^2}.$$

It can be proved that, the system

$$\left\{Z_{-2},Z_{-1},\left\{Z_n/k_n^2\right\}_{n=0}^{\infty}\right\}\in H^2(-h(\mathbf{x}),\eta(\mathbf{x},t)),\tag{2.29}$$

is a Riesz basis of the Sobolev space $H^2(-h(\mathbf{x}),\eta(\mathbf{x},t))$. The proof follows the ideas of (Russel 1982) and will be presented in detail elsewhere.

2.2 The $(\mathbf{x},t)$ derivatives of the eigensystem

The purpose of this section, is the calculation of the $(\mathbf{x},t)-$ derivatives of the eigensystem $\{k_n,Z_n\}$ for $n\geq 0$ as well as the determination of their asymptotic behavior for large values of n, which is crucial for the study of the convergence properties of the expansion (2.4). Calculations for $n=-2,-1$ are more straightforward (Z_{-2} and Z_{-1} depend only on η and h) and are postponed to Appendix B. For $n\geq 0$, special attention is required since k_n, $n\geq 0$ are defined implicitly in terms of the $(\mathbf{x},t)$ functions η and h that parametrize the boundaries. In order to proceed with the calculations pf the $(\mathbf{x},t)$-derivatives, we need the first and second Fréchet (shape) derivatives of the eigensystem $\{k_n,Z_n\}$ with respect to h and η. For example, the first $a-$ derivative, where

a stands for t, x_i, $i = 1, 2$, is written as

$$\partial_a Z_n(z; \mathbf{x}, t) = \partial_\eta Z_n(z; \eta, h)\partial_a \eta(\mathbf{x}, t) + \partial_h Z_h(z; \eta, h)\partial_a h(\mathbf{x}), \tag{2.30}$$

where $\partial_\eta Z_n$ and $\partial_h Z_n$ denote the aforementioned Fréchet derivatives. Unfortunately, their calculation for eigensystems of a general regular Sturm-Liouville problem seems to be an open problem in the mathematical literature, with the notable exception of the first Fréchet derivative of the eigenvalues. The latter problem has been first addressed by Dauge and Helffer in 1993 (Dauge & Helffer 1993), and studied further by various authors (Kong & Zettl 1999, Zettl 2005). We shall content ourselves, from now on, to a constant-parameter reference waveguide, for which the eigenvalues are defined by solving a transcendental equation, and the eigenfunctions are expressed in closed forms in terms of η, h and $k_n(\eta, h)$. For simplicity, and having in mind applications to the nonlinear water waves problem over variable bathymetry (Chapter 3.3), we shall consider the Sturm-Liouville problem (2.5) with $Q(\mathbf{x}, z) = 0$.

$$\partial_z^2 Z_n + k_n^2 Z_n = 0, \quad -h(\mathbf{x}) < z < \eta(\mathbf{x}, t), \tag{2.31a}$$

$$\mathscr{B}_\eta Z_n \equiv [\partial_z Z_n - \mu_0 Z_n]_{z=\eta} = 0, \tag{2.31b}$$

$$\mathscr{B}_h Z_n \equiv [\partial_z Z_n]_{z=-h} = 0. \tag{2.31c}$$

The above problem will be referred to as the *water-wave reference waveguide*. For any $(\mathbf{x}, t)$, the functions $\{ik_0, k_n, n \geq 1\}$ (also called local wave numbers), are defined as roots of the transcendental equations

$$\mu_0 - k_0 \tanh(k_0 H) = 0, \tag{2.32a}$$

$$\mu_0 + k_n \tan(k_n H) = 0, \tag{2.32b}$$

where $H = \eta + h$, and the corresponding eigenfunctions, normalized so that $[Z_n]_{z=\eta} = 1$, are given by the formulae

$$Z_0(z; \eta, h) = \frac{\cosh[k_0(z+h)]}{\cosh[k_0(\eta+h)]}, \tag{2.33a}$$

$$Z_n(z; \eta, h) = \frac{\cos[k_n(z+h)]}{\cos[k_n(\eta+h)]}. \tag{2.33b}$$

At this point, attention should be drawn to the fact that the transcendental equations (2.32) cannot be solved explicitly for $k_n(H)$. However, as shown in the following proposition, the derivatives of the mapping $k_n(H)$ are expressed, via the implicit function theorem, in terms of k_n itself, making possible the determination of their asymptotic behaviour.

Proposition 2.1. *For $n \geq 1$ the first and second derivatives of $k_n(H)$ are given by the following*

equations, and exhibit the asymptotic behaviour indicated therein:

$$\partial_H k_n = -\frac{k_n^2+\mu_0^2}{-\mu_0+H(k_n^2+\mu_0^2)}\,k_n = O(n), \tag{2.34}$$

$$\partial_H^2 k_n = 2\partial_H k_n\left(-\mu_0+\frac{\partial_H k_n}{k_n}(1-H\mu_0)\left(2+H\frac{\partial_H k_n}{k_n}\right)\right) = O(n). \tag{2.35}$$

Further, by the chain rule we obtain

$$\partial_a k_n = \partial_H k_n \partial_a H = O(n), \tag{2.36}$$

$$\partial_{x_i}^2 k_n = \partial_H^2 k_n (\partial_{x_i} H)^2 + \partial_H k_n (\partial_{x_i}^2 H) = O(n), \tag{2.37}$$

Proof. The first equalities appearing in (2.34) and (2.35) are obtained by applying the implicit function theorem to the transcendental Eq. (2.32b). The estimates appearing in the second equalities of (2.34) and (2.35) are obtained by invoking the estimate $k_n = O(n)$, Eq.(2.7a). We give the details bellow.

Setting $G_n(H,k_n) = \mu_0 + k_n\tan(k_nH)$, the local dispersion relation (2.32b), implicitly defining the function $k_n = k_n(H)$, is written in the form $G_n(H,k_n) = 0$. Then, the implicit function theorem yields the following relations

$$\partial_H k_n = -\frac{\partial_H G_n}{\partial_{k_n} G_n}, \tag{2.38}$$

$$\partial_H^2 k_n = -\frac{\partial_H^2 G_n + 2(\partial_{Hk_n} G_n)\partial_H k_n + \partial_{k_n}^2 G_n (\partial_H k_n)^2}{\partial_{k_n} G_n}, \tag{2.39}$$

which can be used for the calculation of $\partial_H k_n$ and $\partial_H^2 k_n$. By straightforward differentiation we find

$$\partial_H G_n = k_n^2 \sec^2(k_nH), \tag{2.40a}$$

$$\partial_{k_n} G_n = \tan(k_nH) + k_nH\sec^2(k_nH), \tag{2.40b}$$

which, in conjunction with Eq. (2.38), yields

$$\partial_H k_n = -\frac{k_n^2\sec^2(k_nH)}{\tan(k_nH)+k_nH\sec^2(k_nH)}. \tag{2.41}$$

Eliminating the trigonometric functions in the right-hand side of the above equation, by using Eq. (2.32b) and the identity $1+\tan^2 a = \sec^2 a$, Eq. (2.41) takes the form

$$\partial_H k_n = -\frac{k_n\,(k_n^2+\mu_0^2)}{-\mu_0+H(k_n^2+\mu_0^2)}, \tag{2.42}$$

which proves the first equality in Eq. (2.34). The second equality in Eq. (2.34), that is the

estimate $\partial_H k_n = O(n)$, follows easily from the estimate $k_n = O(n)$, Eq. (2.7a), and the following limiting relation, that follows easily from the above equation,

$$\frac{\partial_H k_n}{k_n} = -\frac{1 + \frac{\mu_0^2}{k_n^2}}{H - \frac{\mu_0 - H\mu_0^2}{k_n^2}} \xrightarrow[n\to\infty]{} -\frac{1}{H}. \tag{2.43}$$

The proof of Eq. (2.34) is now completed.

Eq. (2.35) is proved by using Eq. (2.39). Differentiating $G_n(H, k_n)$ twice and using Eq. (2.32b), and the trigonometric identity $1 + \tan^2 a = \sec^2 a$, we find

$$\partial_H^2 G_n = 2k_n^3 \sec^2(k_n H)\tan(k_n H) = -2\mu_0(k_n^2 + \mu_0^2), \tag{2.44a}$$

$$\partial_{Hk_n}^2 G_n = 2k_n \sec^2(k_n H) + 2k_n^2 H \sec^2(k_n H)\tan(k_n H) = 2\frac{k_n^2 + \mu_0^2}{k_n}(1 - H\mu_0), \tag{2.44b}$$

$$\partial_{k_n}^2 G_n = 2H \sec^2(k_n H) + 2k_n H^2 \sec^2(k_n H)\tan(k_n H) = 2H\frac{k_n^2 + \mu_0^2}{k_n^2}(1 - H\mu_0). \tag{2.44c}$$

Substituting the derivatives of $G_n(H, k_n)$ from Eqs. (2.40b) and (2.44) to Eq. (2.39), and using Eq. (2.34), we find

$$\partial_H^2 k_n = -2\partial_H k_n \left\{\mu_0 + \frac{\partial_H k_n}{k_n}(H\mu_0 - 1)\left(2 + H\frac{\partial_H k_n}{k_n}\right)\right\}, \tag{2.45}$$

which proves the first equality of Eq. (2.35). The second equality in Eq. (2.35), that is the estimate $\partial_H^2 k_n = O(n)$, follows directly from Eqs. (2.45) and (2.43), in conjunction with the already proved result $\partial_H k_n = O(n)$. This completes the proof of Proposition 2.1. □

In order to proceed with the $(\mathbf{x}, t)-$ derivatives of $Z_n = Z_n(z; \eta(\mathbf{x}, t), h(\mathbf{x}))$, it is useful to introduce the auxiliary function

$$W_n(z; \eta, h) = W_n(\mathbf{x}, z, t) = \frac{\sin[k_n(z + h)]}{\cos[k_n(\eta + h)]} = -\frac{\partial_z Z_n}{k_n}, \tag{2.46}$$

which satisfies the same differential equations as Z_n, namely $\partial_z^2 W_n = -k_n^2 W_n$. Using Eqs. (2.30), (2.32b), (2.33b) and (2.46), in conjunction with Proposition 2.1, we can prove the following

Proposition 2.2. *The space and time derivatives of the vertical functions Z_n, $n \geq 1$ are given by the following equations, and exhibit the asymptotic behaviour indicated therein*

$$\partial_a Z_n = -\left(\partial_a k_n(z + h) + k_n \partial_a h\right) W_n - \mu_0 \frac{\partial_a(k_n H)}{k_n} Z_n = O(n), \tag{2.47}$$

$$
\begin{aligned}
\Delta_{\mathbf{x}} Z_n = &- |\nabla_{\mathbf{x}} k_n|^2 (z+h)^2 Z_n - 2k_n \nabla_{\mathbf{x}} k_n \cdot \nabla_{\mathbf{x}} h (z+h) Z_n, \\
&+ \left[-k_n^2 |\nabla_{\mathbf{x}} h|^2 - |\nabla_{\mathbf{x}} (k_n H)|^2 - \mu_0 \frac{\Delta_{\mathbf{x}} (k_n H)}{k_n} + 2\mu_0^2 \frac{|\nabla_{\mathbf{x}} (k_n H)|^2}{k_n^2} \right] Z_n, \\
&- \left[\Delta_{\mathbf{x}} k_n - 2\mu_0 \frac{\nabla_{\mathbf{x}} k_n \cdot \nabla_{\mathbf{x}} (k_n H)}{k_n} \right] (z+h) W_n, \\
&+ \left[2\nabla_{\mathbf{x}} k_n \cdot \nabla_{\mathbf{x}} h + k_n \Delta_{\mathbf{x}} h - 2\mu_0 \nabla_{\mathbf{x}} h \cdot \nabla_{\mathbf{x}} (k_n H) \right] W_n = O(n^2).
\end{aligned}
\tag{2.48}
$$

Proof. The Fréchet derivatives $\partial_\eta Z_n$ and $\partial_h Z_n$, appearing in Eq. (2.30), are calculated by differentiating $Z_n(z;\eta,h)$, given by Eq. (2.33b), and they can be written as

$$
\partial_\eta Z_n = -\partial_\eta k_n (z+h) W_n + \tan(k_n H) \left(\partial_\eta k_n H + k_n \right) Z_n, \tag{2.49a}
$$

$$
\partial_h Z_n = - \left[\partial_h k_n (z+h) + k_n \right] W_n + \tan(k_n H) \left(\partial_h k_n H + k_n \right) Z_n. \tag{2.49b}
$$

where the definition of W_n, Eq. (2.46), have been used. Recalling that $k_n = k_n(\eta,h) = k_n(\eta+h) = k_n(H)$, we see that $\partial_\eta k_n = \partial_h k_n = \partial_H k_n$, which, upon substitution in Eqs. (2.49), leads to the following expressions

$$
\partial_\eta Z_n = -\partial_H k_n (z+h) W_n + \tan(k_n H) \left(\partial_H k_n H + k_n \right) Z_n, \tag{2.50a}
$$

$$
\partial_h Z_n = - \left[\partial_H k_n (z+h) + k_n \right] W_n + \tan(k_n H) \left(\partial_H k_n H + k_n \right) Z_n. \tag{2.50b}
$$

Substituting Eqs. (2.50) in Eq. (2.30), and taking into account the identities

$$
\begin{aligned}
\partial_a k_n &= \partial_\eta k_n \partial_a \eta + \partial_h k_n \partial_a h, \\
\partial_a (k_n H) &= \partial_a k_n H + k_n \partial_a H,
\end{aligned}
$$

we obtain

$$
\partial_a Z_n = - \left[\partial_a k_n (z+h) + k_n \partial_a h \right] W_n + \tan(k_n H) \partial_a (k_n H) Z_n. \tag{2.51}
$$

Then, the first equality in (2.47) is obtained after eliminating $\tan(k_n H)$ from the above equation using Eq. (2.32b), $\tan(k_n H) = -\mu_0/k_n$.

Let us now turn to the calculation of the second derivative, $\partial_{x_i}^2 Z_n$, $i = 1, 2$, which is more involved. A general formula is obtained by differentiating both members of Eq. (2.30) with respect to $a = x_i$, which reads as follows

$$
\begin{aligned}
\partial_{x_i}^2 Z_n = & \\
&= \partial_\eta^2 Z_n (\partial_{x_i} \eta)^2 + \partial_h^2 Z_n (\partial_{x_i} h)^2 + 2\partial_{\eta h} Z_n (\partial_{x_i} \eta)(\partial_{x_i} h) + \partial_\eta Z_n \partial_{x_i}^2 \eta + \partial_h Z_n \partial_{x_i}^2 h,
\end{aligned}
\tag{2.52}
$$

where the second Fréchet derivatives $\partial_\eta^2 Z_n$, $\partial_h^2 Z_n$ and $\partial_{\eta h}^2 Z_n$ can be calculated by differentiating both members of Eqs. (2.50) with respect to η and h. However, it is more convenient (and

shorter) to proceed differently, differentiating directly both members of Eq. (2.51) with respect to x_i. This approach leads to

$$\begin{aligned}\partial^2_{x_i} Z_n = &-\left[(z+h)\partial^2_{x_i} k_n + 2\partial_{x_i} h \partial_{x_i} k_n + k_n \partial^2_{x_i} h\right] W_n \\ &-\left[(z+h)\partial_{x_i} k_n + k_n \partial_{x_i} h\right] \partial_{x_i} W_n \\ &+\left[\sec^2(k_n H)(\partial_{x_i}(k_n H))^2 + \tan(k_n H)\partial^2_{x_i}(k_n H)\right] Z_n \\ &+\tan(k_n H)\partial_{x_i}(k_n H)\partial_{x_i} Z_n.\end{aligned} \tag{2.53}$$

To proceed further, we need to calculate $\partial_{x_i} W_n$. It is calculated (similarly as $\partial_{x_i} Z_n$) resulting in

$$\partial_{x_i} W_n = -\left[\partial_{x_i} k_n (z+h) + k_n \partial_{x_i} h\right] Z_n + \tan(k_n H)\partial_{x_i}(k_n H) W_n. \tag{2.54}$$

Substituting $\partial_{x_i} Z_n$ and $\partial_{x_i} W_n$, from Eqs. (2.51) and (2.54), into Eq. (2.53), we obtain an expression for $\partial^2_{x_i} Z_n$ in terms of Z_n and W_n, which after elimination of the trigonometric functions gives Eq. (2.48).

The estimates in the rightmost members of Eqs. (2.47), (2.48), are derived by applying the estimates (2.7a) and (2.7b) for k_n and Z_n, the estimate $W_n = O(1)$, the estimates given in Proposition 2.1 for $\partial_a k_n$ and $\partial^2_{x_i} k_n$, and their consequences given in Lemma C.1. Following this procedure for the estimation of $\partial_a Z_n$ leads to

$$\partial_a Z_n = \underbrace{-\left(\partial_a k_n (z+h) + k_n \partial_a h\right)}_{O(n)} W_n - \underbrace{\mu_0 \frac{\partial_a (k_n H)}{k_n}}_{O(n^{-2})} Z_n = O(n), \tag{2.55}$$

which proves Eq. (2.47). The relevant details for the estimation of $\partial^2_{x_i} Z_n$ can be found in Appendix C. □

Remark 2.4. The eigenfunctions (2.33b) coincide with the leading term of the asymptotic expansion of the eigenfunctions for the general Sturm-Liouville problem (2.5). Thus, we may conjecture that the results of Proposition 2.2 represent the leading asymptotic terms of the general case. A rigorous proof of this conjecture remains open.

Following a similar procedure as in the proofs of the above propositions, one can also derive the corresponding analytical expressions for the derivatives of $\{k_0, Z_0\}$.

Proposition 2.3. *The first and second derivatives of $k_0(H)$ are given by the following equations:*

$$\partial_H k_0 = -\frac{k_0^2 - \mu_0^2}{\mu_0 + H(k_0^2 - \mu_0^2)} k_0, \tag{2.56}$$

$$\partial^2_H k_0 = 2\partial_H k_0 \left(-\mu_0 + \frac{\partial_H k_0}{k_0}(1 - H\mu_0)\left(2 + H\frac{\partial_H k_0}{k_0}\right)\right). \tag{2.57}$$

Further, by the chain rule we obtain

$$\partial_a k_0 = \partial_H k_0 \partial_a H, \tag{2.58}$$

$$\partial_{x_i}^2 k_0 = \partial_H^2 k_0 (\partial_{x_i} H)^2 + \partial_H k_0 (\partial_{x_i}^2 H). \tag{2.59}$$

Introducing the auxiliary function

$$W_0(z;\eta,h) = W_0(\mathbf{x},z,t) = \frac{\sinh[k_0(z+h)]}{\cosh[k_0(\eta+h)]} = \frac{\partial_z Z_0}{k_0}, \tag{2.60}$$

and working as in the proof of Proposition 2.2, we arrive at the following

Proposition 2.4. *The space and time derivatives of the Z_0 are given by*

$$\partial_a Z_0 = (\partial_a k_0 (z+h) + k_0 \partial_a h)\, W_0 - \mu_0 \frac{\partial_a (k_0 H)}{k_0} Z_0, \tag{2.61}$$

$$\begin{aligned}
\Delta_{\mathbf{x}} Z_0 =& |\nabla_{\mathbf{x}} k_0|^2 (z+h)^2 Z_0 + 2k_0 \nabla_{\mathbf{x}} k_0 \cdot \nabla_{\mathbf{x}} h (z+h) Z_0 \\
&+ \left[k_0^2 |\nabla_{\mathbf{x}} h|^2 - |\nabla_{\mathbf{x}} (k_0 H)|^2 - \mu_0 \frac{\Delta_{\mathbf{x}} (k_0 H)}{k_0} + 2\mu_0^2 \frac{|\nabla_{\mathbf{x}} (k_0 H)|^2}{k_0^2} \right] Z_0 \\
&+ \left[\Delta_{\mathbf{x}} k_0 - 2\mu_0 \frac{\nabla_{\mathbf{x}} k_0 \cdot \nabla_{\mathbf{x}} (k_0 H)}{k_0} \right] (z+h) W_0 \\
&+ \left[2\nabla_{\mathbf{x}} k_0 \cdot \nabla_{\mathbf{x}} h + k_0 \Delta_{\mathbf{x}} h - 2\mu_0 \nabla_{\mathbf{x}} h \cdot \nabla_{\mathbf{x}} (k_0 H) \right] W_0.
\end{aligned} \tag{2.62}$$

The results of this section provide a non-linear extension of the ones appearing in the context of multi-modal expansions in linearised water waves over varying bathymetry (see e.g., (Massel 1993, Chamberlain & Porter 1995, Porter & Staziker 1995)); the eigensystem $\{k_n(h), Z_n(z;h)\}_{n\geq 1}$ employed in the latter work, called herewith PS95, is obtained by linearisation of the present eigensystem $\{k_n(H), Z_n(z;\eta,h)\}_{n\geq 1}$ about $\eta = 0$. It is also easily checked that the analytical expression for $\partial_h k_n(h)$, found in PS95, p.375, is recovered from (2.41) of Proposition 2.1. Indeed,

$$\begin{aligned}
\partial_H k_n &= -\frac{k_n^2 \sec^2(k_n H)}{\tan(k_n H) + k_n H \sec^2(k_n H)} \\
&= -\frac{k_n^2}{\frac{\tan(k_n H)}{\sec^2(k_n H)} + k_n H} \\
&= -\frac{k_n^2}{\sin(k_n H)\cos(k_n H) + k_n H},
\end{aligned}$$

and the result follows after taking $\eta = 0$ and noting that $H = \eta + h = h$. It should be emphasized that, in the present work, both the first and second derivatives of the eigenfunctions k_n are derived as polynomial expressions of $k_n(H)$ (not containing trigonometric or hyperbolic functions). Apart from the study of their asymptotic behaviour with respect to n, this fact facilitates as well their numerical evaluation. With some more work, involving extensive manipulations and trigonometry, one can also show that $\partial_h Z(z;0,h)$, obtained from Eq. (2.49b), is identical to the

corresponding expression found in PS95, p.375.

Concerning the analytic formulae presented in Propositions 2.2 and 2.4, we stress out the fact that Eqs. (2.47) and (2.48) express the first and the second derivatives of the vertical basis functions Z_n as linear combinations of the functions Z_n and W_n. The coefficients of these linear combinations are given in terms of the corresponding derivatives of the geometric boundary functions (η, h), and the first and the second derivatives of k_n, the latter being expressed by means of k_n themselves through the Eqs. (2.36) and (2.37). Thus, in fact, Eqs. (2.47) and (2.48) reduce the numerical calculation of the derivatives of Z_n to the calculation of geometrical quantities (which are regularly calculated during the numerical solution of the wave propagation problem in the waveguide) and the calculation of k_n, which can be done easily and accurately. This is an important issue, greatly improving both the computational efficiency and the accuracy in various circumstances. For example, in the calculation of the first and second spatial derivatives of the expanded wave field.

2.3 Termwise differentiability of the enhanced expansion

To establish the termwise differentiability of the coupled-mode series (2.4), corresponding to the water waves reference waveguide (2.31) and boundary modes (2.9), we shall estimate the decay rates of the differentiated terms $\varphi_n Z_n$, $n \geq 1$. To this end, consider, for example, the first and second x_i-derivatives of the n^{th} term of the series (2.4):

$$T_n^{\partial x_i} = \partial_{x_i}\varphi_n(\mathbf{x},t)\, Z_n(\mathbf{x},z,t) + \varphi_n(\mathbf{x},t)\, \partial_{x_i} Z_n(\mathbf{x},z,t), \tag{2.63}$$

$$T_n^{\partial^2 x_i} = \partial^2_{x_i}\varphi_n(\mathbf{x},t)\, Z_n(\mathbf{x},z,t) + 2\partial_{x_i}\varphi_n(\mathbf{x},t)\, \partial_{x_i} Z_n(\mathbf{x},z,t) + \varphi_n(\mathbf{x},t)\, \partial^2_{x_i} Z_n(\mathbf{x},z,t). \tag{2.64}$$

The results obtained in Section 2.1, for φ_n , and in Section 2.2, for $\partial_{x_i} Z_n$ and $\partial^2_{x_i} Z_n$, permit us to directly estimate the decay rates of the terms $\varphi_n \partial_{x_i} Z_n$ and $\varphi_n \partial^2_{x_i} Z_n$, appearing in the right-hand sides of Eqs. (2.63), (2.64). Indeed, under the appropriate smoothness assumptions, stated in Corollary 2.1 and in Proposition 2.2, we see that $\varphi_n \partial_{x_i} Z_n = O(1/n^4)O(n) = O(1/n^3)$, and $\varphi_n \partial^2_{x_i} Z_n = O(1/n^4)O(n^2) = O(1/n^2)$. To estimate the rates of the remaining terms of the right-hand sides of Eqs. (2.63) and (2.64) we need estimates of the derivatives ∂_α and $\partial^2_{x_i}$ of the modal amplitudes $\{\varphi_n\}_n$ for large n, where α stands for t or x_i, $i = 1, 2$.

The the modal amplitudes $\{\varphi_n\}_n$, for the case of water-wave reference waveguide, are written in view of (2.28) as follows:

$$\varphi_n(\mathbf{x},t) = \gamma_n(\mathbf{x},t)\lambda_n(\mathbf{x},t)\frac{1}{k_n^4(\mathbf{x},t)}, \quad (\mathbf{x},t) \in X \times I, \tag{2.65}$$

with

$$\gamma_n = \left(\frac{H}{2} + \frac{H\mu_0^2 - \mu_0}{2k_n^2}\right)^{-1} = \frac{2k_n^2}{H(k_n^2 + \mu_0) - \mu_0}, \tag{2.66}$$

$$\lambda_n = \left[\partial_z^2\Phi^* - \partial_z^3\Phi^*\right]_{z=\eta} - \left[\partial_z^3\Phi^*\right]_{z=-h}\sec(k_nH) + \int_{-h}^{\eta}\partial_z^4\Phi^* Z_n dz. \tag{2.67}$$

It is also recalled that Φ^* is given by Eq. (2.11), $\Phi^*(\mathbf{x},z,t) = \Phi(\mathbf{x},z,t) - \varphi_{-2}(\mathbf{x},t)Z_{-2} - \varphi_{-1}(\mathbf{x},t)Z_{-1}$. It is clear that we need estimates of the quantities, γ_n, λ_n and k_n^{-4}, and their derivatives. The relevant results are collected in the following four lemmata. Under the stated assumptions, all order estimates given below are uniform in $\tilde{X}_{\text{part}} \times I$.

Lemma 2.1. *If η and h satisfy the* BSC($\tilde{X}_{part} \times I$)*, then the following estimates hold uniformly in $X_{part} \times I$*

$$k_n^{-4},\ \partial_\alpha k_n^{-4},\ \partial_{x_i}^2 k_n^{-4} \text{ are of order } O(n^{-4}), \tag{2.68}$$

$$\gamma_n,\ \partial_\alpha\gamma_n,\ \partial_{x_i}^2\gamma_n \text{ are of order } O(1), \tag{2.69}$$

$$Z_n(-h) = O(1),\ \partial_\alpha Z_n(-h) = O(n^{-2}),\ \partial_{x_i}^2 Z_n(-h) = O(n^{-2}). \tag{2.70}$$

Proof. The first assertion in (2.68) follows directly from the estimate (2.7a), $k_n = O(n)$. In order to prove the assertions on the derivatives, their calculation is required. Then, their estimates are obtained by invoking the estimate (2.7a) together with the estimates of Proposition 2.1. The proof of Eqs. (2.69) and (2.70) is similar but more tedious; see Appendix D. □

The following lemma provides estimates for integrals involved in the definition of $\lambda_n(\mathbf{x},t)$ and its derivatives $\partial_a\lambda_n(\mathbf{x},t)$, $\partial_{x_i}^2\lambda_n(\mathbf{x},t)$, $i = 1,2$.

Lemma 2.2. *Le F be a function defined on $D_h^\eta \times I$ and assume that $F(\cdot\ \cdot\ t)$ satisfy the local* VSC($k=2;\mathbf{x},t$)*. Then, locally at $(\mathbf{x},t)$, we have*

$$\int_{-h}^{\eta} FZ_n dz = O(n^{-2}), \tag{2.71a}$$

$$\int_{-h}^{\eta} FW_n dz = O(n^{-1}). \tag{2.71b}$$

If, in addition, η and h satisfy the local BSC($\mathbf{x},t$)*, then*

$$\int_{-h}^{\eta} F\partial_a Z_n dz = O(1), \tag{2.72a}$$

$$\int_{-h}^{\eta} F\partial_{x_i}^2 Z_n dz = O(1). \tag{2.72b}$$

Further, if $F(\mathbf{x},\cdot,t)$ satisfies the uniform VSC($k=2;\tilde{X}_{part}\times I$)*, and η, h satisfy the uniform* BSC($\mathbf{x},t$)*, then the estimates (2.71) and (2.72) are uniformly valid in $\tilde{X}_{part}\times I$.*

Remark 2.5. The four integrals in Eqs. (2.71) and (2.72) could be directly estimated under the weaker assumption that F satisfy the VSC($k=0;\mathbf{x},t$), or $F \in L^2(-h,\eta)$, using the

Cauchy-Schwartz inequality. However, the estimates obtained in this way are weaker, namely,

$$\int_{-h}^{\eta} FZ_n dz = O(1), \quad \int_{-h}^{\eta} FW_n dz = O(1),$$
$$\int_{-h}^{\eta} F\partial_a Z_n dz = O(n), \quad \int_{-h}^{\eta} F\partial_{x_i}^2 Z_n dz = O(n^2),$$

and are not satisfactory for our purposes. Assuming that F is sufficiently smooth, namely $F \in H^2(-h, \eta)$ we are able to perform two integrations by parts, leading to the better estimates derived above.

Proof. Using $Z_n = -k_n^{-2}\partial_z^2 Z_n$, performing two integrations by parts in z (permitted by the local VSC($k = 2; \mathbf{x}, t$)), and using the boundary values of the eigenfunctions $\{Z_n\}_{n\geq 0}$, $[Z_n]_{z=\eta} = 1$, $[\partial_z Z_n]_{z=\eta} = \mu_0$ and $[Z_n]_{z=-h} = 0$, we have

$$\begin{aligned}\int_{-h}^{\eta} FZ_n dz &= -k_n^{-2}\int_{-h}^{\eta} F\partial_z^2 Z_n dz \\ &= -k_n^{-2}\left([F]_{z=\eta}\,\mu_0 - [\partial_z F]_{z=\eta} + [\partial_z F Z_n]_{z=-h} + \int_{-h}^{\eta}\partial_z^2 F Z_n dz\right).\end{aligned}$$

Since $F(\mathbf{x}, \cdot, t) \in H^2(-h(\mathbf{x}), \eta(\mathbf{x}, t))$, all boundary values of F appearing in the right-hand side of the above equation are well-defined and bounded. In addition $[Z_n]_{z=-h} = O(1)$ and the integral is bounded by $\|\partial_z^2 F\|_{L^2}\|Z_n\|_{L^2} \leq \|F\|_{H^2}\|Z_n\|_{L2} = O(1)$. Thus, the term in parenthesis has order $O(1)$, and the order of the integral appearing in the left hand side of the above equation is $O(k_n^{-2})O(1) = O(n^{-2})$, as asserted in (2.71a). In order to prove (2.71b), we substitute $W_n = -k_n^{-2}\partial_z^2 W_n$, perform two integrations by parts in z and take into account the relations $[W_n]_{z=\eta} = \tan(k_n H) = -\mu_0/k_n$, $[W_n]_{z=-h} = 0$, $[\partial_z W_n]_{z=\eta} = k_n$ and $[\partial_z W_n]_{z=-h} = k_n \sec(k_n H)$ (directly obtained from Eq. (2.46)):

$$\begin{aligned}\int_{-h}^{\eta} FW_n dz &= -k_n^{-2}\int_{-h}^{\eta} F\partial_z^2 W_n dz \\ &= -k_n^{-2}\left([F]_{z=\eta}\,k_n + [\partial_z F]_{z=\eta}\,\frac{\mu_0}{k_n} - [\partial_z F Z_n]_{z=-h}\,k_n + \int_{-h}^{\eta}\partial_z^2 F W_n dz\right).\end{aligned}$$

Now, the presence of $k_n = O(n)$ in the first and third terms in parenthesis, makes the latter $O(n)$. Thus, the order of the integral is $O(k_n^{-2})O(n) = O(n^{-1})$, as asserted.

The main idea for proving assertions (2.72), is to express $\partial_a Z_n$ and $\partial_{x_i}^2 Z_n$, as linear combinations of Z_n and W_n, using Eqs. (2.47) and (2.48) of Proposition 2.2, and then estimate the arising terms by exploiting assertions (2.71), Eq. (2.7a), and Proposition 2.1. For the integral in (2.72a), we have

$$\int_{-h}^{\eta} F\partial_a Z_n dz =$$

$$= -\partial_a k_n \int_{-h}^{\eta} F(z+h) W_n dz - k_n \partial_a h \int_{-h}^{\eta} F W_n dz - \mu_0 \frac{\partial_a (k_n H)}{k_n} \int_{-h}^{\eta} F Z_n dz. \quad (2.73)$$

The first integral in the right-hand side of the above equation is $O(n^{-1})$ (apply Eq. (2.71b) with $F(z+h)$ in place of F). Using this result, in conjunction with Eq. (2.36) of Proposition 2.1, we see that the first term is $O(1)$. Similarly, the second term is $O(n) \cdot O(n^{-1}) = O(1)$. Finally, using Eqs. (C.1), (2.7a) and (2.71a), we deduce that the order of the third term is $O(n^{-1}) \cdot O(n^{-1}) \cdot O(n^{-2}) = O(n^{-4})$. Thus, the order of the integral is $O(1)$, which proves Eq. (2.72a).

Expressing $\partial_{x_i}^2 Z_n$ in terms of Z_n and W_n, using Eq. (2.48) of Proposition 2.2, the integral in (2.72b) takes the form

$$\begin{aligned}
&- (\partial_{x_i} k_n)^2 \int_{-h}^{\eta} F(z+h)^2 Z_n dz - 2k_n (\partial_{x_i} k_n)(\partial_{x_i} h) \int_{-h}^{\eta} F(z+h) Z_n dz \\
&+ \left[-k_n^2 (\partial_{x_i} h)^2 - (\partial_{x_i}(k_n H))^2 - \mu_0 \frac{\partial_{x_i}^2 (k_n H)}{k_n} + 2\mu_0^2 \left(\frac{\partial_{x_i}(k_n H)}{k_n} \right)^2 \right] \int_{-h}^{\eta} F Z_n dz \\
&- \left[\partial_{x_i}^2 k_n - 2\mu_0 (\partial_{x_i} k_n) \frac{\partial_{x_i}(k_n H)}{k_n} \right] \int_{-h}^{\eta} F(z+h) W_n dz \\
&- \left[k_n \partial_{x_i}^2 h + 2 (\partial_{x_i} k_n)(\partial_{x_i} h) - 2\mu_0 (\partial_{x_i} h) \partial_{x_i}(k_n H) \right] \int_{-h}^{\eta} F W_n dz.
\end{aligned}$$

All integral terms in the above expression can be estimated by invoking the already proved assertions (2.71), applied to the functions F, $F(z+h)$ and $F(z+h)^2$. Using these results, in conjunction with the known estimates for k_n, $\partial_{x_i} k_n$, $\partial_{x_i}^2 k_n$, $\partial_{x_i}(k_n H)$ and $\partial_{x_i}^2 (k_n H)$ (see Eqs. (2.7a), (2.36), (2.36)) we readily prove (2.72b).

The uniform validity of Eqs. (2.71) and (2.72), asserted in the last part of the proposition, under uniformly valid smoothness assumptions, follows easily from the uniform validity of the assumptions.

□

Lemma 2.3. *If η and h satisfy the* BSC($\tilde{X}_{\text{part}} \times I$), $\Phi \in C^1(\overline{D_h^\eta}(X) \times I)$ and Φ, $\partial_\alpha \Phi$, $\partial_{x_i}^2 \Phi$ satisfy the VSC($k = 6; X_{\text{part}} \times I$), then

$$\lambda_n, \ \partial_\alpha \lambda_n, \ \partial_{x_i}^2 \lambda_n \text{ are of order } O(1). \quad (2.74)$$

Proof. The result $\lambda_n(\mathbf{x}, t) = O(1)$ is deduced from Eq. (2.67). Indeed, from the assumption $\Phi \in H^6(-h, \eta)$ and Eq. (2.11), we conclude that $\Phi^* \in H^6(-h, \eta)$, and thus all corresponding boundary values appearing in the right hand side of Eq. (2.67) are well defined and $O(1)$. Since $[Z_n]_{-h} = O(1)$, according to Eq. (2.70), all boundary terms are of order $O(1)$. The integral term is found to be $O(n^{-2})$ by using assertion (2.71a) of Lemma 2.2 with $F = \partial_z^4 \Phi^* \in H^2(-h, \eta)$, consequently $\lambda_n(\mathbf{x}, t) = O(1)$.

To prove that $\partial_\alpha \lambda_n$ and $\partial_{x_i}^2 \lambda_n$ are of order $O(1)$, we first calculate them by differentiating

Eq. (2.67). For $\partial_\alpha \lambda_n$, one finds

$$\begin{aligned}\partial_a \lambda_n = \partial_a \left[\partial_z^2 \Phi^* \mu_0 - \partial_z^3 \Phi^*\right]_{z=\eta} - \partial_a \left(\left[\partial_z^3 \Phi^*\right]_{z=-h} [Z]_{z=-h}\right) \\ + \partial_a \eta \left[\partial_z^4 \Phi^*\right]_{z=\eta} + \partial_a h \left[\partial_z^4 \Phi^*\right]_{z=-h} [Z_n]_{z=-h} \\ + \int_{-h}^{\eta} \partial_a \partial_z^4 \Phi^* Z_n dz + \int_{-h}^{\eta} \partial_z^4 \Phi^* \partial_a Z_n dz. \quad (2.75)\end{aligned}$$

Smoothness assumptions and Eqs. (2.70) of Lemma 2.1 ensure that all boundary terms in the above equation are of order $O(1)$. Applying Lemma 2.2 with $F = \partial_a \partial_z^4 \Phi^* \in H^2(-h, \eta)$ and $F = \partial_z^4 \Phi^* \in H^2(-h, \eta)$, it is easily seen that the integral terms in the third line of (2.75) are estimated as $O(1)$, which proves that $\partial_a \lambda_n = O(1)$. We turn now to $\partial_{x_i}^2 \lambda_n$. Direct differentiation of (2.75) with respect to $a = x_i$ yields the following expression

$$\begin{aligned}\partial_{x_i}^2 \lambda_n = \partial_{x_i}^2 \left[\partial_z^2 \Phi^* \mu_0 - \partial_z^3 \Phi^*\right]_{z=\eta} - \partial_{x_i}^2 \left(\left[\partial_z^3 \Phi^*\right]_{z=-h} [Z]_{z=-h}\right) \\ + \partial_{x_i} \left(\partial_{x_i} \eta \left[\partial_z^4 \Phi^*\right]_{z=\eta}\right) + \partial_{x_i} \left(\partial_{x_i} h \left[\partial_z^4 \Phi^*\right]_{z=-h} [Z_n]_{z=-h}\right) \\ + \partial_{x_i} \eta \left[\partial_{x_i} \partial_z^4 \Phi^* + \partial_x^4 \Phi^* \partial_{x_i} Z_n\right]_{z=\eta} + \partial_{x_i} h \left[\partial_{x_i} \partial_z^4 \Phi^* + \partial_z^4 \partial_{x_i} Z_n\right]_{z=-h} [Z_n]_{z=-h} \\ + \int_{-h}^{\eta} \partial_{x_i}^2 \partial_z^4 \Phi^* Z_n dz + 2 \int_{-h}^{\eta} \partial_{x_i} \partial_z^4 \Phi^* \partial_{x_i} Z_n dz + \int_{-h}^{\eta} \partial_z^4 \Phi^* \partial_{x_i}^2 Z_n dz. \quad (2.76)\end{aligned}$$

Again, under the stated smoothness assumptions and Lemma 2.1, all boundary terms (the first three lines of the right-hand side of Eq. (2.76)) are of order $O(1)$. The integrals, appearing in the last line of the right-hand side of (2.76), are estimated by applying Eqs. (2.71a), (2.72a) and (2.72b) of Lemma 2.2 with $F = \partial_{x_i}^2 \partial_z^4 \Phi^* \in H^2(-h, \eta)$, $F = \partial_z^4 \Phi^*$ and $F = \partial_z^4 \Phi^*$, respectively, and are found to be of order $O(1)$, which proves that $\partial_{x_i}^2 \lambda_n = O(1)$. □

We are now in position of estimating the derivatives of $\{\varphi_n\}_n$, defined by Eq. (2.65). Differentiating the latter equation and estimating the resulting expressions, using the estimates (2.68), (2.69) and (2.74), the following theorem is proved

Theorem 2.2. *Assume that η and h satisfy* BSC$(\mathbf{x}, t)$. *Let $\Phi \in C^1(\overline{D_h^\eta}(X) \times I)$ and assume that for each $t \in I$, $\Phi(\mathbf{x}, \cdot, t)$, $\partial_t \Phi(\mathbf{x}, \cdot, t)$, $\partial_{x_i} \Phi(\mathbf{x}, \cdot, t)$, $\partial_{x_i}^2 \Phi(\mathbf{x}, \cdot, t)$ satisfy the local* VSC$(k = 6; \mathbf{x}, t)$. *Then, the sequences $\partial_\alpha \varphi_n$ and $\partial_{x_i}^2 \varphi_n$, $i = 1, 2$, satisfy the following estimates*

$$\|\partial_\alpha \varphi_n\|_{\infty, X \times I} = O(n^{-4}), \quad (2.77)$$

$$\|\partial_{x_i}^2 \varphi_n\|_{\infty, X \times I} = O(n^{-4}). \quad (2.78)$$

Corollary 2.2. *Under the assumptions stated in Theorem 2.2, $\|\partial_a(\varphi_n Z_n)\|_\infty = O(n^{-3})$ for $a \in \{t, x_1, x_2, z\}$ and $\|\partial_a^2(\varphi_n Z_n)\|_\infty = O(n^{-2})$ for $a \in \{x_1, x_2, z\}$. Thus, the series expansion (2.4) can be differentiated term-by-term once with respect to time t, and twice with respect*

to the spatial variables $(\mathbf{x}, z)$*. The termwise differentiated series are uniformly convergent in* $\overline{D_h^\eta}(\tilde{X}_{part}) \times I$ *or in* $\overline{D_h^\eta}(X) \times I$*, if the smoothness assumptions hold true uniformly in* X*.*

Chapter 3

New variational equations for fully nonlinear water waves

In this chapter, we proceed with a systematic variational treatment of the water waves problem by exploiting the enhanced eigenfunction expansion, established in Chapter 2. It is convenient to introduce some notation first

Notation 3.1. Sequences of functions are denoted by bold letters; a series of the form $\Phi = \sum_n \varphi_n Z_n$ is written as

$$\Phi(\mathbf{x}, z, t) = \boldsymbol{\phi}^{\mathrm{T}}(\mathbf{x}, t)\, \boldsymbol{Z}(z; \eta(\mathbf{x}, t), h(\mathbf{x})). \tag{3.1}$$

The vector of vertical functions $\boldsymbol{Z}(z; \eta, h)$ will be frequently abbreviated as $\boldsymbol{Z}$, or $\boldsymbol{Z}(\eta)$, when the dependence on the unknown surface field η is important and should be emphasized.

The idea is to substitute expression (2.4) (or (3.1), with $\boldsymbol{Z}(z; \eta, h) \equiv \{Z_n(z; \eta, h)\}_{n=-2}^{\infty}$ given by (2.9) and (2.33)), in Luke's integral $S[\eta, \Phi]$, Eq. (1.14), and derive EL equations for the free surface elevation η and the unknown sequence of modal amplitudes $\boldsymbol{\phi}(\mathbf{x}, t) \equiv \{\varphi_n(\mathbf{x}, t)\}_{n=-2}^{\infty}$. This is done in Section 3.1 for the case of a generic series representation of the unknown function Φ given by (3.1). Subsequently, in Section 3.2, we specify (3.1) to be the exact representation provided by the enhanced eigenfunction expansion (2.4).

3.1 Euler-Lagrange equations for a generic series representation of the velocity potential

The transformed action functional, $\tilde{\mathcal{S}}[\eta, \boldsymbol{\phi}] = \mathcal{S}[\eta, \boldsymbol{\phi}^{\mathrm{T}}\boldsymbol{Z}(\eta)]$, is written as

$$\tilde{\mathcal{S}}[\eta, \boldsymbol{\phi}] = \int_{t_0}^{t_1} \int_X \left(\int_{-h}^{\eta} \partial_t(\boldsymbol{\phi}^{\mathrm{T}}\boldsymbol{Z}(\eta)) dz + \tilde{K}[\eta, \boldsymbol{\phi}] + g\frac{\eta^2}{2} \right) d\mathbf{x}dt, \tag{3.2}$$

where we have introduced the transformed kinetic energy density $\tilde{K}[\eta,\boldsymbol{\phi}]=K\left[\eta,\boldsymbol{\phi}^{\mathrm{T}}\boldsymbol{Z}(\eta)\right]$,

$$\tilde{K}[\eta,\boldsymbol{\phi}]=\frac{1}{2}\int_{-h}^{\eta}\left[\nabla(\boldsymbol{\phi}^{\mathrm{T}}\boldsymbol{Z}(\eta))\right]^{2}\,dz. \tag{3.3}$$

Eq. (3.2) is formally the same for any series representation of the form (3.1), finite or infinite. In any case, one could explicitly compute the right hand side of Eq. (3.2) using the specific expressions of the vertical functions $\boldsymbol{Z}$. However, this is not recommended when working with complicated series expansions or representations, since it leads to very heavy calculations. The stationarity of $\tilde{S}\left[\eta,\boldsymbol{\phi}\right]$ shall now be invoked, with the purpose of deriving Euler-Lagrange equations for η and $\boldsymbol{\phi}$. Since $\boldsymbol{\phi}$ depends on $(\mathbf{x},t)$ and the z- dependence of $\boldsymbol{Z}$ can be removed via integration in the right hand side of (3.2), we shall obtain in this way, a semi-discretization of the problem (Kantorovich-type dimensional reduction, (Kantorovich & Krylov 1958, Chapter IV)). Accordingly, in terms of the new functional variables $(\eta,\boldsymbol{\phi})$, we have the following variational equation

$$\delta\tilde{\mathcal{S}}[\eta,\boldsymbol{\phi};\delta\eta,\delta\boldsymbol{\phi}]=\delta_{\eta}\tilde{\mathcal{S}}[\eta,\boldsymbol{\phi};\delta\eta]+\sum_{m}\delta_{\varphi_m}\tilde{\mathcal{S}}[\eta,\boldsymbol{\phi};\delta\varphi_m]=0, \tag{3.4}$$

where $\delta_{\eta}\tilde{\mathcal{S}}[\eta,\boldsymbol{\phi};\delta\eta]$ and $\delta_{\varphi_m}\tilde{\mathcal{S}}[\eta,\boldsymbol{\phi};\delta\varphi_m]$ denote the partial variations of $\mathcal{S}[\eta,\boldsymbol{\phi}]$ in the directions $\delta\eta$ and $\delta\varphi_m$. The variations $(\delta\eta,\delta\boldsymbol{\phi})$ of $(\eta,\boldsymbol{\phi})$ are arbitrary, continuously differentiable functions of $(\mathbf{x},t)$, satisfying essential conditions equivalent with those satisfied by Φ in the classical Luke's variational principle, that is, the isochronality constraint, $\delta\boldsymbol{\phi}(\mathbf{x},t_0)=\delta\boldsymbol{\phi}(\mathbf{x},t_1)=\delta\eta(\mathbf{x},t_0)=\delta\eta(\mathbf{x},t_1)=0$, the vanishing-at-infinity condition, and the constraint $[\delta\eta]_{x_1=a}=0$, due to the fact that the free surface elevation η is assumed known on the excitation boundary S_a. To derive the Euler-Lagrange equations of $\tilde{\mathcal{S}}$ we need first to calculate its variation as the variational equation (3.4) dictates. Although this calculation can be done directly, by expanding the right-hand side of (3.2) and performing straightforward (yet laborious) manipulations, it is more instructive and more economical to exploit the fact that $\tilde{\mathcal{S}}$ is a composite functional and apply the chain rule for functional derivatives (see, e.g., (Flett 1980, 4.1.2), (Gasiński & Papageorgiou 2005, Prop 4.1.12). In this way we are able to utilize the already calculated variations $\delta_{\eta}\mathcal{S}[\eta,\Phi;\delta\eta]$ and $\delta_{\Phi}\mathcal{S}[\eta,\Phi;\delta\Phi]$, given by Eqs. (1.19) and (1.20), respectively, and keep a good track of the various terms arising from the variational procedure. This is accomplished by using the following lemma, which is proved in Appendix E:

Lemma 3.1. *The partial variations $\delta_{\eta}\tilde{\mathcal{S}}[\eta,\boldsymbol{\phi};\delta\eta]$ and $\delta_{\phi_m}\tilde{\mathcal{S}}[\eta,\boldsymbol{\phi};\delta\phi_m]$, appearing in Eq. (3.4), are calculated by the following formulae*

$$\delta_{\eta}\tilde{\mathcal{S}}\left[\eta,\boldsymbol{\phi};\delta\eta\right]=\delta_{\eta}\mathcal{S}\left[\eta,\boldsymbol{\phi}^{T}\boldsymbol{Z}(\eta);\delta\eta\right]+\delta_{\Phi}\mathcal{S}\left[\eta,\boldsymbol{\phi}^{T}\boldsymbol{Z}(\eta);(\boldsymbol{\phi}^{T}\,\partial_{\eta}\boldsymbol{Z}(\eta))\delta\eta\right], \tag{3.5}$$

$$\delta_{\varphi_m}\tilde{\mathcal{S}}\left[\eta,\boldsymbol{\phi};\delta\varphi_m\right]=\delta_{\Phi}\mathcal{S}\left[\eta,\boldsymbol{\phi}^{T}\boldsymbol{Z}(\eta);Z_m(\eta)\delta\varphi_m\right], \tag{3.6}$$

where the variations $\delta_\Phi \mathcal{S}[\eta, \Phi; \delta\Phi]$ and $\delta_\eta \mathcal{S}[\eta, \Phi; \delta\eta]$ are given by Eqs. (1.19) and (1.20), respectively.

Let us start by calculating $\delta_{\varphi_m}\tilde{\mathcal{S}}[\eta, \boldsymbol{\phi}; \delta\varphi_m]$. Applying Eq. (3.6) of Lemma 3.1, we substitute Φ and $\delta\Phi$ in Eq. (1.19), by $\boldsymbol{\phi}^{\mathrm{T}}\boldsymbol{Z}$ and $Z_m\delta\varphi_m$ respectively, obtaining

$$\begin{aligned}\delta_{\varphi_m}\tilde{\mathcal{S}}[\eta, \boldsymbol{\phi}; \delta\varphi_m] = \int_{t_0}^{t_1}\int_X \Big\{ &\big(-\partial_t\eta + N_\eta \cdot [\nabla(\boldsymbol{\phi}^{\mathrm{T}}\boldsymbol{Z})]\big)\,[Z_m\delta\varphi_m]_{z=\eta} \\ &- \int_{-h}^{\eta} \Delta(\boldsymbol{\phi}^{\mathrm{T}}\boldsymbol{Z}) Z_m\delta\varphi_m dz + N_h \cdot \big[\nabla(\boldsymbol{\phi}^{\mathrm{T}}\boldsymbol{Z}) Z_m\delta\varphi_m\big]_{z=-h}\Big\} d\mathbf{x}dt \\ &+ \int_{t_0}^{t_1}\int_{\mathbb{R}}\int_{-h_a}^{\eta_a} \Big(-\big[\partial_{x_1}(\boldsymbol{\phi}^{\mathrm{T}}\boldsymbol{Z})\big]_{x_1=a} + V_a\Big)\,[Z_m\delta\varphi_m]_{x_1=a}\, dz dx_2 dt,\end{aligned} \tag{3.7}$$

where the η dependence of $\boldsymbol{Z}(\eta)$ has been dropped for the sake of clarity. Since $\delta\varphi_m$ do not depend on z, the above equation is easily written as

$$\begin{aligned}\delta_{\varphi_m}\tilde{\mathcal{S}}[\eta, \boldsymbol{\phi}; \delta\varphi_m] = \int_{t_0}^{t_1}\int_X \Big\{ &\Big(-\partial_t\eta + N_\eta \cdot \Big[\nabla(\boldsymbol{\phi}^{\mathrm{T}}\boldsymbol{Z})\Big]\Big)\,[Z_m]_{z=\eta} \\ &- \int_{-h}^{\eta} \Delta(\boldsymbol{\phi}^{\mathrm{T}}\boldsymbol{Z}) Z_m dz + N_h \cdot \big[\nabla(\boldsymbol{\phi}^{\mathrm{T}}\boldsymbol{Z}) Z_m\big]_{z=-h}\Big\} \delta\varphi_m d\mathbf{x}dt \\ &+ \int_{t_0}^{t_1}\int_{\mathbb{R}} \Big\{\int_{-h_a}^{\eta_a} \Big(-\big[\partial_{x_1}(\boldsymbol{\phi}^{\mathrm{T}}\boldsymbol{Z})\big]_{x_1=a} + V_a\Big)\,[Z_m]_{x_1=a}\, dz\Big\}\,[\delta\varphi_m]_{x_1=a}\, dx_2 dt.\end{aligned} \tag{3.8}$$

We shall now turn to the calculation of the variation $\delta_\eta\tilde{\mathcal{S}}[\eta, \boldsymbol{\phi}; \delta\eta]$. Applying Eq. (3.5) of Lemma 3.1, we replace Φ by $\boldsymbol{\phi}^{\mathrm{T}}\boldsymbol{Z}$ in Eqs. (1.20), (1.19), and $\delta\Phi$ by $\boldsymbol{\phi}^{\mathrm{T}}\partial_\eta\boldsymbol{Z}(\eta)\delta\eta$ in Eq. (1.19), obtaining

$$\begin{aligned}\delta_\eta\tilde{\mathcal{S}}[\eta, \boldsymbol{\phi}; \delta\eta] = &\int_{t_0}^{t_1}\int_X \Big\{ \Big[\partial_t(\boldsymbol{\phi}^{\mathrm{T}}\boldsymbol{Z})\Big]_{z=\eta} + \frac{1}{2}\Big[\nabla(\boldsymbol{\phi}^{\mathrm{T}}\boldsymbol{Z})\Big]^2_{z=\eta} + g\eta + \frac{P_{\mathrm{surf}}}{\rho}\Big\}\delta\eta d\mathbf{x}dt \\ &+ \int_{t_0}^{t_1}\int_X \Big\{ \Big(-\partial_t\eta + N_\eta \cdot \Big[\nabla(\boldsymbol{\phi}^{\mathrm{T}}\boldsymbol{Z})\Big]\Big)\Big[\boldsymbol{\phi}^{\mathrm{T}}\partial_\eta\boldsymbol{Z}\Big]_{z=\eta} \\ &\qquad - \int_{-h}^{\eta} \Delta(\boldsymbol{\phi}^{\mathrm{T}}\boldsymbol{Z})\,\boldsymbol{\phi}^{\mathrm{T}}\partial_\eta\boldsymbol{Z}\, dz + N_h \cdot \Big[\nabla(\boldsymbol{\phi}^{\mathrm{T}}\boldsymbol{Z})\,\boldsymbol{\phi}^{\mathrm{T}}\partial_\eta\boldsymbol{Z}\Big]_{z=-h}\Big\}\delta\eta d\mathbf{x}dt \\ &+ \int_{t_0}^{t_1}\int_{\mathbb{R}} \Big\{\int_{-h_a}^{\eta_a} \Big(-\big[\partial_{x_1}(\boldsymbol{\phi}^{\mathrm{T}}\boldsymbol{Z})\big]_{x_1=a} + V_a\Big)\Big[\boldsymbol{\phi}^{\mathrm{T}}\partial_\eta\boldsymbol{Z}\Big]_{x_1=a} dz\Big\}\,[\delta\eta]_{x_1=a}\, dx_2 dt,\end{aligned} \tag{3.9}$$

where $\delta\eta$ has been factored out of the vertical integrals, as was done for $\delta\varphi_m$ in the derivation of Eq. (3.8). Recalling that $\Delta = \Delta_{\mathbf{x}} + \partial_z^2$ and $N_h = (-\nabla_{\mathbf{x}}h, -1)$, the vertical integral and the bottom boundary term, appearing in the second line of Eq. (3.8), are written as

$$\int_{-h}^{\eta} \Delta(\boldsymbol{\phi}^{\mathrm{T}}\boldsymbol{Z}) Z_m dz = \\ = \sum_n \left(\int_{-h}^{\eta} Z_n Z_m dz \right) \nabla_{\mathbf{x}}^2 \varphi_n + 2 \left(\int_{-h}^{\eta} \nabla_{\mathbf{x}} Z_n Z_m dz \right) \cdot \nabla_{\mathbf{x}} \varphi_n + \left(\int_{-h}^{\eta} \Delta Z_n Z_m dz \right) \varphi_n, \quad (3.10)$$

and

$$N_h \cdot \left[\nabla(\boldsymbol{\phi}^{\mathrm{T}}\boldsymbol{Z}) Z_m \right]_{z=-h} = \\ = \sum_n -\nabla_{\mathbf{x}} h \cdot \left(\nabla_{\mathbf{x}} \varphi_n \left[Z_n Z_m \right]_{z=-h} + \varphi_n \left[\nabla_{\mathbf{x}} Z_n Z_m \right]_{z=-h} \right) - \left[\partial_z Z_n Z_m \right]_{z=-h}, \quad (3.11)$$

respectively, while, the vertical integral of the last lateral boundary term of Eq. (3.8) is written as

$$\int_{-h_a}^{\eta_a} \left(\left[\partial_{x_1} (\boldsymbol{\phi}^{\mathrm{T}}\boldsymbol{Z}) \right]_{x_1=a} - V_a \right) \left[Z_m \right]_{x_1=a} dz = \\ = \sum_n \left[\partial_{x_1} \varphi_n \right]_{x_1=a} \int_{-h_a}^{\eta_a} \left[Z_n Z_m \right]_{x_1=a} dz + \left[\varphi_n \right]_{x_1=a} \int_{-h_a}^{\eta_a} \left[\partial_{x_1} Z_n Z_m \right]_{x_1=a} dz - g_m. \quad (3.12)$$

where the notation

$$g_m = \int_{-h_a}^{\eta_a} V_a [Z_m]_{x_1=a} dz \quad (3.13)$$

has been used. Similarly for the corresponding terms appearing in Eq. (3.9) one easily verifies that

$$\int_{-h}^{\eta} \Delta(\boldsymbol{\phi}^{\mathrm{T}}\boldsymbol{Z}) \partial_\eta Z_m dz = \\ = \sum_n \left(\int_{-h}^{\eta} Z_n \partial_\eta Z_m dz \right) \nabla_{\mathbf{x}}^2 \varphi_n + 2 \left(\int_{-h}^{\eta} \nabla_{\mathbf{x}} Z_n \partial_\eta Z_m dz \right) \cdot \nabla_{\mathbf{x}} \varphi_n + \left(\int_{-h}^{\eta} \Delta Z_n \partial_\eta Z_m dz \right) \varphi_n, \quad (3.14)$$

and

$$N_h \cdot \left[\nabla(\boldsymbol{\phi}^{\mathrm{T}}\boldsymbol{Z}) \partial_\eta Z_m \right]_{z=-h} = \\ = \sum_n -\nabla_{\mathbf{x}} h \cdot \left(\nabla_{\mathbf{x}} \varphi_n \left[Z_n \partial_\eta Z_m \right]_{z=-h} + \varphi_n \left[\nabla_{\mathbf{x}} Z_n \partial_\eta Z_m \right]_{z=-h} \right) - \left[\partial_z Z_n \partial_\eta Z_m \right]_{z=-h}, \quad (3.15)$$

Finally, taking into account Eqs. (3.10) - (3.15) in Eqs. (3.8) and (3.9), the variational equation (3.4) yields the following Euler-Lagrange equations for the functional $\tilde{\mathcal{S}}[\eta, \boldsymbol{\phi}]$

$$\left(\partial_t \eta - N_\eta \cdot \left[\nabla(\boldsymbol{\phi}^{\mathrm{T}}\boldsymbol{Z}) \right]_{z=\eta} \right) \left[Z_m \right]_{z=\eta} + \sum_n L_{mn}[\eta, h] \varphi_n = 0, \qquad \text{for all } m, \quad (3.16)$$

$$\sum_n [T_{mn}\varphi_n]_{x_1=a} = g_m, \quad \text{for all } m, \tag{3.17}$$

$$[\partial_t(\boldsymbol{\phi}^{\mathrm{T}}\boldsymbol{Z})]_{z=\eta} + g\eta + \frac{1}{2}[\nabla(\boldsymbol{\phi}^{\mathrm{T}}\boldsymbol{Z})]^2_{z=\eta} - \sum_m \Big(\sum_n \ell_{mn}[\eta,h]\varphi_n\Big)\varphi_m$$
$$+\Big(-\partial_t\eta + N_\eta \cdot [\nabla(\boldsymbol{\phi}^{\mathrm{T}}\boldsymbol{Z})]_{z=\eta}\Big)\Big(\boldsymbol{\phi}^{\mathrm{T}}\,[\partial_\eta \boldsymbol{Z}]_{z=\eta}\Big) = -\frac{P_{\mathrm{surf}}}{\rho}. \tag{3.18}$$

In the above equations, L_{mn} and ℓ_{mn} denote 2$^{\mathrm{nd}}$ order linear differential operators on X and $[T_{mn}\,]_{x_1=a}$ denote boundary operators on the matching surface S_a. They are given by

$$L_{mn}[\eta,h] = A_{mn}\Delta_{\mathbf{x}} + B^i_{mn}\partial_{x_i} + C_{mn}, \tag{3.19}$$
$$\ell_{mn}[\eta,h] = a_{mn}\Delta_{\mathbf{x}} + b^i_{mn}\partial_{x_i} + c_{mn}, \tag{3.20}$$
$$[T_{mn}\,\cdot\,]_{x_1=a} = [A_{mn}]_{x_1=a}\,[\partial_{x_1}\,\cdot\,]_{x_1=a} + \frac{1}{2}\,[B_{mn}]_{x_1=a}\,[\,\cdot\,]_{x_1=a}\,, \tag{3.21}$$

where the matrix functions $A_{mn} = A_{mn}(\eta,h)$ etc. are defined by

$$A_{mn} = \int_{-h}^{\eta} Z_n Z_m dz = A_{nm}, \tag{3.22a}$$
$$B^i_{mn} = 2\int_{-h}^{\eta} \partial_{x_i} Z_n Z_m dz + \partial_{x_i} h\big[Z_n Z_m\big]_{z=-h}, \quad i=1,2, \tag{3.22b}$$
$$C_{mn} = \int_{-h}^{\eta} \Delta Z_n Z_m dz - N_h \cdot \big[\nabla Z_n Z_m\big]_{z=-h}, \tag{3.22c}$$

$$a_{mn} = \int_{-h}^{\eta} Z_n \partial_\eta Z_m dz, \tag{3.23a}$$
$$b^i_{mn} = 2\int_{-h}^{\eta} \partial_{x_i} Z_n \partial_\eta Z_m dz + \partial_{x_i} h\big[Z_n \partial_\eta Z_m\big]_{z=-h}, \quad i=1,2, \tag{3.23b}$$
$$c_{mn} = \int_{-h}^{\eta} \Delta Z_n \partial_\eta Z_m dz - N_h \cdot \big[\nabla Z_n \partial_\eta Z_m\big]_{z=-h}, \tag{3.23c}$$

The above derivation establishes the following identities, that are easily verified, and will be used in the sequel

$$\sum_n L_{mn}[\eta,h]\varphi_n = \int_{-h}^{\eta} \Delta(\boldsymbol{\phi}^{\mathrm{T}}\boldsymbol{Z}) Z_m dz - N_h \cdot \Big[\nabla(\boldsymbol{\phi}^{\mathrm{T}}\boldsymbol{Z})\Big]_{z=-h}\,[Z_m]_{z=-h}\,, \tag{3.24}$$
$$\sum_n \ell_{mn}[\eta,h]\varphi_n = \int_{-h}^{\eta} \Delta(\boldsymbol{\phi}^{\mathrm{T}}\boldsymbol{Z}) \partial_\eta Z_m dz - N_h \cdot \Big[\nabla(\boldsymbol{\phi}^{\mathrm{T}}\boldsymbol{Z})\Big]_{z=-h}\,[\partial_\eta Z_m]_{z=-h}\,. \tag{3.25}$$

The system of equations (3.16) corresponds to the free surface kinematic condition (1.7), the Laplace equation (1.5) and the bottom impermeability condition (1.6) while the system of boundary conditions (3.17) corresponds to the matching condition (1.12). Eq. (3.18) corresponds to the dynamical (Bernoulli) condition on the free surface, Eq. (1.8), but it also contains terms

related to the aforementioned kinematical equations.

The potential usefulness of the formal result (3.17)- (3.23) is twofold, depending on the choice of the vertical system $\boldsymbol{Z}$; it can be used either in conjunction with a simple representation of the velocity potential, leading to a simplified model system, or, in conjunction with an exact series representation of the velocity potential leading to an exact reformulation of the full problem. The latter approach is elaborated in the next two sections with the purpose of exactly reformulating the Hamiltonian equations for water waves through the enhanced eigenfunction expansion (2.4). The former approach and its relation with existing water wave models will be discussed in the next chapter.

3.2 Euler-Lagrange equations for the enhanced eigenfunction expansion

The series representation of the velocity potential is specified here as the exact infinite series expansion (2.4), established in Chapter 2. Consequently, the change of (functional) variables $(\eta, \Phi) \to (\eta, \boldsymbol{\phi})$ is introduced in Luke's action functional $\mathcal{S}[\eta, \Phi]$, Eq. (1.14). Note that, under the assumptions stated in Theorem 2.2, termwise differentiation and integration of the infinite series (2.4) is permissible. Thus, it is legitimate to perform termwise manipulations in the right-hand side of Eq. (1.14), after the substitution of the infinite series $\Phi = \boldsymbol{\phi}^{\mathrm{T}}\boldsymbol{Z}$. Moreover, under the assumption that the (functional) transformation $(\eta, \Phi) \to (\eta, \boldsymbol{\phi})$ is regular and invertible, the critical "points" of $\mathcal{S}$ and $\tilde{\mathcal{S}}$ are essentially the same in the sense that

$$\delta\mathcal{S}[\eta, \Phi; \delta\eta, \delta\Phi] = 0 \Leftrightarrow \delta\tilde{\mathcal{S}}[\eta, \boldsymbol{\phi}; \delta\eta, \delta\boldsymbol{\phi}] = 0.$$

In this case Eqs. (3.16), (3.17) yield the following infinite system of equations

$$\partial_t\eta - N_\eta \cdot \left[\nabla(\boldsymbol{\phi}^{\mathrm{T}}\boldsymbol{Z})\right]_{z=\eta} + \sum_{n=-2}^{\infty} L_{mn}[\eta, h]\varphi_n = 0, \quad \mathbf{x} \in X, \quad m \geq -2, \tag{3.26}$$

$$\sum_{n=-2}^{\infty} [T_{mn}\varphi_n]_{x_1=a} = g_m, \quad m \geq -2, \tag{3.27}$$

where the normalisation $[Z_n]_\eta = 1$ has been used in Eq. (3.26). Eqs. (3.26), (3.27), constitute a modal reformulation of the kinematical problem, Eqs. (1.5), (1.6), (1.12), through the exact series representation (2.4). The matrix coefficients A_{mn}, B_{mn}, C_{mn}, $m, n \geq -2$, of the operators L_{mn} and T_{mn} appearing above, are given in Appendix F. The infinite system (3.26) first appeared in (Athanassoulis & Belibassakis 2000), in a slightly different form where the normal derivative $N_\eta \cdot \left[\nabla(\boldsymbol{\phi}^{\mathrm{T}}\boldsymbol{Z})\right]_{z=\eta}$ does not appear explicitly; the relevant terms are part of the definition of the matrix coefficients of the aforementioned work. The same authors proposed a reformulation of the infinite system (3.26), as one evolution equation on η coupled with a time-independent system of partial differential equations on $\boldsymbol{\phi}$, obtained by subtracting the first equation of (3.26)

from the others (Athanassoulis & Belibassakis 2007, Belibassakis & Athanassoulis 2011). In the lemma below, we follow this approach in order to show that (3.26) implies that $\boldsymbol{\phi}^{\mathrm{T}}\boldsymbol{Z}$ satisfies the kinematics of the problem.

Lemma 3.2. *Let $\boldsymbol{\phi} = \{\varphi_n\}_{n=-2}^{\infty}$ satisfy Eqs. (3.26) at every $t \in I$. Then, the function $\Phi = \boldsymbol{\phi}^T\boldsymbol{Z}$, where $\boldsymbol{Z}$ are given by Eqs. (2.9), (2.33), satisfies the Laplace equation (1.5), and the bottom impermeability condition, Eq. (1.6).*

Proof. Let us pick one of the equations appearing in (3.26), say the one corresponding to $m = m_*$. Subtracting this equation from the others we find that $\boldsymbol{\phi}$ has to satisfy the following time independent system of partial differential equations

$$\sum_{n=-2}^{\infty} \left(L_{mn}[\eta,h] - L_{m_*n}[\eta,h]\right)\varphi_n = 0, \quad \mathbf{x} \in X, \quad m \geq -2. \tag{3.28}$$

The above system, in view of the identity (3.24), is rewritten as

$$\int_{-h}^{\eta} \Delta(\boldsymbol{\phi}^{\mathrm{T}}\boldsymbol{Z})(Z_m - Z_{m_*})dz - N_h \cdot \left[\nabla(\boldsymbol{\phi}^{\mathrm{T}}\boldsymbol{Z})(Z_m - Z_{m_*})\right]_{z=-h} = 0, \quad m \geq -2. \tag{3.29}$$

Consider now a function $\delta\Psi$, defined on the closed domain $\overline{D_h^{\eta}}(X)$, which is zero on the boundary Γ^{η}, arbitrary (admissibly smooth) in the open domain $D_h^{\eta}(X)$ and on the seabed boundary Γ_h, and vanishes as $|\mathbf{x}| \to \infty$. Form Theorem 2.1, we conclude that there exists an admissible sequence, say $\delta\psi_n$, $n \geq -2$, such that $\delta\Psi = \sum_{n=-2}^{\infty} \delta\psi_n Z_n$. Multiplying the m^{th} equation of (3.29) by $\delta\psi_m$, integrating over X, and summing over m, we obtain:

$$\int_X \int_{-h}^{\eta} \Delta(\boldsymbol{\phi}^{\mathrm{T}}\boldsymbol{Z})\delta\Psi' dz d\mathbf{x} - \int_X N_h \cdot [\nabla\Phi]_{z=-h} \left[\delta\Psi'\right]_{z=-h} d\mathbf{x} = 0, \tag{3.30}$$

with $\delta\Psi' = \sum_{m=-2}^{\infty} \delta\psi_m(Z_m - Z_{m_*})$. Noting that $\delta\Psi' = \delta\Psi - Z_{m_*}\left[\delta\Psi\right]_{z=\eta}$ and $\left[\delta\Psi\right]_{z=\eta} = 0$ we observe that $\delta\Psi' = \delta\Psi$ and $\left[\delta\Psi'\right]_{z=\eta} = 0$. Thus, we deduce from equation (3.30), using classical variational arguments, that the function $\Phi = \boldsymbol{\phi}^{\mathrm{T}}\boldsymbol{Z}$ satisfies the Laplace equation (1.5) and the bottom impermeability condition (1.6). □

According to Lemma 3.2, $\Delta(\boldsymbol{\phi}^{\mathrm{T}}\boldsymbol{Z}) = 0$ and $N_h \cdot [\nabla(\boldsymbol{\phi}^{\mathrm{T}}\boldsymbol{Z})] = 0$, which implies, in view of identity (3.24), that $\sum_{n=-2}^{\infty} L_{mn}[\eta,h]\varphi_n = 0$, $m \geq -2$. Thus, the infinite system (3.26) can be stated as one evolution equation on η,

$$\partial_t\eta - N_\eta \cdot \left[\nabla(\boldsymbol{\phi}^{\mathrm{T}}\boldsymbol{Z})\right]_{z=\eta} = 0, \quad \mathbf{x} \in X, \tag{3.31}$$

which is just the kinematic free-surface kinematic condition (1.7) with $\Phi = \boldsymbol{\phi}^{\mathrm{T}}\boldsymbol{Z}$ and an infinite

system of time-independent equations on $\boldsymbol{\phi}$,

$$\sum_{n=-2}^{\infty} L_{mn}[\eta,h]\varphi_n = 0, \quad \mathbf{x}\in X, \quad m\geq -2, \tag{3.32}$$

which corresponds to the kinematical subproblem, Eqs. (1.5), (1.6). Moreover, identity (3.25) implies that $\sum_{n=-2}^{\infty}\ell_{mn}[\eta,h]\varphi_n = 0$, $m\geq -2$. Consequently the double infinite series appearing in Eq. (3.18) vanishes, leading eventually to

$$\left[\partial_t(\boldsymbol{\phi}^{\mathrm{T}}\boldsymbol{Z})\right]_{z=\eta} + g\eta + \frac{1}{2}\left[\nabla(\boldsymbol{\phi}^{\mathrm{T}}\boldsymbol{Z})\right]^2_{z=\eta} = -\frac{P_{\mathrm{surf}}}{\rho}, \tag{3.33}$$

which is the free surface dynamic condition, Eq. (1.8), with $\Phi = \boldsymbol{\phi}^{\mathrm{T}}\boldsymbol{Z}$. The set of equations (3.31)-(3.33), comprises a modal reformulation of the complete hydrodynamical problem through the enhanced eigenfunction expansion (2.4). In the next section, these equations will be further elaborated with purpose of deriving a more convenient, Hamiltonian formulation.

3.3 The Hamiltonian/Coupled-Mode System (HCMS)

In order to derive a Hamiltonian formulation, from Eqs. (3.31)-(3.33), we need to introduce the trace of the velocity potential, or equivalently, the trace of its series expansion (2.4), by

$$\psi(\mathbf{x},t) = [\Phi]_{z=\eta} = \boldsymbol{\phi}^{\mathrm{T}}\,[\boldsymbol{Z}]_{z=\eta} = \sum_{n=-2}^{\infty}\varphi_n(\mathbf{x},t), \tag{3.34}$$

where the normalization of the vertical functions $[Z_n]_{z=\eta} = 1$, $n\geq -2$ (see Eq. (2.6)) has been used in the last equality of (3.34). Then, we can prove the following

Lemma 3.3. *For each $t\in[t_0,t_1]$, the infinite system*

$$\sum_{n=-2}^{\infty} L_{mn}[\eta,h]\varphi_n = 0, \quad m\geq -2, \quad \mathbf{x}\in X, \tag{3.35a}$$

$$\sum_{n=-2}^{\infty}\varphi_n = \psi, \quad \mathbf{x}\in X, \tag{3.35b}$$

$$\sum_{n=-2}^{\infty}[T_{mn}\varphi_n]_{x_1=a} = g_m, \quad m\geq -2, \tag{3.35c}$$

$$\varphi_n\to 0,\ n\geq -2, \quad as \quad |x|\to\infty, \tag{3.35d}$$

is equivalent to the boundary value problem (1.23). That is, $\Phi = \boldsymbol{\phi}^T\boldsymbol{Z} = \sum_{n=-2}^{\infty}\varphi_n Z_n$ satisfies

$$\Delta\Phi = 0, \quad in \quad D_h^\eta, \tag{3.36a}$$

$$N_h\cdot[\nabla\Phi]_{z=-h} = 0, \tag{3.36b}$$

$$[\Phi]_{z=\eta} = \psi, \tag{3.36c}$$

$$[\partial_{x_1}\Phi]_{x_1=a} = V_a, \tag{3.36d}$$

$$\Phi \to 0, \quad as \quad |x| \to \infty. \tag{3.36e}$$

if and only if, $\boldsymbol{\phi} = \{\varphi_n\}_{n=-2}^{\infty}$ *satisfies the problem* (3.35).

Proof. Let Φ be the classical solution of problem (3.36), and consider its modal expansion, $\Phi = \boldsymbol{\phi}^{\mathrm{T}}\boldsymbol{Z}$, in accordance to Theorem 2.1. Then, since $[Z_n]_{z=\eta} = 1,\ n \geq -2$, we see at once that Eq. (3.36c) yields directly Eq. (3.35b). Moreover, with the aid of identity (3.24), we conclude that $\boldsymbol{\phi}$ satisfies the infinite system Eq. (3.35a), provided $\Phi = \boldsymbol{\phi}^{\mathrm{T}}\boldsymbol{Z}$ satisfies (3.36a), (3.36b). Boundary conditions (3.35c) are verified by multiplying (3.36d) by Z_m, integrating over $[-h_a, \eta_a]$ and recalling the definition of T_{mn}, Eq. (3.21).

Now suppose that the (admissible) sequence $\boldsymbol{\phi}$ satisfies Eqs. (3.35), and consider the field $\Phi = \boldsymbol{\phi}^{\mathrm{T}}\boldsymbol{Z}$. Then, using Eqs. (3.35d) we see at once that Eq. (3.36e) is satisfied. Moreover, since $[Z_n]_{z=\eta} = 1$, Eq. (3.35b) yields Eq. (3.36d). In order to prove Eqs. (3.36a), (3.36b) take an arbitrary admissible function $\delta\Psi$ defined on the closed domain $\overline{D_h^\eta}$. Applying Theorem 2.1 we conclude that there exists an admissible sequence $\delta\boldsymbol{\psi}$ such that $\delta\Psi = \delta\boldsymbol{\psi}^{\mathrm{T}}\boldsymbol{Z}$. Multiplying the m^{th} equation of (3.35a) by $\delta\psi_m$, integrating over X, and summing over m, we obtain an equation like Eq. (3.30) in the proof of Lemma 3.2 and we conclude by using the classical variational arguments. The lateral excitation condition (3.36c) is also easily obtained by using Eq. (3.35c) and the series expansion. □

Assuming that the system (3.35) is solved, for some (η, ψ) and g_m, then, we may assume as well that the solution sequence can be expressed as

$$\boldsymbol{\phi} = \{\varphi_n\}_{n=-2}^{\infty} = \boldsymbol{\mathscr{F}}[\eta, h]\psi = \{\mathscr{F}_n[\eta, h]\psi\}_{n=-2}^{\infty}, \tag{3.37}$$

where we have introduced the operator $\boldsymbol{\mathscr{F}}[\eta, h]$ that maps ψ to the modal sequence $\boldsymbol{\phi}$ that solves (3.35). With this convention, the remaining free surface conditions (3.31), (3.33) involve only the unknown fields (η, ψ) and the first one is already written as an evolution equation on η. In order to formulate Eq. (3.33) as an evolution equation on ψ, we first observe that for any smooth functions $\boldsymbol{\phi} = \{\varphi_n(\mathbf{x}, t)\}_n$ and $\boldsymbol{Z} = \{Z_n(z; \eta(\mathbf{x}, t), h(\mathbf{x}))\}_n$ the following identities hold

$$\left[\partial_t(\boldsymbol{\phi}^{\mathrm{T}}\boldsymbol{Z})\right]_{z=\eta} = \partial_t\left[\boldsymbol{\phi}^{\mathrm{T}}\boldsymbol{Z}\right]_{z=\eta} - \boldsymbol{\phi}^{\mathrm{T}}\left[\partial_z\boldsymbol{Z}\right]_{z=\eta}\partial_t\eta, \tag{3.38}$$

$$\left[\nabla_{\mathbf{x}}(\boldsymbol{\phi}^{\mathrm{T}}\boldsymbol{Z})\right]_{z=\eta} = \nabla_{\mathbf{x}}\left[\boldsymbol{\phi}^{\mathrm{T}}\boldsymbol{Z}\right]_{z=\eta} - \boldsymbol{\phi}^{\mathrm{T}}\left[\partial_z\boldsymbol{Z}\right]_{z=\eta}\nabla_{\mathbf{x}}\eta. \tag{3.39}$$

In order to prove Eq. (3.38), we first note that $\partial_t(\boldsymbol{\phi}^{\mathrm{T}}\boldsymbol{Z}) = \partial_t\boldsymbol{\phi}^{\mathrm{T}}\boldsymbol{Z} + \boldsymbol{\phi}^{\mathrm{T}}\partial_\eta\boldsymbol{Z}\partial_t\eta$, hence

$$\left[\partial_t(\boldsymbol{\phi}^{\mathrm{T}}\boldsymbol{Z})\right]_{z=\eta} = \partial_t\boldsymbol{\phi}^{\mathrm{T}}\left[\boldsymbol{Z}\right]_{z=\eta} + \boldsymbol{\phi}^{\mathrm{T}}\left[\partial_\eta\boldsymbol{Z}\right]_{z=\eta}\partial_t\eta. \tag{3.40}$$

Moreover, a straightforward application of the chain rule implies that

$$\partial_t \left[\boldsymbol{\phi}^{\mathrm{T}} \boldsymbol{Z}\right]_{z=\eta} = \partial_t \boldsymbol{\phi}^{\mathrm{T}} \left[\boldsymbol{Z}\right]_{z=\eta} + \boldsymbol{\phi}^{\mathrm{T}} \left[\partial_z \boldsymbol{Z} + \partial_\eta \boldsymbol{Z}\right]_{z=\eta} \partial_t \eta. \tag{3.41}$$

Combining the two last equations we obtain Eq. (3.38). Eq. (3.39) is proved similarly. Returning to Eqs. (3.31), (3.33), we take into account (3.38), (3.39) and (3.37), and after straightforward calculations, we arrive at the following

Theorem 3.1. *The water wave problem is equivalent with the following system of the two nonlinear operator partial differential equations*

$$\partial_t \eta = -\nabla_{\mathbf{x}} \eta \cdot \nabla_{\mathbf{x}} \psi + \left((\nabla_{\mathbf{x}} \eta)^2 + 1\right)\left(h_0^{-1} \mathscr{F}_{-2}[\eta, h]\psi + \mu_0 \psi\right), \quad \mathbf{x} \in X, \tag{3.42}$$

$$\partial_t \psi = -g\eta - \frac{1}{2}(\nabla_{\mathbf{x}} \psi)^2 + \frac{1}{2}\left((\nabla_{\mathbf{x}} \eta)^2 + 1\right)\left(h_0^{-1} \mathscr{F}_{-2}[\eta, h]\psi + \mu_0 \psi\right)^2, \quad \mathbf{x} \in X, \tag{3.43}$$

where $\mathscr{F}_{-2}[\eta, h]\psi$ is determined by solving the time independent coupled-mode problem (3.35).

The nonlocal evolution equations Eqs. (3.42), (3.43), together with the time independent substrate system (3.35), will be called *Hamiltonian/Coupled-Mode System* or HCMS for brevity. Comparing Eq. (3.42) with Eq. (1.26), we easily see that the standard DtN operator is given by

$$G[\eta, h]\psi = -\nabla_{\mathbf{x}} \eta \cdot \nabla_{\mathbf{x}} \psi + \left((\nabla_{\mathbf{x}} \eta)^2 + 1\right)\left(h_0^{-1} \mathscr{F}_{-2}[\eta, h]\psi + \mu_0 \psi\right). \tag{3.44}$$

Eq. (3.44) furnishes a new, modal characterisation of the DtN operator for water waves. In the next section, we give an alternative derivation of (3.44) by a direct variational reformulation of the boundary value problem (3.36).

3.4 On the modal characterization of the DtN operator

The series expansion (2.4) established in Chapter 2, can be employed for the exact reformulation of the boundary value problem (3.36) that defines the DtN operator. This is implemented here by using (2.4) in conjunction with a variational formulation of Eqs. (1.23) (see, e.g., (Babuška 1973)):

$$\delta \mathscr{I}[\Phi, \lambda; \delta\Phi, \delta\lambda] \equiv \delta_\Phi \mathscr{I}[\Phi, \lambda; \delta\Phi] + \delta_\lambda \mathscr{I}[\Phi, \lambda; \delta\lambda] = 0, \tag{3.45}$$

where the functional $\mathscr{I}[\Phi, \lambda]$ is given by

$$\begin{aligned} \mathscr{I}[\Phi, \lambda] =& \frac{1}{2}\int_X \int_{-h}^{\eta} |\nabla\Phi|^2 dz d\mathbf{x} - \int_X \lambda \left(\left[\Phi\right]_{z=\eta} - \psi\right) d\mathbf{x} \\ &+ \int_{\mathbb{R}} \int_{-h_a}^{\eta_a} V_a \left[\Phi\right]_{x_1=a} dz dx_2. \end{aligned} \tag{3.46}$$

Note that, in the above variational formulation, Dirichlet boundary condition is introduced into the functional by means of the Lagrange multiplier $\lambda = \lambda(\mathbf{x}, t)$, leaving Φ unconstrained throughout the closed domain $\overline{D_h^\eta}(X)$, apart from the vanishing at infinity condition $\nabla\Phi \to 0$ as $|\mathbf{x}| \to \infty$. Calculating the first variations of the functional $\mathscr{J}$, in the usual way, we find

$$\begin{aligned}\delta_\Phi \mathscr{J}\left[\Phi, \lambda; \delta\Phi\right] = &- \int_X \int_{-h}^{\eta} \Delta\Phi\delta\Phi dz d\mathbf{x} - \int_X \Big(\lambda - N_\eta \cdot \left[\nabla\Phi\right]_{z=\eta}\Big) \left[\delta\Phi\right]_{z=\eta} \\ &+ \int_X N_h \cdot \left[\nabla\Phi\right]_{z=-h} \left[\delta\Phi\right]_{z=-h} + \int_{\mathbb{R}} \int_{-h_a}^{\eta_a} \Big(- \left[\partial_{x_1}\Phi\right]_{x_1=a} + V_a\Big) \left[\delta\Phi\right]_{x_1=a}\end{aligned} \tag{3.47}$$

$$\delta_\lambda \left[\Phi, \lambda; \delta\lambda\right] = - \int_X \Big(\left[\Phi\right]_{z=\eta} - \psi\Big) \delta\lambda d\mathbf{x}. \tag{3.48}$$

Taking into account Eqs. (3.47), (3.48), the two partial variational equations $\delta_\Phi \mathscr{J}\left[\Phi, \lambda; \delta\Phi\right] = 0$ and $\delta_\lambda \left[\Phi, \lambda; \delta\lambda\right] = 0$, in conjunction with arbitrariness of $\delta\Phi$ and $\delta\lambda$, prove that the variational principle (3.45) is equivalent to the boundary value problem (3.36) and, moreover, the equation

$$\lambda = N_\eta \cdot \left[\nabla\Phi\right]_{z=\eta}. \tag{3.49}$$

The last equation provides a physical interpretation of the Lagrange multiplier $\lambda = \lambda(\boldsymbol{x}, t)$. In fact λ is an alternative representation of the DtN operator (1.22), that is

$$\lambda = G[\eta, h]\psi. \tag{3.50}$$

We shall now apply the variational formulation (3.45) in conjunction with the series representation of the velocity potential (2.4), in order to prove that the sequence $\{\varphi_n\}_{n=-2}^{\infty}$ solves the system (3.35) and the DtN operator $G[\eta, h]\psi$ is given by (3.44). Under the transformation $\Phi \to \boldsymbol{\phi}$ the functional $\mathscr{J}$ takes the form

$$\tilde{\mathscr{J}}[\boldsymbol{\phi}, \lambda] = \mathscr{J}\left[\boldsymbol{\phi}^{\mathrm{T}}\boldsymbol{Z}, \lambda\right]. \tag{3.51}$$

As in the previous section, the assumptions stated in Theorem 2.2, allow termwise differentiation and integration of the infinite series (2.4), after the substitution $\Phi = \boldsymbol{\phi}^{\mathrm{T}}\boldsymbol{Z}$, in the right hand side of of Eq. (3.46). Thus, Φ satisfies (3.45) if and only if $\boldsymbol{\phi}$ satisfies

$$\delta\tilde{\mathscr{J}}[\boldsymbol{\phi}, \lambda; \delta\boldsymbol{\phi}, \delta\lambda] \equiv \delta_{\boldsymbol{\phi}}\tilde{\mathscr{J}}[\boldsymbol{\phi}, \lambda; \delta\boldsymbol{\phi}] + \delta_\lambda\tilde{\mathscr{J}}[\boldsymbol{\phi}, \lambda; \delta\lambda] \tag{3.52}$$

$$= \sum_{m=-2}^{\infty} \delta_{\varphi_m}\tilde{\mathscr{J}}\left[\boldsymbol{\phi}, \lambda; \delta\varphi_m\right] + \delta_\lambda\tilde{\mathscr{J}}[\boldsymbol{\phi}, \lambda; \delta\lambda] = 0, \tag{3.53}$$

Performing the variations indicated above, we easily obtain the following Euler-Lagrange equations

$$\int_{-h}^{\eta} \Delta(\boldsymbol{\phi}^{\mathrm{T}}\boldsymbol{Z}) Z_m dz - N_h \cdot \left[\nabla(\boldsymbol{\phi}^{\mathrm{T}}\boldsymbol{Z})\right]_{z=-h} = -\lambda + N_\eta \cdot \left[\nabla(\boldsymbol{\phi}^{\mathrm{T}}\boldsymbol{Z})\right]_{z=\eta},\ m \geq -2,\ \boldsymbol{x} \in X, \tag{3.54a}$$

$$\sum_{n=-2}^{\infty} \varphi_n \left[Z_n\right]_{z=\eta} = \psi. \tag{3.54b}$$

$$\int_{-h_a}^{\eta_a} \left(\left[\partial_{x_1}(\boldsymbol{\phi}^{\mathrm{T}}\boldsymbol{Z})\right]_{x_1=a} - V_a \right) \left[Z_m\right]_{x_1=a} dz = 0, \quad m \geq -2, \quad x_2 \in \mathbb{R}. \tag{3.54c}$$

Observe now that the right hand side of Eq. (3.54a) is zero because of Eq. (3.49). Consequently Eq. (3.54a) takes the form

$$\int_{-h}^{\eta} \Delta(\boldsymbol{\phi}^{\mathrm{T}}\boldsymbol{Z}) Z_m dz - N_h \cdot \left[\nabla(\boldsymbol{\phi}^{\mathrm{T}}\boldsymbol{Z}) Z_m\right]_{z=-h} = 0, \ m \geq -2, \ \boldsymbol{x} \in X. \tag{3.55}$$

Performing similar calculations as in the derivation of (3.16), the above equations are easily identified with (3.35a). Similarly, we also see that Eq. (3.54c) is identical to (3.35c). Recalling finally that $\left[Z_n\right]_{z=\eta} = 1$, we obtain (3.35b) from (3.54b). It remains to prove the modal form of the DtN operator, Eq. (3.44). Substituting the modal expansion into the right-hand side of Eq. (3.49), and taking into account the condition $\left[Z_n\right]_{z=\eta} = 1$, we find

$$G[\eta,h]\psi = -\nabla_{\mathbf{x}}\eta \cdot \sum_{n=-2}^{\infty} \left(\nabla_{\mathbf{x}}\varphi_n + \varphi_n \left[\nabla_{\mathbf{x}} Z_n\right]_{z=\eta} \right) + \sum_{n=-2}^{\infty} \varphi_n \left[\partial_z Z_n\right]_{z=\eta}. \tag{3.56}$$

The expression in the above right hand side is greatly simplified by using the analytical expressions for the values of $\partial_z Z_n$ and $\nabla_{\mathbf{x}} Z_n$ on the free surface. These are given by

$$\left[\nabla Z_n\right]_{z=\eta} = \begin{pmatrix} -\mu_0 \nabla_{\mathbf{x}}\eta \\ \mu_0 \end{pmatrix}, \quad n \geq 0, \tag{3.57a}$$

$$\left[\nabla Z_{-2}\right]_{z=\eta} = \begin{pmatrix} -\left(\mu_0 + h_0^{-1}\right) \nabla_{\mathbf{x}}\eta \\ \mu_0 + h_0^{-1} \end{pmatrix}, \tag{3.57b}$$

$$\left[\nabla Z_{-1}\right]_{z=\eta} = \begin{pmatrix} -\mu_0 \nabla_{\mathbf{x}}\eta \\ \mu_0 \end{pmatrix}. \tag{3.57c}$$

Substituting Eqs. (3.57) into Eq. (3.56), and interchanging differentiations with the infinite summation, which is permissible under the considered smoothness assumptions (Corollary 2.2), we obtain

$$G[\eta,h]\psi = -\nabla_{\mathbf{x}}\eta \cdot \sum_{n=-2}^{\infty} \nabla_{\mathbf{x}}\varphi_n + (\nabla_{\mathbf{x}}\eta)^2 \left(\mu_0 \sum_{n=-2}^{\infty} \varphi_n + h_0^{-1}\varphi_{-2} \right) + \mu_0 \sum_{n=-2}^{\infty} \varphi_n + h_0^{-1}\varphi_{-2}. \tag{3.58}$$

Finally, using $\psi = \sum_{n=-2}^{\infty} \varphi_n$, Eq. (3.58) becomes

$$G[\eta,h]\psi = -\nabla_{\mathbf{x}}\eta \cdot \nabla_{\mathbf{x}}\psi + \left((\nabla_{\mathbf{x}}\eta)^2 + 1\right)\left(h_0^{-1}\mathscr{F}_{-2}[\eta,h]\psi + \mu_0\psi\right), \tag{3.59}$$

which is the same as Eq. (3.44), since $\varphi_{-2} = \mathscr{F}_{-2}[\eta, h]\psi$ by definition.

3.5 Dispersive properties of the linearised HCMS above flat bottom

In this section, we investigate the dispersive properties of the linearised HCMS in the case of a flat horizontal bottom $\{z = -h_0\}$. In order to answer this question, we follow the analysis of (Belibassakis & Athanassoulis 2011, Section 4.2). Linearising Eqs. (3.42), (3.43) around $(\eta, \psi) = (0, 0)$ we get

$$\partial_t \eta - \left(h_0^{-1} \mathscr{F}_{-2}\left[0, h\right] + \mu_0 \right) \psi = 0, \tag{3.60}$$

$$\partial_t \psi + g\eta = 0, \tag{3.61}$$

where $\mathscr{F}_{-2}\left[0, h\right]\psi$, is the first term of the sequence $\varphi_n = \mathscr{F}_n[0, h]\psi, \quad n \geq -2$, determined by solving the linearized version of the coupled mode substrate system (3.35) on X,

$$\sum_{n=-2}^{\infty} A_{mn}(0, h)\partial_x^2 \varphi_n + B_{mn}(0, h)\partial_x \varphi_n + C_{mn}(0, h)\varphi_n = 0, \quad m \geq -2, \tag{3.62a}$$

$$\sum_{n=-2}^{\infty} \varphi_n = \psi, \tag{3.62b}$$

in conjunction with horizontal periodicity assumptions. It is recalled that the coefficients A_{mn}, B_{mn}, C_{mn}, are formally defined by Eqs. (3.22) and, in the general case, are expressed in terms of $(\eta, h) = (\eta(x, t), h(x))$, $k_n(\eta, h)$ and μ_0 (see Appendix F). In the above special case of linear waves above a variable bottom, A_{mn}, B_{mn}, C_{mn} are just x- dependent functions given in terms of h and μ_0. The further simplification of bottom flatness, $h = h_0$ with $\partial_x h_0 = 0$, leads to $B_{mn}(0, h_0) = 0$ and $C_{mn}(0, h_0) = \int_{-h_0}^{0} \partial_z^2 Z_n Z_m dz$ for any $m, n \geq -2$ (see also Eq. (4.8)). Thus, $A_{mn}(0, h_0)$ and $C_{mn}(0, h_0)$ are constant coefficients that depend solely on h_0, $k_n(h_0)$ and μ_0. They are easily calculated from the results of Appendix F and are given below

$$A = \begin{pmatrix} A_{-2,-2} & A_{-2,-1} & \frac{2\mu_0 a}{h_0 k_0^4} - \frac{1}{h_0 k_0^2} & \frac{2\mu_0 a}{h_0 k_1^4} + \frac{1}{h_0 k_1^2} & \frac{2\mu_0 a}{h_0 k_2^4} + \frac{1}{h_0 k_2^2} & \cdots \\ & A_{-1,-1} & \frac{2\mu_0 b}{k_0^4 h_0} - \frac{\operatorname{sech}(k_0 h_0)}{h_0 k_0^2} & \frac{2\mu_0 b}{k_1^4 h_0} + \frac{\operatorname{sech}(k_1 h_0)}{h_0 k_1^2} & \frac{2\mu_0 b}{k_2^4 h_0} + \frac{\operatorname{sech}(k_2 h_0)}{h_0 k_2^2} & \cdots \\ & & \frac{h_0}{2} - \frac{h\mu_0^2 - \mu_0}{2k_0^2} & 0 & 0 & \cdots \\ & & & \frac{h_0}{2} + \frac{h\mu_0^2 - \mu_0}{2k_1^2} & 0 & \cdots \\ & & & & \frac{h_0}{2} + \frac{h\mu_0^2 - \mu_0}{2k_2^2} & \cdots \\ & & & & & \ddots \end{pmatrix}, \tag{3.63}$$

$$\begin{pmatrix} A_{-2,-2} & A_{-2,-1} \\ & A_{-1,-1} \end{pmatrix} = \begin{pmatrix} \frac{2\mu_0^2 h_0^3}{15} - \frac{2\mu_0 h_0^2}{5} + \frac{7h_0}{15} & \frac{2\mu_0^2 h_0^3}{15} - \frac{11\mu_0 h_0^2}{24} + \frac{23h_0}{40} \\ & \frac{2\mu_0^2 h_0^3}{15} - \frac{31\mu_0 h_0^2}{64} + \frac{43h_0}{40} \end{pmatrix},$$

$$C = \begin{pmatrix} C_{-2,-2} & C_{-2,-1} & k_0^2 A_{-2,0} & -k_1^2 A_{-2,1} & -k_2^2 A_{-2,2} & \dots \\ C_{-1,-2} & C_{-1,-1} & k_0^2 A_{-2,0} & -k_1^2 A_{-1,1} & -k_2^2 A_{-1,2} & \dots \\ \frac{2a\mu_0}{h_0 k_0^2} & \frac{2b\mu_0}{h_0 k_0^2} & k_0^2 A_{00} & 0 & 0 & \dots \\ -\frac{2a\mu_0}{h_0 k_1^2} & -\frac{2b\mu_0}{h_0 k_1^2} & 0 & -k_1^2 A_{11} & 0 & \dots \\ -\frac{2a\mu_0}{h_0 k_2^2} & -\frac{2b\mu_0}{h_0 k_2^2} & 0 & 0 & -k_2^2 A_{22} & \dots \\ \vdots & \vdots & \vdots & \vdots & \vdots & \ddots \end{pmatrix},$$

$$\begin{pmatrix} C_{-2,-2} & C_{-2,-1} \\ C_{-1,-2} & C_{-1,-1} \end{pmatrix} = \begin{pmatrix} -\frac{\mu_0^2 h_0}{3} + \frac{2}{3h_0} + \frac{\mu_0}{3} & -\frac{\mu_0^2 h_0}{3} - \frac{2}{3h_0} + \mu_0 \\ -\frac{\mu_0^2 h_0}{3} - \frac{1}{6h_0} + \frac{\mu_0}{2} & -\frac{\mu_0^2 h_0}{3} + \frac{1}{6h_0} + \frac{\mu_0}{6} \end{pmatrix}.$$

The determination of the infinite matrices A and C requires the parameters $k_n = k_n(0, h_0)$, $n \geq 0$, which are positive real numbers ($\partial_{x_i} k_n = \partial_{x_i}^2 k_n = 0$) obtained as the solutions of the transcendental equations

$$\mu_0 - k_0 \tanh(k_0 h_0) = 0, \quad \mu_0 + k_n \tan(k_n h_0) = 0,$$

for some $\mu_0 > 0$.

In order to investigate the dispersive properties of the above linearized formulation, Eqs. (3.60), (3.61) and (3.62), we consider *plane wave* solutions of the form

$$(\eta(x,t), \psi(x,t)) = \left(\tilde{\eta}, \tilde{\psi}\right) e^{i(\kappa x - \omega t)}, \tag{3.63}$$

where $(\tilde{\eta}, \tilde{\psi})$ are nonzero real numbers. This implies that the solution of the linear substrate system (3.62) is of the form $\varphi_n(x,t) = \tilde{\varphi}_n e^{i(\kappa x - \omega t)}$, $n \geq -2$, where $\tilde{\varphi_n}$ satisfies the algebraic system

$$\sum_{n=-2}^{\infty} \left(-\kappa^2 A_{mn}(0, h_0) + C_{mn}(0, h_0)\right) \tilde{\varphi_n} = 0, \quad m \geq -2, \tag{3.64a}$$

$$\sum_{n=-2}^{\infty} \tilde{\varphi_n} = \tilde{\psi}. \tag{3.64b}$$

Upon the linear transformation $\tilde{\phi}_n = \tilde{\varphi}_n/\tilde{\psi}$, the above system is equivalent to

$$\sum_{n=-2}^{\infty} \left(-\kappa^2 A_{mn}(0,h_0) + C_{mn}(0,h_0)\right) \tilde{\phi}_n = 0, \quad m \geq -2, \tag{3.65a}$$

$$\sum_{n=-2}^{\infty} \tilde{\phi}_n = 1. \tag{3.65b}$$

which can be solved for different values of κ and h_0, once μ_0 is specified. Thus,

$$\mathscr{F}_n[0,h_0]\psi = \tilde{\phi}_n \tilde{\psi} e^{i(\kappa x - \omega t)}, \quad n \geq -2, \tag{3.66}$$

and the evolutionary system (3.60), (3.61) takes the form

$$-i\omega\tilde{\eta} - \left(h_0^{-1}\tilde{\phi}_{-2} + \mu_0\right)\tilde{\psi} = 0, \tag{3.67a}$$

$$-i\omega\tilde{\psi} + g\tilde{\eta} = 0. \tag{3.67b}$$

The vanishing of the determinant of system (3.67) leads to the following dispersion relation

$$\omega(\kappa) = \left(g\left(h_0^{-1}\tilde{\phi}_{-2}(\kappa, h_0, \mu_0) + \mu_0\right)\right)^{1/2}, \tag{3.68}$$

where we have emphasized the dependence of $\tilde{\varphi}_{-2}$ on κ, h_0 and μ_0. The next proposition verifies that (3.68) is the dispersion relation of water waves.

Proposition 3.1. *Let $\mu_0 > 0$. Then (3.68) is identical to $\omega(\kappa) = (gh_0 \tanh(\kappa h_0))^{1/2}$*

Proof. Let us start from the observation that a solution of the system (3.62), with $\psi = \tilde{\psi} e^{i(\kappa x - \omega t)}$, is obtained as the modal decomposition $\boldsymbol{\phi} = \{\varphi_n\}_{n=-2}^{\infty}$ of

$$\Phi = \frac{\cosh\left(\kappa(z+h_0)\right)}{\cosh\left(\kappa h_0\right)} \tilde{\psi} e^{i(\kappa x - \omega t)},$$

furnished by Theorem 2.1. Indeed, since $\Phi = \boldsymbol{\phi}^{\mathrm{T}}\boldsymbol{Z} = \sum_{n=-2}^{\infty} \varphi_n Z_n$, we get that $\Delta(\boldsymbol{\phi}^{\mathrm{T}}\boldsymbol{Z}) = \Delta\Phi = 0$ and $\left[\partial_z\left(\boldsymbol{\phi}^{\mathrm{T}}\boldsymbol{Z}\right)\right]_{z=-h_0} = [\partial_z\Phi]_{z=-h_0} = 0$, and we easily deduce from identity (3.24) that Eqs. (3.62a) are satisfied. Eq. (3.62b) is obtained by recalling that $Z_n = 1$, $n \geq -2$, which implies that $[\Phi]_{z=0} = \left[\boldsymbol{\phi}^{\mathrm{T}}\boldsymbol{Z}\right]_{z=0} = \sum_{n=-2}^{\infty} \varphi_n$. Thus, taking into account Eqs. (2.10) and (2.12) of Theorem 2.1, we find that $\boldsymbol{\phi}$ is explicitly given by

$$\varphi_{-2} = h_0\left(\kappa\tanh(\kappa h_0) - \mu_0\right)\tilde{\psi} e^{i(\kappa x - \omega t)}, \tag{3.69a}$$

$$\varphi_{-1} = 0, \tag{3.69b}$$

$$\varphi_0 = \left[\frac{\kappa\tanh(\kappa h_0) - \mu_0}{\kappa^2 - k_0^2} - h_0\left(\kappa\tanh(\kappa h_0) - \mu_0\right)A_{-2,0}\right]\frac{\tilde{\psi}}{A_{00}} e^{i(\kappa x - \omega t)}, \tag{3.69c}$$

$$\varphi_n = \left[\frac{\kappa\tanh(\kappa h_0) - \mu_0}{\kappa^2 + k_n^2} - h_0\left(\kappa\tanh(\kappa h_0) - \mu_0\right)A_{-2,n}\right]\frac{\tilde{\psi}}{A_{nn}} e^{i(\kappa x - \omega t)}, \quad n \geq 1. \tag{3.69d}$$

Noting that the plane wave assumption (3.63) in conjunction with Eq. (3.69a), implies that $\tilde{\varphi}_{-2} = h_0\left(\kappa\tanh(\kappa h_0) - \mu_0\right)\tilde{\psi}$, the system (3.67) becomes

$$\begin{aligned} -i\omega\tilde{\eta} - \kappa\tanh(\kappa h_0)\tilde{\psi} &= 0, \\ -i\omega\tilde{\psi} + g\tilde{\eta} &= 0, \end{aligned}$$

and the result follows by requiring the determinant of this system to vanish. □

The essence of the above proposition is that, in the linear limit, HCMS is equivalent with the water wave equations. Eventually, a natural question arises concerning the sensitivity of the dispersive properties of HCMS to the choice of μ_0 and the order of truncation of the infinite algebraic system (3.65). In order to investigate this, let us fix a constant depth $h_0 = 1$ m and choose three dimensionless values for $\mu_0 h_0 = 0.1\pi, \pi, 2\pi$. The system (3.65) is truncated by retaining Eqs. (3.65a) for $m = -2, -1, ..., N_{\text{tot}} - 1$, where N_{tot} denotes the total number of terms retained the expansion. This system, together with the truncated version of (3.65b), $\sum_{n=-2}^{N_{\text{tot}}} \varphi_n' = 1$ (see also Chapter 5) is a square linear algebraic system which can be solved for different values of κh_0. Its solution yields a numerical approximation of $\tilde{\phi}_n$, $n \geq -2$ denoted by $\tilde{\phi}_n(\kappa, h_0, \mu_0; N_{\text{tot}})$ and a corresponding approximate dispersion relation which is written as

$$\omega(\kappa; N_{\text{tot}}) = \left(g\left(h_0^{-1}\tilde{\phi}_{-2}(\kappa, h_0, \mu_0; N_{\text{tot}}) + \mu_0\right)\right)^{1/2}. \tag{3.70}$$

It follows that plane waves of the truncated linearized HCMS move with a phase velocity $C^{(N_{\text{tot}})} = \omega(\kappa; N_{\text{tot}})/\kappa$ given by

$$\frac{C^{(N_{\text{tot}})}}{(gh_0)^{1/2}} = \frac{\left(\tilde{\phi}_{-2}(\kappa, h_0, \mu_0; N_{\text{tot}}) + \mu_0 h_0\right)^{1/2}}{(\kappa h_0)^{1/2}(\kappa h_0)^{1/2}}. \tag{3.71}$$

The latter is plotted in the left column of Figure 3.1 together with the exact velocity

$$\frac{C_{\text{WW}}}{(gh_0)^{1/2}} = \frac{(\tanh(\kappa h_0))^{1/2}}{(\kappa h_0)^{1/2}} \tag{3.72}$$

predicted by the linearized water wave equations. Their relative error

$$|1 - \frac{C^{(N_{\text{tot}})}}{C_{WW}}|, \tag{3.73}$$

is shown at the right column of Figure 3.1 in a semilog scale. It is observed that $C^{(N_{\text{tot}})}$ tends to the exact one as N_{tot} increases for all choices of μ_0. When N_{tot} is small, $\omega(\kappa; N_{\text{tot}})$ becomes purely imaginary in a small neighbourhood of $\kappa h_0 = 0$ which grows for increasing μ_0 but shrinks to zero for increasing N_{tot}. A fairly small number of terms ($N_{\text{tot}} = 6 - 8$) is sufficient for the accurate reproduction of the exact velocity in a fairly large range κh_0. In the left column of

Figure 3.1, it is clearly observed that the relative error for increasing N_{tot} always attains a minimum exactly at the value $\kappa h_0 = k_0^* h_0$, where k_0^* denotes the solution of $k_0^* \tanh(k_0^* h) = \mu_0$ for different values of μ_0. This suggests that when N_{tot} is small the region of the highest accuracy of the truncated system is restricted around $k_0^* h_0$. However, as N_{tot} increases, the relative error around $k_0^* h_0$ reaches the precision of our machine and becomes almost independent on κh_0 (in fact it hardly exceeds 10^{-12} for limiting values of κh_0).

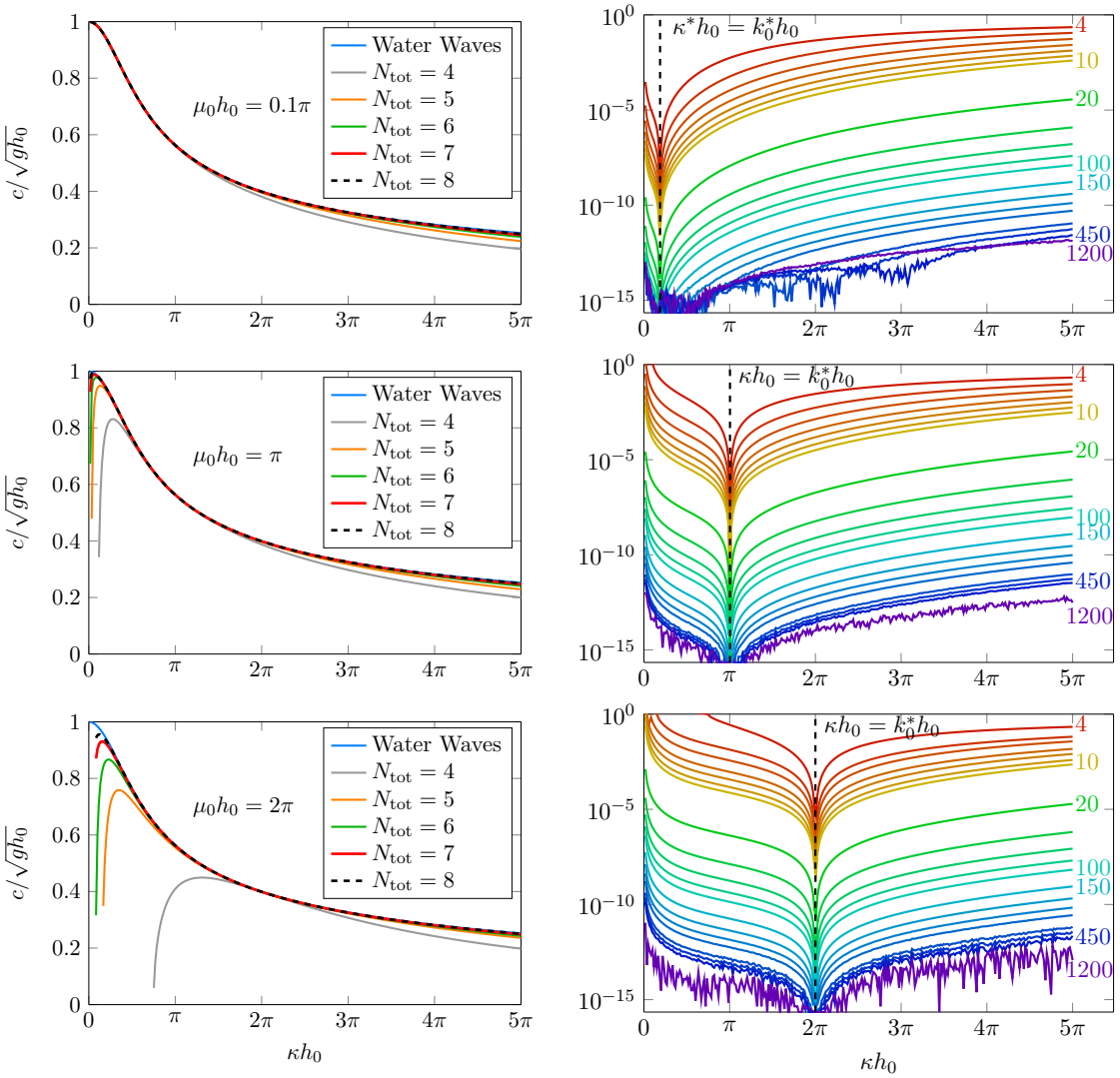

Figure 3.1: Linear phase velocity predicted by HCMS (left) and relative error in semilog scale (right) for $\mu_0 = 0.1\pi, \pi, 2\pi$. The vertical dashed lines correspond to the lines $\kappa h_0 = k_0^* h_0$, where k_0^* denotes the solution of $k_0^* \tanh(k_0^* h) = \mu_0$ for the different values of μ_0.

Chapter 4

Derivation of simple model equations by means of the new variational equations

In this chapter, the Euler-Lagrange equations (3.16)-(3.18), which were derived on the basis of a generic series representation $\Phi(\mathbf{x}, z, t) = \sum_n \varphi_n(\mathbf{x}, t) Z_n(z; \eta(\mathbf{x}, t), h(\mathbf{x}))$, are applied for the case of series representations which are assumed finite. In this framework, the undetermined functions $\varphi_n(\mathbf{x}, t)$ are not a priori defined in terms of the unknown velocity potential Φ and most importantly a notion of convergence of the finite series does not exist. Such a choice is understood as an ansatz and the physical relevance of the resulting models is left to be examined a posteriori. For the remainder of this chapter, we take $P_{\text{surf}} = 0$ and work in the case of a horizontally unbounded fluid, thus the matching boundary condition (3.17) is replaced by vanishing at infinity conditions.

Let us start by rewriting (3.16), (3.18) in a form where the space and time derivatives of the free surface elevation η and bottom surface h appear explicitly. This becomes possible after expanding the horizontal and time derivative of $Z_n(z; \eta, h)$ using the chain rule:

$$\partial_{x_i} Z_n = \partial_\eta Z_n \partial_{x_i} \eta + \partial_h Z_n \partial_{x_i} h, \tag{4.1}$$

$$\begin{aligned} \partial^2_{x_i} Z_n = {} & \partial^2_\eta Z_n (\partial_{x_i} \eta)^2 + \partial_\eta Z_n (\partial^2_{x_i} \eta) + 2 \partial_{\eta\, h} Z_n (\partial_{x_i} \eta)(\partial_{x_i} h) \\ & + \partial^2_h Z_n (\partial_{x_i} h)^2 + \partial_h Z_n (\partial^2_{x_i} h), \end{aligned} \tag{4.2}$$

$$\partial_t Z_n = \partial_\eta Z_n \partial_t \eta. \tag{4.3}$$

By direct differentiation and use of (4.3) one obtains the following expression for the time derivative of the approximate velocity potential

$$\partial_t (\boldsymbol{\phi}^{\mathrm{T}} \boldsymbol{Z}) = \partial_t \boldsymbol{\phi}^{\mathrm{T}} \boldsymbol{Z} + \boldsymbol{\phi}^{\mathrm{T}} \partial_t \boldsymbol{Z} = \partial_t \boldsymbol{\phi}^{\mathrm{T}} \boldsymbol{Z} + \boldsymbol{\phi}^{\mathrm{T}} \partial_\eta \boldsymbol{Z} \partial_t \eta, \tag{4.4}$$

Similarly, using (4.1), the gradient of the approximate velocity potential, takes the form

$$\nabla\left(\boldsymbol{\phi}^{\mathrm{T}}\boldsymbol{Z}\right)=\begin{pmatrix}\nabla_{\mathbf{x}}\boldsymbol{\phi}^{\mathrm{T}}\boldsymbol{Z}+\boldsymbol{\phi}^{\mathrm{T}}\nabla_{\mathbf{x}}\boldsymbol{Z}\\ \boldsymbol{\phi}^{\mathrm{T}}\partial_z\boldsymbol{Z}\end{pmatrix}=\begin{pmatrix}\nabla_{\mathbf{x}}\boldsymbol{\phi}^{\mathrm{T}}\boldsymbol{Z}+\boldsymbol{\phi}^{\mathrm{T}}\partial_\eta\boldsymbol{Z}\nabla_{\mathbf{x}}\eta+\boldsymbol{\phi}^{\mathrm{T}}\partial_h\boldsymbol{Z}\nabla_{\mathbf{x}}h\\ \boldsymbol{\phi}^{\mathrm{T}}\partial_z\boldsymbol{Z}\end{pmatrix}. \tag{4.5}$$

Using Eq. (4.3) in Eq. (3.18), Eqs. (3.16) and (3.18) yield

$$\left(\partial_t\eta-N_\eta\cdot\left[\nabla(\boldsymbol{\phi}^{\mathrm{T}}\boldsymbol{Z})\right]_\eta\right)[Z_m]_\eta+\sum_n L_{mn}\varphi_n=0, \tag{4.6}$$

$$\partial_t\boldsymbol{\phi}^{\mathrm{T}}[\boldsymbol{Z}]_\eta+g\eta+\frac{1}{2}[\nabla(\boldsymbol{\phi}^{\mathrm{T}}\boldsymbol{Z})]^2_\eta+N_\eta\cdot\left[\nabla(\boldsymbol{\phi}^{\mathrm{T}}\boldsymbol{Z})(\boldsymbol{\phi}^{\mathrm{T}}\partial_\eta\boldsymbol{Z})\right]_\eta-\sum_m(\sum_n l_{mn}\varphi_n)\varphi_m=0, \tag{4.7}$$

where we have further abbreviated the notation of the trace from $[\,]_{z=\eta}$ to $[\,]_\eta$. At this point, we shall also reformulate the matrix coefficients A, B, C, Eqs. (3.22a)-(3.23c), of the operators L_{mn} and l_{mn} appearing above. Substituting (4.1) and (4.2) in (3.22a)-(3.23c), we find

$$A_{mn}=\int_{-h}^{\eta}Z_nZ_m dz, \tag{4.8a}$$

$$B^i_{mn}=2\partial_{x_i}h\int_{-h}^{\eta}\partial_hZ_nZ_m dz+2\partial_{x_i}\eta\int_{-h}^{\eta}\partial_\eta Z_nZ_m dz+\partial_{x_i}h\left[Z_nZ_m\right]_{z=-h}, \tag{4.8b}$$

$$\begin{aligned}C_{mn}=&(\nabla_x h)^2\int_{-h}^{\eta}\partial_h^2Z_nZ_m dz+(\nabla_x^2h)\int_{-h}^{\eta}\partial_hZ_nZ_m dz+(\nabla_x\eta)^2\int_{-h}^{\eta}\partial_\eta^2Z_nZ_m dz\\&+(\nabla_x^2\eta)\int_{-h}^{\eta}\partial_\eta Z_nZ_m dz+2(\nabla_x h)\cdot(\nabla_x\eta)\int_{-h}^{\eta}\partial^2_{h\eta}Z_nZ_m dz+\int_{-h}^{\eta}\partial_z^2Z_nZ_m dz\\&+(\nabla_{\mathbf{x}}h)^2\left[\partial_hZ_nZ_m\right]_{z=-h}+(\nabla_{\mathbf{x}}h)\cdot(\nabla_{\mathbf{x}}\eta)\left[\partial_\eta Z_nZ_m\right]_{z=-h}+\left[\partial_zZ_nZ_m\right]_{z=-h},\end{aligned} \tag{4.8c}$$

$$a_{mn}=\int_{-h}^{\eta}Z_n\partial_\eta Z_m dz, \tag{4.9a}$$

$$b^i_{mn}=2\partial_{x_i}\eta\int_{-h}^{\eta}\partial_\eta Z_n\partial_\eta Z_m dz+2\partial_{x_i}h\int_{-h}^{\eta}\partial_hZ_n\partial_\eta Z_m dz+\partial_{x_i}h\left[Z_n\partial_\eta Z_m\right]_{z=-h} \tag{4.9b}$$

$$\begin{aligned}c_{mn}=&(\nabla_x h)^2\int_{-h}^{\eta}\partial_h^2Z_n\partial_\eta Z_m dz+(\nabla_x^2h)\int_{-h}^{\eta}\partial_hZ_n\partial_\eta Z_m dz+(\nabla_x\eta)^2\int_{-h}^{\eta}\partial_\eta^2Z_n\partial_\eta Z_m dz\\&+(\nabla_x^2\eta)\int_{-h}^{\eta}\partial_\eta Z_nZ_m dz+2(\nabla_x h)\cdot(\nabla_x\eta)\int_{-h}^{\eta}\partial^2_{h\eta}Z_n\partial_\eta Z_m dz+\int_{-h}^{\eta}\partial_z^2Z_n\partial_\eta Z_m dz\\&+(\nabla_{\mathbf{x}}h)^2\left[\partial_hZ_n\partial_\eta Z_m\right]_{z=-h}+(\nabla_{\mathbf{x}}h)\cdot(\nabla_{\mathbf{x}}\eta)\left[\partial_\eta Z_n\partial_\eta Z_m\right]_{z=-h}+\left[\partial_zZ_n\partial_\eta Z_m\right]_{z=-h}.\end{aligned} \tag{4.9c}$$

Assuming now that the smooth vertical functions $Z_n(z;\eta,h)$, for any n, do not depend explicitly on the derivatives (slopes) of η and h, it is easily seen that the above matrix functions have the following order

$$A_{mn}=O(1),\quad B^i_{mn}=O(|\partial_{x_i}\eta|,|\partial_{x_i}h|),\qquad C_{mn}=O(|\nabla_{\mathbf{x}}\eta|^2,|\nabla_{\mathbf{x}}h|^2,\Delta_{\mathbf{x}}\eta,\Delta_{\mathbf{x}}h), \tag{4.10}$$

$$a_{mn}=O(1),\quad b^i_{mn}=O(|\partial_{x_i}\eta|,|\partial_{x_i}h|),\qquad c_{mn}=O(|\nabla_{\mathbf{x}}\eta|^2,|\nabla_{\mathbf{x}}h|^2,\Delta_{\mathbf{x}}\eta,\Delta_{\mathbf{x}}h). \tag{4.11}$$

In the next section, we shall derive two different formal results, already appeared in literature, as special cases of Eqs. (4.6), (4.7).

4.1 Derivation of some existing models

In an attempt to derive extended versions of classical water wave models, (Isobe & Abohadima 1998) and (Klopman et al. 2010) called herein IA98 and KVGD10, invoked Luke's variational principle in conjunction with finite series representations of the velocity potential and appropriate simplifications. In this section, we shall briefly present how one can obtain the results of the aforementioned works from Eqs. (4.6), (4.7).

Euler-Lagrange equations of IA98

Following IA98, we represent the velocity potential by the following expression

$$\Phi(x,z,t)=\sum_{n=1}^{N}\varphi_n(x,t)Z_n(z;h(x,t)). \tag{4.12}$$

Since Z_n are chosen here to be independent of η, we see immediately that $\partial_\eta Z_n=0$, so that in view of Eqs. (4.9a)-(4.9c), the double series in Eq. (4.7) vanishes. Also, the third term of the left-hand side of Eq. (4.7) vanishes for the same reason. Thus, Eqs. (4.6), (4.7) take the following form

$$\left(\partial_t\eta-N_\eta\cdot\left[\nabla(\boldsymbol{\phi}^{\mathrm{T}}\boldsymbol{Z})\right]_{z=\eta}\right)[Z_m]_{z=\eta}+\sum_{n=1}^{N}L_{mn}\varphi_n=0,\quad m=1,...,N, \tag{4.13}$$

$$\partial_t\boldsymbol{\phi}^{\mathrm{T}}[\boldsymbol{Z}]_{z=\eta}+g\eta+\frac{1}{2}[\nabla(\boldsymbol{\phi}^{\mathrm{T}}\boldsymbol{Z})]^2_{z=\eta}=0. \tag{4.14}$$

Eq. (4.14) is easily identified with Eq. (9) of IA98. In order to verify that Eq. (4.13) is the same as Eq. (8) of IA98, we reformulate the coefficients of the operators L_{mn}, given in the general case by Eqs. (4.8a)-(4.8c), by taking into account once again that $\partial_\eta Z_n=0$. Then, we easily obtain from Eqs. (4.8a)-(4.8c) the following expressions

$$A_{mn}=\int_{-h}^{\eta}Z_nZ_m dz, \tag{4.15a}$$

$$B^i_{mn}=2\partial_{x_i}h\int_{-h}^{\eta}\partial_hZ_nZ_m dz+\partial_{x_i}h[Z_nZ_m]_{-h}, \tag{4.15b}$$

$$C_{mn}=(\nabla_x h)^2\int_{-h}^{\eta}\partial_h^2Z_nZ_m dz+(\nabla_x^2h)\int_{-h}^{\eta}\partial_hZ_nZ_m dz+\int_{-h}^{\eta}\partial_z^2Z_nZ_m dz + (\nabla_{\mathbf{x}}h)^2[\partial_hZ_nZ_m]_{-h}+[\partial_zZ_nZ_m]_{-h}. \tag{4.15c}$$

As shown in IA98, linearisation of (4.13), (4.14) in conjunction with the choice of a single term representation $\Phi=\varphi Z(z;h)$, $Z(z;h)=\mathrm{sech}(\kappa h)\cosh(\kappa(z+h))$ with κ satisfying the linear

dispersion relation, leads to the standard mild slope equation of (Berkhoff 1972). Further, preserving the non-linearity of Eqs. (4.13), (4.14) and choosing $\Phi = \varphi Z(z;h)$, $Z(z;h) = 1$, leads to a two component system on (η, φ), which after the introduction of the approximate horizontal velocity can be easilly identified with the nonlinear shallow-water equations. Choosing a two term representation for Φ, IA98 also derived a three component model which, upon appropriate simplifications, leads to the Boussinesq equations in the form given by Peregrine (Peregrine 1967). Recently, (Murakami & Iguchi 2015) proved the solvability of the initial value problem for the original three component system of IA98.

Euler-Lagrange equations of KVGD10

The derivation of the general series model of KVGD10 is more involved due to the fact that all but one of the prescribed vertical functions are allowed to depend on the free surface elevation η. In particular, it is assumed in KVGD10 that Z_n have they following form

$$Z_0 = 1, \qquad Z_n = Z_n\left(z; \eta(\mathbf{x},t), h(\mathbf{x})\right), \tag{4.16}$$

and, for $n \geq 1$, they satisfy the following essential conditions

$$[Z_n]_{z=\eta} = 0, \qquad n \geq 0. \tag{4.17}$$

The corresponding representation of the velocity potential is written

$$\Phi(\mathbf{x}, z, t) = \psi(\mathbf{x}, t) Z_0 + \sum_{n=1}^{N} \varphi_n(\mathbf{x}, t) Z_n(z; \eta(\mathbf{x}, t), h(\mathbf{x})). \tag{4.18}$$

In view of Eqs. (4.16)-(4.18), the Euler-Lagrange equations (4.6), (4.7) take the following form

$$\partial_t \eta - N_\eta \cdot \left[\nabla(\psi + \boldsymbol{\phi}^{\mathrm{T}} \boldsymbol{Z})\right]_{z=\eta} + H\Delta\psi + \sum_{n=1}^{N} L_{0n}\varphi_n = 0, \tag{4.19}$$

$$\int_{-h}^{\eta} Z_m dz \Delta\psi + \sum_{n=1}^{N} L_{mn}\varphi_n = 0, \quad m = 1, ..., N, \tag{4.20}$$

$$\partial_t \psi + g\eta + \frac{1}{2}\left[\nabla(\psi + \boldsymbol{\phi}^{\mathrm{T}} \boldsymbol{Z})\right]^2_{z=\eta} + N_\eta \cdot \left[\nabla(\psi + \boldsymbol{\phi}^{\mathrm{T}} \boldsymbol{Z})(\boldsymbol{\phi}^{\mathrm{T}} \partial_\eta \boldsymbol{Z})\right]_{z=\eta}$$
$$-\Delta\psi \sum_{n=1}^{N} \varphi_n \int_{-h}^{\eta} \partial_\eta Z_n dz - \sum_{m=1}^{N} \Big(\sum_{n=1}^{N} l_{mn}\varphi_n\Big)\varphi_m = 0. \tag{4.21}$$

The matrix coefficients of the horizontal differential operators L_{mn} and l_{mn}, in conformity with Klopman's simplification ($\partial_{x_i} h = 0$), are given by

$$A_{mn} = \int_{-h}^{\eta} Z_n Z_m dz, \tag{4.22a}$$

$$B^i_{mn} = 2\partial_{x_i}\eta \int_{-h}^{\eta} \partial_\eta Z_n Z_m dz, \tag{4.22b}$$

$$C_{mn} = (\nabla_{\mathbf{x}}\eta)^2 \int_{-h}^{\eta} \partial^2_\eta Z_n Z_m dz + (\nabla^2_{\mathbf{x}}\eta) \int_{-h}^{\eta} \partial_\eta Z_n Z_m dz + \int_{-h}^{\eta} \partial^2_z Z_n Z_m dz + \left[\partial_z Z_n Z_m\right]_{z=-h}, \tag{4.22c}$$

$$a_{mn} = \int_{-h}^{\eta} Z_n \partial_\eta Z_m dz, \tag{4.23a}$$

$$b^i_{mn} = 2\partial_{x_i}\eta \int_{-h}^{\eta} \partial_\eta Z_n \partial_\eta Z_m dz, \tag{4.23b}$$

$$c_{mn} = (\nabla_{\mathbf{x}}\eta)^2 \int_{-h}^{\eta} \partial^2_\eta Z_n \partial_\eta Z_m dz + (\nabla^2_{\mathbf{x}}\eta) \int_{-h}^{\eta} \partial_\eta Z_n \partial_\eta Z_m dz + \int_{-h}^{\eta} \partial^2_z Z_n \partial_\eta Z_m dz + \left[\partial_z Z_n \partial_\eta Z_m\right]_{z=-h}. \tag{4.23c}$$

Performing appropriate algebraic manipulations, and discarding all terms containing horizontal derivatives of h, we find that our Eqs. (4.19), (4.20) and (4.21) reduce to Eqs. (4.3a), (4.3c) and (4.3b) of KVGD10 respectively.

One obvious advantage of Klopman et al's choice of vertical functions, Eq. (4.16), is that it directly yields two evolution equations on (η, ψ) coupled with a time independent system of partial differential equations on φ_n, $n \geq 1$. Moreover, as one might expected in this non-pertubative framework, the maximum order of spatial derivatives in the evolution equations never exceeds two, independently of the number of vertical functions used in (4.18).

4.2 Derivation of a new model system

In this section, we derive a water wave model as an application of Eqs. (4.19)-(4.21). Focusing our attention to the modelling of long waves propagating in shallow water over a horizontal seabed $z = -h$, we recall that the velocity potential is well approximated by even order polynomials in z (see e.g., (Witham 1974, Chapter 13), (Massel 1989, Chapter 4), (Lannes 2013, Chapter 3.6)). Motivated by this fact, we choose a simple two term representation of the velocity potential ($N = 1$ in Eq. (4.18)) given by

$$\Phi(\mathbf{x}, z, t) = \psi(\mathbf{x}, t) + \varphi(\mathbf{x}, t) Z(z; \eta(\mathbf{x}, t), h), \tag{4.24a}$$

$$Z(z; \eta(\mathbf{x}, t), h) = \frac{1}{2}\left(z - \eta(\mathbf{x}, t)\right)^2 + \left(\eta(\mathbf{x}, t) + h\right)\left(z - \eta(\mathbf{x}, t)\right). \tag{4.24b}$$

A similar representation was also used in KVGD10 for the derivation of the so called parabolic model. In fact, the choice (4.24) is an attempt to extend the asymptotic expansion of the velocity potential that derives the Green-Nagdhi equations (see Eqs. (17), (20), (21) of (Lannes

& Bonneton 2009)); the functions ψ and $\Delta\psi$ appearing in Eqs. (21), (22) of (Lannes & Bonneton 2009) (determined by the perturbation procedure), are replaced here by the undetermined functions ψ and φ which will eventually appear in the resulting Euler-Lagrange equations. In this case, Eqs. (4.19)-(4.21), after some straightforward calculations, yield the following system

$$\partial_t\eta + \nabla_{\boldsymbol{x}}\eta\cdot\nabla_{\boldsymbol{x}}\psi - [(\nabla_{\boldsymbol{x}}\eta)^2+1]\varphi H + H\Delta_{\boldsymbol{x}}\psi + L_{0,1}\varphi = 0, \tag{4.25}$$

$$\partial_t\psi + \frac{1}{2}(\nabla_{\boldsymbol{x}}\psi)^2 - \frac{1}{2}[(\nabla_{\boldsymbol{x}}\eta)^2+1](\varphi H)^2 - \frac{1}{2}H^2\Delta_{\boldsymbol{x}}\psi\varphi - (l_{1,1}\varphi)\,\varphi = 0, \tag{4.26}$$

$$-\frac{H^3}{3}\Delta_{\boldsymbol{x}}\psi + L_{11}\varphi = 0, \tag{4.27}$$

with $H=\eta(\boldsymbol{x},t)+h$ and

$$L_{0,1} = -\frac{1}{3}H^3\Delta_{\boldsymbol{x}} - 2H^2\nabla_{\boldsymbol{x}}\eta\cdot\nabla_{\boldsymbol{x}} - H(\nabla_{\boldsymbol{x}}\eta)^2 - H^2\Delta_{\boldsymbol{x}}\eta + H, \tag{4.28a}$$

$$L_{1,1} = \frac{2}{15}H^5\Delta_{\boldsymbol{x}} + \frac{2}{3}H^4\nabla_{\boldsymbol{x}}\eta\cdot\nabla_{\boldsymbol{x}} + \frac{1}{3}\left(H^4\Delta_{\boldsymbol{x}}\eta + H^3\left(\nabla_{\boldsymbol{x}}\eta\right)^2 - H^3\right), \tag{4.28b}$$

$$l_{1,1} = -\frac{1}{3}H^4\Delta_{\boldsymbol{x}} + 2H^3\nabla_{\boldsymbol{x}}\eta\cdot\nabla_{\boldsymbol{x}} + \left(H^2\left(\nabla_{\boldsymbol{x}}\eta\right)^2 + H^3\Delta_{\boldsymbol{x}}\eta - H^2\right). \tag{4.28c}$$

The two component system (4.25), (4.26), is an evolutionary system on (η,ψ) coupled with the time independent partial differential equation (4.27) which determines φ at time t. Introducing the operator $\mathscr{F}[\eta,h]$ that maps ψ to the solution of (4.27), $\varphi=\mathscr{F}[\eta,h]\psi$, and performing straightforward manipulations, the above system is written as

$$\partial_t\eta + \nabla_{\boldsymbol{x}}\cdot\left[H\nabla_{\boldsymbol{x}}\psi - \frac{1}{3}\nabla_{\boldsymbol{x}}\left(H^3\mathscr{F}[\eta,h]\psi\right)\right] = 0, \tag{4.29a}$$

$$\begin{aligned}\partial_t\psi + g\eta + \frac{1}{2}\left(\nabla_{\boldsymbol{x}}\psi\right)^2 - \left(\frac{3}{2}|\nabla_{\boldsymbol{x}}\eta|^2 - \frac{1}{2}\right)\left(H\mathscr{F}[\eta,h]\psi\right)^2 \\ + \left\{H\Delta_{\boldsymbol{x}}\psi - \nabla_{\boldsymbol{x}}\cdot\left[\frac{1}{3}\nabla_{\boldsymbol{x}}\left(H^3\mathscr{F}[\eta,h]\psi\right)\right]\right\}H\mathscr{F}[\eta,h]\psi = 0.\end{aligned} \tag{4.29b}$$

In order to gain some insight on the physical properties of above the model, we pursue a linear analysis. Linearising Eqs. (4.29a), (4.29b) around $(\eta,\psi)=(0,0)$, we get

$$\partial_t\eta + \nabla_{\boldsymbol{x}}\cdot\left[h\nabla_{\boldsymbol{x}}\psi - \frac{1}{3}\nabla_{\boldsymbol{x}}\left(h^3\mathscr{F}[0,h]\psi\right)\right] = 0, \tag{4.30a}$$

$$\partial_t\psi + g\eta = 0, \tag{4.30b}$$

where $\mathscr{F}[0,h]\psi=\varphi$ is determined by the solution of

$$\nabla_{\boldsymbol{x}}\cdot\left(\frac{2}{15}h^5\nabla_{\boldsymbol{x}}\varphi\right) - \frac{1}{3}h^3\varphi - \frac{h^3}{3}\Delta_{\boldsymbol{x}}\psi = 0. \tag{4.31}$$

Looking for plane wave solutions of Eqs. (4.30a)-(4.30b) in the form

$$(\eta(x,t),\psi(x,t),\varphi(x,t)) = (\tilde{\eta},\tilde{\psi},\tilde{\varphi})e^{i(\kappa x-\omega t)},$$

we find from (4.31) that

$$\varphi = \mathscr{F}[0,h]\psi = \frac{\kappa^2}{1+\frac{2}{5}h^2\kappa^2}\tilde{\psi}e^{i(\kappa x-\omega t)}, \tag{4.32}$$

consequently, Eqs. (4.30a)-(4.30b) take the form of an homogeneous algebraic system on $(\tilde{\eta},\tilde{\psi})$

$$\begin{pmatrix} -i\omega & -h\kappa^2+\frac{h\kappa^2}{3}\frac{h^2\kappa^2}{1+\frac{2}{5}h^2\kappa^2} \\ g & -i\omega \end{pmatrix}\begin{pmatrix}\tilde{\eta}\\ \tilde{\psi}\end{pmatrix} = \begin{pmatrix}0\\0\end{pmatrix}.$$

For this system to have a non-trivial solution, the determinant of its matrix must vanish, thus yielding the dispersion relation

$$\omega^2(k) = gh\kappa^2\frac{1+\frac{1}{15}h^2\kappa^2}{1+\frac{2}{5}h^2\kappa^2}. \tag{4.33}$$

It follows from (4.33) that the speed $C=\omega/k$, is

$$\frac{C}{\sqrt{gh}} = \left(\frac{1+\frac{1}{15}h^2\kappa^2}{1+\frac{2}{5}h^2\kappa^2}\right)^{1/2}, \tag{4.34}$$

which coincides with the one predicted by the parabolic model of KVGD10, the three component model of IA98 and the (improved) Green-Nagdhi equations of (Bonneton et al. 2011, Section 2.6) with $a=6/5$. In the following figure, the wave speed given by (4.34) is compared with the exact,

$$\frac{C_{\mathrm{WW}}}{\sqrt{gh}} = \left(\frac{\tanh(\kappa h)}{\kappa h}\right)^{1/2}, \tag{4.35}$$

the one predicted by HCMS with $N_{\mathrm{tot}}=6$ (including the sloping bottom mode) and $\mu_0 h_0 = 0.1\pi$, as well as, the ones predicted by the usual and higher order Green-Nagdhi (GN) equations derived in (Matsuno 2016). The latter are denoted as GN^{2n}, where the exponent signifies the asymptotic order $\delta^{2n}=(h_0/L_0)^{2n}$. As shown in the latter work, when n is even the dispersion relation becomes singular. Eqs. (4.29a), (4.29b) give a more accurate wave speed than the usual GN equations, GN^2. GN^4 and GN^6 perform better than Eqs. (4.29a), (4.29b) up to some values of κh_0. The wave speed predicted by HCMS with $N_{\mathrm{tot}}=6$ is the most close to the exact one, provided that the waves are not too shallow. Although further investigation is required, the present results show that nonlocal simplified models that retain a substrate time independent structure have better dispersive properties than two component models. Moreover, HCMS, being

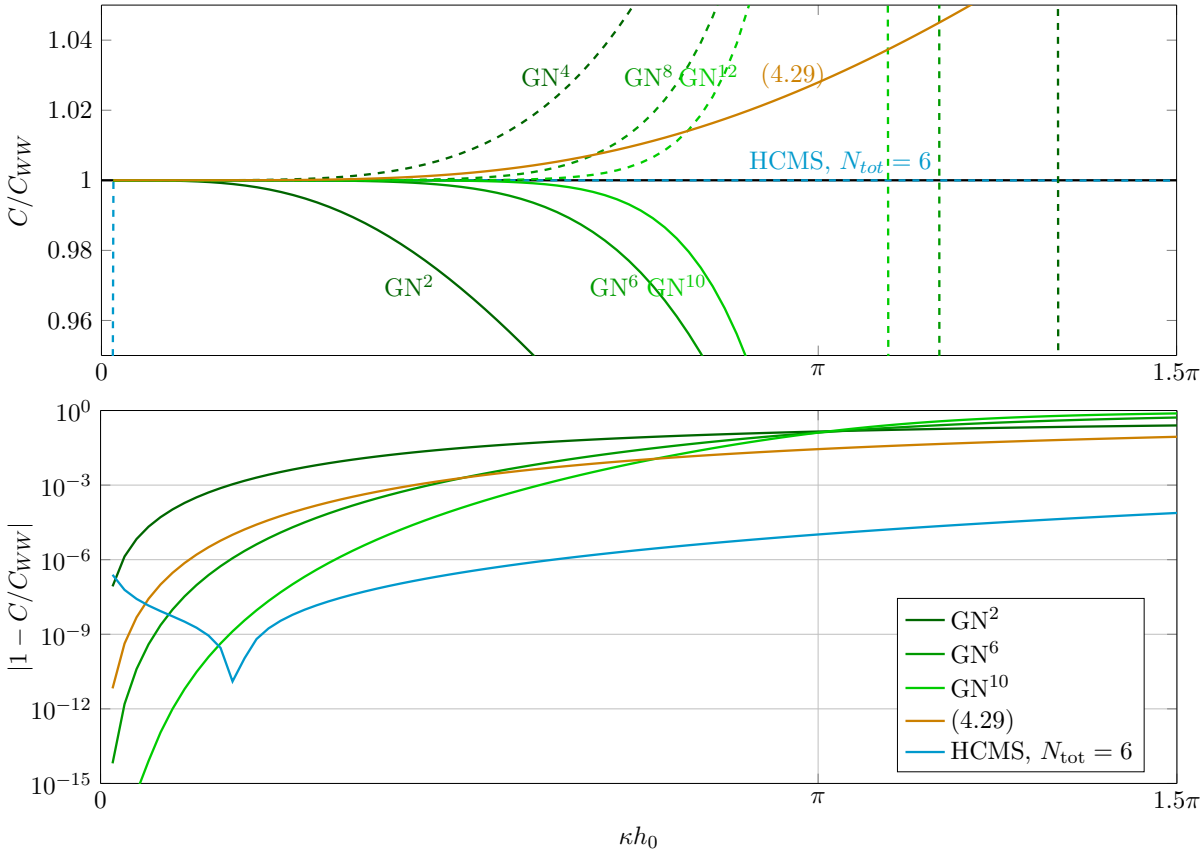

Figure 4.1: Errors on the linear wave speed predicted by (4.29a), (4.29b), the HCMS with $N_{\text{tot}} = 6$ and the Green-Nagdhi equations for several orders.

derived through an exact representation of the wave potential, reproduces the wave velocity with very high accuracy using only $N_{\text{tot}} = 5, 6$ modes.

Part II

Numerical method and results

Chapter 5

Truncation and spatial discretisation of the Coupled-Mode System

As already mentioned, the numerical implementation of the ZCS formulation requires the computation of the non-local DtN operator, which takes care of the substrate kinematics of the fluid. This is the most crucial step for demanding numerical simulations of nonlinear water-waves, in terms of both computational time and accuracy. This happens since the boundary value problem (1.23) (together with appropriate lateral boundary conditions) has to be solved at every time step during the numerical integration of the Hamiltonian evolution Eqs. (1.26), (1.27), and $G[\eta, h]\psi$ enters quadratically in Eq. (1.27), making its contribution crucial for highly nonlinear effects.

For the numerical implementation of HCMS, Eqs. (3.42), (3.43), one needs to compute an approximation of the free surface amplitude $\mathscr{F}_{-2}[\eta, h]\psi$ (and thus of the DtN operator in view of Eq. (3.44)). This requires the reduction (truncation) of the infinite substrate system (3.35) to a finite system, the spatial discretization of the truncated system, and its solution with a certain numerical method. Restricting our attention to the convergence properties of the coupled mode method for large values of n, the modes $n = -2, -1, 0$ are always kept in the expansion (2.4). Denoting by M the number of evanescent modes ($n \geq 1$) kept in the truncated series, the total number of unknown functions $\{\varphi_n\}_{n=-2}^{M}$ is $N_{\text{tot}} = M + 3$. These are computed by solving the system of equations which consists of the first $M + 2$ differential equations of (3.35a), supplemented by the linear algebraic constraint obtained by truncating the series appearing in Eq. (3.35b) at $n = M$.

Once the finite system is formulated, a fourth order finite difference method is employed for its discretization and reduction to a square system of linear algebraic equations. The corresponding approximate free surface amplitude, denoted by $\mathscr{F}_{-2}^{(M)}[\eta, h]\psi$, can then be used in Eq. (3.44), for the computation of an approximation of the DtN operator $G[\eta, h]\psi$:

$$G^{(M)}[\eta, h]\psi = -\nabla_{\mathbf{x}}\eta \cdot \nabla_{\mathbf{x}}\psi + \left((\nabla_{\mathbf{x}}\eta)^2 + 1\right)\left(h_0^{-1}\mathscr{F}_{-2}^{(M)}[\eta, h]\psi + \mu_0\psi\right). \tag{5.1}$$

Restricting for simplicity to the case of waves of one horizontal dimension (i.e., $\partial_{x_1} \equiv \partial_x$, $\partial_{x_2} = \partial/\partial_{x_2} \equiv 0$) in which X is a finite interval, say $X = [a, b]$, the truncated version of Eqs. (3.35a), (3.35b) takes the form:

$$\sum_{n=-2}^{M} A_{mn}\partial_x^2\varphi_n + B_{mn}\partial_x\varphi_n + C_{mn}\varphi_n = 0, \quad m = -2, ..., M-1, \quad x \in X, \tag{5.2a}$$

$$\sum_{n=-2}^{M} \varphi_n = \psi, \quad x \in X. \tag{5.2b}$$

It should be noted that, independently of the numerical method chosen for the solution of the truncated substrate system (5.2a)-(5.2b), the matrix coefficients A, B and C appearing in (5.2a) can be efficiently evaluated, at every time t, since they are explicitly expressed, through Eqs. (3.22a), (3.22b) and (3.22c), in terms of the parameters h_0, μ_0, the free surface elevation η, the bottom surface h and the local wavenumber functions $k_n(\eta, h)$ (see Appendix F). The latter are computed as highly accurate solutions to the local transcendental equations (2.32) using the Newton-Raphson method.

The organisation of the remainder of this chapter is as follows. In Section 5.1 we describe the lateral boundary conditions which can possibly complete the substrate system (5.2). In Section 5.2 we provide the corresponding discrete equations obtained by spatial discretization using fourth order finite differences. Finally, in Section 5.3 we assess the accuracy and convergence of the DtN approximation, furnished by Eq. (5.1). The results of Theorem 2.2 concerning the decay of the modal amplitudes are also verified through the solution of the substrate system (5.2).

5.1 Lateral boundary conditions

5.1.1 Matching condition at $x = a$

In this case, we assume that η, ψ and lateral data g_m of φ_m, $m = -2, ..., M-1$ are known on $x = a$. The matching of the velocity potential is then implemented by the following system of coupled boundary conditions

$$\sum_{n=-2}^{M} [A_{mn}]_{x=a} [\partial_x\varphi_n]_{x=a} + \frac{1}{2} [B_{mn}]_{x=a} [\varphi_n]_{x=a} = g_m, \quad m = -2, ..., M-1. \tag{5.3}$$

5.1.2 Vertical impermeable walls at $x = a$ and $x = b$

The boundary conditions for fully reflecting vertical walls at $x = a$ and $x = b$ read

$$\sum_{n=-2}^{M} [A_{mn}]_{x=a} [\partial_x\varphi_n]_{x=a} + \frac{1}{2} [B_{mn} - \partial_x h Z_n Z_m]_{x=a} [\varphi_n]_{x=a} = 0, \quad m = -2, ..., M-1, \tag{5.4a}$$

$$\sum_{n=-2}^{M} [A_{mn}]_{x=b} [\partial_x \varphi_n]_{x=b} + \frac{1}{2} [B_{mn} - \partial_x h Z_n Z_m]_{x=b} [\varphi_n]_{x=b} = 0, \quad m = -2, ..., M-1, \quad (5.4b)$$

Note that the slope of the bathymetry at $x = a, b$ can be non-zero.

5.1.3 Periodic boundary conditions

Periodicity on the modal amplitudes is imposed by

$$\varphi_m(a) = \varphi_m(b), \quad m = -2, ..., M-1. \quad (5.5)$$

5.2 Discretization using fourth-order finite-differences

The system of differential equations (5.2a) is discretised using the finite difference method on a uniform grid of N_X points at fourth order of accuracy. In order to avoid the use of fictitious points and at the same time keep fourth order of accuracy near the boundaries of the computational domain, we use asymmetric and one sided formulae for $i = 2, N_X - 1$ and $i = 1, N_X$ respectively. Thus, the first and second derivative of a function u at x_i are approximated by

$$(\partial_x u)_i = \begin{cases} \frac{1}{\delta}\left(-\frac{25}{12}u_i + 8u_{i+1} - 3u_{i+2} + \frac{4}{3}u_{i+3} - \frac{1}{4}u_{i+4}\right), & i = 1 \\ \frac{1}{\delta}\left(\frac{1}{4}u_{i-1} + \frac{5}{6}u_i - \frac{3}{2}u_{i+1} + \frac{1}{2}u_{i+2} - \frac{1}{12}u_{i+3}\right), & i = 2 \\ \frac{1}{12\delta}\left(u_{i-2} - 8u_{i-1} + 8u_{i+1} - u_{i+2}\right), & i = 3, ..., N_X - 2 \\ \frac{1}{\delta}\left(\frac{1}{12}u_{i-3} - \frac{1}{2}u_{i-2} + \frac{3}{2}u_{i-1} - \frac{5}{6}u_i - \frac{1}{4}u_{i+1}\right), & i = N_X - 1 \\ \frac{1}{\delta}\left(\frac{1}{4}u_{i-4} - \frac{4}{3}u_{i-3} + 3u_{i-2} - 8u_{i-1} + \frac{25}{12}u_i\right), & i = N_X \end{cases} \quad (5.6)$$

$$(\partial_x^2 u)_i = \begin{cases} \frac{1}{\delta^2}\left(\frac{15}{4}u_i - \frac{77}{6}u_{i+1} + \frac{107}{6}u_{i+2} - 13u_{i+3} - \frac{61}{12}u_{i+4} - \frac{5}{6}u_{i+5}\right), & i = 1 \\ \frac{1}{\delta^2}\left(\frac{5}{6}u_{i-1} - \frac{5}{5}u_i - \frac{1}{3}u_{i+1} + \frac{7}{6}u_{i+2} - \frac{1}{2}u_{i+3} + \frac{1}{12}u_{i+4}\right), & i = 2 \\ \frac{1}{12\delta^2}\left(-u_{i-2} + 16u_{i-1} - 30u_i + 16u_{i+1} - u_{i+2}\right), & i = 3, ..., N_X - 2 \\ \frac{1}{\delta^2}\left(\frac{5}{6}u_{i+1} - \frac{5}{5}u_i - \frac{1}{3}u_{i-1} + \frac{7}{6}u_{i-2} - \frac{1}{2}u_{i-3} + \frac{1}{12}u_{i-4}\right), & i = N_X - 1 \\ \frac{1}{\delta^2}\left(-\frac{15}{4}u_i + \frac{77}{6}u_{i-1} - \frac{107}{6}u_{i-2} + 13u_{i-3} + \frac{61}{12}u_{i-4} + \frac{5}{6}u_{i-5}\right), & i = N_X \end{cases} \quad (5.7)$$

In the case of a periodic problem, we use the following central formulae

$$(\partial_x u)_i = \frac{1}{12\delta}\left(u_{i-2} - 8u_{i-1} + 8u_{i+1} - u_{i+2}\right), \quad (5.8)$$

$$(\partial_x^2 u)_i = \frac{1}{12\delta^2}\left(-u_{i-2} + 16u_{i-1} - 30u_i + 16u_{i+1} - u_{i+2}\right), \quad (5.9)$$

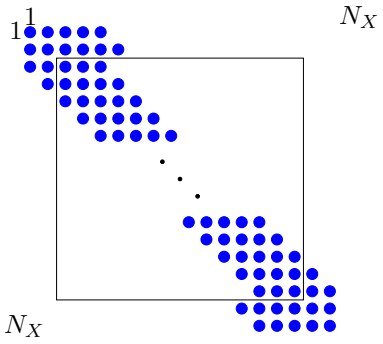

Figure 5.1: Sparsity pattern of the submatrices D_{mn} for the case of two vertical walls.

with the usual modifications at the ends of the periodic domain and its vicinities.

5.2.1 Discretisation of the field equations

Using Eqs. (5.6) and (5.7) for the approximation of $\partial_x\varphi_n$ and $\partial_x^2\varphi_n$, $n=-2,...,M$, the system of differential equations (5.2a) at the nodes $i=3,...,N_X-2$ takes the following form

$$\sum_{n=-2}^{M}\Big(-\frac{1}{12\delta^2}A^i_{mn}+\frac{1}{12\delta}B^i_{mn}\Big)\varphi_n^{i-2}+\Big(\frac{4}{3\delta^2}A^i_{mn}-\frac{2}{3\delta}B^i_{mn}\Big)\varphi_n^{i-1}+\Big(-\frac{5}{2\delta^2}A^i_{mn}+C^i_{mn}\Big)\varphi_n^{i}$$
$$+\Big(\frac{4}{3\delta^2}A^i_{mn}+\frac{2}{3\delta}B^i_{mn}\Big)\varphi_n^{i+1}+\Big(\frac{1}{12\delta^2}A^i_{mn}-\frac{1}{12\delta}B^i_{mn}\Big)\varphi_n^{i+2}=0, \quad (5.10)$$

where the superscript denotes local value of the corresponding quantity at the indicated node. Similar equations are obtained for $i=2, N_X-1$:

$$\sum_{n=-2}^{M}\Big(\frac{5}{6\delta^2}A^i_{mn}-\frac{1}{4\delta}B^i_{mn}\Big)\varphi_n^{i-1}+\Big(-\frac{5}{4\delta^2}A^i_{mn}-\frac{5}{6\delta}B^i_{mn}+C^i_{mn}\Big)\varphi_n^{i}+\Big(-\frac{1}{3\delta^2}A^i_{mn}+\frac{3}{2\delta}B^i_{mn}\Big)\varphi_n^{i+1}$$
$$+\Big(\frac{7}{6\delta^2}A^i_{mn}-\frac{1}{2\delta}B^i_{mn}\Big)\varphi_n^{i+2}+\Big(-\frac{1}{2\delta^2}A^i_{mn}+\frac{1}{12\delta}B^i_{mn}\Big)\varphi_n^{i+3}+\frac{1}{12\delta^2}A^i_{mn}\varphi_n^{i+4}=0. \quad (5.11)$$

5.2.2 Discretization of lateral boundary conditions

The discretised version of Eq. (5.3) reads

$$\sum_{n=-2}^{M}\Big(-\frac{25}{12\delta}A^1_{mn}+\frac{1}{2}B^1_{mn}\Big)\varphi_n^1+\frac{1}{\delta}A^1_{mn}\Big(4\varphi_n^2-3\varphi_n^3+\frac{4}{3}\varphi_n^4-\frac{1}{4}\varphi_n^5\Big)=g_m. \quad (5.12)$$

The discretisation of Eq. (5.4a) is the same as above with $g_m=0$. The latter equation evaluated at $i=N_X$ is the discretised version of Eq. (5.4b).

5.2.3 The structure of the linear system

The final discrete problem consists of a linear algebraic system with $(M+3)N_X$ unknowns and $(M+3)N_X$ equations. This system is written as $P\mathbf{y} = \mathbf{b}$, where $\mathbf{y} = \{y_j\}_{j=1}^{(M+3)N_X} = \{\{\varphi_m^i\}_{i=1}^{N_X}\}_{m=-2}^{M}$ is the vector of unknown values and $P \in \mathbb{R}^{(M+3)N_X \times (M+3)N_X}$, reads

$$P = \begin{pmatrix} D_{-2,-2} & D_{-2,-1} & D_{-2,0} & \cdots & D_{-2,M} \\ D_{-1,-2} & D_{-1,-1} & D_{-1,0} & \cdots & D_{-1,M} \\ D_{0,-2} & D_{0,-1} & D_{0,0} & \cdots & D_{0,M} \\ \vdots & \vdots & \vdots & \ddots & \vdots \\ D_{M-1,-2} & D_{M-1,-1} & D_{M-1,0} & \cdots & D_{M-1,M} \\ I_{N_X} & I_{N_X} & I_{N_X} & I_{N_X} & I_{N_X} \end{pmatrix} \tag{5.13}$$

where the square sub-matrices $D_{m,n} \in \mathbb{R}^{N_X \times N_X}$, $m = -2, ..., M$, are almost penta-diagonal (except for entries corresponding to $i, j = 1, 2, N_X - 1, N_X$, see Figure 5.1) and I_{N_X} denotes the unit matrix.

The sub-matrices D_{mn} correspond to the left hand sides of Eqs. (5.10)-(5.12), while the unitary sub-matrices appearing in the last line of P correspond to the algebraic constraint (5.2b). The components b_j, $j = 1, ..., (M+2)N_X$, are non-zero only in the case of excitation boundary (see Eqs. (5.12)), while for $j = (M+2)N_X, ..., (M+3)N_X$, b_j are equal to the local values of ψ (Eq. (5.2b)). The above system can be solved for y by means of several available tools. Here we use `mldivide` ("$\mathbf{y} = P\backslash\mathbf{b}$") of MATLAB which implements an LU solver. Thus, the solution vector y contains the local values of the modal amplitudes $\{\varphi_m^i\}_{i=1}^{N_X}$ for $m = -2, ..., M$ that correspond to the local values of η, ψ and boundary data g_m if they exist. This eventually leads to an approximation of the free-surface amplitude $\mathscr{F}_{-2}^{(M)}[\eta, h]\psi$ and the corresponding DtN operator $G^{(M)}[\eta, h]\psi$ at every node $i = 1, ..., N_X$.

5.3 Convergence and accuracy of the method

To demonstrate the numerical performance of the present approach and to assess the accuracy of the approximate DtN operator as given by Eq. (5.1), use will be made of some indicative examples involving highly non-uniform domains.

We first consider two examples for the flat bottom case, introduced in (Nicholls & Reitich 2001*b*) for the assessment of petrurbative computations of the DtN operator, and often used for similar purposes (see e.g. (Xu & Guyenne 2009, Fazioli & Nicholls 2010, Wilkening & Vasan

2015)). These examples are constructed by using the function

$$\Phi_\kappa = \cosh(\kappa(z+h))\cos(\kappa x), \tag{5.14}$$

which is a particular solution of the Laplace Eq. (1.5), with horizontal spatial period $2\pi/\kappa$, and satisfies the Neumann boundary condition (1.6) at a flat seabed $z = -h$. In addition, two "free surface" profiles are introduced, defined by $\eta(x) = \varepsilon\cos(\kappa x)$, where γ is an indifferent constant, and $\eta = \varepsilon f_r(x)$, $f_r(x) = Ax^4(2\pi - x)^4 + B$, where A and B are constants chosen so that $\int_0^{2\pi} f_r(x)dx = 0$ and $\max\{f_r(x)\} = f_r(\pi) = 1$. Following (Nicholls & Reitich 2001*b*), we call the first surface *smooth* ($\eta \in C^\infty(X)$), and the second *rough* ($\eta \in C^4(X)$). The constant ε determines the amplitude of the surfaces and represents the order of the deformed domain. The Dirichlet data of the harmonic function Φ_κ are given by $\psi = [\Phi_\kappa]_{z=\eta} = \cos(\kappa(\eta+h))\cos(\kappa x)$, so that the action of DtN operator on ψ is explicitly given by

$$\begin{aligned} G[\eta,h]\psi &= -\partial_x\eta\,[\partial_x\Phi_\kappa]_{z=\eta} + [\partial_z\Phi_\kappa]_{z=\eta} \\ &= [-\partial_x\eta\cos(\kappa(\eta+h)) + \sinh(\kappa(\eta+h))]\,\kappa\cos(\kappa x). \end{aligned} \tag{5.15}$$

In order to compute the DtN operator using (5.1), we solve the coupled mode system (5.2) with $\psi = [\Phi_\kappa]_{z=\eta}$, and periodic boundary conditions on φ_n (see Eqs. (5.5)). This gives an approximation $G^{(M)}[\eta,h]\psi$ where M denotes the number of modes ($n \geq 0$) kept in the enhanced eigenfunction expansion (2.4). Computations presented below correspond to $\kappa = 1$, $h_0 = 1$, and values of the deformation parameter ε, from $\varepsilon = 0.1$ to $\varepsilon = 0.9$; see Figure 5.2. For the construction of the vertical basis functions Z_n we choose $\mu_0 = \kappa\tanh(\kappa h_0)$. The horizontal grid consists of $N_X = 256$, uniformly distributed points on the interval $X = [0, 2\pi]$. The bottom mode, $n = -1$, is dropped in these examples, since the seabed is globally flat and the bottom boundary condition of the reference waveguide and the problem are consistent. Thus, in this case, the total number of modes is $M + 2$.

The first issue addressed in the context of our numerical investigation concerns the rate of decay of the numerically computed modal amplitudes $\{\varphi_n\}_{n=-2}^M$ and their horizontal derivatives, measured by the $C^2(X)$ norm, $X = [0, 2\pi]$,

$$\|\varphi_n\|_{C^2(X)} = \|\varphi_n\|_\infty + h_0^{-1}\|\partial_x\varphi_n\|_\infty + h_0^{-2}\|\partial_x^2\varphi_n\|_\infty \tag{5.16}$$

Numerical results for $\|\varphi_n\|_{C^2(X)}$, obtained by solving the truncated substrate problem (5.2a) with periodic boundary conditions are shown in Figure 5.3. The calculations have been performed with a great number of modes (-2,0, and 67 evanescent modes) in order to reveal the asymptotic behaviour for large values of n. Two conclusions can be readily drawn: First, for large values of n, $\|\varphi_n\|_{C^2(X)} = O(n^{-4})$, as predicted by Theorem 2. Second, and most importantly, the decay rate of the first few modal amplitudes, up to $n = 3, 4$, is almost exponential. This phenomenon is an inherent, generic feature of the CCMM, appearing consistently in all geometric configurations,

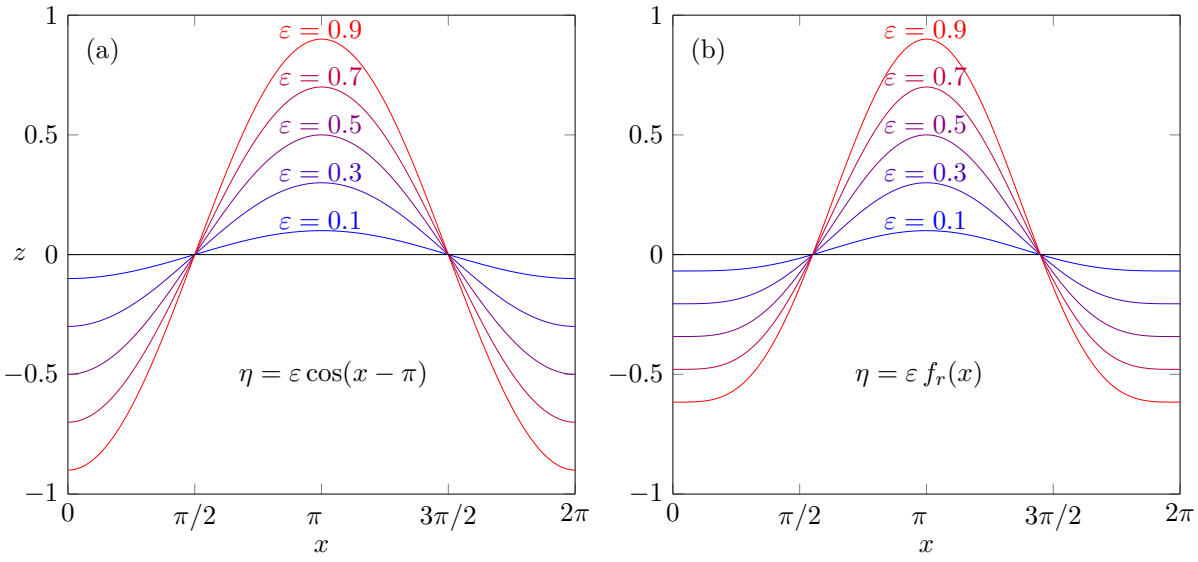

Figure 5.2: Periodic domains used in the computations (a) Smooth case, (b) Rough case.

even in very complicated ones. It is reasonable to assume that this phenomenon plays an essential role in the efficiency of the present method.

The second and more important issue concerns the numerical investigation of the convergence and accuracy properties of the DtN operator computed by (5.1). Following the usual practice, we will be interested in the following relative error

$$\mathscr{E}^{(M)}[G] = \frac{\|G^{(M)}[\eta, h_0]\psi - G[\eta, h_0]\psi\|_{L^2(X)}}{\|G[\eta, h_0]\psi\|_{L^2(X)}}. \tag{5.17}$$

where $G[\eta, h]\psi$ is given by Eq. (5.15). Numerical results for $\mathscr{E}^{(M)}[G]$ have been obtained by using various values of M, from $M+2=3$ up to $M+2=70$, for both the smooth and the rough cases. In Figure 5.4, $\mathscr{E}^{(M)}[G]$ is shown for five increasing values of the deformation parameter $\varepsilon = 0.1\,(0.2)\,0.9$. In both (smooth and rough) cases, $\mathscr{E}^{(M)}[G]$ decays rapidly, up to a plateau limit, which is reached for $M+2 \backsimeq 20$. The following three conclusions are readily drawn from the results shown in Figure 5.4.

1) The decay rate $M^{-6.5}$ applies to all cases, even the for large value of the deformation parameter ε.

2) The accuracy of DtN operator is only slightly affected by the reduction of smoothness of η from $C^\infty(X)$ to $C^4(X)$.

3) To achieve an accuracy 10^{-5}, which is satisfactory in many applications, we need four evanescent modes for $\varepsilon \leq 0.5$, or five evanescent modes, for any $\varepsilon \leq 0.9$.

The computations up to now were performed for the same spatial discretisation. In order to quantify the convergence of the present finite difference scheme we compute the DtN operator

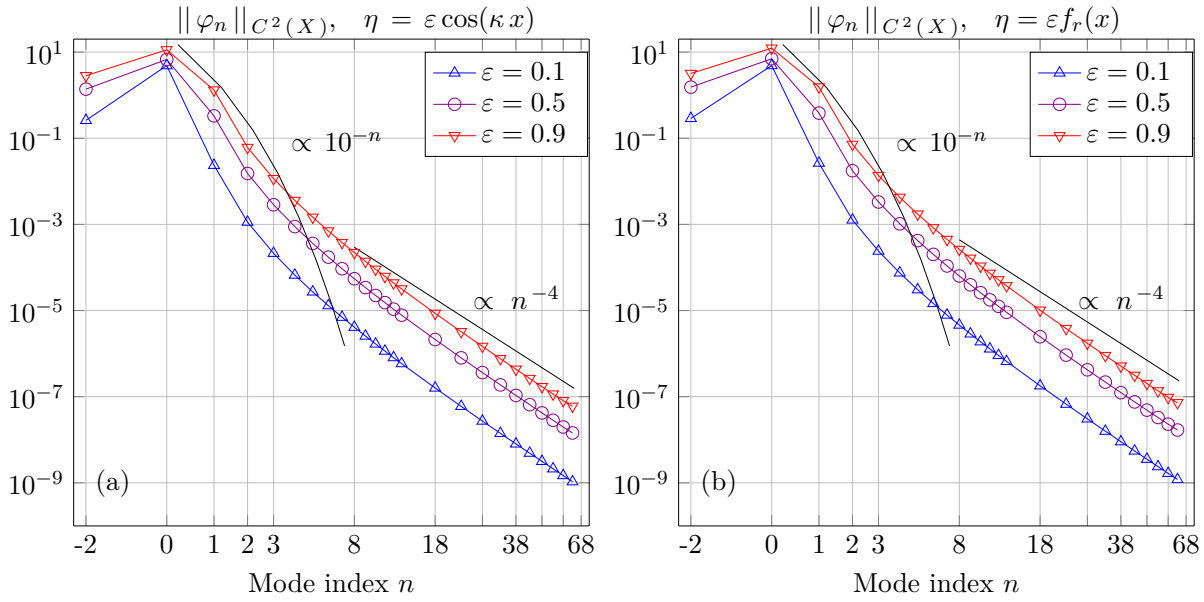

Figure 5.3: Decay of the computed $||\varphi_n||_{C^2(X)}$ for $\varepsilon = 0.1, 0.5, 0.9$. (a) Smooth case, (b) Rough case.

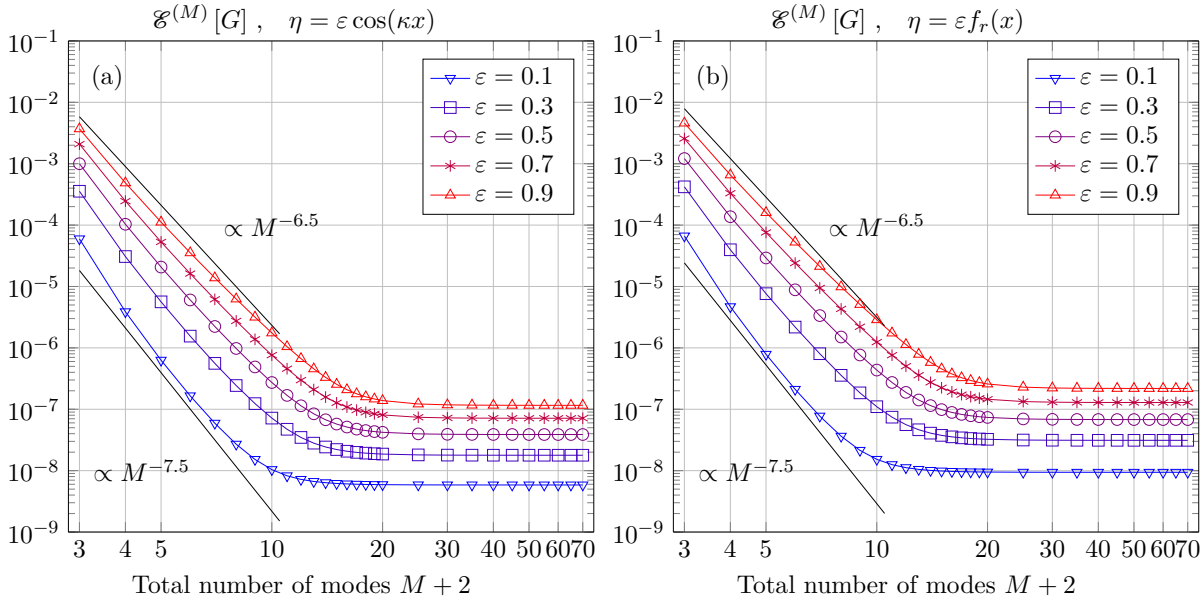

Figure 5.4: L^2-error of the DtN operator, Eq. (5.17), as a function of the total number of modes, for $\varepsilon = 0.1, 0.5. 0.9$. (a) Smooth case, (b) Rough case.

for the smooth case with $\varepsilon = 0.5$ for several values (N_X, M). In Figure 5.5(a) we show $\mathscr{E}^M[G]$ as a function of N_X for different values of M. It is observed that as the total number of modes increases, $\mathscr{E}^M[G]$ becomes proportional to δx^4 which is consistent with the fourth order accuracy of the present scheme. In other words, as soon as the total number of modes is large enough the error due to spatial discretization becomes dominant. The error $\mathscr{E}^M[G]$ as a function of the total number of modes for different values of N_X is plotted in Figure 5.5(b). As the spatial discretization becomes finer the rate of diminution of $\mathscr{E}^M[G]$ with respect to M tends to become proportional to $1/M^7$. The plateau limit of $\mathscr{E}^{(M)}[G]$ significantly decreases and shifts towards larger values of M ($\min \mathscr{E}^M[G] = \mathscr{E}^{(6)}[G] = 2 \times 10^{-4}$ for $N_X = 32$ and $\min \mathscr{E}^{(M)}[G] = \mathscr{E}^{(40)}[G] = 2 \times 10^{-9}$ for $N_X = 512$). The relative error as a function of (N_X, M) is depicted in Figure 5.5.

Notwithstanding the interest and the significance of the above results, the main advantage of the present approach (the CCMM) seems to us to be its ability to treat cases with varying bathymetry $h = h(x)$ without any additional cost apart from the inclusion of the bottom boundary mode, $n = -1$. As a demonstration of this ability, we consider the DtN operator corresponding to the complex domain and Dirichlet data ψ shown in Figure 5.6(a). Homogeneous Neumann boundary conditions are applied to the bottom and lateral boundaries. Including now the mode $n = -1$, the DtN is computed with a total number of four and seven modes. For comparison purposes, the same problem is solved by a standard Boundary Element Method (BEM) ((Fillipas & Belibassakis 2014)) and the results are plotted in Figure 5.6(b). The differences between $G^{(1)}[\eta, h]\psi$ and $G^{(4)}[\eta, h]\psi$ are minor, and mainly restricted near the ends of the boundary nonuniformities. The relative discrepancy between the BEM solution and $G^{(4)}[\eta, h]\psi$ is of order $O(10^{-4})$, while the CCMM solution is much faster. The above results justify the expectation that the DtN operator in the presence of complex, variable bathymetries, is accurately and efficiently computed by CCMM, using a small total number of horizontal modal amplitudes φ_n in the series expansion 2.4.

Closing this section, we shall comment on how the present method compares with perturbative methods. The latter are based on the approximation of the DtN operator by an operator-Taylor series, with respect to the field η. They were initially introduced for the flat bottom case in (Craig & Sulem 1993) and have been extended to variable bottoms in (Craig et al. 2005, Guyenne & Nicholls 2005). First of all, in contrast with the present method, perturbative methods are limited by horizontal periodicity and smallness assumptions on the deformation of the horizontal boundaries. For the flat bottom case, Nicholls and Reitich (Nicholls & Reitich 2001*b*), called herewith NR01, presented three variants, called the operator expansion (OE) method, the field expansion (FE) method, and the transformed field expansion (TFE) method, and used the periodic examples described above to compare their numerical performance. A first qualitative comparison between these pertubative methods and the CCMM is summarised by the following points:

1) The OE and the FE methods always diverge as the order of truncation of the Taylor series exceeds some value (about 10 or smaller, dependent on ε and N_x, see, e.g., Figures 1 to 6 in

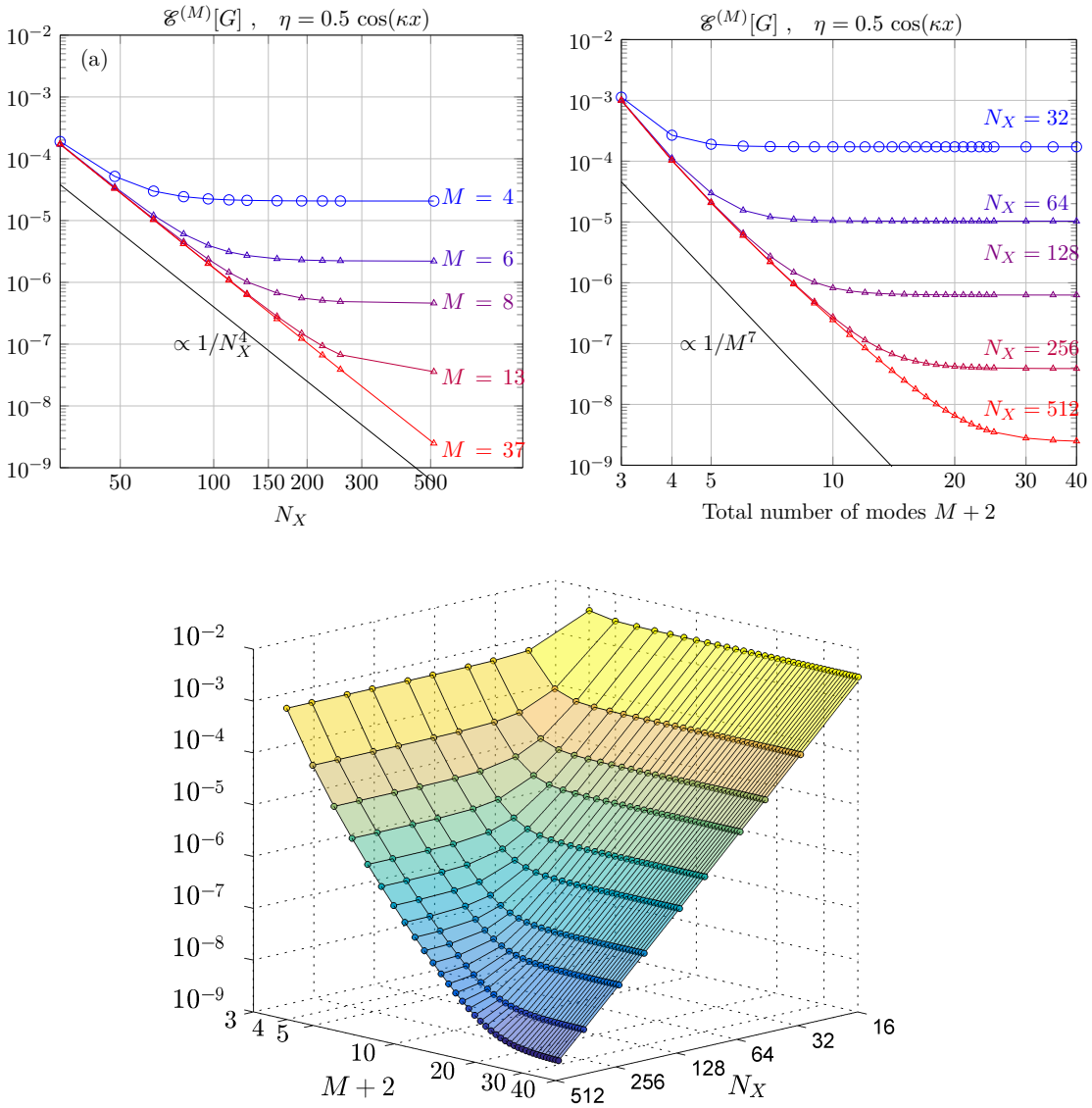

Figure 5.5: $\mathscr{E}^{(M)}[G]$ for the smooth case $\varepsilon = 0.5$. (a) $\mathscr{E}^{(M)}[G]$ as a function of N_X for different values of $M+2$. (b) $\mathscr{E}^{(M)}[G]$ as a function of $M+2$ for different values of N_X. (c) $\mathscr{E}^{(M)}[G]$ as a function of (N_X, M).

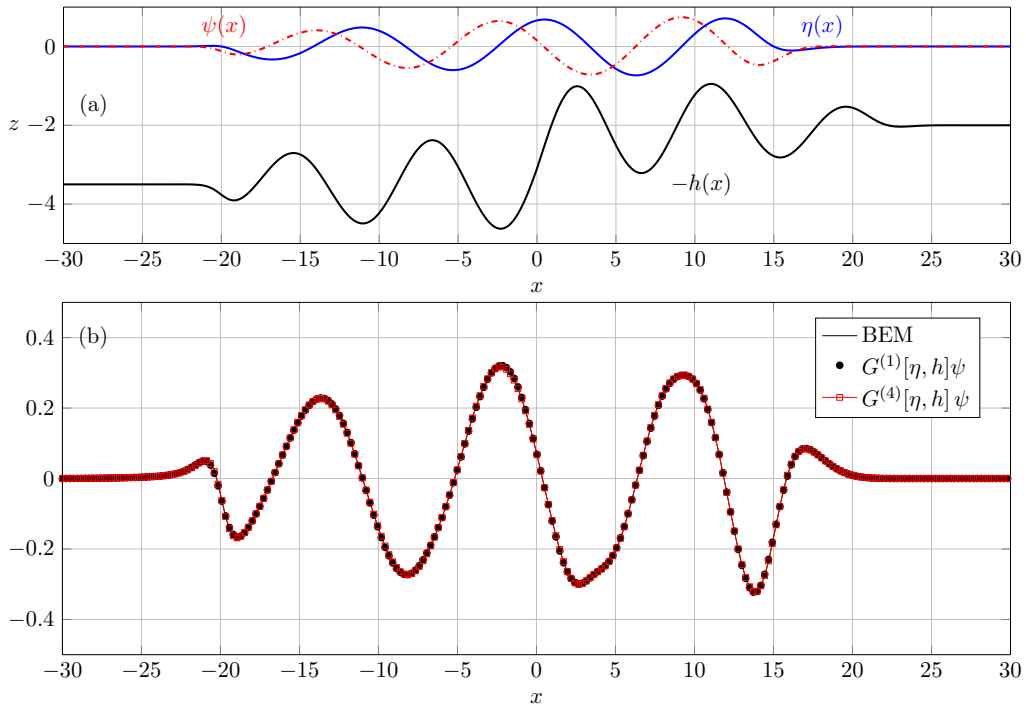

Figure 5.6: (a) Non-uniform domain and Dirichlet data ψ used in the computations. (b) Comparison of the DtN operator computed by using CCMM and BEM.

NR01, while CCMM does not diverge for any number of terms M.

2) CCMM with 6 or 7 modes provides better accuracy in comparison with the best accuracy possible by OE and FE before their divergence.

3) The TFE does not diverge, reaching a plateau limit, with a limiting accuracy which is slightly better than that of CCMM for small values of ε (see Figs. 1 to 5 in NR01 in comparison with Figure 5.4, above), but it is worse for high values of ε; for example, for the "rough" profile and $\varepsilon = 0.8$, the limiting accuracy of TFE is a little more than 10^{-4} (see Figure 6 of NR01), while the limiting accuracy of CCMM is less than 10^{-4} and is reached by CCMM with only 7 modes.

It should be noted here that the TFE is implemented by using both operator-Taylor expansion and vertical discretization of the domain in order to calculate each term of the expansion, which makes it comparable with direct numerical methods concerning the computational burden.

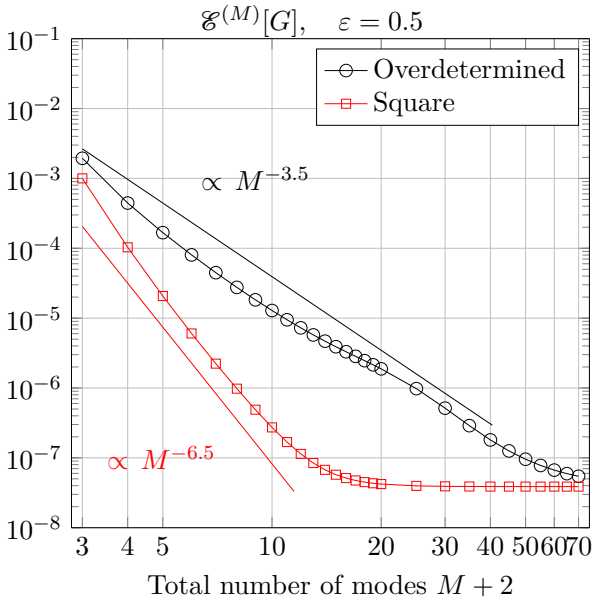

Figure 5.7: L^2-error of the DtN operator, Eq. (5.17)

5.4 On the solution strategy of the substrate CMS

The strategy proposed for the truncation of the infinite substrate system (3.35), is not the only possible. In fact, in the initial implementations of the method the first $M+2$ equations of (3.35) where kept, leading to the following truncated CMS

$$\sum_{n=-2}^{M} A_{mn}\partial_x^2\varphi_n + B_{mn}\partial_x\varphi_n + C_{mn}\varphi_n = 0, \quad m = -2, ..., M, \quad x \in X, \tag{5.18a}$$

$$\sum_{n=-2}^{M} \varphi_n = \psi, \quad x \in X. \tag{5.18b}$$

The finite-difference discretization of the above system leads to an overdetermined linear system which cannot be treated with direct numerical methods and its solution is calculated up to a round-off error. We have observed that this strategy significantly slows down the rate of convergence of $G^{(M)}[\eta, h]\psi$ to the exact solution, see Figure 5.7. Moreover, it increases the computational time, which is inappropriate for simulations in large domains and had to be avoided.

Chapter 6

Computation of travelling periodic waves above a flat bottom

The search of solutions to the problem of steadily travelling water waves goes back to Stokes (Stokes 1847) who employed Fourier series in the horizontal direction and noticed that the free boundary nature of this problem can be treated by perturbation methods, essentially by employing a Taylor series expansion for the velocity potential. This approach was further developed by several authors leading to several variants concerning the type and the order of the employed perturbation expansion, see e.g., (Cokelet 1976, Fenton 1985). As the deficiency of higher order Stoke's expansions, in computing waves of high amplitude, was becoming evident, several authors turned to alternative methods of solution, free of restrictions concerning the nonlinearity or the shallowness of the wave. We mention, for example, the classical works of Longuet-Higgins (Longuet-Higgins 1978*a*,*b*) and (Williams 1981). Another method, perhaps the most popular among the engineering community, is the Fourier approximation method in the context of stream function theory, which was initiated in (Rienecker & Fenton 1981) and further elaborated in (Fenton 1988), leading eventually to a code which is now available online. More recent formulations, applied to the study of the dynamics of steady water waves, include the Zakharov/Craig-Sulem formulation (Nicholls 1998, Craig & Nicholls 2002) and the Ablowitz-Fokas-Muslimani formulation (Deconinck & Oliveras 2011). The present chapter is devoted to the computation of periodic travelling waves above a flat bottom through the HCMS formulation. The methodology followed is similar to (Rienecker & Fenton 1981, Belibassakis & Athanassoulis 2011, Zhao et al. 2016) and aims at the accurate computation of fully nonlinear travelling periodic waves which will serve as data in simulations.

The organisation of the present chapter is as follows. In Section 6.1 we formulate the equations of travelling periodic waves governed by HCMS and, in Section 6.2, we propose a numerical scheme for its solution. Numerical results are presented in the last section.

6.1 Mathematical formulation

The classical differential formulation describing a perfect two dimensional fluid with a free surface in the presence of gravity and under the assumption of irrotational flow consists of the following set of equations

$$\Delta\Phi = 0, \quad \text{in } D^{\eta}_{h_0}, \tag{6.1}$$

$$\partial_z\Phi = 0, \quad \text{on } z = -h_0, \tag{6.2}$$

$$\partial_t\eta + \partial_x\eta\,\partial_x\Phi - \partial_z\Phi = 0, \quad \text{on } z = \eta, \tag{6.3}$$

$$\partial_t\Phi + \frac{1}{2}(\nabla\Phi)^2 + g\eta = C(t), \quad \text{on } z = \eta. \tag{6.4}$$

Eq. (6.1) is the Laplace equation for the velocity potential, accounting for the irrotationality and incompressibility of the fluid flow in the two dimensional domain D^{η}_{h}. Eq. (6.2) is the impermeability boundary condition on the flat seabed $z = -h_0$. Eq. (6.3) and (6.4) are the kinematic and dynamic free-surface conditions, respectively ((Stoker 1957)). In the Bernoulli equation Eq. (6.4), we have chosen to keep the function $C(t)$, emerging from the integration of Euler equations. Following the procedure of Chapter 3.3 the above set of equations can be equivalently reformulated as

$$\partial_t\eta = -\partial_x\eta\,\partial_x\psi + \big((\partial_x\eta)^2 + 1\big)\big(h_0^{-1}\mathscr{F}[\eta, h_0]\psi + \mu_0\psi\big), \quad x \in X, \tag{6.5a}$$

$$\partial_t\psi = -g\eta - \frac{1}{2}(\partial_x\psi)^2 + \frac{1}{2}\big((\partial_x\eta)^2 + 1\big)\big(h_0^{-1}\mathscr{F}[\eta, h_0]\psi + \mu_0\psi\big)^2 + C(t), \quad x \in X, \tag{6.5b}$$

where $\mathscr{F}[\eta, h_0]\psi$ is the free surface amplitude φ_{-2} defined through the infinite time-independent system of second order horizontal ordinary differential equations.

$$\sum_{n=-2}^{\infty} A_{mn}\partial_x^2\varphi_n + B_{mn}\partial_x\varphi_n + C_{mn}\varphi_n = 0, \quad m \geq -2, \quad x \in X. \tag{6.6a}$$

$$\sum_{n=-2}^{\infty} \varphi_n = \psi, \quad x \in X, \tag{6.6b}$$

$$\varphi_n(0) = \varphi_n(L). \tag{6.6c}$$

In (6.6a) the variable coefficients are given by

$$A_{mn} = \int_{-h}^{\eta} Z_n Z_m dz, \tag{6.7a}$$

$$B_{mn} = 2\int_{-h}^{\eta} \partial_x Z_n Z_m dz, \tag{6.7b}$$

$$C_{mn} = \int_{-h}^{\eta} \left(\partial_x^2 Z_n + \partial_z^2 Z_n\right) Z_m dz. \tag{6.7c}$$

To find steady travelling wave solutions, apart from spatial periodicity, one assumes that waves propagate towards one direction, say towards the right, with an unknown uniform speed $c > 0$. Thus, we search for solutions of the form $\eta(x,t) = \tilde{\eta}(\xi)$ and $\psi(x,t) = \tilde{\psi}(\xi)$ where $\xi = x - ct$. Substituting these expressions in Eqs. (6.5a)-(6.5b), dropping tildes and writing x instead of ξ we obtain the following time-independent system

$$c\,\partial_x\eta - \partial_x\eta\,\partial_x\psi + \left((\partial_x\eta)^2 + 1\right)\left(h_0^{-1}\mathscr{F}[\eta, h_0]\psi + \mu_0\psi\right) = 0, \quad x \in X, \tag{6.8a}$$

$$c\,\partial_x\psi - g\eta - \frac{1}{2}(\partial_x\psi)^2 + \frac{1}{2}\left((\partial_x\eta)^2 + 1\right)\left(h_0^{-1}\mathscr{F}[\eta, h_0]\psi + \mu_0\psi\right)^2 + E = 0, \quad x \in X, \tag{6.8b}$$

coupled with the substrate system (6.6), which remains the same under the travelling wave assumption, since it does not contain time derivatives. The arbitrary constant E appearing in Eq. (6.8b) is the Bernoulli constant. Its inclusion, technically speaking, is not of fundamental importance for the numerical solution of the system (6.8). If the time dependent function $C(t)$, appearing in Eq. (6.4), have been absorbed in Φ, then a constant E would not appear in Eq. (6.8b). The equivalence of these two possibilities was recently discussed in (Vasan & Deconinck 2013), where it is shown that taking $E = 0$ results in a steady flow with uniform current.

6.2 Numerical Scheme

A uniformly distributed grid, x_i, $i = 1, ..., N_X + 1$, is introduced in the interval $[0, \lambda]$, where λ denotes the wavelength of the unknown wave. The derivatives of η and ψ, in Eqs. (6.8a), (6.8b), are approximated by using fourth-order central finite-differences for periodic functions,

$$(\partial_x u)_i = \frac{1}{12\delta}\left(u_{i-2} - 8u_{i-1} + 8u_{i+1} - u_{i+2}\right),$$

where the index i denotes the value at x_i and $\delta = \lambda/N_X$. Using the above formula with $f = \eta$ and ψ, in Eqs. (6.8a), (6.8b), we find that (η_i, ψ_i), c and E must satisfy the following nonlinear algebraic system

$$c(\partial_x\eta)_i - (\partial_x\eta)_i(\partial_x\psi)_i + ((\partial_x\eta)_i^2 + 1)\left(\frac{1}{h_0}\left(\mathscr{F}^{(M)}[\eta, h_0]\psi\right)_i + \mu_0\psi_i\right) = 0, \tag{6.9}$$

$$c(\partial_x\psi)_i - g\eta_i - \frac{1}{2}(\partial_x\psi)_i^2 + \frac{1}{2}((\partial_x\eta)_i^2 + 1)\left(\frac{1}{h_0}\left(\mathscr{F}^{(M)}[\eta, h_0]\psi\right)_i + \mu_0\psi_i\right)^2 + E = 0. \tag{6.10}$$

The grid values of the approximate free surface amplitude, $\left(\mathscr{F}^{(M)}[\eta, h_0]\psi\right)_i$, $i = 1, ..., N_X$, are determined by the grid values of the solution of the substrate coupled mode system (6.6). System (6.9), (6.10) involves $2N_X + 2$ unknowns, η_i, ψ_i, $i = 1, ..., N_X + 1$, c and E, but consists of $2(N_X + 1)$ equations. Thus, in order to obtain a closed system we need to impose additional conditions (Rienecker & Fenton 1981, Belibassakis & Athanassoulis 2011, Zhao et al. 2016). The first condition corresponds to the restriction to unimodal waves (one trough in one wavelength)

of specified wave height H:

$$\eta_1 - \eta_{\frac{1}{2}(N_X+1)} = H. \tag{6.11}$$

The last condition expresses the conservation of mass and is obtained by using a numerical integration formula for the approximation of

$$\int_0^\lambda \eta(x)dx = 0. \tag{6.12}$$

Given the wave-height H and wavelength λ, steady water waves for the HCMS are computed by the following iterative procedure

Algorithm 1 Steady Water Wave

Input: λ/h_0 and H/h_0

for $k = 0 \to N_{\text{iter}}$ **do**

Evaluate $A(\eta^k, h_0)$, $B(\eta^k, h_0)$, $C(\eta^k, h_0)$ and compute $\mathscr{F}[\eta^k, h_0]\psi^k$

Solve the system (6.9), (6.10), (6.11), (6.12), with $\mathscr{F}[\eta, h_0]\psi = \mathscr{F}[\eta^k, h_0]\psi^k$

by the Newton-Raphson method, in order to obtain $(\eta^{k+1}, \psi^{k+1}, c^{k+1}, K^{k+1})$

Repeat until $|\eta^{k+1}| + |\psi^{k+1}| + |c^{k+1}| + |K^{k+1}| > |\eta^k| + |\psi^k| + |c^k| + |K^k|$.

end for

The initial guess ($k = 0$) is made on the basis of linear theory

$$\eta^0(x) = \frac{H}{2}\cos(\kappa_0 x), \quad \psi^0(x) = g\frac{H}{2\omega_0}\sin(\kappa_0 x), \quad c^0 = \frac{\omega_0}{\kappa_0}, \quad K^0 = 0, \tag{6.13}$$

where H is the sought for wave height, and the frequency ω_0 and wavenumber κ_0 are related by the well-known dispersion relation

$$\omega_0^2(\kappa_0) = g\kappa_0 \tanh(\kappa_0 h_0).$$

The Jacobian needed for the solution of Eqs. (6.9), (6.10), (6.11),(6.12), at every iteration k, is computed analytically by keeping $\mathscr{F}^{(M)}[\eta^k, h_0]\psi^k$ fixed with respect to the local values η_i, ψ_i. The Newton-Rapshon procedure performed at every iteration k is terminated when the maximum difference between two consecutive iterations becomes less that 10^{-15}. It should be emphasized that the present algorithm executes a double iteration procedure. Other implementations are possible and are left for future study.

λ/h_0	$0.8H_{\max}/h_0$	c/c_0
1	0.1132	0.4250
4	0.4016	0.8127
7	0.5230	0.9608
12	0.5832	1.0668
28	0.7741	1.1724

Table 6.1: Wave speed c/c_0 of strongly nonlinear waves for different shallowness conditions.

6.3 Results and discussion

In this section, Algorithm 1 is implemented for the computation of steady water waves governed by the HCMS. In particular, we examine a well known property of nonlinear waves, that is the dependence of their speed c on their height H. As already mentioned, in order to obtain travelling wave solutions, using the present algorithm, we need to specify λ/h_0 and H/h_0. Algorithm 1 is implemented by gradually increasing H/h_0 for a wide range of shallowness conditions $\lambda/h_0 = 1, 4, 7, 12, 20, 28$. The largest value of H/h_0 is specified by the maximum wave height H/h_0 for which convergence is achieved. For comparison purposes, we introduce the following expression for the extremal value of the wave height with respect to wave length,

$$\frac{H_{\max}}{h_0} = \frac{0.141063(\frac{\lambda}{h_0}) + 0.0095721(\frac{\lambda}{h_0})^2 + 0.0077829(\frac{\lambda}{h_0})^3}{1 + 0.00788340(\frac{\lambda}{h_0}) + 0.0317567(\frac{\lambda}{h_0})^2 + 0.0093407(\frac{\lambda}{h_0})^3}, \tag{6.14}$$

which is given in (Fenton 1990, Section 6) through fitting on the data of (Williams 1981). Throughout our computations we have used a fine spatial discretisation of $N_X = 1000$ points per wavelength and $N_{\text{tot}} = 4, 6, 8$ for the solution of HCMS. Results are shown in Figure 6.1, where they are compared with the corresponding (digitized) data (for $\lambda/h_0 = 4, 7, 12, 20, 28$) presented in (Zhao et al. 2016, Figure 2). The latter are obtained by using modified a version of Fenton's code, able to reach waves of highest amplitude. For waves of height less than 90% of H_{max}/h_0 the results corresponding to $N_{\text{tot}} = 4, 6, 8$ are almost indistinguishable. The convergence of the method with respect to N_{tot} is better observed in the vicinity of H_{max}/h_0. The agreement with stream function theory is evident almost for all values H/h_0. Slight discrepancies are only observed for waveheights larger than 99% of H_{max}/h_0.

In order to illustrate the convergence of the present algorithm we consider strongly nonlinear waves of height equal to 80% of H_{max}/h_0. The corresponding computed velocities are shown in Table 6.1 and are in agreement with the output of Fenton's original code. In Figure 6.2 we have plotted the successive iterations of the free surface elevation for the above five cases. Convergence is always achieved starting from the initial guess corresponding to the desired wave

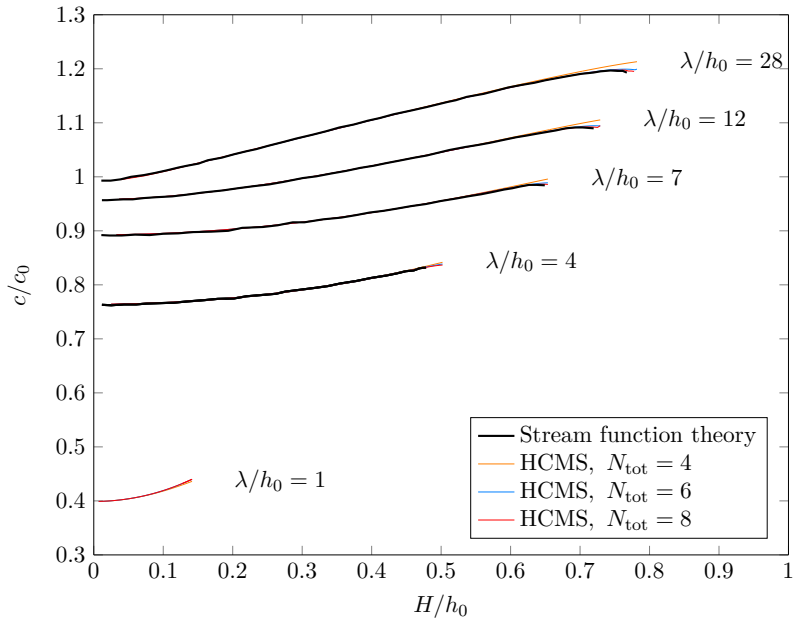

Figure 6.1: The dependence of the wavespeed on the waveheight for different values of wavelength.

height. One might say that the present algorithm implements a "nonlinearization" of the initial linear guess (6.13), which nevertheless is quite naive for that wave height. The investigation of this remarkable feature is left for future work. As the conditions become shallower and the wave height comparable to the depth, more iterations are needed for the fulfillment of the stopping criterion. Furthermore, we have observed that the range of applicability of the present scheme, concerning the shallowness conditions, broadens as nonlinearity becomes smaller.

An important by-product of our approach is that the velocity potential can also be computed in a straightforward way, in view of the solution of the substrate system (6.6). In fact, having computed the numerical solution φ_n, $n = -2, 0, 1, ..., N_{\text{tot}}$, of the latter system for some N_{tot}, the velocity potential on the whole fluid domain is efficiently reconstructed by $\Phi = \sum_{n=-2}^{N_{\text{tot}}} \varphi_n Z_n$, where Z_n are given by Eqs. (2.9) and (2.33). This is very useful because the modal decomposition φ_n, $n = -2, 0, 1, ..., N_T$ provides useful data for the vertical matching of the velocity potential in time-domain computations. Additionally, in view of the analytical expressions for the derivatives of Z_n, derived in Chapter 2, the computation of the velocity $V = \nabla\Phi$ becomes a matter of multiplication and addition. Thus, we also easily retract the data g_m (see Eq. (3.13)) needed for the vertical matching of the horizontal velocity in the substrate system, Eq. (3.35c). As an example, we provide Figures 6.3 and 6.4 the computed horizontal and vertical velocity fields for the studied travelling waves of wave height 80% of H_{max}/h_0. For an interesting discussion on the structure of these fluid quantities we refer to (Clamond 2012).

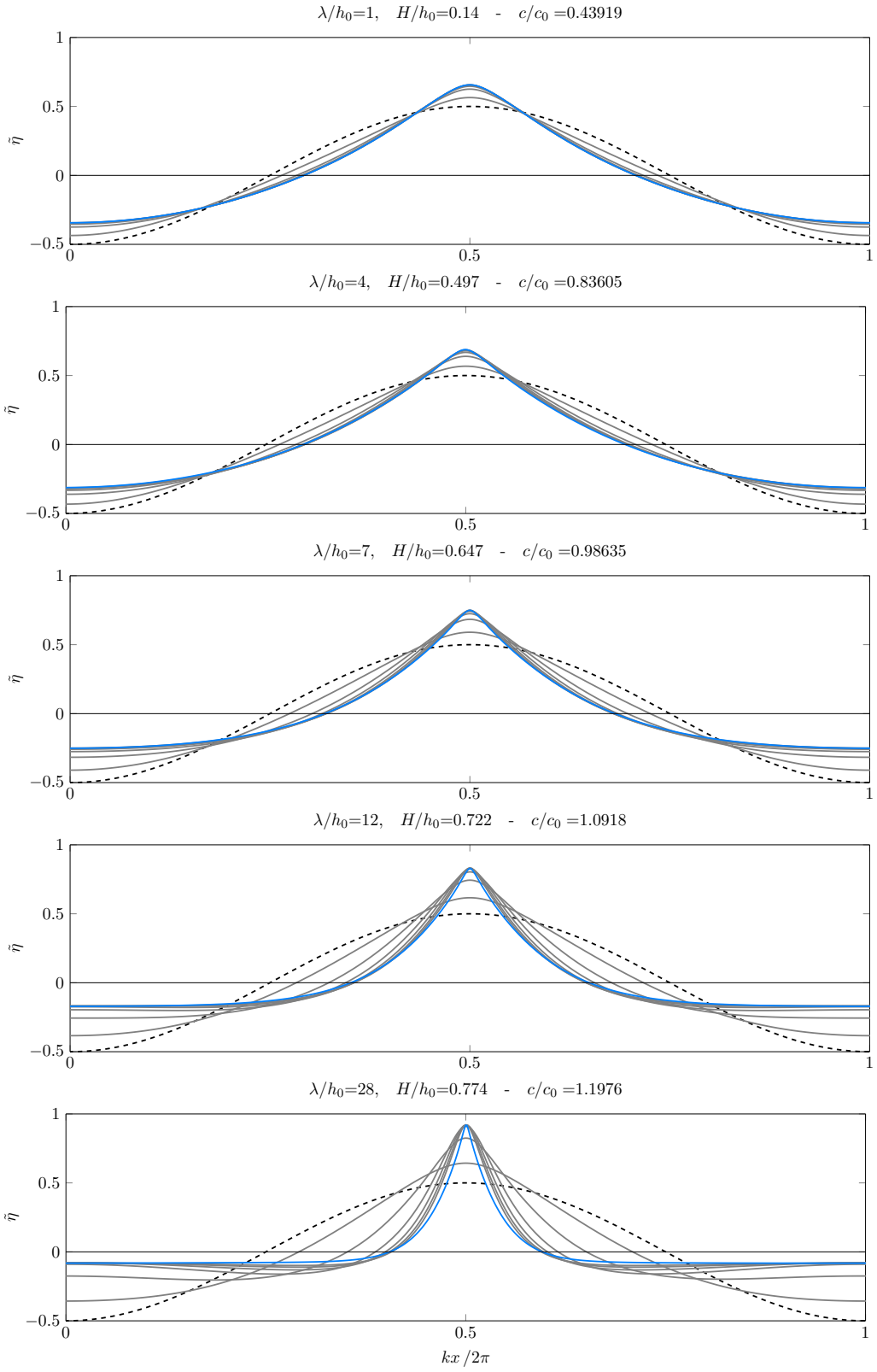

Figure 6.2: Convergence of the nondimensional free surface elevation $\tilde{\eta} = \eta/H$ for waves of wave height H_{max}/h_0. Initial guess and final solution are shown with broken and light blue lines respectively. Grey lines correspond to solutions along the iterations.

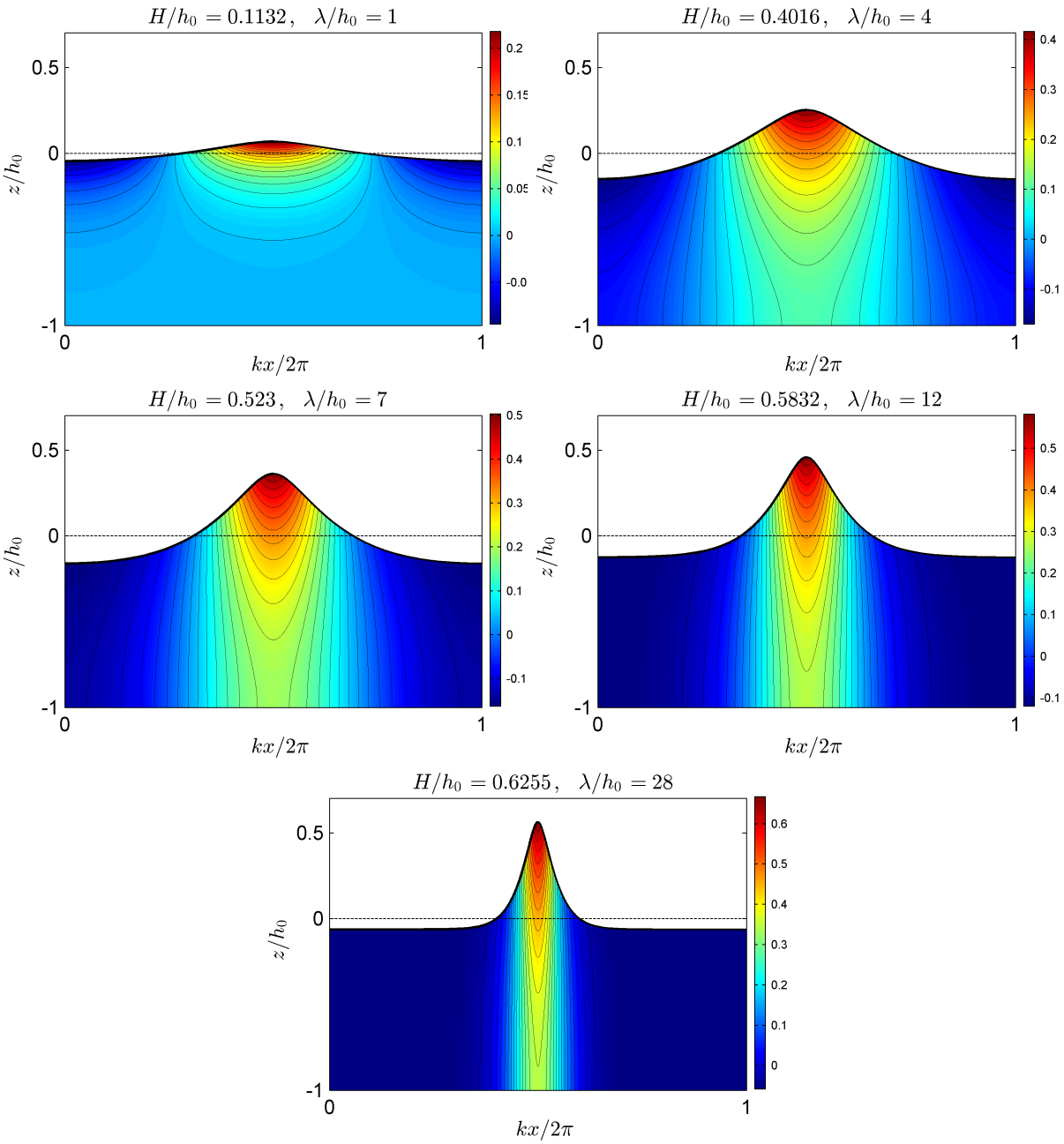

Figure 6.3: Horizontal velocity field $\partial_x \Phi / c_0$ of traveling periodic waves of wave height $0.8 H_{\max}/h_0$.

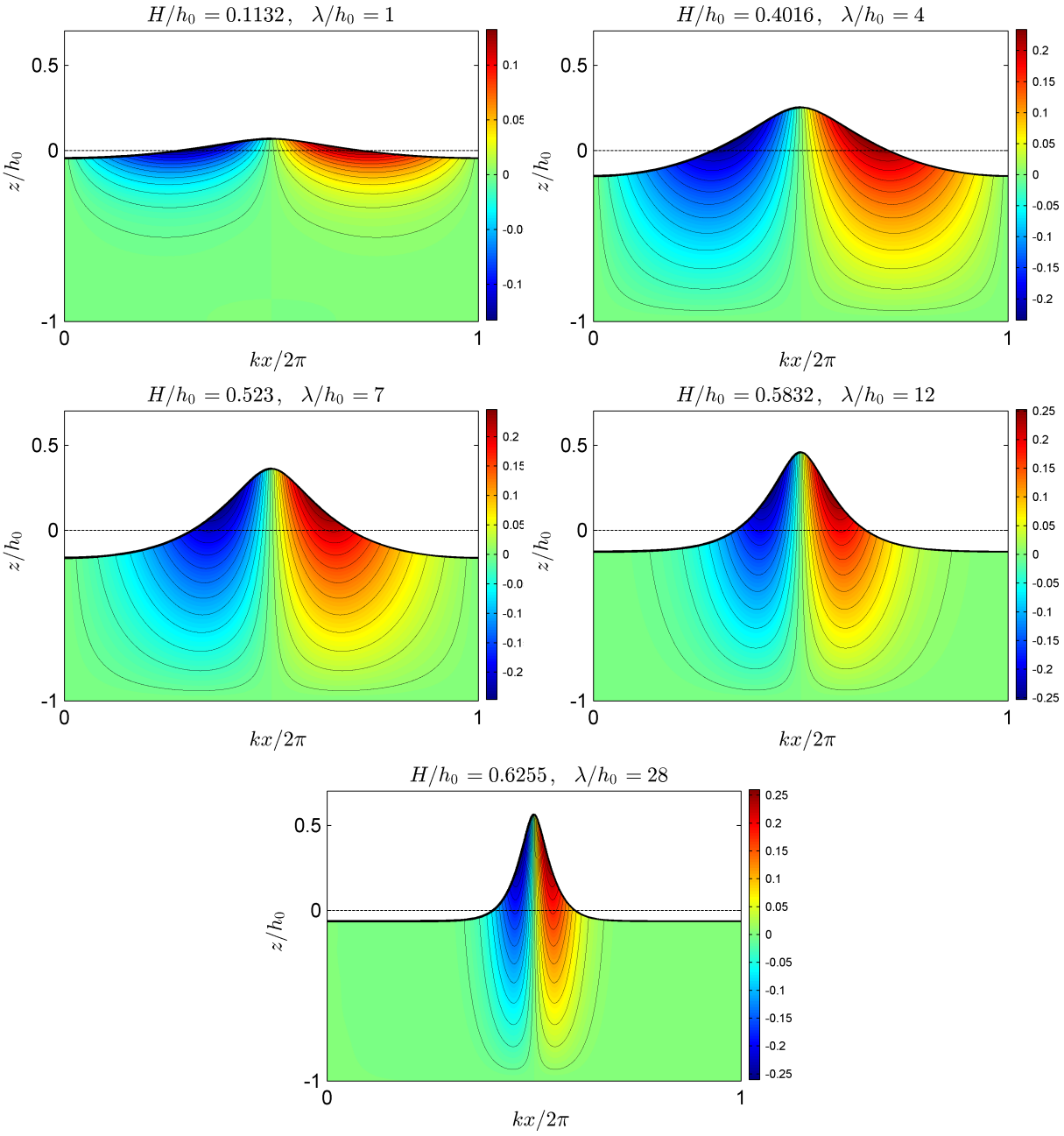

Figure 6.4: Vertical velocity field $\partial_z \Phi / c_0$ of traveling periodic waves of wave height $0.8 H_{\max}/h_0$.

Chapter 7

Time stepping scheme

In this chapter, we describe two numerical schemes applicable to the Hamiltonian Coupled Mode System (HCMS) in one horizontal dimension. The first one corresponds to the case of a basin laterally confined by vertical impermeable walls. This configuration is suitable for simulating the evolution of water waves starting from an initial condition and it can be used to study wave-wave and wave-bottom interactions and the reflection of waves on vertical walls. The second one concerns the case of a numerical wave-tank, able to account for wave generation and absorption. This configuration is suitable for numerical experiments involving the transformation of incident wave fields due to variable bathymetry.

7.1 Closed tank with vertical walls

Assuming that the two fully reflecting walls are located at $x = a, b$, HCMS consists of the following two component system on $X = [a, b]$

$$\partial_t \eta = -\partial_x \eta \, \partial_x \psi + \big((\partial_x \eta)^2 + 1\big)\big(h_0^{-1} \mathscr{F}_{-2}^{(M)}[\eta, h]\psi + \mu_0 \psi\big), \quad x \in X, \tag{7.1a}$$

$$\partial_t \psi = -g\eta - \frac{1}{2}(\partial_x \psi)^2 + \frac{1}{2}\big((\partial_x \eta)^2 + 1\big)\big(h_0^{-1} \mathscr{F}_{-2}^{(M)}[\eta, h]\psi + \mu_0 \psi\big)^2, \quad x \in X, \tag{7.1b}$$

where the (nonlocal) operator $\mathscr{F}_{-2}^{(M)}[\eta, h]\psi = \varphi_{-2}$ is determined by solving the following (substrate) system of second order variable coefficient differential equations on X

$$\sum_{n=-2}^{M} A_{mn} \partial_x^2 \varphi_n + B_{mn} \partial_x \varphi_n + C_{mn} \varphi_n = 0, \quad m = -2, ..., M-1, \quad x \in X, \tag{7.2a}$$

$$\sum_{n=-2}^{M-1} \varphi_n = \psi, \quad x \in X, \tag{7.2b}$$

$$\sum_{n=-2}^{M-1} A_{mn} \partial_x \varphi_n + \frac{1}{2}\big(B_{mn} - \partial_x h Z_n Z_m\big)\varphi_n = 0, \quad m = -2, ..., M-1, \quad x = a,\, b. \tag{7.2c}$$

The matrix coefficients appearing in Eqs. (7.2a) are given by

$$A_{mn} = \int_{-h}^{\eta} Z_n Z_m dz, \tag{7.3a}$$

$$B_{mn} = \int_{-h}^{\eta} \partial_x Z_n Z_m dz + \partial_x h [Z_n Z_m]_{z=-h}, \tag{7.3b}$$

$$C_{mn} = \int_{-h}^{\eta} \Delta Z_n Z_m dz - N_h \cdot [\nabla Z_n Z_m]_{z=-h}, \tag{7.3c}$$

and the system (7.1) is supplemented by initial conditions

$$\eta(x, t_0) = \eta_0(x), \quad \psi(x, t_0) = \psi_0(x). \tag{7.4}$$

For the spatial discretization of the evolutionary system (7.1), we use fourth order central finite differences (see Eqs. (5.6)) on a uniform grid x_i, $i = 1, ..., N_X$, of X, obtaining the following semi-discretized system

$$\partial_t \eta_i = -(\partial_x \eta)_i (\partial_x \psi)_i + \left((\partial_x \eta)_i^2 + 1\right) \left(h_0^{-1} \mathscr{F}_{-2}^{(M)}[\eta, h]\psi + \mu_0 \psi\right)_i, \tag{7.5a}$$

$$\partial_t \psi_i = -g\eta_i - \frac{1}{2}(\partial_x \psi)_i^2 + \frac{1}{2}\left((\partial_x \eta)_i^2 + 1\right) \left(h_0^{-1} \mathscr{F}_{-2}^{(M)}[\eta, h]\psi + \mu_0 \psi\right)_i^2, \tag{7.5b}$$

For the time integration of this evolutionary nonlocal system (7.5), we employ the fourth order Runge-Kutta method, which is a classical explicit method. At every time step, the computation of the free surface amplitude $\mathscr{F}_{-2}^{(M)}[\eta, h]\psi$, required for the evaluation of the right hand sides of (7.5), is accomplished by the finite difference method described in Chapter 5. In order to describe this procedure, let us write the system (7.5) in the compact form $\partial_t U = N[U]$, where $U = U(x_i, t)$. Introducing a temporal grid $t^n = n\delta t$ and $U^n \equiv U(x, t^n)$, the time-stepping is implemented by Algorithm 2. The coefficients α, β and γ are given by the well known Butcher tableau

$$\begin{array}{c|c} \gamma & \alpha_{ij} \\ \hline & \beta \end{array} = \begin{array}{c|cccc} 0 & 0 & 0 & 0 & 0 \\ 1/2 & 1/2 & 0 & 0 & 0 \\ 1/2 & 0 & 1/2 & 0 & 0 \\ 1 & 0 & 0 & 1 & 0 \\ \hline & 1/6 & 1/3 & 1/3 & 1/6 \end{array}$$

It should be emphasized that Algorithm 2, requires four evaluations of $A(\bar{\eta}^k, h)$, $B(\bar{\eta}^k, h)$, $C(\bar{\eta}^k, h)$ and four inversions of the corresponding substrate linear system. Modifications of the above algorithm for the use of other explicit methods of time integration are straightforward.

Algorithm 2 IBVP for the HCMS (7.1)

Given $U^0 \equiv (\eta^0, \psi^0)$

for $n = 1 \to N_{\text{time}}$ **do**

for $i = 1 \to 4$ **do**

$\bar{U}_i \equiv (\bar{\eta}_i, \bar{\psi}_i) = U^n + \delta t \sum_{j=1}^{i-1} \alpha_{ij} K_j^n$

Evaluate $A(\bar{\eta}_i, h)$, $B(\bar{\eta}_i, h)$, $C(\bar{\eta}_i, h)$ and solve the substrate system (7.2) with $\psi = \bar{\psi}_i$

$K_i^n = N(t^n + \gamma_i \delta t, \bar{U}_i)$

end for

$U^{n+1} = U^n + \delta t \sum_{j=1}^{4} \beta_j K_j^n$

end for

7.2 Periodic domain

The HCMS formulation in the periodic case becomes

$$\partial_t \eta = -\partial_x \eta \, \partial_x \psi + \big((\partial_x \eta)^2 + 1\big)\big(h_0^{-1} \mathscr{F}_{-2}^{(N_{\text{tot}})}[\eta, h]\psi + \mu_0 \psi\big), \quad x \in X, \tag{7.6a}$$

$$\partial_t \psi = -g\eta - \frac{1}{2}(\partial_x \psi)^2 + \frac{1}{2}\big((\partial_x \eta)^2 + 1\big)\big(h_0^{-1} \mathscr{F}_{-2}^{(N_{\text{tot}})}[\eta, h]\psi\big)^2, \quad x \in X, \tag{7.6b}$$

where $X = [0, \lambda]$. The (nonlocal) operator $\mathscr{F}_{-2}^{(N_{\text{tot}})}[\eta, h]\psi = \varphi_{-2}$ is determined by solving

$$\sum_{n=-2}^{M} A_{mn} \partial_x^2 \varphi_n + B_{mn} \partial_x \varphi_n + C_{mn} \varphi_n = 0, \quad m = -2, ..., M-1, \quad x \in X, \tag{7.7a}$$

$$\sum_{n=-2}^{M-1} \varphi_n = \psi, \quad x \in X, \tag{7.7b}$$

$$\varphi_n(0) = \varphi_n(\lambda), \quad m = -2, ..., M-1. \tag{7.7c}$$

Eventually, the initial conditions (η_0, ψ_0) and the bathymetry h must be periodic in this case. The time marching of Eqs. (7.6) is implemented by the obvious modification of Algorithm 2.

7.3 Wave tank with generation and absorption layers

A common feature of wave simulations in finite domains is that reflections are expected to occur at the boundaries, at a finite time during the simulation. An approach to cope with this

burden in water waves is to surround the boundaries of the computational domain by absorbing layers appropriately designed to absorb outgoing waves. This method, also called sponge layer technique, is very popular in the engineering community and has been implemented in several variants see e.g. (Cao et al. 1993, Jensen 1998, Clamond et al. 2005, Zhang et al. 2014). In order to describe the implementation of this method in the present context, let us first write the Hamiltonian Coupled Mode system in one horizontal dimension, in the case of a matching condition at $x = a$ and a vertical wall at $x = b$:

$$\partial_t \eta = -\partial_x \eta \, \partial_x \psi + \left((\partial_x \eta)^2 + 1\right)\left(h_0^{-1} \mathscr{F}_{-2}^{(N_{\text{tot}})}[\eta, h]\psi + \mu_0 \psi\right), \quad x \in X, \tag{7.8a}$$

$$\partial_t \psi = -g\eta - \frac{1}{2}(\partial_x \psi)^2 + \frac{1}{2}\left((\partial_x \eta)^2 + 1\right)\left(h_0^{-1} \mathscr{F}_{-2}^{(N_{\text{tot}})}[\eta, h]\psi + \mu_0 \psi\right)^2, \quad x \in X, \tag{7.8b}$$

where $N_{\text{tot}} = M + 3$, M denoting the number of evanescent modes ($n \geq 1$), and $\mathscr{F}_{-2}^{(N_{\text{tot}})}[\eta, h]\psi$ is obtained by solving the following system

$$\sum_{n=-2}^{M} A_{mn} \partial_x^2 \varphi_n + B_{mn} \partial_x \varphi_n + C_{mn} \varphi_n = 0, \quad m = -2, ..., M-1, \quad x \in X. \tag{7.9a}$$

$$\sum_{n=-2}^{M-1} \varphi_n = \psi, \quad x \in X, \tag{7.9b}$$

$$\sum_{n=-2}^{M-1} A_{mn} \partial_x \varphi_n + \frac{1}{2} B_{mn} \varphi_n = g_m, \quad m = -2, ..., M-1, \quad x = a, \tag{7.9c}$$

$$\sum_{n=-2}^{M-1} A_{mn} \partial_x \varphi_n + \frac{1}{2} B_{mn} \varphi_n = 0, \quad m = -2, ..., M-1, \quad x = b. \tag{7.9d}$$

An important question, regarding the numerical wave generation scheme, is how to initialize the wave propagation process. Since an instantaneous non-trivial configuration of the wave field is not known, it seems natural to assume that the fluid is initially ($t = 0$) at rest and it is gradually excited at $x = a$. This is implemented by imposing the conditions

$$\eta(x, 0) = 0, \quad \psi(x, 0) = 0, \ x \in X, \quad g_m(0) = 0, \ m = -2, ..., M-1, \tag{7.10}$$

and

$$g_m(t) = D(t) g_{m,\,\text{imp}}(t), \tag{7.11}$$

where

$$D(\tau) = \begin{cases} e^{1 - \frac{1}{1-(\tau-1)^2}}, & \tau \in (0, 1) \\ 1, & \text{otherwise} \end{cases} \tag{7.12}$$

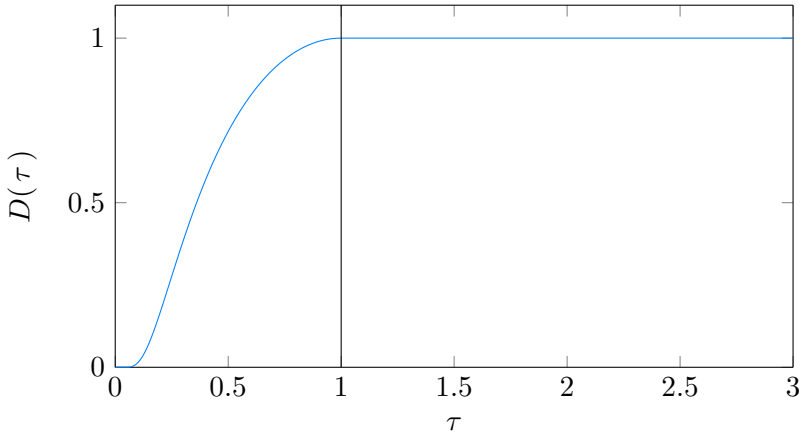

Figure 7.1: The transition function $D(\tau)$

is a smooth transition function and $g_{m,\,\mathrm{imp}}$ denote the data we desire to impose at $x = a$ after some appropriate time $t_c > 0$. In the case of a Dirichlet matching condition we can use instead

$$\eta(a,t) = D(t)\eta_{\mathrm{imp}}(t), \quad \psi(a,t) = D(t)\psi_{\mathrm{imp}}(t), \quad \varphi_m(t) = D(t)\varphi_{m,\,\mathrm{imp}}(t). \tag{7.13}$$

Condition Eq. (7.11) in conjunction with the matching condition Eq. (7.9c) might ensure the generation of a predefined wave at the entrance section $x = a$. However, this is not enough for an efficient, long-lasting, numerical simulation. The reason is that, because of the variations of the bathymetry, backscattered waves are developed, propagating towards $x = a$ and these waves will be reflected within the computational domain (in positive direction) if we do not apply a specific absorption procedure.

We proceed by applying appropriate modifications on the evolutionary system Eqs. (7.8) in an entrance layer (starting at $x = a > 0$) and in an absorption layer (near the end of the finite computational domain at $x = b > a$). Using the notation $U = (\eta, \psi)^{\mathrm{T}}$, the right hand sides of (7.8), denoted by $N(U,t)$, are modified by the introduction of two terms proportional to prescribed smooth functions $c_a(x)$ and $c_b(x)$ supported in small regions before the boundaries $x = a$ and $x = b$:

$$\partial_t U = N(U,t) - c_a(U_{\mathrm{imp}} - U) - c_b U := \tilde{N}(U,t). \tag{7.14}$$

The spatial variation of c_a and c_b is chosen to be polynomial as in (Zhang et al. 2014).

$$c_a = \begin{cases} C_a \left(\dfrac{a + L_a - x}{L_a} \right)^p, & x \in [a, a + L_a] \\ 0, & x \in [a + L_a, b] \end{cases} \tag{7.15}$$

$$c_b = \begin{cases} 0, & x \in [a, b - L_b] \\ C_b \left(\dfrac{x - (b - L_b)}{L_b} \right)^p, & x \in [b - L_b, b] \end{cases} \tag{7.16}$$

where L_a and L_b denote the lengths of the entrance and absorbing layer. The algorithm for time stepping in this case is shown Algorithm 3. It should be noted that no modification takes place on the substrate system, that is, the sponge layers affects only the free surface boundary conditions. Concerning the vertical wall conditions of φ_n at $x = b$, Eqs. (7.9d), we have observed that as soon as no disturbance reaches $x = b$, up to some level of accuracy, it does not play a significant role and could be replaced for example by homogeneous Dirichlet conditions.

Algorithm 3 HCMS (7.14) with Generation and Absorption Layers

$U^0 \equiv (\eta^0, \psi^0) = 0$

for $n = 1 \to N_{\text{time}}$ **do**

for $i = 1 \to 4$ **do**

Calculate $\bar{U}_{\text{imp}}(t^n + \gamma_i \delta t)$ and $\bar{g}_m(t^n + \gamma_i \delta t)$

$\bar{U}_i \equiv (\bar{\eta}_i, \bar{\psi}_i) = U^n + \sum_{j=1}^{i-1} \alpha_{ij} K_j^n$

Evaluate $A(\bar{\eta}_i, h)$, $B(\bar{\eta}_i, h)$, $C(\bar{\eta}_i, h)$ and solve (7.9) with $\psi = \bar{\psi}_i$ and $g_m = \bar{g}_m(t^n + \gamma_i \delta t)$

$K_i^n = \tilde{N}(t^n + \gamma_i \delta t, \bar{U}^i)$

end for

$U^{n+1} = U^n + \delta t \sum_{j=1}^{4} \beta_j K_j^n$

end for

Chapter 8

Simulations of water waves in one horizontal dimension

In this chapter, the numerical schemes presented previously are implemented for the simulations of nonlinear water waves over flat or varying bathymetry. Our aim is to provide sufficient evidence of the nonlinear accuracy of HCMS and its applicability in demanding cases. First, in Section 8.1 we consider the long-time steady propagation of nonlinear water waves above flat bottom. In Sections 8.2 and 8.3, we consider experiments involving the nonlinear transformation of solitary waves, due to their interaction with vertical impermeable walls and varying bathymetry. In Sections 8.4 and 8.5, we consider the transformation of incident regular waves in the presence of varying bathymetry. Finally, in order to demonstrate the applicability of the method in a quite complicated case, we provide, in Section 8.6, numerical results on the interaction of a solitary wave with an undulating bathymetry.

8.1 Propagation of steady travelling waves over flat bottom

In this section, we illustrate the nonlinear accuracy of the present numerical method and its capability in reproducing the long-time propagation of travelling nonlinear waves above a flat bottom. In order to assess the conservation properties of our numerical scheme, we introduce the relative error on the conservation of energy

$$\mathscr{E}\left[H\right] = \left| \frac{H_0 - H^{(N_{\text{tot}})}(t)}{H_0} \right| \tag{8.1}$$

where

$$H_0 = \frac{1}{2} \int_X \left(\psi_0 G^{(N_{\text{tot}})} \left[\eta_0, h\right] \psi_0 + g\eta_0^2 \right) dx. \tag{8.2}$$

is the initial energy, and $H^{(N_{\rm tot})}(t)$ is the energy during the simulation, computed by

$$H^{(N_{\rm tot})}(t) = \frac{1}{2}\int_X \left(\psi G^{(N_{\rm tot})}\left[\eta, h\right]\psi + g\eta^2\right) dx. \tag{8.3}$$

The X integrals in the above equations are calculated by the trapezoidal rule and $N_{\rm tot} = M + 3$, where M denotes the number of evanescent modes ($n \geq 1$) kept in the enhanced eigenfunction expansion (2.4).

8.1.1 Periodic nonlinear waves

The initial conditions $(\eta(x,0), \psi(x,0)) = (\eta_0, \psi_0)$ for (7.6) are specified as travelling wave numerical solutions (regular waves) obtained by the method developed in Chapter 6. The substrate periodic CMS (7.7) is solved by the finite difference method presented in Chapter 5. Eqs. (7.6) are marched in time by a straightforward adaptation of Algorithm 2 in the present periodic case.

We consider a deep steady wave of wave length $\lambda = 1$ m over a depth $h_0 = 1$ m (shallowness $kh_0 = 2\pi$). The wave height is $H = 0.1132$ m which corresponds to 80% of the maximum value, predicted by (Williams 1981), for the specific choise of λ, h_0. This wave is characterised by nonlinearity $H/h_0 = 0.1132$ (steepness $kH/2 = 0.3555$) which is quite significant. The nondimensional wave speed and period are $c/(gh_0)^{1/2} = 0.4249$ and $T/(g/h_0)^{1/2} = 2.3534$ respectively. The parameter μ_0 is chosen to be $\mu_0 = k\tanh(kh_0)$, where $k = 2\pi\lambda$. The uniform spatio-temporal discretisation is $\delta x = 0.01$ m and $\delta t = 0.05$ s which corresponds to a Courant-Friedrichs-Lewy (CFL) number CFL $= c\delta t/\delta x = 0.667$ and the wave is left to propagate for a duration $30T$ s. Starting with $N_{\rm tot} = 4$ we have observed that high frequency instabilities deteriorate the evolution after $t = 6T$ s. The same happens for $N_{\rm tol} = 5$ after $t = 14T$ s. A choice $N_{\rm tot} \geq 6$ proved sufficient for the completion of the present simulation. The free surface elevation at $t = 30T$ s is shown in Figure 8.1 (a). Its shape and phase is well preserved for $N_{\rm tot} = 7, 8$ (results for $N_{\rm tot} = 9 - 12$ are indistinguishable and therefore omitted). The mass $M(t) = \int_X \eta dx$ as a function of time t is shown in Figure 8.1 (b) and the relative error on the Hamiltonian in Figure 8.1 (c). Both quantities are well conserved, bearing in mind that Eqs. (7.6) are marched in time with the classical Runge-Kutta method.

8.1.2 Solitary waves

We shall now consider the closed wave tank case, Eqs. (7.1), (7.2). The initial conditions (η_0, ψ_0) of (7.1) are specified as a highly accurate solitary wave solutions of the complete water wave problem produced by the code of (Clamond & Dutykh 2013). Specifically, we use the version of the code that takes as input a prescribed amplitude, say a/h_0, and returns the free surface elevation, potential and constant velocity c. The length L of the constructed wave is used for the calculation of $\mu_0 = (2\pi/L)\tanh((2\pi/L)h_0)$.

In the first simulation we consider HCMS with $N_{\rm tot} = 7$. We note that $N_{\rm tot} = M + 3$ where

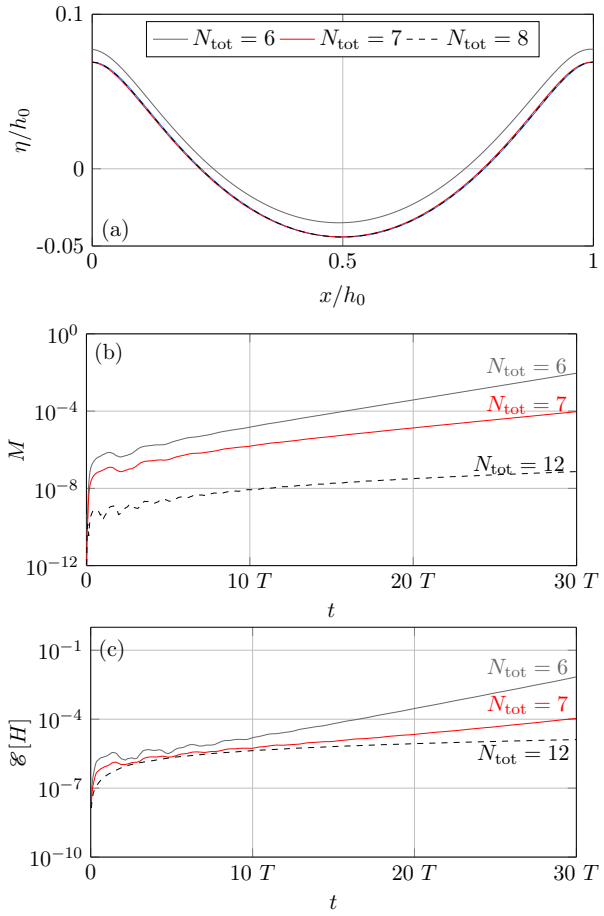

Figure 8.1: Errors during the evolution of a travelling periodic wave of wave height $H/h_0 = 0.113$, $\lambda/h_0 = 1$ (steepness $ka = 0.355$) for different values of N_{tot}: Free surface elevation (a), error on mass as a function of time (b), and relative error on energy as a function of time (c).

M denotes the number of evanescent modes ($n \geq 1$ in (2.4)). This means that we have included the sloping bottom mode despite the fact that the bottom is flat. The sloping bottom amplitude φ_{-1} that is computed during the simulation is practically negligible and no significant differences are observed when the latter mode is neglected from the series expansion. The initial solitary wave has normalized amplitude $a/h = 0.5$ and nondimensional wave speed $c = 1.21$. The constant depth is taken $h_0 = 1$ m and the computational domain is 600 m long. The initial free surface elevation and potential are centered 25 m from the left wall which is a sufficiently long distance in order for the interaction with the wall to be negligible. The spatial and temporal discretization is $\delta x = 0.1$ m and $\delta t = 0.02$ s respectively. Snapshots of the free surface elevation are shown in Figure 8.2. The computed solitary wave maintains its shape even after it has propagated 500 times its depth. The characteristic trail, appearing in the evolution of "exact" solitary wave solutions with asymptotic models (see Figure 5 of (Mitsotakis et al. 2016)) is not noticeable.

The next test concerns the assessment of the convergence our numerical scheme with respect to the spatial discretization. For this purpose we have propagated a solitary wave of amplitude

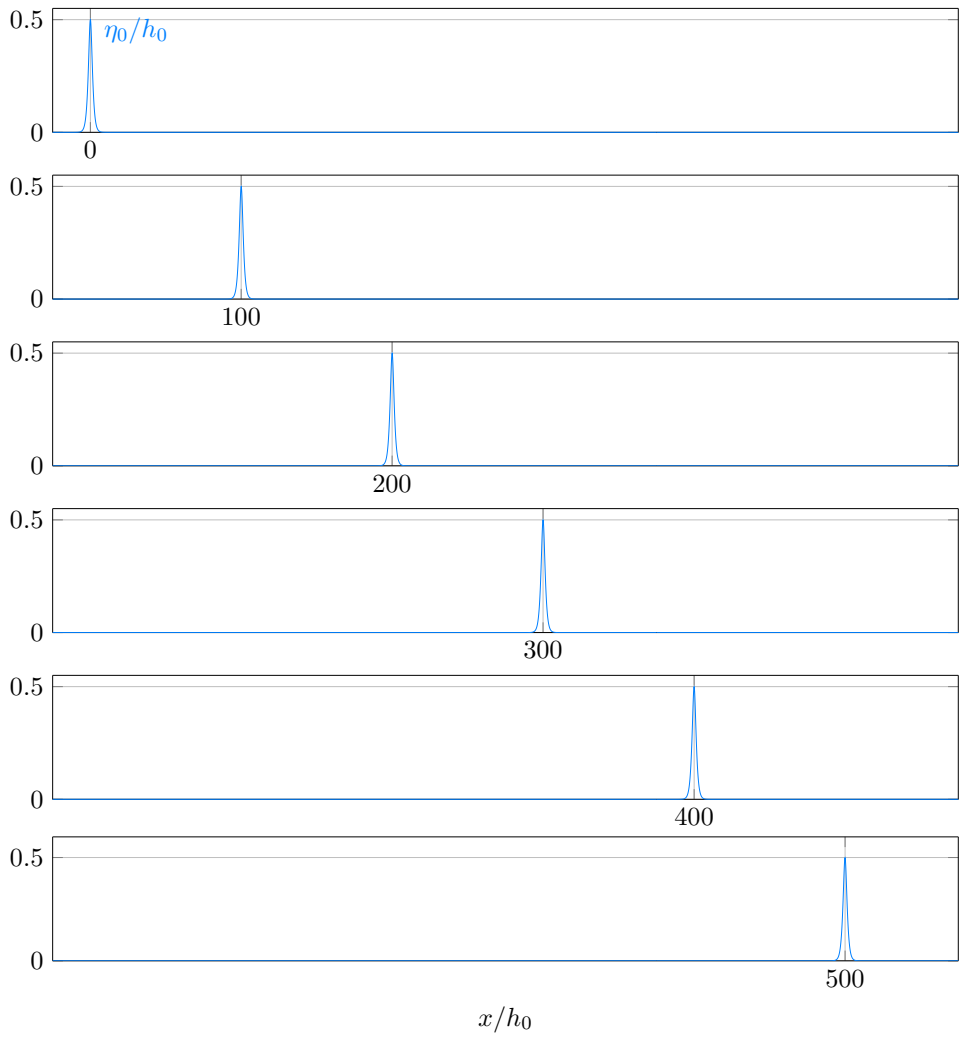

Figure 8.2: Propagation of a solitary wave of amplitude $a/h_0 = 0.5$. Snapshots correspond to $t = 0$, 26.24, 52.50, 78.76, 105.04, 131.30 s.

$a = 0.5$ m over depth $h_0 = 1$ and constant speed $c = 3.8073$ m/s for a duration of approximately 5 s using HCMS $N_{\text{tot}} = 7$. Simulations were performed with $\delta x = 0.5, 0.5, 0.25, 0.125, 0.0625, 0.03125$ and a time step sufficiently small, so that errors from the time integration can be considered insignificant. In Figure 8.3 we monitor the relative L^2 error for η and ψ, denoted by $\mathscr{E}_{L^2}[\eta]$ and $\mathscr{E}_{L^2}[\psi]$ respectively. The scheme clearly convergences with a rate $O(\delta x^4)$ up to $\delta x = 0.0625$ m. For smaller δx the rate of convergence decreases and this might be related to a similar behaviour already observed in the numerical solution of the substrate problem (see Figure 5.5). To investigate the present numerical scheme concerning the number of modes N_{tot} used for the solution of the substrate system, we performed the same computation with $N_{\text{tot}} = 4, 6, 8$. As shown in Figure 8.4 the speed of the computed solitary waves is in very good agreement with the exact one. A slight phase shift is observed only for the case $N_{\text{tot}} = 4$. Finally, in order to examine the sensitivity of the conservation properties on the spatio temporal discretization and

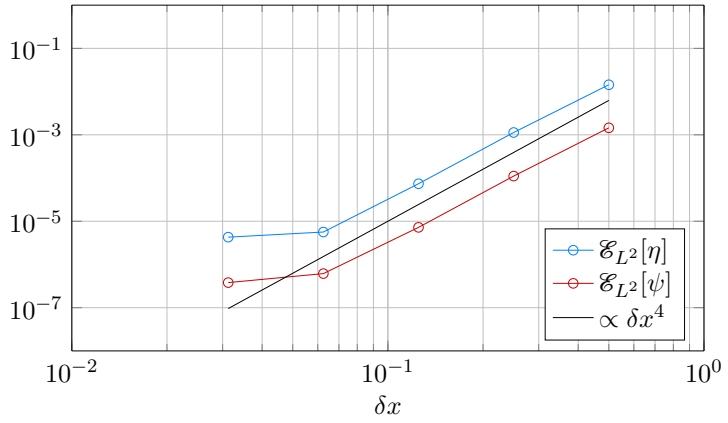

Figure 8.3: Propagation of a solitary wave of normalised amplitude $a/h_0 = 0.4$: L^2 error on the free surface elevation η and potential ψ.

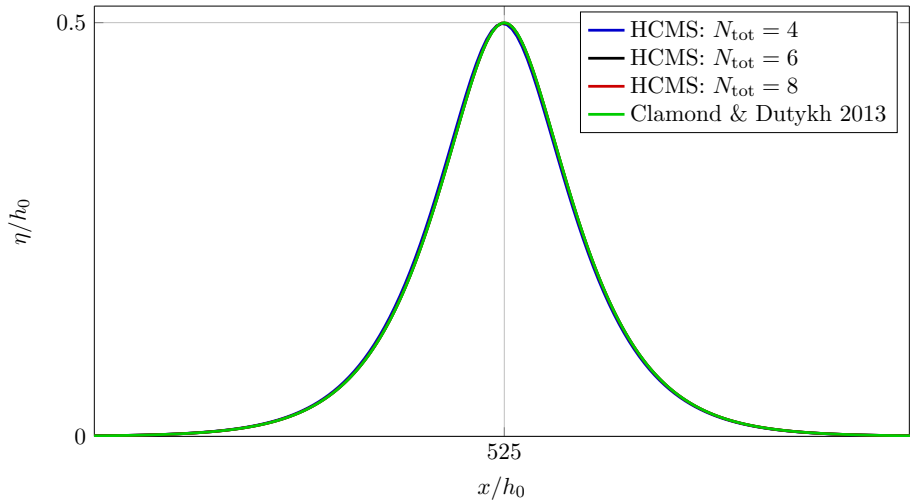

Figure 8.4: Comparison of the computed solitary wave with the exact one after it has travelled 525 times its depth.

N_{tot}, we propagated a solitary wave with $a = 0.4$ m by using CFL $= 0.5$ and $N_{\text{tot}} = 4, 6, 8, 10, 12$. The results are gathered in Tables 8.1 and 8.2. The conserved quantities are very well reproduced for a wide range of numerical parameters.

Despite the fact that the cases studied in this and the previous section are simple, they offer a convenient framework for a detailed numerical investigation of the present scheme which is planned for the near future. Due to the structure of the HCMS, such a study is not classical and requires special attention, since, apart from the discretization in space and time, one must take also into account the errors induced by the truncation of the substrate system.

Table 8.1: Error in the conservation of mass $\mathscr{E}^{(N_{\text{tot}})}[M]$.

N_{tot}	$\delta x = 0.8$	$\delta x = 0.4$	$\delta x = 0.2$	$\delta x = 0.1$	$\delta x = 0.05$	$\delta x = 0.025$
4	$1.01 \cdot 10^{-4}$	$3.00 \cdot 10^{-6}$	$7.24 \cdot 10^{-8}$	$2.40 \cdot 10^{-8}$	$1.42 \cdot 10^{-8}$	$5.31 \cdot 10^{-9}$
6	$9.25 \cdot 10^{-5}$	$2.40 \cdot 10^{-6}$	$3.31 \cdot 10^{-8}$	$2.31 \cdot 10^{-8}$	$1.58 \cdot 10^{-8}$	$1.87 \cdot 10^{-9}$
8	$9.11 \cdot 10^{-5}$	$2.33 \cdot 10^{-6}$	$3.12 \cdot 10^{-8}$	$2.09 \cdot 10^{-8}$	$1.87 \cdot 10^{-8}$	$3.04 \cdot 10^{-9}$
10	$9.06 \cdot 10^{-5}$	$2.31 \cdot 10^{-6}$	$3.12 \cdot 10^{-8}$	$2.12 \cdot 10^{-8}$	$1.51 \cdot 10^{-8}$	$4.68 \cdot 10^{-9}$
12	$9.04 \cdot 10^{-5}$	$2.30 \cdot 10^{-6}$	$3.50 \cdot 10^{-8}$	$1.84 \cdot 10^{-8}$	$1.51 \cdot 10^{-8}$	$7.60 \cdot 10^{-9}$

Table 8.2: Error in the conservation of energy $\mathscr{E}^{(N_{\text{tot}})}[H]$.

N_{tot}	$\delta x = 0.8$	$\delta x = 0.4$	$\delta x = 0.2$	$\delta x = 0.1$	$\delta x = 0.05$	$\delta x = 0.025$
4	$1.73 \cdot 10^{-3}$	$7.84 \cdot 10^{-5}$	$1.71 \cdot 10^{-6}$	$3.36 \cdot 10^{-7}$	$1.61 \cdot 10^{-7}$	$1.19 \cdot 10^{-7}$
6	$1.74 \cdot 10^{-3}$	$8.19 \cdot 10^{-5}$	$2.89 \cdot 10^{-6}$	$9.50 \cdot 10^{-8}$	$4.42 \cdot 10^{-9}$	$3.76 \cdot 10^{-9}$
8	$1.74 \cdot 10^{-3}$	$8.19 \cdot 10^{-5}$	$2.90 \cdot 10^{-6}$	$9.76 \cdot 10^{-8}$	$6.54 \cdot 10^{-9}$	$1.37 \cdot 10^{-9}$
10	$1.74 \cdot 10^{-3}$	$8.19 \cdot 10^{-5}$	$2.90 \cdot 10^{-6}$	$9.80 \cdot 10^{-8}$	$5.29 \cdot 10^{-9}$	$6.10 \cdot 10^{-9}$
12	$1.74 \cdot 10^{-3}$	$8.19 \cdot 10^{-5}$	$2.91 \cdot 10^{-6}$	$9.85 \cdot 10^{-8}$	$7.10 \cdot 10^{-9}$	$1.14 \cdot 10^{-8}$

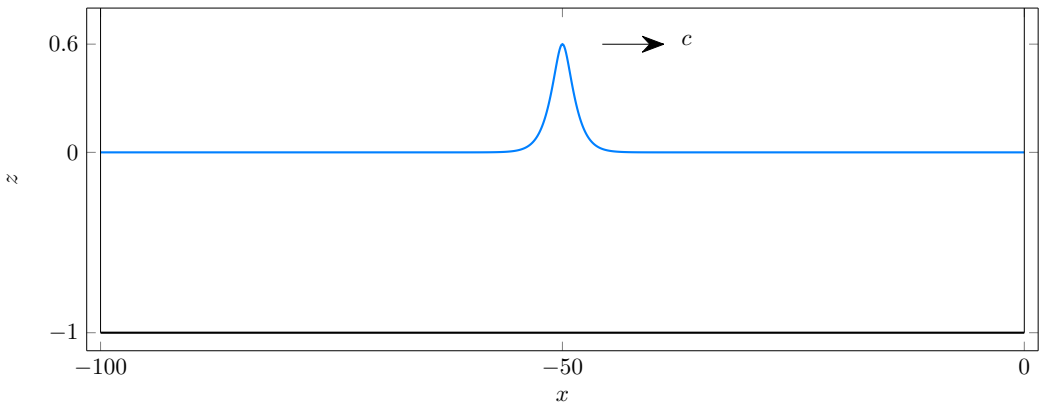

Figure 8.5: Initial free surface and configuration of the domain for the study of the reflection of solitary waves on a vertical wall.

8.2 Reflection of solitary waves on a vertical wall

In order to examine the interaction of nonlinear waves with vertical impermeable boundaries we study the reflection of incident solitary waves on a vertical wall located at the right end ($x = b$) of a flat bottom basin ($h(x) = h_0$), see Figure 8.5. It is recalled that the no-flux condition on the vertical boundaries is implemented by the coupled Robin type boundary conditions (7.2c). This

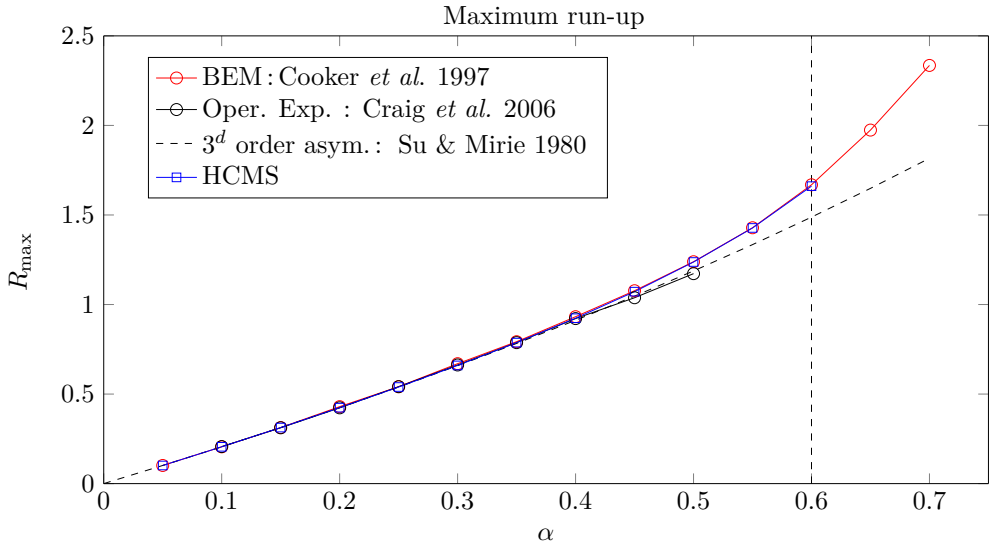

Figure 8.6: Comparison of the maximum run-up, computed by several methods, as a function of incident wave height.

phenomenon has been studied theoretically, numerically and experimentally by several authors. A quantity of interest during this interaction is the (normalised) maximum run-up of the wave on the wall, defined as $R_{\max} = \max\{\eta(b,t)\}/h_0$. An asymptotic formula for $R_{\max}$ is available (Su & Mirie 1980),

$$R_{\max} \sim 2\alpha + \frac{1}{2}\alpha^2 + \frac{3}{4}\alpha^3, \tag{8.4}$$

where α is the normalised amplitude of the initial solitary wave. As it was shown in (Cooker et al. 1997), the maximum run-up predicted by direct numerical simulations for the full problem using the boundary element method, does not agree with the above formula as α approaches its largest possible value. Numerical computations of $R_{\max}$ are also provided in (Craig et al. 2006), using the Zakharov/Craig-Sulem formulation in conjunction with a Taylor series expansion of the DtN operator, and in (Chambarel et al. 2009) using a Boundary Integral Equation Method for the direct solution of the full problem. The same computations are undertaken here by using the HCMS with $N_{\text{tot}} = 8$. The closed basin is extended from $x = -100$ to $x = 0$ and the depth is $h_0 = 1$ m. The spatial and temporal discretisation is $\delta x = 0.05$ and $\delta t = 0.01$ respectively for solitary waves with initial amplitude less than 0.35. For larger values, a finer resolution was required ($\delta x = 0.025$ and $\delta t = 0.005$) in order to obtain stable simulations during the runup and rundown on the wall. Results are shown in Figure 8.6 where several other computations are plotted for comparison purposes. The present method is able to successfully simulate the reflection process for incident solitary waves of amplitude up to $\alpha = 0.6$, showing excellent agreement with the direct BEM method. For values slightly larger than $\alpha = 0.6$ the simulations were interrupted during the rundown process when the free surface becomes almost vertical. BEM

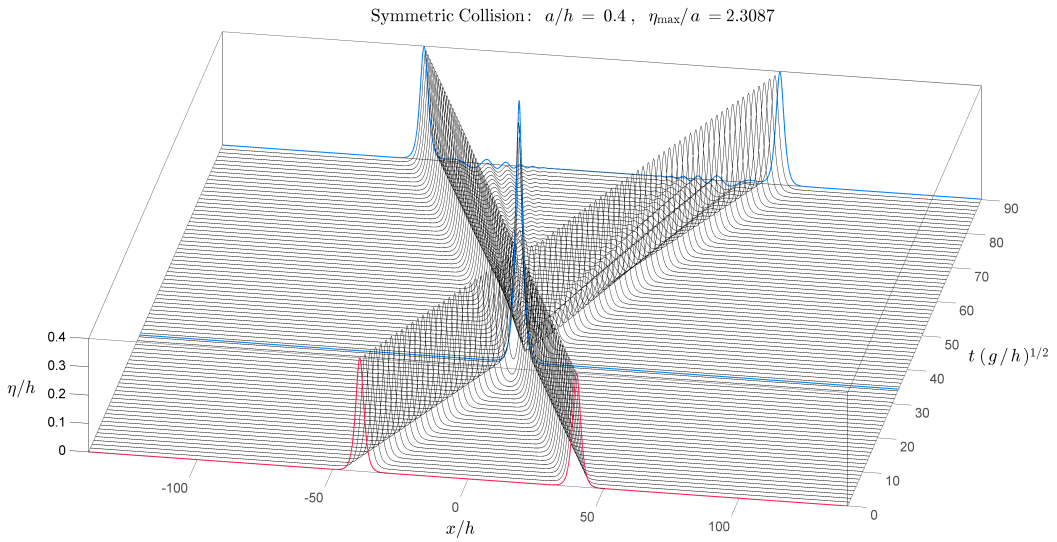

Figure 8.7: Symmetric collision of solitary waves of normalised amplitude $a/h_0 = 0.4$.

computations of (Chambarel et al. 2009) suggest that above this threshold value a residual jet appears. More details and discussions on the reflection of solitary waves as well as its reproduction in the laboratory we refer to (Chambarel et al. 2009, Chen et al. 2015) and the references therein. Closing this section, we present in Figure 8.7 the time history of the symmetric collision of two solitary waves of amplitude $\alpha = 0.4$. It is well known that this interaction is equivalent with the reflection on a vertical wall. For this amplitude, the maximum run-up for both the collision and reflection was $R_{\max} = 0.936$. Further validations as well as numerical results on the velocity field and pressure predicted by HCMS during these interactions can be found in (Charalampopoulos 2016).

8.3 Transformation of solitary waves over varying bathymetry

8.3.1 Shoaling of solitary waves on a plane beach

A solitary wave, initially travelling over a flat bottom, shoals when it encounters a seabed of gradually diminishing topography, usually a plane beach, that ends up to the shore line. During shoaling, the solitary wave undergoes a severe nonlinear transformation which eventually leads to more complex phenomena such as overturning, breaking and run-up.

To show the applicability of HCMS to the simulation of shoaling solitary waves we consider the benchmark test of (Grilli et al. 1994) in which solitary waves are generated in a laboratory wave tank and propagate towards a plane beach of slope 1/35. Since our formulation requires a non-vanishing water depth, we have slightly modified the sloping beach just before the end of the domain. The configuration of the numerical experiment and the position of the measuring gauges is shown in Figure 8.8.

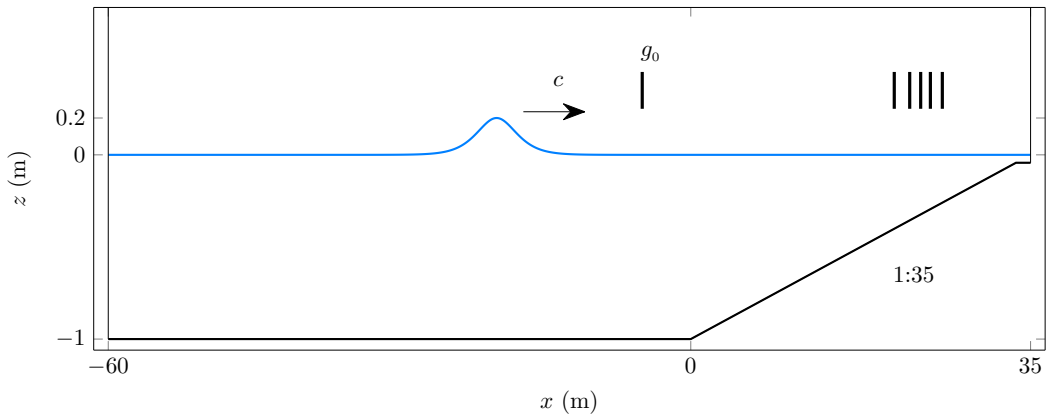

Figure 8.8: Initial free surface and configuration of the computational domain for the experiment of (Grilli et al. 1994). Vertical black line segments correspond to the position of the gauges g_0, g_1, g_3, g_5, g_7 and g_9.

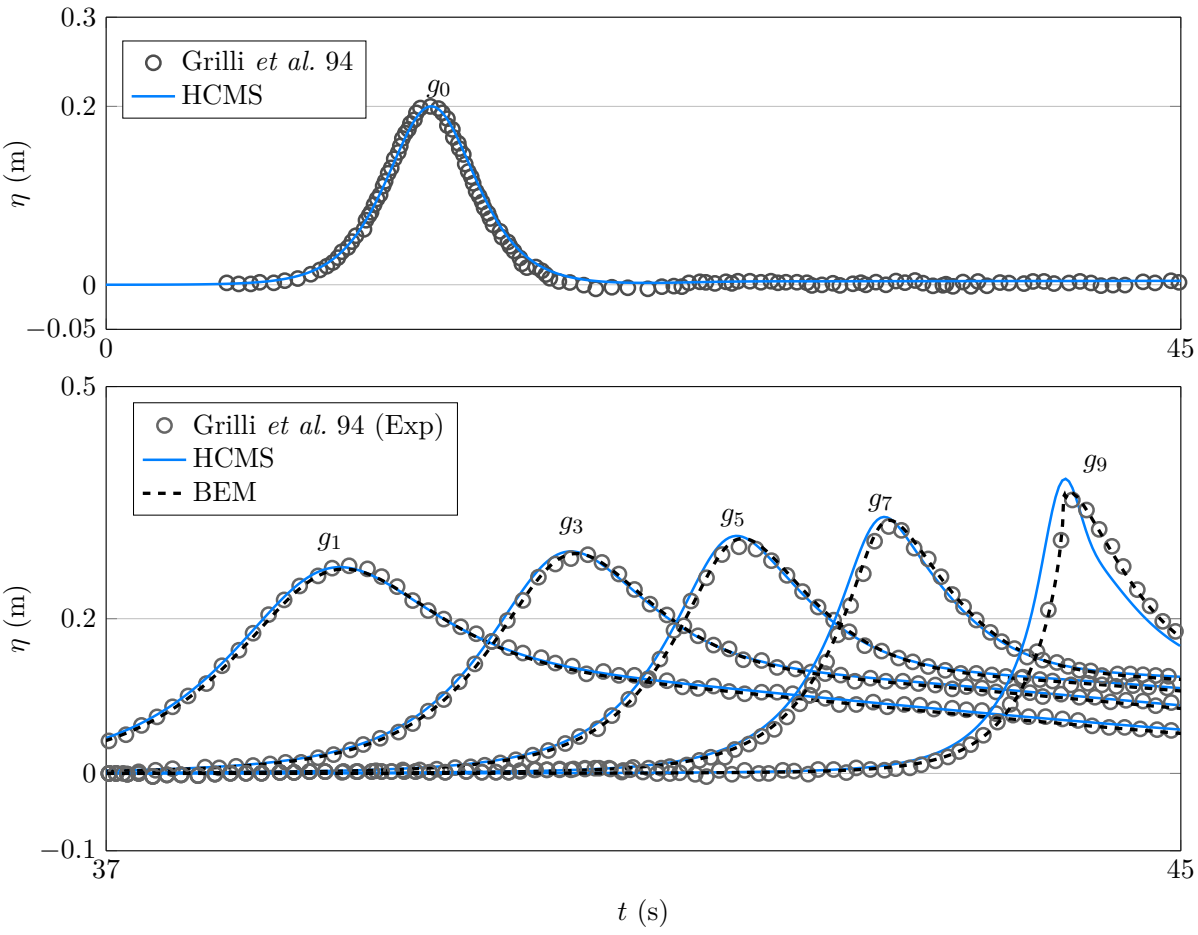

Figure 8.9: Time series of the free surface elevation at several gauges along the wave tank.

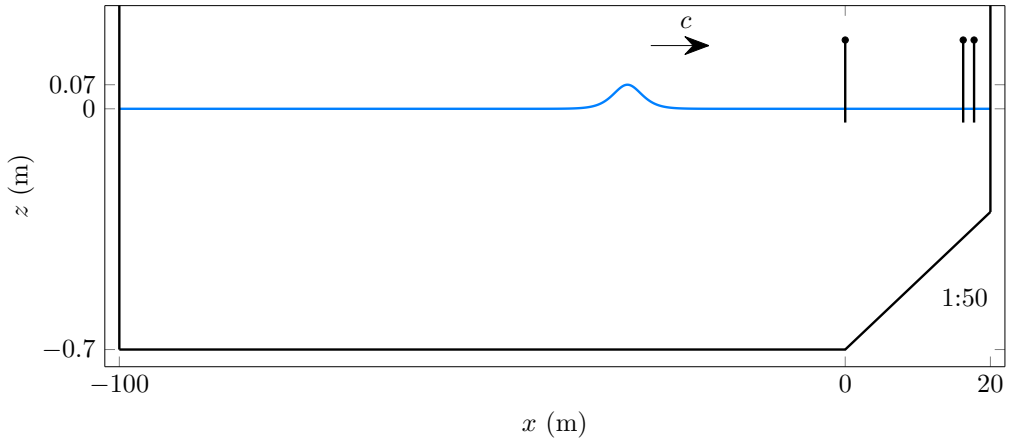

Figure 8.10: Initial free surface and computational domain for the experiment of (Dodd 1998). Vertical black line segments correspond to the measuring stations #1, #2 and #3, located at $x = 0, 16.25$ and 17.75 m.

We consider the case of an initial solitary wave of amplitude $a/h_0 = 0.2$. For the simulation of this experiment we have used HCMS with a total number of modes $N_{\text{total}} = 8$ and a uniform spatio-temporal discretisation $\delta x = 0.1$ and $\delta t = 0.01$. Comparison of our computations with the measurements of (Grilli et al. 1994) and the BEM method (Manolas 2015) are shown in Figure 8.9. The computed free surface elevation is in very good agreement with the measurements at first three gauges g_1, g_3, g_5. A small discrepancy starts to appear at g_7 and becomes more significant at g_9 which is closest to the point where breaking occurs in the laboratory. Agreement of computations and experimental measurements is also observed for the rest of the cases examined in (Grilli et al. 1994) (see (Charalampopoulos 2016)). Shoaling is overall very well reproduced by the HCMS and the phenomenon is captured with adequate accuracy even before breaking.

8.3.2 Reflection of shoaling solitary waves on a vertical wall at the end of a sloping beach

In this numerical test, we simulate a solitary wave that shoals, climbing up a sloping plane beach, and reflects on a vertical wall without breaking. Experiments for this configuration have been conducted in (Dodd 1998) and have been used for the validation of the numerical scheme solving Nwogu's extended Boussinesq equations (Wakley & Berzins 1999). These model equations, being weakly non-linear and weakly dispersive, capture the phenomenon with moderate accuracy, especially when the amplitude of the incident solitary wave is significant (see Section 5.2, Figures 3 and 4 of (Wakley & Berzins 1999)). Recently, (Mitsotakis et al. 2015) demonstrated that the (fully nonlinear) Serre-Green-Nagdhi equations simulate this experiment with higher accuracy than weakly nonlinear models.

The horizontal computational domain extends from $x = -100$ to $x = 20$ m where vertical impermeable walls are located. The depth, for $x \in [-100, 0]$ is constant, $h_0 = 0.7$ m, and the

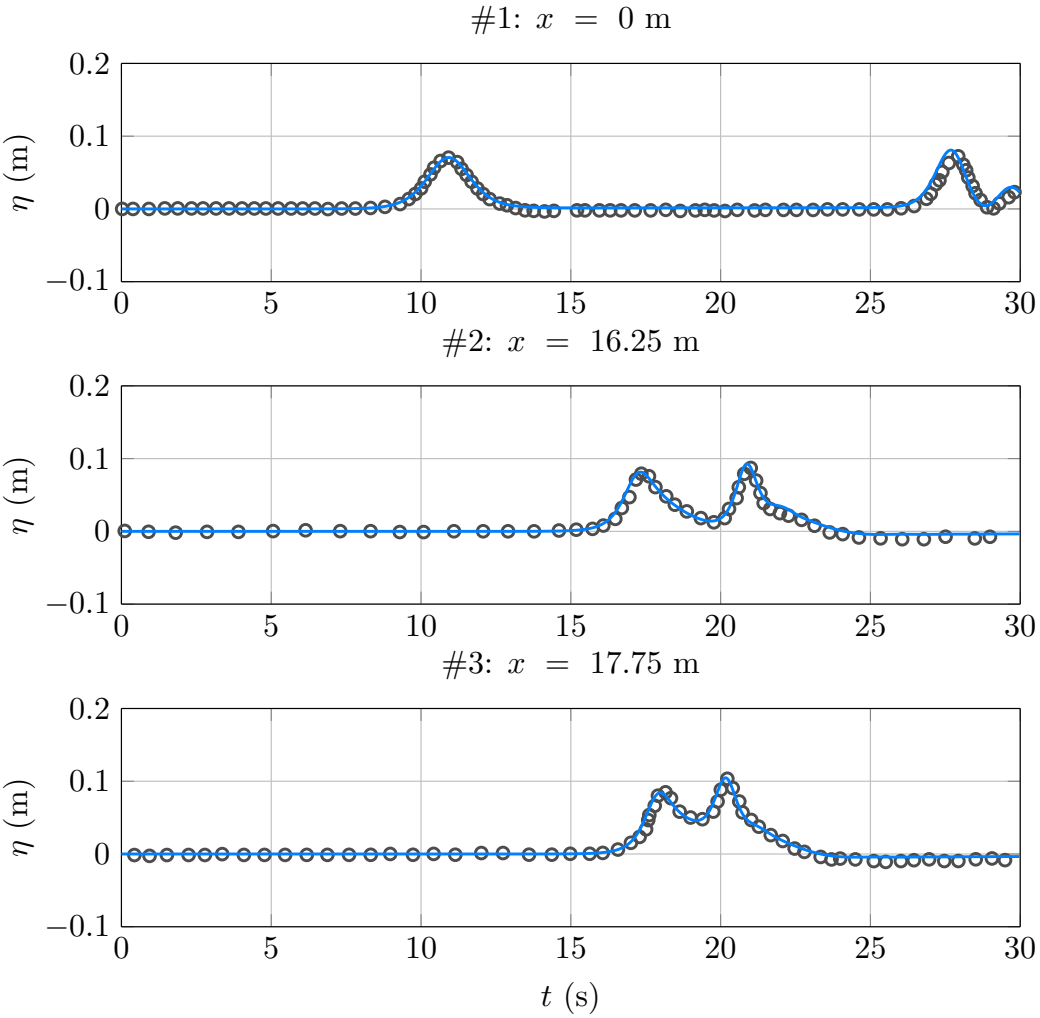

Figure 8.11: Reflection of a shoaling solitary wave, of initial amplitude $a = 0.07$ m, on a vertical wall located at $x = 20$ m. Time series of the free surface elevation, at gauges 1-3. Numerical solution is shown with a light blue line and experimental data with grey circles. The solitary wave is initially centered at $x = -30$.

plane beach of slope 1/50, starts at $x = 0$ m and ends at $x = 20$ m. The initial solitary wave is centered at at $x = -30$, see Figure 8.10. We have considered both cases of (Dodd 1998), corresponding to solitary waves of amplitude $a = 0.07$ m and $a = 0.12$ m, with corresponding velocities $c = 2.7472$ and $c = 2.8337$ m/s. For the numerical solution of HCMS, we have used $N_{\text{tot}} = 7$ modes for the substrate coupled mode system and a spatio-temporal discretization $\delta x = 0.08$ m and $\delta t = 0.015$ s. Comparisons of our computations with experimental measurements are shown in Figures 8.11 and 8.12. The agreement is evident, demonstrating that the present method can accurately simulate the strongly nonlinear reflection process.

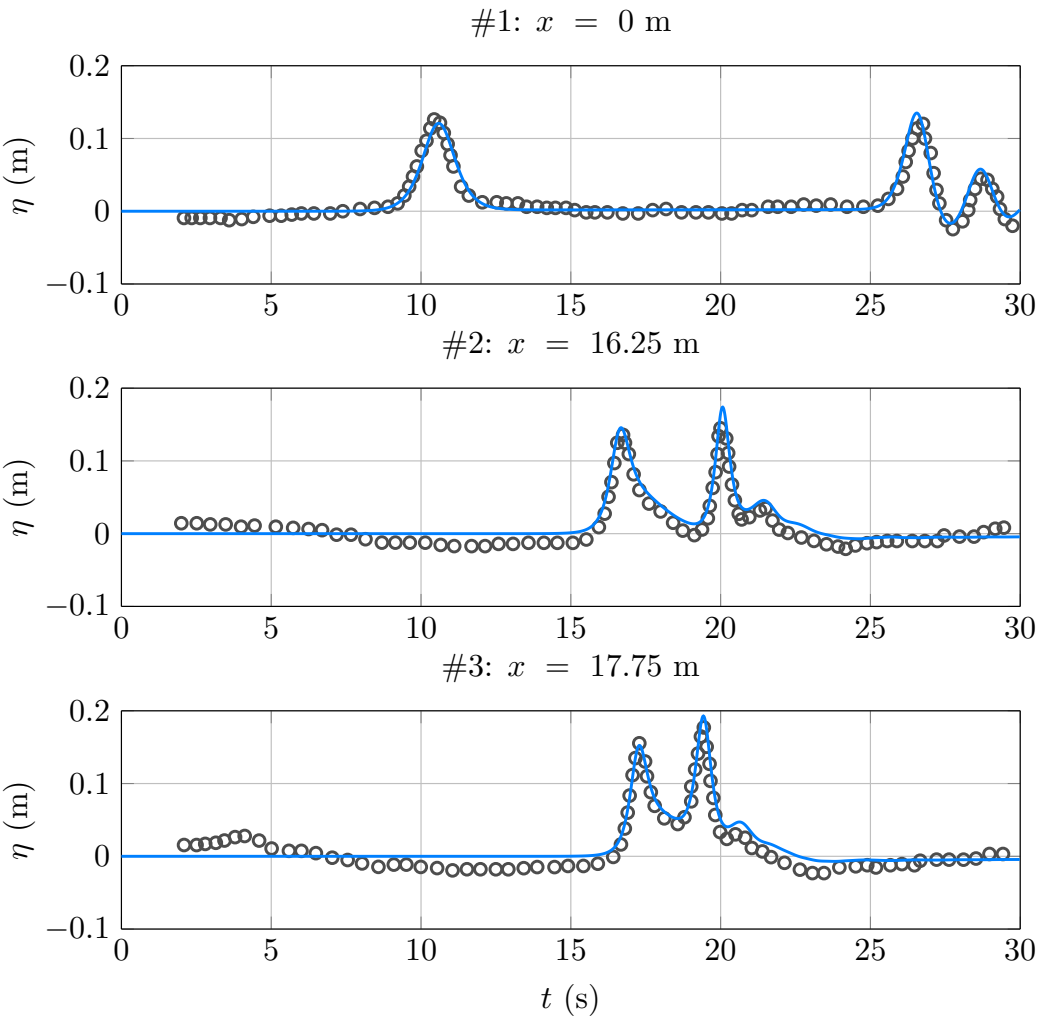

Figure 8.12: Reflection of a shoaling solitary wave of initial amplitude $a = 0.12$ m, on a vertical wall located at $x = 20$ m. Time series of the free surface elevation, at gauges 1-3. Numerical solution is shown with a light blue line and experimental data with grey circles. The solitary wave is initially centered at $x = -30$.

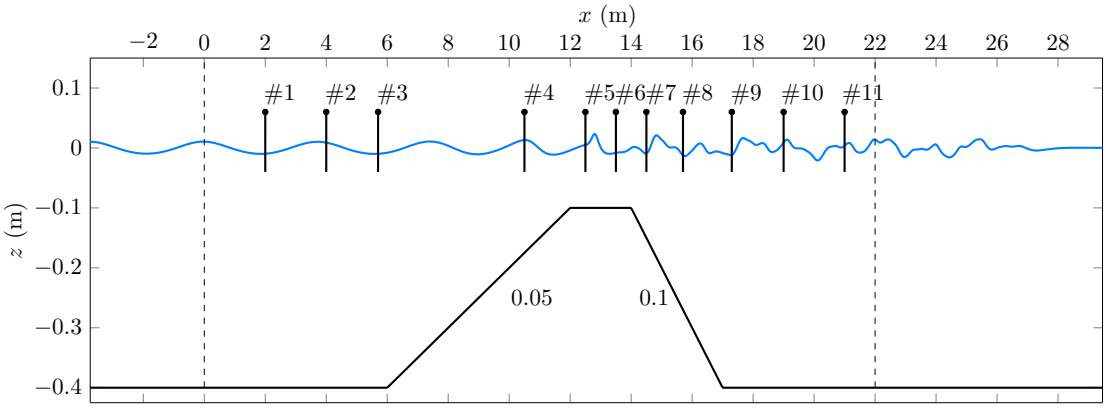

Figure 8.13: Geometric configuration of the numerical wave tank and locations of the measuring stations 1-11 used in (Dingemans 1994). Vertical dashed lines correspond to the ends of the generation and absorbing layers.

8.4 Transformation of regular waves past a submerged obstacle. Harmonic Generation

8.4.1 Trapezoid with mild front and back slopes

We simulate here the experiment conducted by Beji and Battjes in the 90s (Beji & Battjes 1993), which examines the transformation that incident long waves undergo as they propagate past a region characterised by a trapezoidal shoal with mild front and back slopes; see Figure 8.13.

On the one side of the laboratory tank, a wavemaker generates regular waves of relatively small amplitude that propagate towards a submerged bar of trapezoidal shape. As the wave approaches the front side of the bar the shoaling process is initiated, during which the wave amplitude increases. When the wave reaches the horizontal side, it steepens, exhibiting a substantial increase of wave height, just before it is abruptly released towards the deeper region of the tank where it transforms to a rapidly changing dispersive wave pattern. The transmitted wave-field heads towards a region where it is absorbed, allowing the wave-tank to reach a steady state. The free surface elevation is recorded at eight locations along the wave tank, making possible the quantification and further study of the wave transformation. A spectral analysis of the time history of the free surface elevation reveals that the incident monochromatic wave-field is decomposed into higher frequency components, thus this procedure is also called *harmonic generation*. The same experiment, in a different scale, was also conducted by (Dingemans 1994) who measured the free surface elevation in three additional locations after the last station of Beji and Battjes. These type of experimental measurements were used thenceforth for the evaluation of the performance of several numerical water wave models in the case of varying bathymetry and are now widespread (Beji & Battjes 1994, Dingemans 1994, Wakley & Berzins 1999, Woo & Liu 2001, Guyenne & Nicholls 2007, Klopman et al. 2010, Chazel et al. 2011, Belibassakis & Athanassoulis 2011, Chondros & Memos 2014, Zhao et al. 2014, Gouin et al. 2016, Rault et al.

2016).

The case considered herewith is Case A of (Dingemans 1994) in which the wave generation procedure ensures incident periodic wave conditions of wave-height $H = 0.02$ m and period $T = 2.02$ sec that corresponds, according to linear theory, to a wavelength $\lambda_0 = 3.7365$. In the language of asymptotic modelling such a wave is characterized by mild nonlinearity $\varepsilon = H/h = 0.05$, quite small shallowness $\sigma = (h/l_0) = 0.01$, and it can be considered as a shallow or long wave. In order to impose these incident wave conditions, we have first computed a travelling wave numerical solution, by using our Hamiltonian Coupled Mode System (see Chapter 6). The computed wave speed is $c = 1.8518308\ m/s$ and the wavelength $l = 3.7407\ m$. Wave generation/absorption and wave absorption are achieved with the sponge layer approach described in Section 7.3. The length of layers at the left (generating area) and the right (absorbing area) ends of the wave tank is l and $2l$, respectively. The absorbing sponge layer starts acting one meter after the last station (#11) of the experiment. The total length of the computational domain (including sponge layers) is 33.2 m. The spatio-temporal discretisation is $\delta x = l/80 = 0.0468$ m ($N_X = 711$ grid points) and $\delta t = T/100 = 0.0202$ s. The geometric configuration of the numerical wave tank and a snapshot of the computed free surface are shown in Figure 8.13.

In Figure 8.14 we compare the experimental time series of the free surface elevation with our computations by using a total number of 7 modes, for the time window [35,39] s, in which the wave kinematics are adequately established in the laboratory wave tank. The computations show excellent agreement with the experimental measurements concerning both the amplitude and the phase of the free surface elevation. The phenomenon is accurately captured by the present method even in the region after Station #6 where strong dispersion is present and weakly dispersive models give inaccurate predictions (Woo & Liu 2001).

Convergence with respect to M

In order to understand how the performance of the present method depends on the number of modes kept in the enhanced series expansion (2.4), we provide the results obtained for increasing number of modes. The rest of the numerical parameters (spatio-temporal discretisation and sponge layers are kept the same). This type of convergence has also been examined in other numerical models that are based on series representations (Zhao et al. 2014, Rault et al. 2016). Here we take $M = 1, 2, 3, 4, 7$, that corresponds to a total number of modes $N_{\text{tot}} = M + 3 = 4, 5, 6, 7, 10$. For stations #1 - #7, the results are almost identical. Differences start to become significant after station #7 (in the strongly dispersive region of the experiment), and are more pronounced at stations #9 and #11; see Figures 8.15 and 8.16. More specifically, using $M = 2$ ($N_{\text{tot}} = 5$) the results are overall in good agreement with the measurements, except for stations #9 and #11, where they slightly miss to represent the higher harmonics. Using $M = 4$ ($N_{\text{tot}} = 7$) is enough for an accurate reproduction of the experimental results up to station #11. Tiny differences between $M = 4$ and $M = 7$ are observed only in the last three stations (and they are local in time).

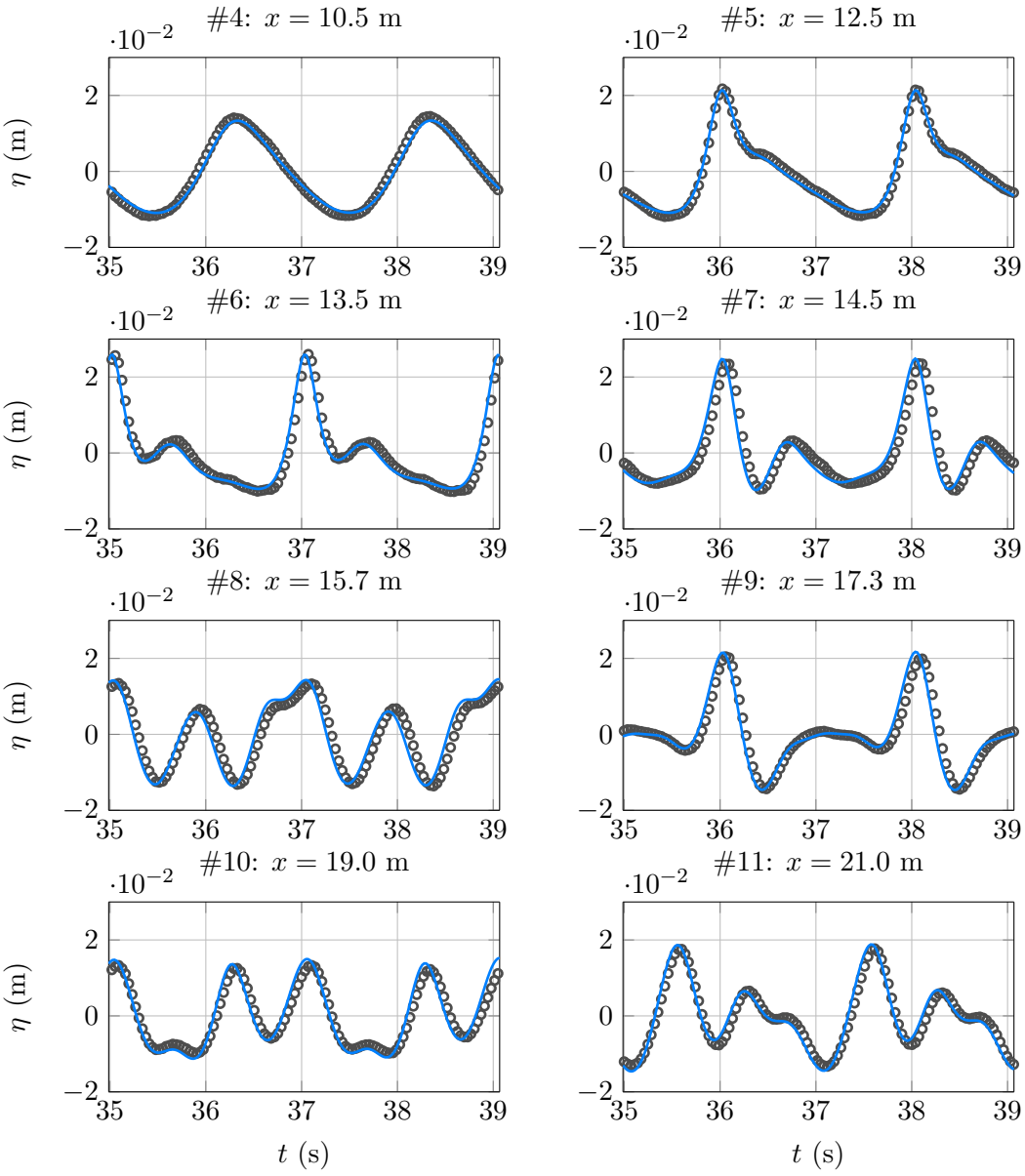

Figure 8.14: Comparison between the time series of the computed free surface elevation (light blue lines) and experimental data from (Dingemans 1994) (grey circles). Measuring stations #4-#11 (see Figure 8.13).

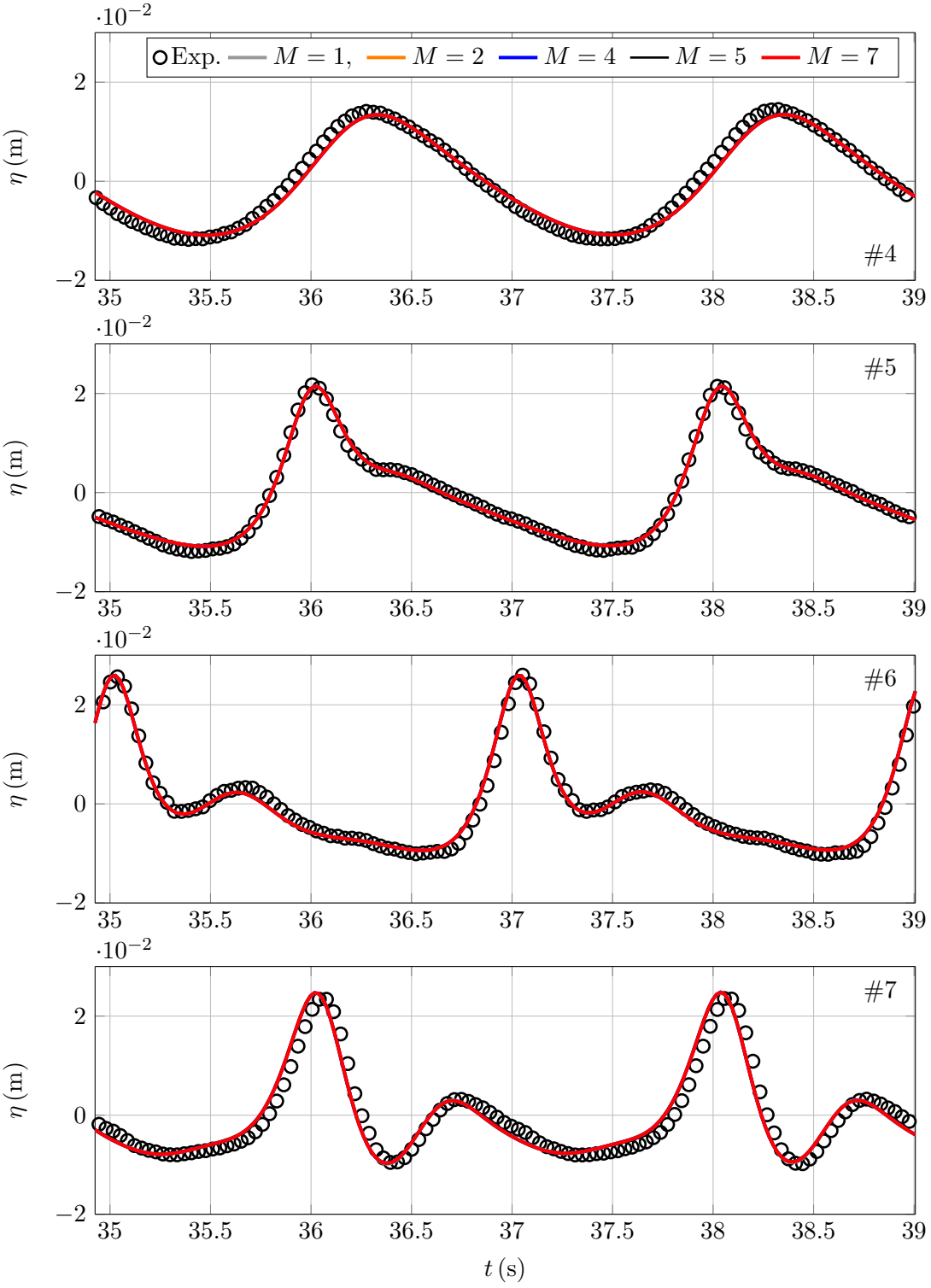

Figure 8.15: Numerical convergence of HCMS with respect to the number of modes used in the series expansion, for the experiment of (Dingemans 1994). Measuring gauges #4 – #7.

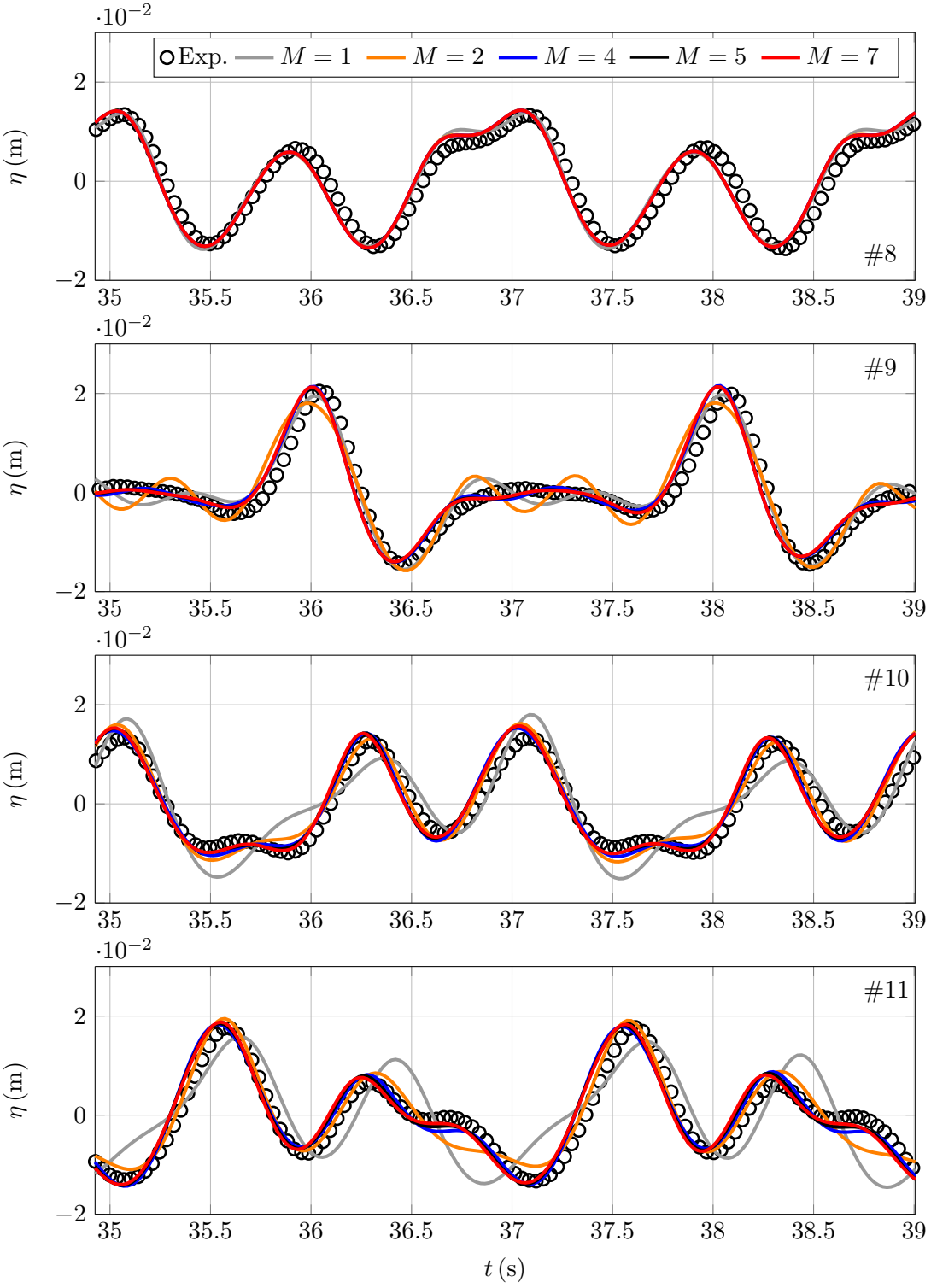

Figure 8.16: Numerical convergence of HCMS with respect to the number of modes used in the series expansion, for the experiment of (Dingemans 1994). Measuring gauges #8 – #11.

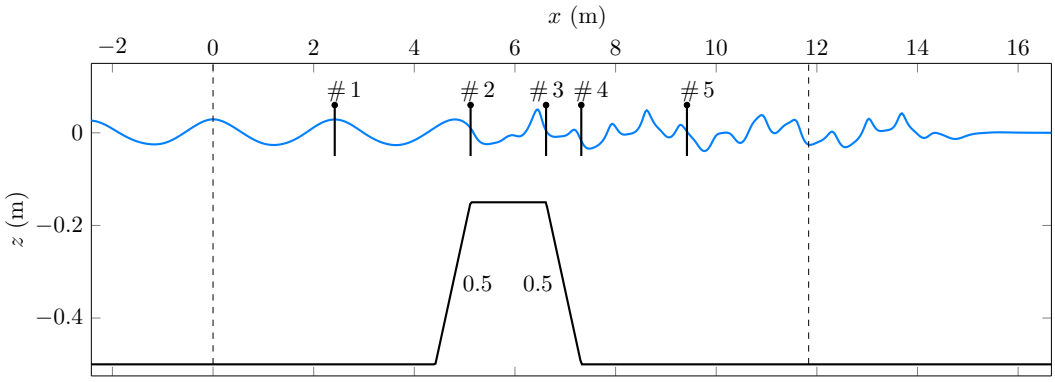

Figure 8.17: Geometric configuration of the numerical wave-tank and locations of the measuring stations 1-5 used in (Ohyama et al. 1995). Vertical dashed lines correspond the ends of the generation and absorbing layers.

Case	Wave height H_0 (m)	Wave period T_0 (s)	Nonlinearity H_0/h_0
2	0.05	1.341	0.1
4	0.05	2.010	0.1
6	0.05	2.683	0.1

Table 8.3: Incident wave conditions for the experiment of (Ohyama et al. 1995)

8.4.2 Isosceles trapezoid with steep slope

We shall now examine the applicability of HCMS in more demanding cases where the trapezoidal bathymetry is characterised by steeper slopes. For this purpose, the experiment of (Ohyama et al. 1995) is considered, in which regular incident waves are transformed past a submerged isosceles trapezoid which compels the depth to range from $h_0 = 0.5$ to 0.15 m with a slope 0.5, see Figure 8.17. (Ohyama et al. 1995) used this experiment to test the ability of a Stokes 2^{nd} order model, the improved Boussinesq equations of (Nwogu 1993) and a fully nonlinear model based on the boundary element method (BEM). This test was recently used for the validation of several other numerical models, including the higher order Green-Nagdhi equations (Zhang et al. 2014), the High Order Spectral method (Gouin et al. 2016) and even a solver for the incompressible Navier-Stokes equations with free surface (Chen et al. 2016). In this work, we consider Case 2, 4 and 6 of (Ohyama et al. 1995) which correspond to the "short", "intermediate" and "long" incident wave conditions. The relevant parameters are shown in Table 8.3. Simulations were performed by gradually increasing the total number of modes N_{tot} until convergence is achieved. For all cases $N_{\text{tot}} = 8$ was sufficient. Denoting by L_0 and T_0 the incident wave length and wave period, the spatio-temporal discretization is $\delta x = L_0/160 = 0.015$ m and $\delta t = T_0/200 = 0.007$ s for Case 2, $\delta x = L_0/200 = 0.02$ m and $\delta t = T_0/200 = 0.013$ s for Case 4, $\delta x = L_0/150 = 0.026$ m and $\delta t = T_0/150 = 0.018$ s for Case 6.

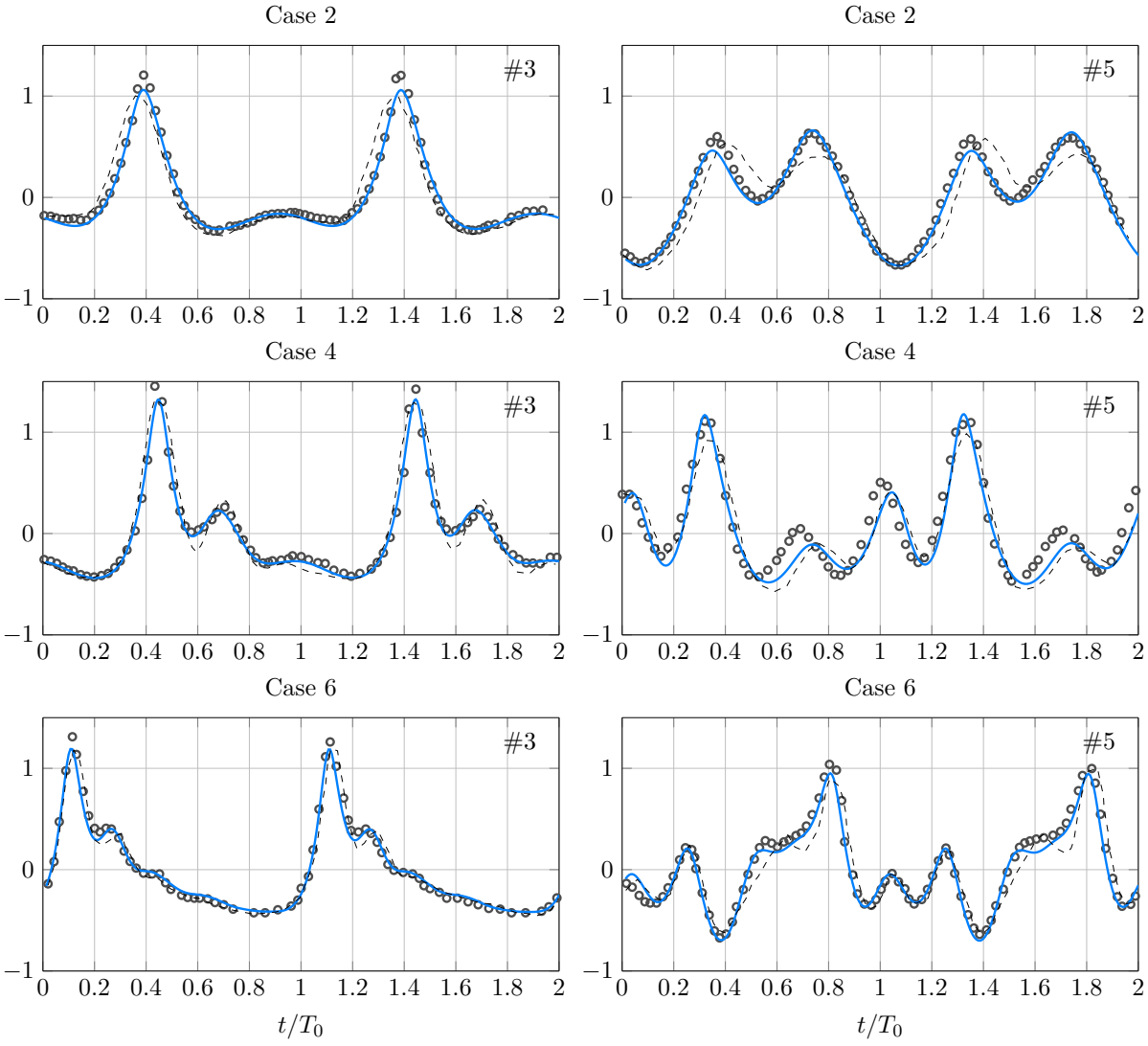

Figure 8.18: Comparison of the computed free surface elevation η/H_0 using HCMS (light blue line) with experimental data (grey circles) and BEM computations (dashed line) of (Ohyama et al. 1995). Measuring stations #3 and #5 (see Figure 8.17).

Comparisons of the computed dimensionless free surface elevation η/H_0 with the digitised experimental data and BEM computations of (Ohyama et al. 1995), at stations #3 and #5, are shown in Figure 8.18. Our computations are time shifted so that their phase matches the experimental ones at station #3, which is located above the right end of the shorter base edge of the trapezoidal bar. The agreement for all cases at station #3 is evident. A slight difference is observed concerning the maximum free surface elevation at station #3 which is also observed in the BEM computations of (Ohyama et al. 1995) as well as in the recent results of (Zhao et al. 2014, Gouin et al. 2016, Chen et al. 2016). It should be noted that according to the computations of (Ohyama et al. 1995), the Stokes 2^{nd} order model provides inaccurate predictions for these cases while the improved Boussinesq equations perform much better despite their weak

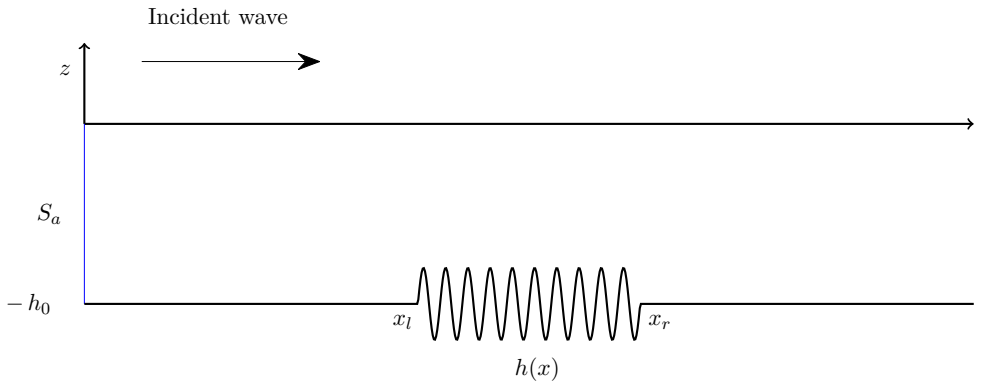

Figure 8.19: Configuration of the wave-tank for the study of Bragg reflection due to the presence of a sinusoidal patch.

nonlinearity. The situation at station #5 is more complicated. Station #5 is located at the lee side of the bar, which is characterised by strongly nonlinear and dispersive effects that cannot be captured by models based on weak nonlinearity and weak dispersion assumptions. In Case 6, our computations are in agreement with the experimental measurements. In Case 4, a significant difference in the phase of higher harmonics is evident between the present computations and the experiment. This difference also appears in the computations of (Ohyama et al. 1995, Zhang et al. 2014, Chen et al. 2016). (Ohyama et al. 1995) and (Chen et al. 2016) argued that this discrepancy is basically due to insufficient resolution in their computations. However, the results of (Zhang et al. 2014), as well as our results are obtained with much finer resolution than the one used in (Ohyama et al. 1995). Finally, our predictions in Case 2 are in very good agreement with the experimental measurements, despite the significant steepness of the free surface elevation. These results indicate that HCMS is capable of modelling strongly nonlinear and dispersive waves that develop during free surface flows past submerged obstacles.

8.5 Reflection of incident waves on a patch of bottom corrugations. Bragg reflection

We study here the transformation of incident regular periodic waves that propagate towards a region characterized by a periodic variation of the seabed. For the case of sinusoidal non-uniformity this wave-bottom interaction was studied theoretically and experimentally in (Davies & Heathersaw 1983, 1984) for the first time. It is shown there that a bottom patch composed by sinusoidal ripples is able to reflect a significant amount of the incident wave energy impinging transversely to the patch. More precisely, it was observed that the incident wave is strongly reflected if its wavelength equals to two times the wavelength of the ripples. This was understood as the hydrodynamic analogue of a phenomenon discovered in 1912, in the context of solid state

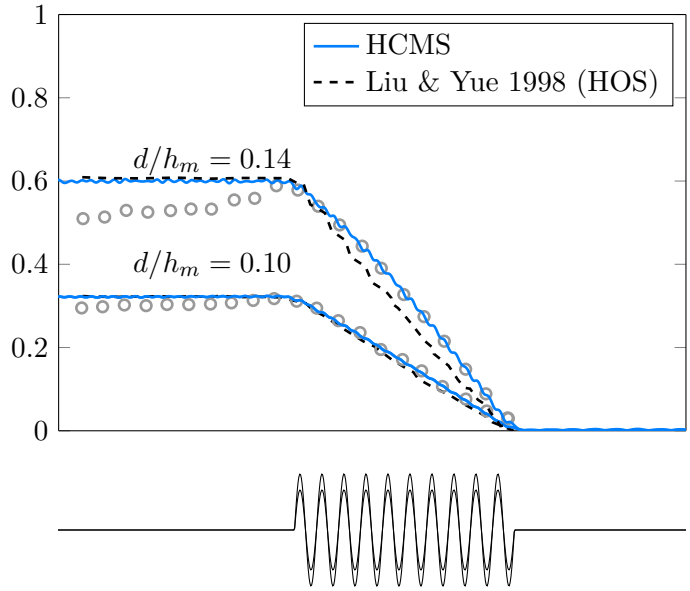

Figure 8.20: Estimation of the local Bragg reflection coefficient in the experiments of (Davies & Heathersaw 1984), for two bottom amplitudes d/h_0 of steepness $k_b d = 0.31$ and incident wave of steepness $kA = 0.05$.

physics, by William Lawrence Bragg and his father William Henry Bragg and is now known as *Bragg scattering*. In the sediment transport literature, this mechanism is employed for the study of formation of sinusoidal sandbars in coastal regions due to surface waves. The original work of DH84 was followed by several others developing the subject in various directions. We mention the work of (Mei 1985) who proposed a theory able to take into account large reflections and (Liu & Yue 1998) who extended the study to three dimensional wave-bottom interactions. Recently, (Couston et al. 2015) studied a closely related phenomenon which can be characterised as the hydrodynamic analogue of the Fabry-Pérrot resonance encountered in optics.

In the following numerical tests we consider a sinusoidal bottom patch of wavenumber $k_b = \frac{2\pi}{l_b}$. The bathymetry $h(x)$ is given by

$$h(x) = \begin{cases} h_0 + d\sin\left(k_b(x - x_l)\right), & x \in [\,x_l, x_r\,] \\ h_0, & \text{elsewhere} \end{cases} \tag{8.5}$$

where x_l and $x_r = x_l + L$ denote the left and right ends of a sinusoidal patch of total length $L = n\lambda_b$, where n is the number of the ripples and $\lambda = 2\pi/k_b$ the bottom wave length, see Figure 8.19.

The amplitude, the wave number and the frequency of the incident waves are denoted by A, k and ω correspondingly. It is known that near the linear Bragg condition ($2k/k_b = 1$) when incident waves and bottom slopes are significant, non-linear effects arise. In order to compare our computations with experimental measurements of (Davies & Heathersaw 1984) we consider

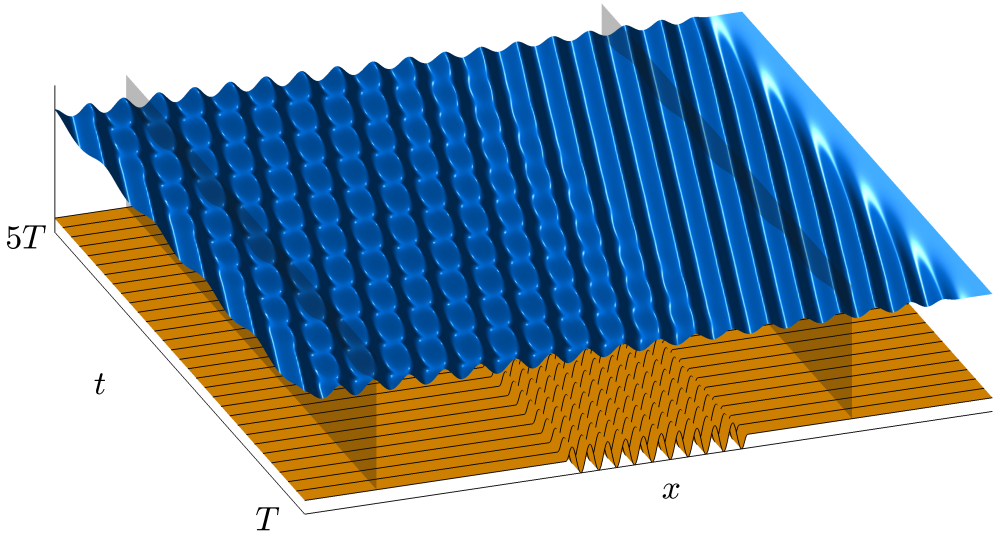

Figure 8.21: Bragg scattering for the case $d/h_0 = 0.14$. Evolution of the free surface between 5 periods.

a patch of 10 ripples for two bottom slopes $d/h_0 = 0.1$ and $d/h_0 = 0.14$ of steepness $k_b d = 0.31$ and incident waves of steepness $kA = 0.05$ with periods $T = 1.20$ s and $T = 1.28$ s. The spatial and temporal discretization is $\delta x = 0.03$ m and $\delta t = T/60$ s. Simulations were performed by using $M = 4$ modes (7 modes totally) for the solution of the substrate system until a steady state was reached in the numerical wave tank. The spatial variation of the reflection coefficient $R(x)$ is estimated by time-harmonic analysis on the local free surface elevation time-series following the method of (Goda & Suzuki 1976). Results in the case where the condition $2k/k_b = 1$ is satisfied are shown in Fig. 8.20. Experimental measurements (DH84) and computations with the High Order Spectral of (Liu & Yue 1998) (LY98), are also plotted, both digitized from LY98. For the case $d/h_0 = 0.1$ experimental and numerical results are almost identical. For the case $d/h_0 = 0.14$, our computations show excellent agreement with the measurements of DH84 over the rippled patch and a slight difference with the computations of LY98. On the upwave side our computations are indistinguishable from the ones of LY98 but both differ from the measurements of DH84 which show a significant decrease on the reflection coefficient. This is attributed in unwanted interference effects present in the tank (see (Davies & Heathersaw 1984)). The results are overall satisfactory illustrating the accuracy of the method and the good performance of the sponge layers. The evolution of the free surface in the (x, t) space during the resonant reflection is depicted in Figure 8.21. A snapshot of the horizontal velocity field and the free surface elevation for the case $d/h_0 = 0.16$ is provided in Figure 8.22.

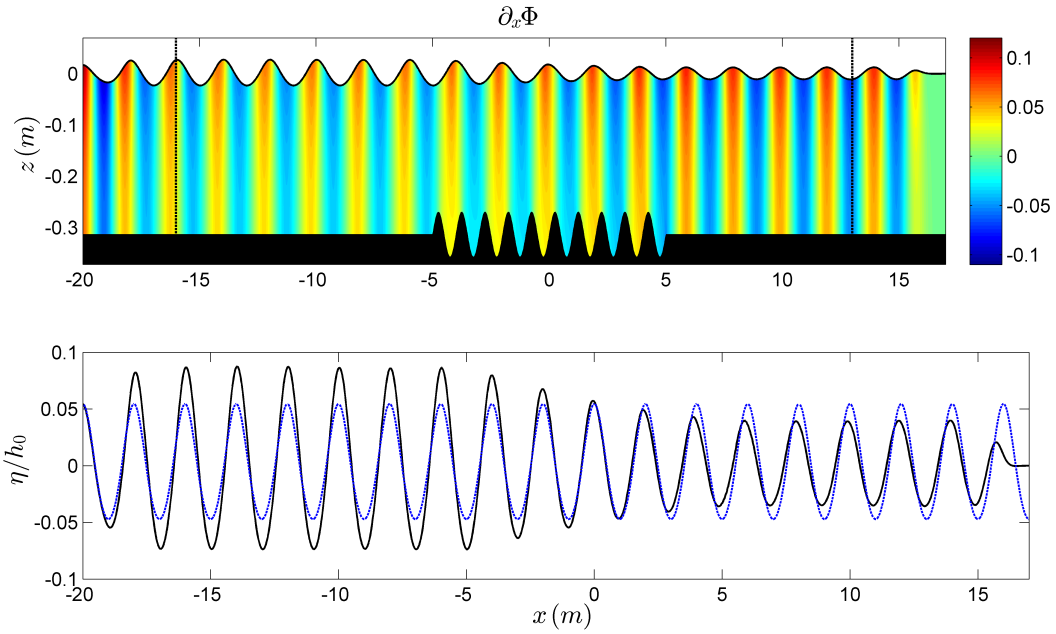

Figure 8.22: (top) Snapshot of the horizontal velocity $\partial_x\Phi$. The vertical black lines represent the edges of the "sponge layers". (bottom) Nondimensionalised free surface elevation η/h_0 for the case $d/h_0 = 0.16$ (black line). The blue dashed line corresponds to the same incident wave travelling over flat bottom.

8.6 Transformation of a solitary wave due to a sinusoidal bottom patch

We consider here the transformation of a solitary wave that initially propagates above a flat bottom and then passes over a sinusoidal patch without breaking. In the present simulation, the initial amplitude of the solitary wave is $a = 0.4$ m, the constant depth is $h_0 = 1$ m, and the varying bathymetry consists of 4 sinusoidal ripples of wave length $L = 12.5$ m (total length 50 m) and amplitude $\beta = 0.3$ m. It is observed that, as the solitary wave passes above the undulation, its crest oscillates and, at the same time, an irregular wave pattern of small amplitude is generated consisting of two distinct parts. The first one is a wave-train travelling steadily in the opposite direction of the incidence as a reflecting wave. The second part is a rapidly changing wave form, trailing the main solitary wave. Long time after the wave-bottom interaction, the solitary wave detaches from its trailing wave, maintaining its shape, with a slightly reduced amplitude and speed. The maximum wave height of the trailing and reflected wave patterns does not exceed $0.050h_0$ and $0.054h_0$, thus both lie the linear regime. The trailing wave assumes the form a wave group with a very broad frequency content. Indeed, the characteristic depth to wave length ratio ranges from 1/2 to 1/25, and as it can be deduced from the figure, dominant frequencies do exist which travel at distinct speeds. On the other hand, the reflected wave train remains practically unchanged after the interaction, with a characteristic depth to length ratio

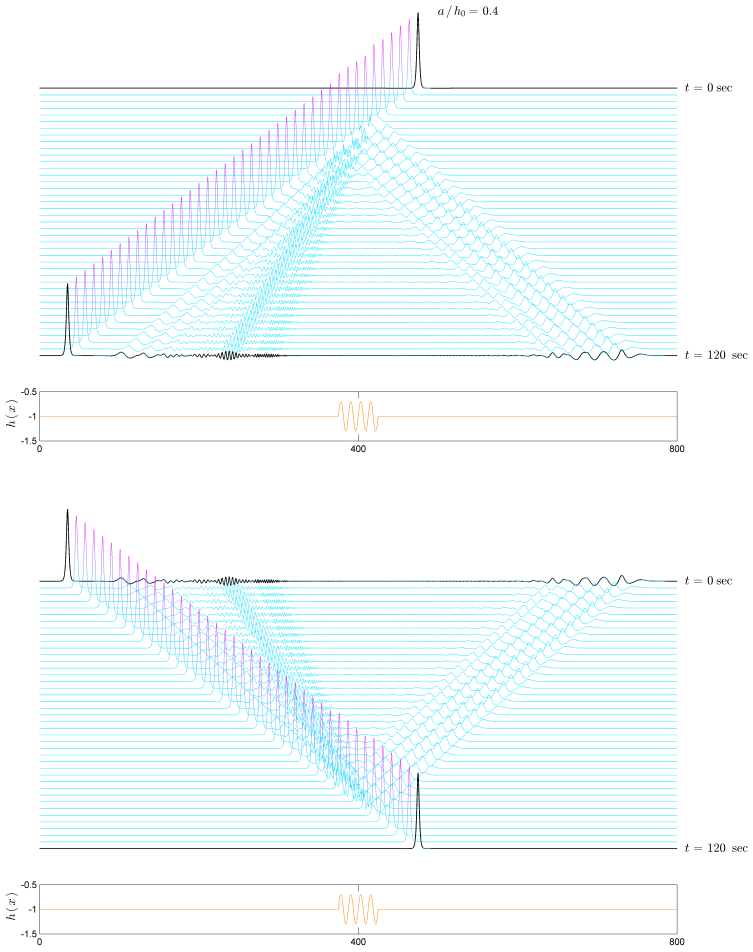

Figure 8.23: (top) Transformation of a solitary wave $a/h = 0.4$ passing over a sinusoidal patch. (bottom) Time reversal of the evolution.

approximately equal to 1/25 and almost constant speed. The characteristics of both products of the wave-bottom interaction depend on the characteristics of the sinusoidal patch (amplitude and wave length). The investigation of their precise relation requires extensive numerical work which is in progress. The error in the conservation of mass and energy remains under 10^{-7} and 10^{-5}, respectively, during this simulation. For validation purposes, we have also considered the time-reversal of this evolution. HCMS is solved with initial conditions $(\eta_0, \psi_0) = (\eta_\mathrm{f}, -\psi_\mathrm{f})$, where η_f, ψ_f denote the computed free surface elevation and free surface potential at the final instant of the already performed simulation. The highly irregular initial condition evolves in time taking the shape of the localised solitary wave which initialised the previous simulation, as it should.

8.7 General comment

The numerical results presented previously demonstrate that the present method can successfully simulate nonlinear and dispersive waves for a wide range of shallowness conditions in the presence of mildly or strongly varying bathymetry. In their majority, the examined cases concern benchmark experiments and were chosen for validation purposes. Several existing models, of low or higher asymptotic order, accurately reproduce the phenomena to these experiments, provided that the involved physical parameters lie in their range of validity. Although, these models allow efficient computations, we are not aware of any model of this type that have reproduced the totality of the cases studied previously. This is understood as a confirmation of the *unified non-pertubative character* of HCMS.

Emphasis should also be placed on the fact that the accuracy of HCMS is comparable to that of direct numerical methods while its numerical solution does not require the discretization of the time dependent free surface or the vertical variable. Moreover, the evaluation of higher-order polynomial nonlinearities and horizontal spatial derivatives, required in pertubative methods, is also avoided. The main computational burden is the solution of the substrate linear system which nonetheless is sparse. Although a systematic investigation of the computational efficiency is required, we might say that HCMS is placed between pertubative and direct methods for that matter. Precise statements require extensive numerical work which is out of the scope of this thesis. Nevertheless, it seems attractive to retain the nonlocal character of water waves, through a substrate modal system, bearing in mind that the range of validity of the numerical model is significantly increased and at the same time the dimension of computations is genuinely reduced. Additionally, owing to the modal representation of the velocity potential, all the physically interesting fluid quantities (velocity, pressure) can be computed at any local position by straightforward differentiation. Thus, an accurate solution of the irrotational Euler equations with free surface can be efficiently constructed. Some examples in this direction are given in Figures 6.3, 6.4 and 8.22 where the velocity field of nonlinear water waves over flat or variable bottom is depicted. More detailed results and validations can be found in (Charalampopoulos 2016).

Conclusions and Future directions of research

The main objective of this thesis was the study of the fully nonlinear problem of water waves over varying bathymetry following the approach typified in (Athanassoulis & Belibassakis 1999, 2000, 2003, Belibassakis & Athanassoulis 2006, 2011). This study led to several contributions which are summarised bellow.

The analysis deployed in the first part of this thesis extends and justifies previous results of the aforementioned authors who promoted the use of enhanced modal expansions for the solution of water wave problems. In particular we have proved that an expansion of this type in the case of fairly general eigensystem is rapidly convergent. Moreover, assuming appropriate smoothness, we proved that the expansion can be termwise differentiated twice with respect to space and once with respect to time. This finding justifies the use of the modal expansion in the variational analysis of the hydrodynamic problem which is undertaken subsequently. Invoking Luke's variational principle in conjunction with the previously established exact representation of the velocity potential, we derived Euler-Lagrange equations with respect to the free surface elevation and modal amplitudes. Using this result, we pursued with the derivation of a an exact reformulation of the problem in the form of two Hamiltonian evolution equations, coupled with a system of horizontal partial differential equations with respect to the modal amplitudes. This novel formulation, named Hamiltonian Coupled Mode System or HCMS, is a modal version of the Zakharov/Craig-Sulem formulation. In our framework, the computation of the Dirichlet to Neumann operator (DtN) requires the solution of the aforementioned substrate coupled mode system on the fixed horizontal domain. Thus, the computationally expensive solution of Laplace equation in the unknown fluid domain is avoided.

In a numerical level, we implemented a fourth-order finite-difference approach for the numerical solution of HCMS. First of all, we assessed the numerical convergence and accuracy of the new modal characterisation of the DtN operator by considering periodic test cases where closed form solutions are available. It was demonstrated that a small number of modes suffices for the accurate computation of the DtN operator in strongly deformed domains. Moreover, the theoretical findings on the rate of decay of the modal the amplitudes and their spatial derivatives were numerically verified. In the sequel, several computations of nonlinear waves were

performed. Specifically we first considered steady traveling periodic waves above flat bottom. The proposed numerical scheme produces solutions in the whole range of nonlinearity and shallowness parameters, up to the breaking limit. Subsequently, we developed numerical schemes devoted to the solution of HCMS in the time domain. Several benchmark tests are considered, illustrating the ability of the HCMS and the overall numerical scheme to describe nonlinear phenomena such as the reflection and shoaling of solitary waves, the harmonic generation emerging when regular incident waves travel past submerged obstacles, and the Bragg scattering in the presence of a bottom sinusoidal patch. Numerical results on the transformation of a solitary wave due to a sinusoidal bottom patch are also given. It seems that this case have never been considered up to now. The physical parameters involved in the examined cases cover a wide range of nonlinearity, shallowness and bottom variation conditions. This is interpreted as a strong confirmation of the non-pertubative character of HCMS. No filtering technique was necessary during the simulations even in cases involving strong nonlinearity and dispersion. The maximum number of modes, needed in order to obtain highly accurate solutions does not exceed 7 or 8 in the most demanding applications. This fact positively predisposes us for the practical effectiveness of the present method and lead to the conclusion that HCMS can be successfully applied to realistic coastal environments with reasonable computational cost. A remarkable feature of our approach, is that, owing to the modal representation of the wave potential, all important hydrodynamic fields (velocity, pressure etc.) can be very easily and efficiently computed.

As already mentioned in the main part of this manuscript, HCMS formulation opens several directions of research, some of which are already in progress. We shall summarize bellow some important points that deserve attention in the future.

- ➢ The mathematical properties of enhanced modal expansions and corresponding coupled mode systems can be further investigated. The numerical results of this thesis indicate the existence of some interesting properties concerning the convergence of the truncated coupled mode system and the dependence of the solution on the free surface elevation and bathymetry. The analyticity properties of the underlying potential can be exploited in order to infer the (shape) derivative of the modal solution sequence and especially of the free surface modal amplitude. This will be particularly useful in the further theoretical and numerical study of HCMS.

- ➢ Detailed numerical investigation of the computational efficiency of HCMS and comparison with other numerical wave models based on direct numerical methods, petrubative expansions or other representations of the velocity potential. Although the present explicit scheme (RK4) provides stable simulations and was sufficient to demonstrate the ability of HCMS to describe strongly nonlinear and dispersive waves, one might consider the exploitation of the nonlocal Hamiltonian structure of HCMS for the development of implicit symplectic integrators. It is expected that this approach will increase the accuracy and

improve the conservation properties in long-time simulations without compromising the computational efficiency. Concerning the spatial discretization and the solution of the substrate problem other numerical methods can also be considered (e.g. finite-elements), which are more appropriate for the extension of the numerical method in the case of two horizontal dimensions and realistic non-orthogonal horizontal domains. In this direction, the parallelization of the code is of paramount importance and is already in progress (Charalampopoulos 2016).

➢ Calculation of hydrodynamic quantities during the interaction of free surface waves with variable bathymetry or vertical boundaries. First results on the velocity field in some cases have been already presented in this thesis. Calculation and validation of the force on a vertical wall during the reflection of solitary waves can be found in the diploma thesis (Charalampopoulos 2016). Reflection of regular nonlinear waves can easily be treated as well. This direction of research can be useful in engineering applications and could potentially lead to the improvement of our understanding concerning the kinematics and dynamics of the fluid and its free surface in physically interesting cases, such as near vertical impermeable boundaries, past submerged obstacles or even before breaking.

➢ Further study and extension of algorithms devoted to the computation of steady water waves governed by HCMS. Although the finite-difference approach followed in this thesis led to meaningful solutions even in extremal cases, one might also consider a spectral representation in the direction of propagation which is more appropriate in periodic problems and potentially useful in unsteady wave propagation. This axis of work can lead to a detailed numerical study of the stability of steady travelling irrotational water waves in interesting cases such as periodic bottoms, uniform current and two horizontal dimensions. Investigation of the corresponding hydrodynamic fields and particle velocities is also possible.

➢ Examination of the influence of other bathymetric configurations to the propagation of solitary waves or regular nonlinear waves. Examples that are currently under investigation include underwater steps, trenches, shoals, corrugations and investigation of moving bottoms as a mechanism for tsunami generation (see (Charalampopoulos 2016)). We also plan to investigate other types of waves and phenomena and compare HCMS with weakly nonlinear, weakly dispersive and other models. We mention for example the interaction of envelope solitary waves that can lead to freak wave formation (see e.g. (Clamond et al. 2006)), dispersive shock waves emerging from abrupt initial conditions (see e.g. (Mitsotakis et al. 2016)) and the Fabry-Pérot resonance phenomenon occurring when regular waves imping on two separated sinusoidal bottom patches on an otherwise flat seabed (see (Couston et al. 2015)).

Part III

Appendices

Appendix A

Auxiliary results for Section 2.1

A.1 Vertical derivatives and bounds of functions $Q_n^*(\mathbf{x}, z)$

The coefficient function $Q(\mathbf{x}, z)$, appearing in the Sturm-Liouville problem of the reference waveguide, Eq. (2.5), is assumed to be a continuous and bounded function, defined throughout of $D_h^\eta(X)$. Its continuity ensures the validity of all classical results concerning Sturm-Liouville theory invoked in this work, including the asymptotic ones (Ince 1956, p. 271).

In the proof of Theorem 2.1 use is made of the function (for large values of n)

$$Q_n^* \equiv Q_n^*(\mathbf{x}, z) = \frac{1}{1 - Q(\mathbf{x}, z)/k_n^2} \tag{A.1}$$

Under the assumption $Q \in C_b\left(D_h^\eta(X)\right)$, this function is well-defined, continuous and bounded for large values of . Indeed, since $|Q| \leq \bar{Q_0} = \text{const.}$ and the fact that $k_n \to \infty$ as $n \to \infty$, it is clear that, for n greater than an appropriate n_0 , we have $|Q| \leq /k_n^2 < \alpha < 1$. Thus,

$$0 < Q_n^* < \frac{1}{1-\alpha} < \infty \tag{A.2}$$

and the following asymptotic expansion of Q_n^*, for large values of n, holds true

$$Q_n^* = 1 + \frac{Q(\mathbf{x}, z)}{k_n^2} + \frac{2Q(\mathbf{x}, z)^2}{k_n^4} + \frac{O(1)}{n^6} = 1 + O(n^{-2}). \tag{A.3}$$

The assumption $Q \in C_b(D_h^\eta(X))$ is enough in order to ensure the validity of part (i) of Theorem 2.1. In proving the estimates (2.13) and (2.14), in parts (ii) and (iii) of Theorem 2.1, use is made of the vertical derivatives up to the second and the fourth order, respectively, of the function Q. Accordingly, in these cases we need to assume $Q(\mathbf{x}, \cdot) \in C^m\left([-h, \eta]\right)$, for $m = 2$ and $m = 4$, respectively, and calculate the corresponding derivatives $\partial_z^m Q_n^*$ and their asymptotics.

By straightforward calculations we obtain

$$\partial_z Q_n^* = \frac{\partial_z Q}{\left(1 - Q/k_n^2\right)^2} \tag{A.4a}$$

$$\partial_z^2 Q_n^* = \frac{\partial_z^2 Q/k_n^2}{\left(1 - Q/k_n^2\right)^2} + \frac{2\left(\partial_z Q/k_n^2\right)^2}{\left(1 - Q/k_n^2\right)^3} \tag{A.4b}$$

$$\partial_z^3 Q_n^* = \frac{\partial_z^3 Q/k_n^2}{\left(1 - Q/k_n^2\right)^2} + \frac{6\partial_z Q \partial_z^2 Q/k_n^4}{\left(1 - Q/k_n^2\right)^3} + \frac{6\partial_z Q(\partial_z Q)^3/k_n^6}{\left(1 - Q/k_n^2\right)^4} \tag{A.4c}$$

$$\partial_z^4 Q_n^* = \frac{\partial_z^4 Q/k_n^2}{\left(1 - Q/k_n^2\right)^2} + \frac{\left(6(\partial_z^2 Q)^2 + 8\partial_z Q \partial_z^3 Q\right)/k_n^4}{\left(1 - Q/k_n^2\right)^3} + \frac{36(\partial_z Q)^2 \partial_z^2 Q/k_n^6}{\left(1 - Q/k_n^2\right)^4} + \frac{24(\partial_z Q)^4/k_n^8}{\left(1 - Q\kappa_n^2\right)^5} \tag{A.4d}$$

Using the above results and the eigenvalue asymptotics, $k_n = O(n)$, we obtain the bounds for $\partial_z^m Q_n^*$, $m = 1, 2, 3, 4$, presented in the following

Proposition A.1. *If $Q(\mathbf{x}, z) \in C^m([-h, \eta])$, $m \geq 1$, and n is greater than an appropriate number n_0, in which case we have $|Q/k_n^2| < a < 1$, then, $Q_n^*(\mathbf{x}, \cdot) \in C^m([-h, \eta])$ and, for $\mathbf{x} \in X$, we have*

$$|Q_n^*(\mathbf{x}, z)| \leq \bar{a} = O(1), \quad \textit{for all} \quad z \in [-h, \eta], \tag{A.5}$$

$$|\partial_z^m Q_n^*(\mathbf{x}, z)| \leq \bar{A}_m \frac{\|Q(\mathbf{x}, \cdot)\|_{C^m}}{k_n^2} = O(n^{-2}), \quad \textit{for all} \quad z \in [-h, \eta], \tag{A.6}$$

where $\bar{A}_m$ is an absolute positive constant (independent from n and $\mathbf{x}$), and $\|Q(\mathbf{x}, \cdot)\|_{C^m}$ is the vertical C^m norm of the coefficient function $Q(\mathbf{x}, z)$, considered as a function of z, defined by

$$\|Q(\mathbf{x}, \cdot)\|_{C^m} \equiv \|Q(\mathbf{x}, \cdot)\|_{C^m([-h,\eta])} = \sum_{l=0}^{m} \max\left\{|\partial_z^l Q(\mathbf{x}, z)|, \;\; z \in [-h, \eta]\right\}. \tag{A.7}$$

Further, if

$$\sup\left\{\|\partial_z^m Q_n^*(\mathbf{x}, z)\|\right\} \leq \frac{\bar{B}_m}{n^2}, \quad \textit{for all} \quad (\mathbf{x}, z) \in D_h^\eta(X), \tag{A.8}$$

where $\bar{B}_m$ is another absolute positive constant.

A.2 Proof of Eqs. (2.23) and (2.26)

In this appendix we shall prove the inequalities (2.23) and (2.26), which have been used in the proof of Theorem 2.1. To simplify the writing and make the arguments clearer, we rewrite the integrals appearing in the right hand sides of (2.23) and (2.26) as

$$I_1 = \int_{-h}^{\eta} (qf)'' g dz, \tag{A.9}$$

$$I_2 = \int_{-h}^{\eta} \left(q(qf)''\right)'' g dz, \tag{A.10}$$

where $q(z)$, $f(z)$, $g(z)$ stand for Q_n^*, Φ^*, Z_n and prime denotes the $z-$ derivative.

Proposition A.2. *Under the assumptions*

$$q \in C^2\left([-h,\eta]\right), \quad f \in H^2\left(-h,\eta\right), \quad g \in L^2(-h,\eta),$$

the following inequality, that is (2.23), holds true:

$$I_1 \leq 2\|q\|_{C^2}\|f\|_{H^2}\|g\|_{L^2}. \tag{A.11}$$

Proof. By applying simple algebraic manipulations and the Cauchy-Schwartz inequality, we obtain

$$\begin{aligned}
|I_1| &= |\int_{-h}^{\eta} \left(q''f + 2q'f' + qf''\right) g dz| \\
&\leq \int_{-h}^{\eta} \left(|q''fg| + 2|q'f'g| + |qf''g|\right) dz \\
&\leq \|q\|_{C^2} \left(\int_{-h}^{\eta} |fg| dz + 2\int_{-h}^{\eta} |f'g| dz + \int_{-h}^{\eta} |f''g| dz\right) \\
&\leq \|q\|_{C^2} \left(\|f\|_{L^2}\|g\|_{L^2} + 2\|f'\|_{L^2}\|g\|_{L^2} + \|f''\|_{L^2}\|g\|_{L^2}\right) \\
&\leq 2\|q\|_{C^2}\|f\|_{H^2}\|g\|_{L^2},
\end{aligned}$$

which is exactly what we wanted to prove. □

Proposition A.3. *Under the assumptions*

$$q \in C^4\left([-h,\eta]\right), \quad f \in H^4\left(-h,\eta\right), \quad g \in L^2(-h,\eta),$$

the following inequality, that is (2.26), holds true:

$$I_1 \leq 13\|q\|_{C^4}\|f\|_{H^4}\|g\|_{L^2}. \tag{A.12}$$

Proof. First we calculate the derivatives appearing in the integrand:

$$\begin{aligned}
\left(q(qf)''\right)'' = q^{(4)}qf + 2q'''q'f + 4q'''qf' + q''q''f + 8q''q'f' \\
+ 7q''qf'' + 6q'q'f'' + 6q'qf''' + qqf^{(4)}.
\end{aligned} \tag{A.13}$$

Then, observe that each $q-$quadratic factor, in the right-hand side of the above equation, is

absolutely bounded by $\|q\|_{C^4}$; for example,

$$|q^{(4)}q| \leq \max_{z\in[-h,\eta]} \left\{|q^{(4)}q|\right\} \leq \|q\|^2_{C^4}, \tag{A.14a}$$

$$|q'''q| \leq \max_{z\in[-h,\eta]} \{|q'''q'|\} \leq \|q\|^2_{C^4}, \tag{A.14b}$$

and so on. Now, using Eq. (A.13), inequalities (A.14), and simple properties of the integral, we find

$$|I_2| \leq \|q\|^2_{C^4}\Big(4\int_{-h}^{\eta}|fg|dz + 12\int_{-h}^{\eta}|f'g|dz + 13\int_{-h}^{\eta}|f''g|dz + 6\int_{-h}^{\eta}|f'''g|dz + \int_{-h}^{\eta}|f^{(4)}g|dz\Big) \tag{A.15}$$

Finally, by increasing all factors in front of the integrals to 13 (the maximum one), and applying Cauchy-Schwarz inequality, we reformulate the right-hand side of the above inequality, obtaining

$$|I_2| \leq 13\|q\|^2_{C^4}\left(\|f\|_{L^2} + \|f'\|_{L^2} + \|f''\|_{L^2} + \|f'''\|_{L^2} + \|f^{(4)}\|_{L^2}\right) \tag{A.16}$$

$$13\|q\|^2_{C^4}\|f\|^2_{H^4}\|g\|^2_{L^2}, \tag{A.17}$$

that is what we wanted to prove. □

Appendix B

Derivatives of $Z_n(z;\eta,h),\ n=-2,-1$

In this appendix, we derive closed form expressions for the derivatives of functions $Z_n = Z_n(z;\eta,h)$, $n=-2,-1$, used for the enrichment of the $L^2(-h,\eta)-$ basis, $Z_n = Z_n(z;\eta,h)$, $n\geq 0$. It is recall that Z_n, $n=-2,-1$ are chosen as second order polynomials in $z+h$ with coefficients dependent on $(\mathbf{x},t)$, through η, h (see Eqs. (2.9a), (2.9b)). In order to abbreviate the presentation we write them in the form

$$Z_n = \zeta_n^2(z+h)^2 + \zeta_n^1(z+h) + \zeta_n^0, \quad n=-2,-1, \tag{B.1}$$

where $\zeta_n^k = \zeta_n^k(\mathbf{x},t)$, $k=0,1,2$ are given by

$$\begin{aligned}
\zeta_{-2}^2 &= \frac{\mu_0 h_0 + 1}{2h_0 H} = \frac{a}{H}, \quad \zeta_{-2}^1 = 0, \quad \zeta_{-2}^0 = aH+1,\\
\zeta_{-1}^2 &= \frac{\mu_0 h_0 - 1}{2h_0 H} = \frac{b}{H}, \quad \zeta_{-1}^1 = \frac{1}{h_0}, \quad \zeta_{-1}^0 = aH+1,
\end{aligned} \tag{B.2}$$

with $H=\eta+h$ denoting the local fluid depth. The vertical derivatives of Z_n, $n=-2,-1$ are easily computed:

$$\begin{aligned}
\partial_z Z_{-2} &= 2\zeta_{-2,2}(z+h),\\
\partial_z Z_{-1} &= 2\zeta_{-1,2}(z+h) + \frac{1}{h_0},\\
\partial_z^2 Z_{-2} &= 2\zeta_{-2,2},\\
\partial_z^2 Z_{-1} &= 2\zeta_{-1,2}.
\end{aligned} \tag{B.3}$$

In order to calculate the horizontal derivatives, one can use the following identities obtained by direct differentiation of (B.1) with respect to $a=x_1$ or x_2:

$$\partial_{x_i} Z_n = f_n^{2,i}(z+h)^2 + f_n^{1,i}(z+h) + f_n^{0,i}, \tag{B.4}$$

$$\begin{aligned} f_n^{2,i} &= \partial_{x_i}\zeta_n^2, \\ f_n^{1,i} &= \partial_{x_i}\zeta_n^1 + 2\zeta_n^i\partial_{x_i}h, \\ f_n^{0,i} &= \partial_{x_i}\zeta_n^0. \end{aligned} \tag{B.5}$$

The coefficients $f_n^{k,i}$, $n=-2,-1$, $k=0,1,2$ are given by

$$\begin{aligned} f_{-2}^2 &= -\frac{a}{H^2}\partial_x H, \quad f_{-2}^1 = 0, \quad f_{-2,0} = a\partial_x H, \\ f_{-1}^2 &= -\frac{a}{H^2}\partial_x H, \quad f_{-1}^1 = \frac{2\partial_a h}{h_0}, \quad f_{-1}^0 = a\partial_x H, \end{aligned} \tag{B.6}$$

Similarly, one finds

$$\Delta_{\mathbf{x}} Z_n = g_n^2(z+h)^2 + g_n^1(z+h) + g_n^0, \tag{B.7}$$

where g_n^k, $n=-2,-1$, $k=1,2,3$ are given by

$$\begin{aligned} g_n^2 &= \Delta_{\mathbf{x}}\zeta_n^2, \\ g_n^1 &= \Delta_{\mathbf{x}}\zeta_n^1 + 4\nabla_{\mathbf{x}}h\cdot\nabla_{\mathbf{x}}\zeta_n^2 + 2\Delta_{\mathbf{x}}h\partial_{n,2}, \\ g_n^0 &= 2\nabla_{\mathbf{x}}h\cdot\nabla_{\mathbf{x}}\zeta_n^1 + 2(\nabla_{\mathbf{x}}h)^2\zeta_n^2 + \zeta_n^1\Delta_{\mathbf{x}}h. \end{aligned} \tag{B.8}$$

Appendix C

Auxiliary results for Section 2.2

We first state and prove a useful consequence of Proposition 2.1:

Lemma C.1. *If the boundary functions η and h satisfy the* BSC($\tilde{X}_{\text{part}} \times I$), then the $(\mathbf{x}, t)$-derivatives of $k_n H$ satisfy the following asymptotic estimates, uniformly in $\tilde{X}_{\text{part}} \times I$,

$$\partial_a(k_n H) = O(n^{-1}), \tag{C.1}$$

$$\partial_{x_i}^2(k_n H) = O(n^{-1}). \tag{C.2}$$

Proof. By a straightforward calculation and use of Eqs. (2.36) and (2.37), we obtain

$$\begin{aligned} \partial_{x_i}(k_n H) &= H\partial_{x_i} k_n + k_n \partial_{x_i} H \\ &= \partial_{x_i} H \left(H\partial_H k_n + k_n\right), \end{aligned} \tag{C.3}$$

and

$$\begin{aligned} \partial_{x_i}^2(k_n H) &= H\partial_{x_i}^2 k_n + 2\partial_{x_i} k_n \partial_{x_i} H + k_n \partial_{x_i}^2 H \\ &= (\partial_{x_i} H)^2 \left(H\partial_H k_n^2 + 2\partial_H k_n\right) + \partial_{x_i}^2 H \left(H\partial_H k_n + k_n\right). \end{aligned} \tag{C.4}$$

In order to obtain estimates for the quantities $\partial_{x_i}(k_n H)$ and $\partial_{x_i}^2(k_n H)$ we have to study the terms in parentheses in the right-hand side of Eqs. (C.3) and (C.4). Using Eq. (2.34), we obtain

$$\begin{aligned} H\partial_H k_n + k_n &= -k_n \left(\frac{H\left(k_n^2 + \mu_0^2\right)}{-\mu_0 + H\left(k_n^2 + \mu_0^2\right)} - 1\right) \\ &= -k_n \left(\frac{\mu_0}{H\left(k_n^2 + \mu_0^2\right)} + O(k_n^{-4})\right) \\ &= -\frac{\mu_0}{H k_n} + O(k_n^{-3}) = O(n^{-1}), \end{aligned} \tag{C.5}$$

which proves (C.1). Further, using Eq. (2.35) and performing some simple algebraic manipula-

tions, we obtain

$$H\partial_H^2 k_n + 2\partial_H k_n = -2\partial_H k_n \left[\mu_0 + \frac{\partial_H k_n}{k_n}(H\mu_0 - 1)\left(2 + H\frac{\partial_H k_n}{k_n}\right)\right] H + 2\partial_H k_n$$
$$= -2\partial_H k_n (H\mu_0 - 1)\left(\frac{H\partial_H k_n + k_n}{k_n}\right)^2 = O(n^{-3}). \tag{C.6}$$

The last estimate in (C.6) is obtained by using $\partial_H k_n = O(n)$ and the already proved Eq. (C.5). Combining now the above two results with Eq. (C.4), gives Eq. (C.2) which completes the proof. □

Detailed proof of the asymptotic estimates appearing in Proposition 2.2

The asymptotic estimates indicated in the second equalities of Eqs. (2.47) and (2.48) are obtained by using the derived analytic expressions in (2.47) and (2.48), in conjunction with $k_n = O(n)$, Eq. (2.7a), $Z_n = O(1)$, $W_n = O(1)$ and the previously established estimates in Proposition 2.1 and Lemma C.1. As an example, we give the details of the estimation $\Delta_{\mathbf{x}} Z_n = O(n^2)$. Considering the analytic expression of the second derivative, Eq. (2.48), and using the above mentioned estimates, we see that

$$\Delta_{\mathbf{x}} Z_n = \underbrace{-|\nabla_{\mathbf{x}} k_n|^2 (z+h)^2 Z_n}_{O(n^2)} - \underbrace{2k_n \nabla_{\mathbf{x}} k_n \cdot \nabla_{\mathbf{x}} h (z+h) Z_n}_{O(n^2)}$$
$$+ \left[\underbrace{-k_n^2 |\nabla_{\mathbf{x}} h|^2}_{O(n^2)} - \underbrace{|\nabla_{\mathbf{x}}(k_n H)|^2}_{O(n^{-2})} - \underbrace{\mu_0 \frac{\Delta_{\mathbf{x}}(k_n H)}{k_n} + 2\mu_0^2 \frac{|\nabla_{\mathbf{x}}(k_n H)|^2}{k_n^2}}_{O(n^{-4})}\right] Z_n$$
$$- \left[\underbrace{\Delta_{\mathbf{x}} k_n}_{O(n)} - \underbrace{2\mu_0 \frac{\nabla_{\mathbf{x}} k_n \cdot \nabla_{\mathbf{x}}(k_n H)}{k_n}}_{O(n^{-1})}\right] (z+h) W_n$$
$$+ \big[\underbrace{2\nabla_{\mathbf{x}} k_n \cdot \nabla_{\mathbf{x}} h}_{O(n)} + \underbrace{k_n \Delta_{\mathbf{x}} h}_{O(n)} - \underbrace{2\mu_0 \nabla_{\mathbf{x}} h \cdot \nabla_{\mathbf{x}}(k_n H)}_{O(n^{-1})}\big] W_n = O(n^2).$$

Appendix D

Detailed proof of Lemma 2.1

Proof of estimates (2.69)

The sequence of functions $\gamma_n(\boldsymbol{x},t)$ and the corresponding sequences of derivatives, $\partial_a\gamma_n(\boldsymbol{x},t)$ and $\partial^2_{x_i}\gamma_n(\boldsymbol{x},t)$, are uniformly convergent to finite limits that can be calculated explicitly in terms of $k_n(\boldsymbol{x},t)$ and $H=\eta+h$. The existence of these limits trivializes the proof of Eq. (4.6). By direct calculation of the integral involved in the definition of the L^2- norm, in conjunction with Eq. (3.1b), we find that $\gamma_n=\gamma_n(\boldsymbol{x},t)$ is given by the formula

$$\gamma_n=\sec^{-2}\left(\frac{H}{2}+\frac{\sin(k_nH)\cos k_nH}{2k_n}\right)^{-1}=\frac{2k_n^2}{Hk_n^2+f}, \tag{D.1}$$

where $f=f(\boldsymbol{x},t)=\mu^2H-\mu_0=O(1)$. Then, by straightforward calculations, we find (recall that a stands for t,x_i, $i=1,2$.):

$$\begin{aligned}\partial_a\gamma_n&=\partial_a(2k_n^2)\frac{1}{Hk_n^2+f}+2k_n^2\partial_a\left(\frac{1}{Hk_n^2+f}\right)\\&=\frac{4k_n\partial_ak_n}{Hk_n^2+f}-\frac{2k_n^2\left(k_n^2\partial_aH+2Hk_n\partial_ak_n+\partial_af\right)}{\left(Hk_n^2+f\right)^2}.\end{aligned} \tag{D.2}$$

The above equations, in conjunction with the fundamental estimate $k_n=n\pi/H+O(n^{-1})$, Eq. (2.7a) and Proposition 2.1, permits us to calculate the limits

$$\lim_{n\to\infty}\gamma_n=\frac{2}{H}\equiv\gamma, \tag{D.3a}$$

$$\lim_{n\to\infty}\partial_a\gamma_n=-\frac{2\partial_aH}{H^2}=\partial_a\gamma, \tag{D.3b}$$

$$\lim_{n\to\infty}\partial^2_{x_i}\gamma_n=-2\left(\frac{\partial^2_{x_i}H}{H^2}-\frac{2\left(\partial_{x_i}H\right)^2}{H^3}\right), \tag{D.3c}$$

Note that the convergence of the three sequences is uniform in $(\boldsymbol{x},t)\in\tilde{X}_{\text{part}}$. The fact that the sequences γ_n, $\partial_a\gamma_n$ and $\partial^2_{x_i}\gamma_n$ have finite limits proves Eqs. (2.69). It is worth noting that the

commutation between the operations of taking the limit (as $n \to \infty$) and the differentiation, which is apparent in Eqs. (D.3), is also justified by standard theorems of Calculus. See, for example (Rudin 1964, Theorem 7.17).

Proof of estimates (2.70)

From Eq. (2.33b) we have $[Z_n]_{z=-h} = \sec(k_n H)$, which, after straightforward differentiations and use of the local dispersion relation (2.32b), leads to

$$[\partial_a Z_n]_{z=-h} = -\mu_0 \, [Z_n]_{z=-h} \, \frac{\partial_a(k_n H)}{k_n}, \tag{D.4}$$

$$\left[\partial_{x_i}^2 Z_n\right]_{z=-h} = \mu_0^2 \, [Z_n]_{z=-h} \left(\frac{\partial_{x_i}(k_n H)}{k_n}\right)^2 + [Z_n]_{z=-h}^3 \, (\partial_{x_i}(k_n H))^2 - \mu_0 \, [Z_n]_{z=-h} \, \frac{\partial_{x_i}^2(k_n H)}{k_n}. \tag{D.5}$$

The proof of the estimates appearing in Eq. (2.70) is now straightforward. Since $k_n H$ tends to $n\pi$, we get $|\sec(k_n H)| \to 1$, as $n \to \infty$, and thus $[Z_n] = O(1)$. Using this result, and Eq. (D.4), in conjunction with $k_n = O(n)$, Eq. (2.7a), and $\partial_a(k_n H) = O(n^{-1})$, Eq. (C.1) of Lemma C.1, we find that $[\partial_a Z_n]_{z=-h} = O(n^{-2})$. Finally, Eq. (D.5), in conjunction with Eqs. (2.7a) and (C.1), (C.2) of Lemma C.1, leads to $\left[\partial_{x_i}^2 Z_n\right] = O(n^{-2})$.

Appendix E

Proof of composition rule for functionals, Lemma 3.1

We start by invoking the chain rule for composite operators (see, e.g., (Flett 1980, 4.1.2), (Gasiński & Papageorgiou 2005, Prop 4.1.12)). Assuming that $G : X \longrightarrow Y$ has a Gâteaux variation at $x \in X$ for the increment h, say $\delta G(x;h)$, and $F : Y \longrightarrow Z$ is Fréchet differentiable at $y = G(x)$, with Fréchet derivative $DF(y)$, the composition $W = F \circ G$ has a Gâteaux variation at $x \in X$ for the increment h, $\delta W(x;h)$, given by

$$\delta W(x;h) = \delta F\left(G(x); \delta G(x;h)\right). \tag{E.1}$$

In our case $x = (x_1, x_2) = (\eta, \phi)$, $y = (y_1, y_2) = (\eta, \Phi)$, W and F are (action) functionals on (x_1, x_2) and (y_1, y_2), respectively, and G is the operator transforming (x_1, x_2) to (y_1, y_2), having the form $(y_1, y_2) = G(x_1, x_2) = (G_1(x_1, x_2), G_2(x_1, x_2))$. Then, functional W takes the form $W(x_1, x_2) = F\left(G(x_1, x_2)\right) = F\left(G_1(x_1, x_2), G_2(x_1, x_2)\right)$. The partial variations $\delta_{x_1} W(x;h_1)$ and $\delta_{x_2}(x;h_2)$ are calculated by applying the chain rule (E.1) separately, in the directions h_1 and h_2:

$$\delta_{x_1} W(x;h_1) = \delta_{y_1} F\left(G(x); \delta_{x_1} G_1(x;h_1)\right) + \delta_{y_2} F\left(G(x); \delta_{x_1} G_2(x;h_1)\right), \tag{E.2}$$

$$\delta_{x_2} W(x;h_2) = \delta_{y_1} F\left(G(x); \delta_{x_2} G_1(x;h_2)\right) + \delta_{y_2} F\left(G(x); \delta_{x_2} G_2(x;h_2)\right). \tag{E.3}$$

For the specific application considered in this thesis, the composite functional is $W(x_1, x_2) \equiv \tilde{\mathcal{S}}[\eta, \boldsymbol{\phi}] = \mathcal{S}\left[G_1(\eta, \boldsymbol{\phi}), G_2(\eta, \boldsymbol{\phi})\right]$, where $\mathcal{S}$ is Luke's functional, given by (1.18) and $G_1(\eta, \boldsymbol{\phi}) = \eta$, $G_2(\eta, \boldsymbol{\phi}) = \Phi(\eta, \boldsymbol{\phi})$, the latter being expressed by means of the series representation (3.1). In order to apply results (E.2), (E.3) in our case, we calculate

$$\delta_\eta G_1(\eta, \boldsymbol{\phi}; \delta\eta) = \delta\eta, \tag{E.4a}$$

$$\delta_{\boldsymbol{\phi}} G_1(\eta, \boldsymbol{\phi}; \delta\boldsymbol{\phi}) = 0, \tag{E.4b}$$

$$\delta_\eta G_2(\eta, \boldsymbol{\phi}; \delta\eta) = \delta_\eta \Phi(\eta, \boldsymbol{\phi}; \delta\eta) = \partial_\eta \Phi(\eta, \boldsymbol{\phi}) \delta\eta, \tag{E.4c}$$

$$\delta_{\boldsymbol{\phi}} G_2(\eta, \boldsymbol{\phi}; \delta\boldsymbol{\phi}) = \delta_{\boldsymbol{\phi}} \Phi(\eta, \boldsymbol{\phi}; \delta\boldsymbol{\phi}) = \partial_{\boldsymbol{\phi}} \Phi(\eta, \boldsymbol{\phi}) \delta\boldsymbol{\phi}. \tag{E.4d}$$

Note that the last members of the two last equations are expressed in terms of usual partial derivatives of $\Phi(\eta, \boldsymbol{\phi})$, given respectively by $\partial_\eta \Phi = \boldsymbol{\phi} \partial_\eta \boldsymbol{Z}(\eta)$ and $\partial_{\boldsymbol{\phi}} \Phi = \boldsymbol{Z}$ in view of Notation 3.1. The partial variations $\delta_\eta \tilde{\mathcal{S}}\,[\eta, \boldsymbol{\phi}; \delta\eta]$ and $\delta_{\boldsymbol{\phi}} \tilde{\mathcal{S}}\,[\eta, \boldsymbol{\phi}; \delta\boldsymbol{\phi}]$ are obtained by applying chain rule (E.1) and taking into account Eqs. (E.4):

$$\delta_\eta \tilde{\mathcal{S}}[\eta, \boldsymbol{\phi}; \delta\eta] = \delta_\eta \mathcal{S}[\eta, \boldsymbol{\phi}\, \boldsymbol{Z}(\eta); \delta\eta] + \delta_\Phi \mathcal{S}[\eta, \boldsymbol{\phi}\, \boldsymbol{Z}(\eta); (\boldsymbol{\phi}\, \partial_\eta \boldsymbol{Z}(\eta))\, \delta\eta], \tag{E.5}$$

$$\delta_{\boldsymbol{\phi}} \tilde{\mathcal{S}}[\eta, \boldsymbol{\phi}; \delta\boldsymbol{\phi}] = \delta_\Phi \mathcal{S}[\eta, \boldsymbol{\phi}\, \boldsymbol{Z}(\eta); \boldsymbol{Z}(\eta) \delta\boldsymbol{\phi}]. \tag{E.6}$$

Eq. (E.5) is identical to (3.5). Let us prove Eq. (3.6). Invoking the linearity of the variation with respect to the increment, i.e. $\delta_{\boldsymbol{\phi}} \tilde{\mathcal{S}}[\eta, \boldsymbol{\phi}; \delta\boldsymbol{\phi}] = \sum_m \delta_{\varphi_m} \tilde{\mathcal{S}}[\eta, \boldsymbol{\phi}; \delta\varphi_m]$, and observing that the Fréchet differentiability of $S[\eta, \Phi]$ implies that $\delta_\Phi \mathcal{S}[\eta, \Phi; \cdot\,]$ is a linear operator in $\delta\Phi$, we can write $\delta_{\boldsymbol{\phi}} \tilde{\mathcal{S}}[\eta, \boldsymbol{\phi}, \delta\boldsymbol{\phi}]$ and $\boldsymbol{Z}(\eta)\delta\boldsymbol{\phi}$ as sums in Eq. (E.6). Invoking the arbitrariness of $\delta\varphi_m$, Eq. (3.6) is obtained and the proof is complete.

Appendix F

Analytical expressions of the matrix functions A, B, C

In this Appendix, we derive analytical expressions of the matrix coefficients A_{mn}, B^i_{mn}, $i = 1, 2$, C_{mn}, given by Eqs. (3.22a), (3.22b), (3.22c), where the vertical functions Z_n, are given by Eqs. (2.9) for $n = -2, -1$, and Eqs. (2.33), for $n \geq 0$. It is recalled that the first and second horizontal derivatives $\partial_{x_i} Z_n$ and $\partial^2_{x_i} Z_n$, appearing in the definitions of B^i_{mn}, $i = 1, 2$ and C_{mn}, have been already calculated in Appendix B, for $n = -2, -1$, and Propositions 2.2, 2.4, for $n \geq 0$. These coefficients contain both vertical integrals and bottom boundary terms, and are written here as

$$B^i_{mn} = 2B^{\text{int},i}_{m,n} + B^{\text{bot}}_{mn}, \tag{F.1}$$

$$C^i_{mn} = C^{\text{int},i}_{m,n} + C^{\text{bot}}_{mn}. \tag{F.2}$$

In the remainder of this Appendix we deal with the integral terms appearing above. The bottom boundary terms are more straightforward and are omitted. In order to proceed with the presentation of the results, we introduce the following notation for the required integrals

Notation F.1. Integrals involving products of vertical functions $Z_n = Z_n(z; \eta(\mathbf{x}, t), h(\mathbf{x}))$, (2.9), (2.33), and $(z + h)$ are collectively denoted by

$$J^s_n = \int_{-h}^{\eta} (z+h)^s Z_n dz, \quad n \geq -2, \tag{F.3}$$

$$J^s_{mn} = \int_{-h}^{\eta} (z+h)^s Z_m Z_n dz, \quad m \geq -2, \quad n \geq 0, \tag{F.4}$$

$$\bar{J}^s_{mn} = \int_{-h}^{\eta} (z+h)^s Z_m W_n dz, \quad m \geq -2, \quad n \geq 0, \tag{F.5}$$

Using the above notation one can easily check that Eq. (3.22a) is written as $A_{mn} = J^0_{mn}$. For Eqs. (3.22b), (3.22c) one needs to take into account the analytical expressions of Appendix B and Propositions 2.2, 2.4. Then, after some straightforward manipulations and use of the above

notation, we find that

$$A_{m,n} = J^0_{mn}, \quad m, n \geq -2, \tag{F.6}$$

$$B^{\text{int},i}_{m,n} = f^{0,i}_n J^0_m + f^{1,i}_n J^1_m + f^{2,i}_n J^2_m, \quad m \geq -2,\ n = -2, -1, \tag{F.7}$$

$$B^{\text{int},i}_{m,n} = f^{0,i}_n J^0_{mn} + f^{1,i}_n \bar{J}^0_{mn} + f^{2,i}_n \bar{J}^1_{mn}, \quad m \geq -2,\ n \geq 0, \tag{F.8}$$

$$C^{\text{int}}_{m,n} = (g^0_n + 2\zeta^2_n) J^0_m + g^1_n J^1_m + g^2_n J^2_m, \quad m \geq -2,\ n = -2, -1, \tag{F.9}$$

$$C^{\text{int}}_{m,n} = \begin{cases} (g^0_0 + k^2_0) J^0_{m0} + g^1_0 J^1_{m0} + g^2_0 J^2_{m0} + g^3_0 \bar{J}^0_{m0} + g^4_0 \bar{J}^1_{m0}, & m \geq -2,\ n = 0, \\ (g^0_n - k^2_n) J^0_{mn} + g^1_n J^1_{mn} + g^2_n J^2_{mn} + g^3_n \bar{J}^0_{mn} + g^4_n \bar{J}^1_{mn}, & m \geq -2,\ n \geq 1. \end{cases} \tag{F.10}$$

where the coefficients $f^{k,i}_n$ and g^k_n, for $n = -2, -1$ and $k = 0, 1, 2, 3, 4$, are given by Eqs. (B.5) and (B.8) respectively. The rest of $f^{k,i}_n$ and g^k_n, $n \geq 0$, are given by

$$f^{0,i}_0 = -\mu_0 \frac{\partial_{x_i}(k_0 H)}{k_0} \tag{F.11a}$$

$$f^{1,i}_0 = k_0 \partial_{x_i} h, \tag{F.11b}$$

$$f^{2,i}_0 = \partial_{x_i} k_0, \tag{F.11c}$$

$$f^{0,i}_n = -\mu_0 \frac{\partial_{x_i}(k_n H)}{k_n}, \tag{F.11d}$$

$$f^{1,i}_n = -k_n \partial_{x_i} h, \tag{F.11e}$$

$$f^{2,i}_n = -\partial_{x_i} k_n, \tag{F.11f}$$

and

$$g^0_0 = k^2_0 |\nabla_{\mathbf{x}} h|^2 - |\nabla_{\mathbf{x}}(k_0 H)|^2 - \mu_0 \frac{\Delta_{\mathbf{x}}(k_0 H)}{k_0} + 2\mu^2_0 \frac{|\nabla_{\mathbf{x}}(k_0 H)|^2}{k^2_0}, \tag{F.12a}$$

$$g^1_0 = 2k_0 \nabla_{\mathbf{x}} k_0 \cdot \nabla_{\mathbf{x}} h, \tag{F.12b}$$

$$g^2_0 = |\nabla_{\mathbf{x}} k_0|^2, \tag{F.12c}$$

$$g^3_0 = 2\nabla_{\mathbf{x}} k_0 \cdot \nabla_{\mathbf{x}} h + k_0 \Delta_{\mathbf{x}} h - 2\mu_0 \nabla_{\mathbf{x}} h \cdot \nabla_{\mathbf{x}}(k_0 H), \tag{F.12d}$$

$$g^4_0 = \Delta_{\mathbf{x}} k_0 - 2\mu_0 \frac{\nabla_{\mathbf{x}} k_0 \cdot \nabla_{\mathbf{x}}(k_0 H)}{k_0}, \tag{F.12e}$$

$$g^0_n = -k^2_n |\nabla_{\mathbf{x}} h|^2 - |\nabla_{\mathbf{x}}(k_n H)|^2 - \mu_0 \frac{\Delta_{\mathbf{x}}(k_n H)}{k_n} + 2\mu^2_0 \frac{|\nabla_{\mathbf{x}}(k_n H)|^2}{k^2_n}, \tag{F.12f}$$

$$g^1_n = -2k_n \nabla_{\mathbf{x}} k_n \cdot \nabla_{\mathbf{x}} h, \tag{F.12g}$$

$$g^2_n = -|\nabla_{\mathbf{x}} k_n|^2, \tag{F.12h}$$

$$g^3_n = -2k_n \nabla_{\mathbf{x}} k_n \cdot \nabla_{\mathbf{x}} h \tag{F.12i}$$

$$g^4_n = \Delta_{\mathbf{x}} k_n - 2\mu_0 \frac{\nabla_{\mathbf{x}} k_n \cdot \nabla_{\mathbf{x}}(k_n H)}{k_n}. \tag{F.12j}$$

Thus, the calculation of the coefficients A_{mn}, B^i_{mn}, $i = 1, 2$, and C_{mn}, is reduced to the calculation of vertical integrals of the form (F.3), (F.4), (F.5) for $s = 0, 1, 2$ and $m, n \geq -2$.

Integrals of the form J^s_m

For any $s = 0, 1, 2, 3, ...$, we easily find from (F.3) that

$$J^s_m = \zeta^2_m \frac{H^{s+3}}{s+3} + \zeta^1_m \frac{H^{s+2}}{s+2} + \zeta^0_m \frac{H^{s+1}}{s+1}, \quad m = -2, -1. \tag{F.13}$$

For $m \geq 0$, straightforward integration and elimination of trigonometric functions, using the local dispersion relations (2.32), yields

$$J^0_0 = \frac{\mu_0}{k_0^2}, \tag{F.14a}$$

$$J^0_m = -\frac{\mu_0}{k_m^2}, \quad m \geq 1, \tag{F.14b}$$

$$J^1_0 = -\frac{1}{k_0^2}(1 - H\mu_0) + \frac{1}{k_0^2}\sqrt{1 - \frac{\mu_0^2}{k_0^2}}, \tag{F.14c}$$

$$J^1_m = \frac{1}{k_m^2}(1 - H\mu_0) + \frac{1}{k_m^2}\sqrt{1 + \frac{\mu_0^2}{k_m^2}}, \quad m \geq 1, \tag{F.14d}$$

$$J^2_0 = \frac{1}{k_0^2}\left(H^2\mu_0 - 2H\right) + \frac{2\mu_0}{k_0^4}, \tag{F.14e}$$

$$J^2_m = -\frac{1}{k_m^2}\left(H^2\mu_0 - 2H\right) + \frac{2\mu_0}{k_m^4}, \quad m \geq 1. \tag{F.14f}$$

Eqs. (F.13) and (F.14) suffice for the evaluation of the coefficients appearing in Eqs. (F.7) and (F.9), thus, at this point we are left with the integrals appearing in Eqs. (F.6), (F.8) and (F.10). These are calculated similarly and are given below.

Integrals of the form J^s_{mn}

- For $s = 0$, we obtain from (F.4) that

$$J^0_{-2,-2} = \frac{8a^2}{15}H^3 - \frac{4a}{3}H^2 + H \tag{F.15a}$$

$$J^0_{-2,-1} = \left(\frac{2a^3}{3} - \frac{2ab}{15} - \frac{a}{4h_0}\right)H^3 + \left(-\frac{5a}{3} + \frac{b}{3} + \frac{1}{2h_0}\right) + H^2 + H, \tag{F.15b}$$

$$J^0_{-2,0} = \frac{2\mu_0 a}{k_0^4 H} - \frac{1}{h_0 k_0^2}, \tag{F.15c}$$

$$J^0_{-2,n} = \frac{2\mu_0 a}{k_n^4 H} + \frac{1}{h_0 k_n^2}, \quad n \geq 1, \tag{F.15d}$$

$$J^0_{-1,0} = \frac{2\mu_0 b}{k_0^4 H} - \frac{\operatorname{sech}(k_0 H)}{h_0 k_0^2}, \tag{F.15e}$$

$$J^0_{-2,n} = \frac{2\mu_0 a}{k_n^4 H} + \frac{1}{h_0 k_n^2}, \quad n \geq 1. \tag{F.15f}$$

$$J^0_{0,0} = \frac{H}{2} - \frac{H\mu_0^2 - \mu_0}{2k_0^2}, \tag{F.15g}$$

$$J^0_{n,n} = \frac{H}{2} + \frac{H\mu_0^2 - \mu_0}{2k_n^2}, \tag{F.15h}$$

and $J^0_{mn} = 0$, for $m, n \geq 0$.

- For $s = 1$, we find from (F.4) that

$$J^1_{-2,-2} = \frac{a^2}{6}H^4 - \frac{a}{2}H^3 + \frac{H^2}{2}, \tag{F.16a}$$

$$J^1_{-2,-1} = \left(\frac{a^2}{4} - \frac{ab}{12} - \frac{2a}{15h_0}\right)H^4 + \left(-\frac{3a}{4} + \frac{b}{4} - \frac{1}{3h_0}\right), \tag{F.16b}$$

$$\begin{aligned} J^1_{-2,0} = \; & \frac{6a(\mu_0 H - 1) + 6a\,\mathrm{sech}(k_0 H)}{H k_0^4} \\ & + \frac{-H(1+2aH) + H^2\mu_0 + H(1-aH)\,\mathrm{sech}(k_0 H)}{H k_0^2} \end{aligned} \tag{F.16c}$$

$$\begin{aligned} J^1_{-2,n} = \; & \frac{6a(\mu_0 H - 1) + 6a\sec(k_n H)}{H k_n^4} \\ & + \frac{H(1+2aH) - H^2\mu_0 - H(1-aH)\sec(k_n H)}{H k_n^2}, \quad n \geq 1, \end{aligned} \tag{F.16d}$$

$$\begin{aligned} J^1_{-1,0} = \; & \frac{-6b + 2\mu_0 H/h_0 + 6bH\mu_0 + 6b\,\mathrm{sech}(k_0 H)}{H k_0^4} \\ & + \frac{-H\left(1 + H\left(\frac{2}{h_0} - a + 3b\right)\right) + H^2\left(\frac{H}{h_0} + 1 - (a-b)H\right)\mu_0 + H(1-aH)\,\mathrm{sech}(k_0 H)}{H k_0^2} \end{aligned} \tag{F.16e}$$

$$\begin{aligned} J^1_{-1,n} = \; & \frac{-6b + 2\mu_0 H/h_0 + 6bH\mu_0 + 6b\sec(k_n H)}{H k_n^4} \\ & - \frac{-H\left(1 + H\left(\frac{2}{h_0} - a + 3b\right)\right) + H^2\left(\frac{H}{h_0} + 1 - (a-b)H\right)\mu_0 + H(1-aH)\sec(k_n H)}{H k_n^2} \end{aligned} \tag{F.16f}$$

$$J^1_{0,0} = -\frac{\mu_0}{k_0^4} - \frac{1}{k_0^2}\left(\frac{H^2\mu_0^2}{4} - \frac{H\mu_0}{2}\right) + \frac{H^2}{4}, \tag{F.16g}$$

$$J^1_{n,n} = -\frac{\mu_0}{k_n^4} + \frac{1}{k_n^2}\left(\frac{H^2\mu_0^2}{4} - \frac{H\mu_0}{2}\right) + \frac{H^2}{4}, \quad n \geq 1. \tag{F.16h}$$

$$J^1_{0,n} = \frac{k_n^2 - k_0^2 + 2\mu_0^2 + (k_0^2 - k_n^2)\sec(k_n H)\,\mathrm{sech}(k_0 H)}{\left(k_0^2 + k_n^2\right)^2}, \quad n \geq 1. \tag{F.16i}$$

$$J^1_{m,n} = \frac{(k_m^2 + k_n^2 + 2\mu_0^2 - (k_m^2 + k_n^2)\sec(k_m H)\sec(k_n H))}{((k_m - k_n)^2(k_m + k_n)^2)}, \quad m, n \geq 1. \tag{F.16j}$$

- For $s = 2$, (F.4) yields

$$J^2_{-2,-2} = \frac{8a^2}{105}H^5 + \frac{4a}{15}H^4 + \frac{H^3}{3}, \tag{F.17a}$$

$$J^2_{-2,-1} = \frac{a(-35/h_0 + 56a - 24b)}{420}H^5 + \frac{105/h_0 - 196a + 84b}{420}H^4 + \frac{H^3}{3}, \tag{F.17b}$$

$$\begin{aligned} J^2_{-2,0} = {} & \frac{6a(\mu_0 H - 1) + 6a\,\mathrm{sech}(k_0 H)}{Hk_0^4} \\ & + \frac{-H(1+2aH) + H^2\mu_0 + H(1-aH)\,\mathrm{sech}(k_0 H)}{Hk_0^2} \end{aligned} \tag{F.17c}$$

$$\begin{aligned} J^2_{-2,n} = {} & \frac{6a(\mu_0 H - 1) + 6a\,\mathrm{sec}(k_n H)}{Hk_n^4} \\ & + \frac{H(1+2aH) - H^2\mu_0 - H(1-aH)\,\mathrm{sec}(k_n H)}{Hk_n^2}, \quad n \geq 1, \end{aligned} \tag{F.17d}$$

$$\begin{aligned} J^2_{-1,0} = {} & \frac{-6b + 2\mu_0 H/h_0 + 6bH\mu_0 + 6b\,\mathrm{sech}(k_0 H)}{Hk_0^4} \\ & + \frac{-H\left(1 + H\left(\frac{2}{h_0} - a + 3b\right)\right) + H^2\left(\frac{H}{h_0} + 1 - (a-b)H\right)\mu_0 + H(1-aH)\,\mathrm{sech}(k_0 H)}{Hk_0^2} \end{aligned} \tag{F.17e}$$

$$\begin{aligned} J^2_{-1,n} = {} & \frac{-6b + 2\mu_0 H/h_0 + 6bH\mu_0 + 6b\,\mathrm{sec}(k_n H)}{Hk_n^4} \\ & - \frac{-H\left(1 + H\left(\frac{2}{h_0} - a + 3b\right)\right) + H^2\left(\frac{H}{h_0} + 1 - (a-b)H\right)\mu_0 + H(1-aH)\,\mathrm{sec}(k_n H)}{Hk_n^2} \end{aligned} \tag{F.17f}$$

$$J^2_{0,0} = -\frac{\mu_0}{k_0^4} - \frac{1}{k_0^2}\left(\frac{H^2\mu_0^2}{4} - \frac{H\mu_0}{2}\right) + \frac{H^2}{4}, \tag{F.17g}$$

$$J^2_{n,n} = -\frac{\mu_0}{k_n^4} + \frac{1}{k_n^2}\left(\frac{H^2\mu_0^2}{4} - \frac{H\mu_0}{2}\right) + \frac{H^2}{4}, \quad n \geq 1. \tag{F.17h}$$

$$J^2_{0,n} = \frac{k_n^2 - k_0^2 + 2\mu_0^2 + (k_0^2 - k_n^2)\,\mathrm{sec}(k_n H)\,\mathrm{sech}(k_0 H)}{\left(k_0^2 + k_n^2\right)^2}, \quad n \geq 1. \tag{F.17i}$$

$$J^2_{m,n} = \frac{(k_m^2 + k_n^2 + 2\mu_0^2 - (k_m^2 + k_n^2)\,\mathrm{sec}(k_m H)\,\mathrm{sec}(k_n H))}{(k_m - k_n)^2(k_m + k_n)^2}, \quad m, n \geq 1. \tag{F.17j}$$

Integrals of the form $\bar{J}^s_{mn}$

- For $s = 0$ we obtain from (F.5) that

$$\bar{J}^0_{-2,0} = \frac{2a(1-\mu_0 H - \operatorname{sech}(k_0 H))}{k_0^3 H} + \frac{1+(aH-1)\operatorname{sech}(k_0 H)}{k_0} \tag{F.18a}$$

$$\bar{J}^0_{-2,n} = \frac{2a(1-\mu_0 H - \sec(k_n H))}{k_n^3 H} - \frac{1+(aH-1)\sec(k_n H)}{k_n}, \quad n \geq 1, \tag{F.18b}$$

$$\bar{J}^0_{-1,0} = \frac{2bh_0(1-\mu_0 H - \operatorname{sech}(k_0 H)) - H}{h_0 k_0^3 H} + \frac{2h_0 - (2h_0 - H(1+\mu_0 h_0))\operatorname{sech}(k_0 H)}{2h_0 k_0}, \tag{F.18c}$$

$$\bar{J}^0_{-1,n} = \frac{2bh_0(1-\mu_0 H - \sec(k_n H)) - H}{h_0 k_n^3 H} - \frac{2h_0 - (2h_0 - H(1+\mu_0 h_0))\sec(k_n H)}{2h_0 k_n}, \tag{F.18d}$$

$$\bar{J}^0_{0,0} = \frac{\mu_0^2}{2k_0^3}, \tag{F.18e}$$

$$\bar{J}^0_{0,n} = -\frac{k_n^2+\mu_0^2}{k_n^3+k_0^2 k_n} + \frac{k_n \sec(k_n H)\operatorname{sech}(k_0 H)}{k_0^2+k_n^2}, \quad n \geq 1, \tag{F.18f}$$

$$\bar{J}^0_{m,0} = \frac{k_0^2 H + \mu_0 - H\mu_0^2}{k_0^3 + k_0 k_m^2}, \quad m \geq 1, \tag{F.18g}$$

$$\bar{J}^0_{m,n} = \frac{k_n^2 H - \mu_0 + H\mu_0^2}{k_m^2 k_n - k_n^3}, \quad m \geq 1, \quad n \geq 1, \quad m \neq n, \tag{F.18h}$$

$$\bar{J}^0_{m,m} = -\frac{-\mu_0^2 H + \mu_0}{4k_m^3} - \frac{H}{4k_m}, \quad m \geq 1. \tag{F.18i}$$

- For $s = 1$ we obtain from (F.5) that

$$\bar{J}^1_{-2,0} = -\frac{6a\mu_0}{k_0^5 H} + \frac{6aH - H(1+2aH)\mu_0}{k_0^3 H} + \frac{H}{k_0} \tag{F.19a}$$

$$\bar{J}^1_{-2,n} = \frac{6a\mu_0}{k_n^5 H} + \frac{6aH - H(1+2aH)\mu_0}{k_n^3 H} - \frac{H}{k_n}, \quad n \geq 1, \tag{F.19b}$$

$$\bar{J}^1_{-1,0} = -\frac{3\mu_0(\mu_0 h_0 - 1)}{h_0 k_0^5 H} + \frac{-H^2 h_0 \mu_0^2 + H(2h_0\mu_0 - 1) - 2H\operatorname{sech}(k_0 H)}{h_0 k_0^3 H} + \frac{H}{k_0}, \tag{F.19c}$$

$$\bar{J}^1_{-1,n} = \frac{3\mu_0(\mu_0 h_0 - 1)}{h_0 k_0^5 H} + \frac{-H(1+h_0\mu_0(H\mu_0 H)) - 2H\sec(k_n H)}{h_0 k_n^3 H} - \frac{H}{k_n}, \quad n \geq 1. \tag{F.19d}$$

$$\bar{J}^1_{0,0} = \frac{\mu_0^2 H - \mu_0}{4k_0^3} + \frac{H}{4k_0}, \tag{F.19e}$$

$$\bar{J}^1_{0,n} = -\frac{-H(k_n^2+\mu_0^2)+\mu_0}{k_n^3+k_0^2 k_n}, \quad n \geq 1, \tag{F.19f}$$

$$\bar{J}^1_{m,0} = \frac{k_0^2-\mu_0^2}{k_0^3+k_0 k_m^2} - \frac{k_0 \sec(k_m H)\operatorname{sech}(k_0 H)}{k_0^2+k_m^2}, \quad m \geq 1, \tag{F.19g}$$

$$\bar{J}^1_{m,n} = \frac{k_n^2+\mu_0^2}{-k_n^3+k_n k_m^2} - \frac{k_n \sec(k_m H)\sec(k_n H)}{-k_n^2+k_m^2}, \quad m \geq 1, \quad n \geq 1, \quad m \neq n, \tag{F.19h}$$

$$\bar{J}^1_{m,m} = \frac{\mu_0^2}{2k_m^3}, \quad m \geq 1. \tag{F.19i}$$

Bibliography

Ambrose, D., Bona, J. & Nicholls, D. (2014), 'On ill-posedness of truncated series models for water waves', *Proc. R. Soc. A* **470**(20130849). (Cited on page 4).

Athanassoulis, G. A. & Papanicolaou, V. G. (1997), 'Eigenvalue asymptotics of layered media and their applications to the inverse problem', *SIAM Journal of Applied Mathematics* **57**, 453—-471. (Cited on page 22).

Athanassoulis, G. & Belibassakis, K. (1998), Water-wave green's function for a 3d uneven-bottom problem with different depths at infinity, *in* 'IUTAM Symposium on Computational Methods for Unbounded domains', pp. 21–32. (Cited on page 20).

Athanassoulis, G. & Belibassakis, K. (1999), 'A consistent coupled-mode theory for the propagation of small-amplitude water waves over variable bathymetry regions.', *J. Fluid Mech.* **389**, 275–301. (Cited on pages , 5, 6, 20, and 123).

Athanassoulis, G. & Belibassakis, K. (2000), A complete modal expansion of the wave potential and its application to linear and nonlinear water-wave problems, *in* 'Rogue Waves'. (Cited on pages , 5, 20, 46, and 123).

Athanassoulis, G. & Belibassakis, K. (2003), Rapidly-convergent local-mode representations for wave propagation and scattering in curved-boundary waveguides, *in* 'Mathematical and Numerical Aspects of Wave Propagation WAVES', pp. 451–456. (Cited on pages 5, 28, and 123).

Athanassoulis, G. & Belibassakis, K. (2007), 'New evolution equations for non-linear water waves un general bathymetry with application to steady travelling solutions in constant, but arbritary depth', *Discrete and Continuous Dynamical Systems* pp. 75–84. (Cited on pages 5, 20, and 47).

Athanassoulis, G. & Papoutsellis, C. (2015*a*), New form of the Hamiltonian equations for the nonlinear water-wave problem, based on a new representation of the DtN operator, and some applications., *in* 'Proceedings of the 34th International Conference on Ocean, Offshore and Arctic Engineering.'. (Cited on page 8).

Athanassoulis, G. & Papoutsellis, C. (2015*b*), Nonlinear irrotational water waves over variable bathymetry. the Hamiltonian approach with a new efficient representation of the Dirichlet to Neumann operator., *in* 'Proceedings of the International Conference DAYS on DIFFRACTION 2015.', pp. 20–26. (Cited on page 8).

Athanassoulis, G., Papoutsellis, C. & Belibassakis, K. (2013), New form of the Hamiltonian equations for the nonlinear water-wave problem, based to a new representation of DtN operator, and some applications, *in* 'Geophysical Research Abstracts.', Vol. 15 of *EGU General Assembly 2013*. (Cited on page 8).

Babuška, I. (1973), 'The Finite Element Method with Lagrangian Multipliers', *Numer. Math.* **20**, 79–92. (Cited on page 50).

Barthelemy, E. (2004), 'Nonlinear shallow water theories for coastal waves', *Surv. Geophys.* **25**. (Cited on page 4).

Barybin, A. A. & Dimitriev, V. (2002), *Modern Electrodynamics and Coupled-mode Theory: Application to Guided-wave Optics*, Rinton Press. (Cited on page 20).

Bateman, W., Swan, C. & Taylor, P. (2001), 'On the Efficient Numerical Simulation of Directionally Spread Surface Water Waves', *Journal of Computational Physics* **174**, 277–305. (Cited on page 3).

Beji, S. & Battjes, J. (1993), 'Experimental investigation of wave propagation over a bar', *Coast. Eng.* **19**, 151–163. (Cited on page 109).

Beji, S. & Battjes, J. (1994), 'Numerical simulation of nonlinear wave propagation over a bar', *Coast. Eng.* **23**, 1–16. (Cited on page 109).

Belibassakis, K. & Athanassoulis, G. (2002), 'Extension of second order stokes theory to variable bathymetry', *J. Fluid Mech.* **464**(8), 35–80. (Cited on page 5).

Belibassakis, K. & Athanassoulis, G. (2006), 'A coupled-mode technique for weakly nonlinear wave interaction with large floating structures lying over variable bathymetry regions', *Appl. Ocean Res.* **28**, 59—-76. (Cited on pages 20, 28, and 123).

Belibassakis, K. & Athanassoulis, G. (2011), 'A coupled-mode system with application to nonlinear water waves propagating in finite water depth and in variable bathymetry regions', *Coast. Eng.* **58**, 337–350. (Cited on pages 5, 6, 20, 47, 53, 81, 83, 109, and 123).

Belibassakis, K., Athanassoulis, G. & Gerostathis, T. (2001), 'A coupled-mode model for the refraction-diffraction of linear waves over steep three-dimensional bathymetry', *Appl. Ocean Res.* **23**, 319–336. (Cited on pages 5 and 20).

Belibassakis, K., Athanassoulis, G., Papathanasiou, T., Filopoulos, S. & Markolefas, S. (2014), 'Acoustic wave propagation in inhomogeneous , layered waveguides based on modal expansions and hp-fem', *Wave Motion* **51**, 1021–1043. (Cited on page 20).

Belibassakis, K., Gerostathis, T. & Athanassoulis, G. (2011), 'A coupled-mode model for water wave scattering by horizontal, non-homogeneous current in general bottom topography', *Appl. Ocean Res.* **33**(4), 384–397. (Cited on pages 5 and 20).

Benjamin, T. & Olver, P. (1982), 'Hamiltonian structure, symmetries and conservation laws for water waves', *J. Fluid Mech.* **125**, 137–185. (Cited on page 3).

Berkhoff, J. (1972), Computation of combined refraction-diffraction, *in* '13th International Conference on Coastal Engineering', pp. 471–490. (Cited on pages 5 and 62).

Bi, W., Pagneux, V., Lafarge, D. & Aurégan, Y. (2007), 'An improved multimodal method for sound propagation in nonuniform lined ducts.', *J. Acoust. Soc. Am.* **122**(1), 280–290. (Cited on page 20).

Bingham, H. B., Madsen, P. A. & Fuhrman, D. (2009), 'Velocity potential formulations of highly accurate Boussinesq-type models', *Coast. Eng.* **56**(2009), 467–478. (Cited on page 4).

Bingham, H. & Zhang, H. (2007), 'On the accuracy of finite difference solutions for nonlinear water waves', *Journal of Engineering Mathematics* **58**, 211–228. (Cited on page 4).

Birkhoff, G. & Rota, C. (1989), *Ordinary Differential Equations*, John Wiley and Sons. (Cited on page 23).

Bonneton, P., Chazel, F., Lannes, D., Marche, F. & Tissier, M. (2011), 'A splitting approach for the fully nonlinear and weakly dispersive Green-Naghdi model', *J. Comp. Phys* **230**, 1479–1498. (Cited on pages 4 and 65).

Boussinesq, J. (1872), 'Théorie des ondes et des remous qui se propagent le long d'un canal rectangulaire horizontal, en communiquant au liquide contenu dans ce canal des vitesses sensiblement pareilles de la surface au fond', *J. Math. Pures Appl.* **17**. (Cited on page 2).

Brekhovskikh, L. & Godin, O. (1992), *Acoustics of Layered Media II: point sources and bounded beams*, Vol. 10, Springer Series on Wave Phenomena. (Cited on pages 19 and 20).

Brezis, H. (2011), *Functional Analysis, Sobolev Spaces and Partial Differential Equations*, Universitext. (Cited on page 24).

Brocchini, M. (2013), 'A reasoned overview on Boussinesq-type models: the interplay between physics, mathematics and numerics', *Proc. R. Soc. A* **469**(20130496). (Cited on page 4).

Broer, L. J. (1974), 'On the Hamiltonian theory of surface waves', *Appl. Sci. Res* **30**, 430—-446. (Cited on pages 3 and 17).

Cai, X., Langtangen, H. P., Nielsen, B. F. & Tveito, A. (1998), 'A Finite Element Method for Fully Nonlinear Water Waves', *J. Comput. Phys.* **143**, 544–568. (Cited on page 4).

Cao, Y., Beck, R. & Schultz, W. (1993), An absorbing beach for numerical simulations of nonlinear waves in a wave tank., *in* '8th Intl. Workshop Water Waves and Floating Bodies', pp. 17–20. (Cited on page 94).

Chambarel, J., Touboul, J. & Kharif, C. (2009), 'Head-on collision of two solitary waves and residual falling jet formation', *Nonlin. Processes Geophys.* **16**, 111–122. (Cited on pages 103 and 104).

Chamberlain, P. & Porter (2006), 'Multi-mode approximations to wave scattering by an uneven bed', *J. Fluid Mech.* **556**(8), 421–441. (Cited on page 5).

Chamberlain, P. & Porter, D. (1995), 'The modified mild-slope equation', *J . Fluid Mech* **291**, 393–407. (Cited on pages 20 and 34).

Charalampopoulos, A. (2016), 'A Hamiltonian Coupled Mode method for the fully nonlinear water wave problem, including the case of the moving seabed'. Diploma Thesis. (Cited on pages 104, 106, 121, and 125).

Chazel, F., Lannes, D. & Marche, F. (2011), 'Numerical Simulation of Strongly Nonlinear and Dispersive Waves Using a Green-Naghdi Model', *J. Sci. Comput.* **48**, 105–116. (Cited on page 109).

Chen, Q., Kelly, D., Dimakopoulos, A. & Zang, J. (2016), 'Validation of the PICIN solver for 2D coastal flows', *Coast. Eng.* **112**, 87–98. (Cited on pages 114, 115, and 116).

Chen, Y., Kharif, C., Yang, J., H. Hsu, J. T. & Chambarel, J. (2015), 'An experimental study of steep solitary wave reflection at a vertical wall', *European Journal of Mechanics B/Fluids* **49**, 20–28. (Cited on page 104).

Chondros, M. & Memos, C. (2014), 'A 2DH nonlinear Boussinesq-type wave model of improved dispersion, shoaling, and wave generation characteristics', *Coast. Eng.* **91**, 99–122. (Cited on page 109).

Clamond, D. (2012), 'Note on the velocity and related fields of steady irrotational two-dimensional surface gravity waves.', *Phil. Trans. R. Soc. A* **370**, 1572—-1586. (Cited on page 86).

Clamond, D. & Dutykh, D. (2012), 'Practical use of variational principles for modeling water waves', *Physica D* **241**, 25–36. (Cited on page 5).

Clamond, D. & Dutykh, D. (2013), 'Fast accurate computation of the fully nonlinear solitary surface gravity waves', *Computers and Fluids* **84**, 35–38. (Cited on page 98).

Clamond, D., Francius, M., Grue, J. & Kharif, C. (2006), 'Long time interaction of envelope solitons and freak wave formations', *Eur. J. Mech. B-Fluid* **25**, 536–553. (Cited on page 125).

Clamond, D., Fructus, D., Grue, J. & Kristiansen, O. (2005), 'An efficient model for three-dimensional surface wave simulations. part ii: Generation and absorption', *J. Comput. Phys.* **205**, 686–705. (Cited on page 94).

Clamond, D. & Grue, J. (2001), 'A fast method for fully nonlinear water-wave computations', *J. Fluid Mech.* **447**, 337–355. (Cited on page 4).

Coddington & Levinson (1955), *Theory of ordinary differential equations*, TATA MacGraw-Hill. (Cited on page 25).

Cokelet, E. (1976), 'Steep gravity waves in water of arbritary uniform depth', *Phil. Trans. R. Soc. A* **286**(1335), 183–230. (Cited on page 81).

Cooker, M., Weidman, P. & Bale, D. (1997), 'Reflection of a high-amplitude solitary wave at a vertical wall', *J. Fluid Mech.* **342**, 141–158. (Cited on page 103).

Couston, L.-A., Guo, Q., Chamanzar, M. & Alam1, M.-R. (2015), 'Fabry-Perot resonance of water waves', *Physical Review E* **92**. (Cited on pages 117 and 125).

Craig, W. & Groves, M. (1994), 'Hamiltonian long-wave approximations to the water-wave problem', *Wave Motion* **19**, 367–389. (Cited on page 4).

Craig, W., Guyenne, P., Hammack, J., Henderson, D. & Sulem, C. (2006), 'Solitary water wave interactions', *Physics of Fluids* **18**. (Cited on pages 3 and 103).

Craig, W., Guyenne, P., Nicholls, D. & Sulem, C. (2005), 'Hamiltonian long-wave expansions for water waves over a rough bottom', *Proc. R. Soc. A* **461**, 839–873. (Cited on pages 3 and 77).

Craig, W. & Nicholls, D. (2002), 'Traveling gravity water waves in two and three dimensions', *European Journal of Mechanics B/Fluids* **21**, 615–641. (Cited on pages 3 and 81).

Craig, W., Schanz, U. & Sulem, C. (1997), 'The modulational regime of three-dimensional water waves and the davey-stewartson system', *Ann. Inst. Henri Poincaré (C) Non Linear Analysis* **14**(5), 615 – 667. (Cited on page 4).

Craig, W. & Sulem, C. (1993), 'Numerical simulation of gravity waves', *J. Comp. Phys.* **108**, 73–83. (Cited on pages , 3, 6, 15, 16, and 77).

Craik, A. (2004), 'The Origins of Water Wave Theory', *Annu. Rev. Fluid Mech.* **36**, 1–28. (Cited on page 1).

Dauge, M. & Helffer, B. (1993), 'Eigenvalues Variation. I. Neumann Problem for Sturm-Liouville Operators', *Journal of Differential Equations* **104**, 243–262. (Cited on page 29).

Davies, D. & Heathersaw, A. (1983), Surface wave propagation over sinusoidally topography: Theory and observation, Technical Report 159, Institute of Oceanographic Sciences. (Cited on page 116).

Davies, G. & Heathersaw, A. (1984), 'Surface wave propagation over sinusoidally varying topography', *J. Fluid. Mech.* **144**, 419–443. (Cited on pages 116, 117, and 118).

Debnath, L. (1994), *Nonlinear Water Waves*, Academic Press. (Cited on pages 12 and 14).

Deconinck, B. & Oliveras, K. (2011), 'The instability of periodic surface gravity waves', *J. Fluid Mech.* **675**, 141–167. (Cited on page 81).

Devillard, P., Dunlop, F., & Souillard, B. (1988), 'Localization of gravity waves on a channel with a random bottom', *J. Fluid Mech.* **186**, 521–538. (Cited on page 21).

Dias, F. & Bridges, T. J. (2006), 'The numerical computation of freely propagating time-dependent irrotational water waves', *Fluid Dynamics Research* **38**, 803–830. (Cited on page 4).

Dingemans, M. (1994), Comparison of computations with Boussinesq-like models and laboratory measurements, Technical report, Delft Hydraulics. (Cited on pages 109 and 110).

Dingemans, M. (1997), *Water wave propagation over uneven bottoms," Non- Linear Wave Propagation"*, Vol. 13, World Scientific, Singapore. (Cited on page 4).

Dodd, N. (1998), 'A numerical model of wave run-up, overtopping and regeneration', *J. Waterway, Port, Coastal, Ocean Eng.* **124**, 73–81. (Cited on pages 106 and 107).

Dommermuth, D. & Yue, D. (1987), 'A high-order spectral method for the study of nonlinear gravity waves.', *J. Fluid Mech.* **184**, 267 – 288. (Cited on page 3).

Dusseaux, R. & Faure, C. (2008), 'Telegraphist's equations for rectangular waveguides and analysis in nonorthogonal coordinates', *Progress in Electromagnetics Research* (3), 53–71. (Cited on page 20).

Engsig-Karup, A., Bingham, H. & Lindberg, O. (2009), 'An efficient flexible-order model for 3D nonlinear water waves', *J. Comput. Phys.* **228**, 2100–2118. (Cited on page 4).

Fazioli, C. & Nicholls, D. (2010), 'Stable computation of the functional variation of the dirichlet-neumann operator', *J. Comput. Phys* **229**, 906–920. (Cited on page 73).

Fenton, J. (1985), 'A fifth-order stokes theory for steady waves', *J. Waterway, Port, Coastal, Ocean Eng.* **111**, 216–234. (Cited on page 81).

Fenton, J. (1988), 'The numerical solution of steady water wave problems', *Computers and Geosciences* **14**(3), 357–368. (Cited on page 81).

Fenton, J. (1990), 'Nonlinear wave theories', *The Sea: Ocean Engineering Science* **9**. (Cited on page 85).

Feynman, R., Leighton, R. B. & Sands, M. (1964), *The Feynman Lectures on Physics*, Addison Wesley. (Cited on page 1).

Fillipas, E. & Belibassakis, K. (2014), 'Hydrodynamic analysis of flapping-foil thrusters operating beneath the free surface and in waves', *Eng. Anal. Bound. Elem.* **41**, 47–59. (Cited on page 77).

Flett, T. (1980), *Differential Analysis*, Cambridge University Press. (Cited on pages 42 and 139).

Gagarina, E., Ambatia, V., van der Vegt, J. & Bokhove, O. (2014), 'Variational space–time (dis)continuous galerkin method for nonlinear free surface water waves', *J. Comput. Phys.* **275**, 459–483. (Cited on page 4).

Gasiński, L. & Papageorgiou, N. (2005), *Nonlinear Analysis*, Chapman and Hall/CRC. (Cited on pages 42 and 139).

Goda, Y. & Suzuki, Y. (1976), Estimation of incident and reflected waves in random wave experiments., *in* 'Proc. 15th Coastal Engng Conference, Honolulu, Hawaii.', pp. 828–845. (Cited on page 118).

Godin, O. A. (1997), 'A note on differential equations of coupled-mode propagation in fluids', *J. Acoust. Soc. Am.* **103**, 159—-168. (Cited on page 21).

Gouin, M., Ducrozet, G. & Ferrant, P. (2016), 'Development and validation of a non-linear spectral model for water waves over variable depth', *European Journal of Mechanics B/Fluids* **57**, 115–128. (Cited on pages 3, 109, 114, and 115).

Green, E. & Naghdi, P. M. (1976), 'A derivation of equations for wave propagation in water of variable depth', *J. Fluid Mech* **78**(237–246). (Cited on page 4).

Grilli, S., Guyenne, P. & Dias, F. (2001), 'A fully non-linear model for three-dimensional overturning waves over an arbitrary bottom', *Int. J. Numer. Meth. Fluids* **35**(829–867). (Cited on page 4).

Grilli, S., Subramanya, R., Svendsen, T. & Veeramony, J. (1994), 'Shoaling of solitary waves on plane beaches', *J. Waterway, Port, Coastal, Ocean Eng.* **120**(6), 609–628. (Cited on pages 4, 104, and 106).

Guyenne, P. & Nicholls, D. (2005), 'Numerical simulation of solitary waves on plane slopes', *Math. Comput. Simul.* **69**, 269–281. (Cited on pages 3 and 77).

Guyenne, P. & Nicholls, D. (2007), 'A high-order spectral method for nonlinear water waves over moving bottom topography', *SIAM J. Sci. Comput* **30**, 81–101. (Cited on pages 3 and 109).

Harris, J. G. & Block, G. (2005), 'The coupling of elastic, surface-wave modes by a slow, interfacial inclusion', *Proc. R. Soc. A* **461**, 3765–3783. (Cited on page 20).

Huang, W. (1994), 'Coupled-mode theory for optical waveguides: an overview', *J. Opt. Soc. Am. A* **11**(3), 963–983. (Cited on page 20).

Ince, E. (1956), *Ordinary Differential Equations.*, Dover. (Cited on page 129).

Isobe, M. & Abohadima, S. (1998), 'Numerical model of fully-nonlinear wave refraction and diffraction', *Coast. Eng.* . (Cited on pages 5 and 61).

Jensen, T. (1998), 'Open boundary conditions in stratified ocean models', *J. Marine Syst.* **16**, 297–322. (Cited on page 94).

Kakinuma, T. (2001), *A set of fully nonlinear equations for surface and internal gravity waves*, Environmental Studies, WIT Press. (Cited on page 5).

Kantorovich, L. & Krylov, V. (1958), *Approximate methods of higher analysis*, Interscience Publishers, New York. (Cited on page 42).

Kim, J. W., Bai, K. J., Ertekin, R. C. & Webster, W. C. (2001), 'A derivation of the green-naghdi equations for irrotational flows', *J. Eng. Math.* **40**, 17–42. (Cited on page 5).

Klopman, G., Groesen, B.-V. & Dingemans, M. (2010), 'A variational approach to Boussinesq modelling of fully nonlinear water waves', *J. Fluid Mech.* **657**, 36–63. (Cited on pages 5, 61, and 109).

Kong, Q. & Zettl, A. (1999), 'Dependence of Eigenvalues of Sturm–Liouville Problems on the Boundary', *Journal of Differential Equations* **126**(2), 289–407. (Cited on page 29).

Korteweg, D. & de Vries, G. (1895), 'On the change of form of long waves advancing in a rectangular canal, and on a new type of long stationary waves', *Phil. Mag.* **39**(5), 422–443. (Cited on page 2).

Lannes, D. (2005), 'Well-posedness of the water wave equations', *J. Am. Math. Soc.* **18**(3), 605–654. (Cited on pages 15 and 17).

Lannes, D. (2013), *The Water Waves Problem. Mathematical Analysis and Asymptotics*, American Mathematical Society. (Cited on pages 4, 12, and 63).

Lannes, D. & Bonneton, P. (2009), 'Derivation of asymptotic two-dimensional time-dependent equations for surface water wave propagation', *Physics of Fluids* **21**(016601). (Cited on pages 4, 63, and 64).

Liu, Y. & Yue, D. (1998), 'On generalized Bragg scattering of surface waves by bottom ripples', *J. Fluid Mech* **35**, 829–867. (Cited on pages 3, 117, and 118).

Longuet-Higgins, M. S. (1978*a*), 'The instabilities of gravity waves of finite amplitude in deep water I. superharmonics', *Proc. R. Soc. A* (360), 471–488. (Cited on page 81).

Longuet-Higgins, M. S. (1978*b*), 'The instabilities of gravity waves of finite amplitude in deep water II. subharmonics', *Proc. R. Soc. A* (360), 489–505. (Cited on page 81).

Longuet-Higgins, M. S., F.R.S. & Cokelet, E. (1976), 'The deformation of steep surface waves on water i. a numerical method of computation', *Proc. R. Soc. A* **350**, 1–26. (Cited on page 4).

Luke, J. (1967), 'A variational principle for a fluid with a free surface', *J. Fluid Mech.* **27**, 395–397. (Cited on pages , 2, and 14).

Luo, W., Zhang, R. & Schmidt, H. (2011), 'Three-dimensional mode coupling around a seamount', *Sci. China Physics, Mech. Astron.* **54**(9), 1561–1569. (Cited on page 21).

Ma, Q. (2010), *Advances in Numerical Simulation of Nonlinear Water Waves*, World Scientific. (Cited on page 4).

Madsen, P., Bingham, H. & Liu, H. (2002), 'A new Boussinesq method for fully nonlinear waves from shallow to deep water', *J. Fluid Mech.* **462**, 1–30. (Cited on page 4).

Manolas, D. (2015), Development of simulation tools for the integrated analysis of offshore wind turbines, PhD thesis, School of Mechanical Engineering, National Technical University of Athens. (Cited on page 106).

Massel, S. (1989), *Hydrodynamics of coastal zones*, number 48 *in* 'Elsevier Oceanography Series', Elsevier. (Cited on page 63).

Massel, S. (1993), 'Extended refraction-diffraction equation for surface waves', *Coast. Eng.* **19**, 97–126. (Cited on pages 5, 20, and 34).

Matsuno, Y. (2016), 'Hamiltonian structure for two-dimensional extended Green-Naghdi equations', *Proc. R. Soc. A* **472**(2190). (Cited on pages 4 and 65).

Maupin, V. (1988), 'Surface waves across 2-D structures: a method based on coupled local modes', *Geophys. J. Int.* **93**, 173–185. (Cited on page 20).

Maurel, A., Mercier, J.-F. & Felix, S. (2014), 'Propagation in waveguides with varying cross section and curvature: a new light on the role of supplementary modes in multi-modal methods.', *Proc. R. Soc. A* **470**(20140008). (Cited on page 20).

Mcdonald, B. E. (1996), 'Bathymetric and volumetric contributions to ocean acoustic mode coupling', *J. Acoust. Soc. Am.* **100**(1), 219–224. (Cited on page 20).

Mei, C. (1985), 'Resonant reflection of surface water waves by periodic sandbars', *J. Fluid Mech.* **152**, 315–335. (Cited on page 117).

Mélinand, B. (2015), 'A mathematical study of meteo and landslide tsunamis : The proudman resonance', *Nolinearity* **28**(2), 4037–4080. (Cited on page 18).

Memos, C., Klonaris, G. & Chondros, M. (2015), 'On Higher-Order Boussinesq-Type Wave Models', *J. of Waterway, Port, Coastal, and Ocean Eng.* **142**. (Cited on page 4).

Mercier, J.-F. & Maurel, A. (2013), 'Acoustic propagation in non-uniform waveguides: revisiting webster equation using evanescent boundary modes.', *Proc. R. Soc. A* **469**(20130186). (Cited on page 20).

Mercier, J. & Maurel, A. A. (2015), Improved Multimodal Methods for the Acoustic Propagation in Waveguides With a Wall Impedance and a Uniform Flow., *in* 'International Congress of Sound and Vibration'. (Cited on page 20).

Milder, D. M. (1990), 'The effects of truncation on surface-wave hamiltonians', *J. Fluid Mech* **216**, 249–262. (Cited on pages 3 and 4).

Miles, J. & Salmon, R. (1985), 'Weakly dispersive nonlinear gravity waves', *J. Fluid Mech* **157**(519–531). (Cited on page 4).

Miles, J. W. (1977), 'On Hamilton's principle for surface waves', *J. Fluid Mech* **83**, 153–158. (Cited on pages 3, 14, and 17).

Mitsotakis, D., Dutykh, D. & Carter, J. (2016), 'On the nonlinear dynamics of the traveling-wave solutions of the Serre equations', *Wave Motion* . (Cited on pages 99 and 125).

Mitsotakis, D., Synolakis, C. & McGuiness, M. (2015), 'A modified Galerkin/Finite Element Method for the numerical solution of the Serre-Green-Nagdhi system', *Int. J. Numer. Meth.* . (Cited on page 106).

Murakami, Y. & Iguchi, T. (2015), 'Solvability of the initial value problem to a model system for water waves', *Kodai Mathematical Journal* **38**, 470–491. (Cited on page 62).

Nicholls, D. (1998), 'Traveling water waves: Spectral continuation methods with parallel implementation', *J. Cpmput. Physics* **143**, 224–240. (Cited on pages 3 and 81).

Nicholls, D. (2007), 'Spectral stability of traveling water waves: Analytic dependence of the spectrum', *J. Nonlinear Sci.* **17**, 369–397. (Cited on pages 3 and 4).

Nicholls, D. & Reitich, F. (2001*a*), 'A new approach to analyticity of Dirichlet to Neumann operators', *Proceedings of the Royal Society of Edinburgh* **131**, 1411–1433. (Cited on page 3).

Nicholls, D. & Reitich, F. (2001*b*), 'Stability of High-Order Perturbative Methods for the Computation of Dirichlet-Neumann Operators', *J. Comput. Phys.* **70**, 276–298. (Cited on pages 3, 73, 74, and 77).

Nicholls, D. & Reitich, F. (2006), 'Stable, high-order computation of traveling water waves in three dimensions', *European Journal of Mechanics B/Fluids* **25**, 406–424. (Cited on page 3).

Nwogu, O. (1993), 'Alternative form of Boussinesq equations for nearshore wave propagation', *J. Waterway, Port, Coastal, Ocean Eng.* **119**, 618–638. (Cited on pages 4 and 114).

Ohyama, T., Kioka, W. & Tada, A. (1995), 'Applicability of numerical models to nonlinear dispersive waves', *Coast. Eng.* **24**, 297–313. (Cited on pages 114, 115, and 116).

Pannatoni, R. F. (2016), 'Coupled mode theory of scattering by a cylindrically symmetric seamount', *Proc. R. Soc. A* **472**(20150465). (Cited on page 20).

Papoutsellis, C. (2015), Numerical simulation of non-linear water waves over variable bathymetry, *in* 'YSC 2015. 4th International Young Scientists Conference on Computational Science', Procedia Computer Science., Elsevier, pp. 1–10. (Cited on page 8).

Papoutsellis, C., Athanassoulis, G. & Charalampopoulos, A. (2016), Interaction of solitary water waves with uneven bottom using a Hamiltonian Coupled-Mode System., *in* 'Frontiers of Nonlinear Physics'. (Cited on page 8).

Papoutsellis, C. E. (2012), Nonlinear Water Waves: Comparison of different variational methods, Master's thesis, School of Applied Mathematics and Physical Sciences, NTUA.
URL: *dspace.lib.ntua.gr/handle/123456789/38248* (Cited on page 17).

Peregrine, D. (1967), 'Long waves on a beach', *J. Fluid Mech.* **27**, 815–827. (Cited on pages 4 and 62).

Petrov, A. A. (1964), 'Variational treatment of the problem of liquid motion in container of finite dimensions', *PMM* **28**, 754–758. (Cited on page 2).

Porter, D. & Staziker, D. (1995), 'Extensions of the mild-slope equation', *J . Fluid Mech* **300**, 367–382. (Cited on pages 5, 20, and 34).

Rault, C., Benoit, M. & Yates, M. (2016), 'Validation of a fully nonlinear and dispersive wavemodelwith laboratory non-breaking experiments', *Coast. Eng.* **114**, 194–207. (Cited on pages 6, 109, and 110).

Rienecker, M. & Fenton, J. (1981), 'A fourier approximation method for steady water waves', *J. Fluid Mech.* **104**, 119–137. (Cited on pages 81 and 83).

Rudin, W. (1964), *Principles of Mathematical Analysis*, McGraw-Hill, Inc. (Cited on page 138).

Russel, D. (1982), 'On Exponential Bases for the Sobolev Spaces over an Interval', *Journal of Mathematical Analysis and Applications* **87**, 528–550. (Cited on page 28).

Rutherford, S. R. & Hawker, K. E. (1981), 'Consistent coupled mode theory of sound propagation for a class of nonseparable problems', *J. Acoust. Soc. Am.* **70**(2), 554–564. (Cited on page 21).

Rycroft, C. H. & Wilkening, J. (2013), 'Computation of three-dimensional standing water waves', *J. Comput. Phys.* **255**, 612–638. (Cited on page 4).

Saint-Venant, A. (1871), 'Théorie du mouvement non permanent des eaux, avec application aux crues des rivières et á l'introduction de marées dans leurs lits', *Comptes rendus des séances de l'Académie des Sciences* **73**, 147–154. (Cited on page 2).

Schaffer, H. (2008), 'Comparison of dirichlet–neumann operator expansions for nonlinear surface gravity waves', *Coast. Eng.* **55**, 288–294. (Cited on page 3).

Seo, S. N. (2014), 'Transfer matrix of linear water wave scattering over a stepwise bottom', *Coast. Eng.* **88**, 33–42. (Cited on page 21).

Serre, F. (1953), 'Contribution à l'étude des écoulements permanents et variables dans les canaux', *Houille Blanche* **8**(374). (Cited on page 4).

Smith, R. (1983), 'A coupled mode solution for acoustic propagation in a waveguide with stepwise depth variations of a penetrable bottom', *J. Acoust. Soc. Am.* **74**(1), 188–195. (Cited on page 21).

Smith, R. (1998), 'An operator expansion formalism for nonlinear surface waves over variable depth', *J. Fluid Mech.* **363**, 333–347. (Cited on page 3).

Stevenson, A. (1951*a*), 'Exact and Approximate Equations for Wave Propagation in Acoustic Horns', *J. Appl. Phys.* **22**, 1461. (Cited on page 20).

Stevenson, A. (1951*b*), 'General Theory of Electromagnetic Horns', *J. Appl. Phys.* **22**, 1447. (Cited on page 20).

Stoker, J. (1957), *Water Waves*, Interscience, NY. (Cited on pages 12 and 82).

Stokes, G. (1847), 'On the theory of oscillatory waves', *Trans. Camb. Phil. Soc.* **8**, 441–455. (Cited on pages 2 and 81).

Stotts, S. & Koch, R. (2015), 'A two-way coupled mode formalism that satisfies energy conservation for impedance boundaries in underwater acoustics', *J. Acoust. Soc. Am.* **138**, 3383—-3396. (Cited on page 20).

Su, C. & Mirie, S. (1980), 'On head-on collisions between two solitary waves', *J. Fluid Mech.* **98**, 509–525. (Cited on page 103).

Tian, Y. & Sato, S. (2008), 'A numerical model on the interaction between nearshore nonlinear waves and strong currents', *Coast. Eng.* **50**(4), 369–395. (Cited on page 6).

van Groesen, E. & Molenaar, J. (2007), *Continuum Modeling in the Physical Sciences*, Society for Industrial and Applied Mathematics. (Cited on page 14).

Vasan, V. & Deconinck, B. (2013), 'The Bernoulli boundary condition for traveling water waves', *Applied Mathematics Letters* . (Cited on page 83).

Wakley, M. & Berzins, M. (1999), 'A finite element method for the one-dimensional extended Boussinesq equations', *Int. J. Numer. Meth. Fluids* **29**, 143–157. (Cited on pages 106 and 109).

Watson, K. & B.West (1975), 'A transport-equation description of nonlinear ocean surface wave interactions', *J. Fluid Mech.* **70**, 815–826. (Cited on page 16).

West, B., Brueckner, K., Janda, R., Milder, M. & Milton, R. (1987), 'A new numerical method for surface hydrodynamics', *J. Geophys. Res.* **92**, 11803 – 11824. (Cited on page 3).

Whitham, G. B. (1967), 'Variational methods and applications to water waves', *Proc. R. Soc. A* **299**(1456), 6–25. (Cited on page 3).

Wilkening, J. & Vasan, V. (2015), 'Comparison of five methods of computing the Dirichlet - Neumann Operator for the water wave problem', *Contemporary Mathematics* **635**. (Cited on pages 4 and 73).

Williams, J. (1981), 'Limiting gravity waves in water of finite depth', *Philos. Trans. R. Soc. Lond.* **302**, 139–188. (Cited on pages 81, 85, and 98).

Witham, G. (1974), *Linear and Non Linear Waves*, Wiley, NY. (Cited on pages 12, 14, and 63).

Woo, S.-B. & Liu, P. L. (2001), 'A Petrov - Galerkin finite element model for one-dimensional fully non-linear and weakly dispersive wave propagation', *Int. J. Numer. Meth. Fluids* **37**, 541–575. (Cited on pages 109 and 110).

Xu, L. & Guyenne, P. (2009), 'Numerical simulation of three-dimensional nonlinear water waves. water waves', *J. Comput. Phys.* **228**(22), 8446–8466. (Cited on pages 3 and 73).

Yates, M. & Benoit, M. (2015), 'Accuracy and efficiency of two numerical methods of solving the potential flow problem for highly nonlinear and dispersive water waves', *Int. J. Numer. Methods Fluids* **77**, 616–640. (Cited on page 6).

Zakharov, V. (1968), 'Stability of periodic waves of finite amplitude on the surface of a deep fluid', *J. Appl. Mech. Tech. Phys* **9**, 86–94. (Cited on pages , 2, 6, 15, and 17).

Zettl, A. (2005), *Sturm-Liouville Theory*, American Mathematical Society. (Cited on page 29).

Zhang, Y., Kennedy, A., Panda, N., Dawson, C. & Westerink, J. (2014), 'Generating-absorbing sponge layers for phase-resolving wave models.', *Coast. Eng.* **84**, 1–9. (Cited on pages 94, 95, 114, and 116).

Zhao, B., Duan, W., Demirbilek, Z., Ertekin, R. & Webster, W. (2016), 'A comparative study between the IGN-2 equations and the fully nonlinear, weakly dispersive Boussinesq equations', *Coast. Eng.* **11**, 60–69. (Cited on pages 81, 83, and 85).

Zhao, B., Duan, W. & Ertekin, R. (2014), 'Application of higher-level gn theory to some wave transformation problems', *Coast. Eng.* **83**, 177–189. (Cited on pages 5, 109, 110, and 115).

Zou, Z. & Fang, K. (2008), 'Alternative forms of the higher-order boussinesq equations: Derivations and validations', *Coast. Eng.* **55**, 506–521. (Cited on page 4).